

International University Science Forum



**SCIENCE
EDUCATION
PRACTICE**



Toronto 2021

International University
Science Forum

**SCIENCE
EDUCATION
PRACTICE**

Part 1

TORONTO, 2021

Forum Scientifique
International des Universités

SCIENCE
ÉDUCATION
PRATIQUER

Partie 1

TORONTO, 2021



Science. Education. Practice : proceedings of the
International University Science Forum (Canada, Toronto), April
8, 2021. Part 1 - Infinity Publishing.

S67

ISBN 978-5-905695-60-6

The collection includes scientific articles of participants of the International University Science Forum, the purpose of which is to present significant results of scientific research in the field of humanities, natural and technical sciences; the formation of a modern level of scientific knowledge, experience in transformation of theoretical science into the sphere of practical application of innovations; generalization of research and practical experience. The forum is a tool for establishing sustainable ties, as well as the exchange of experience between teachers and researchers of universities and research organizations.

Le recueil comprend des articles scientifiques des participants du Forum Scientifique International des Universités, dont l'objectif est la présentation des résultats significatifs de la recherche dans le domaine des sciences humaines, de la nature et de l'ingénieur; la formation du niveau contemporain des connaissances scientifiques, de l'expérience de la transformation de la science théorique au champ de l'application pratique des innovations; la synthèse de l'expérience des recherches scientifiques et pratiques. Le forum est un instrument permettant d'établir des liens durables et d'échanger des données d'expérience entre les enseignants et les chercheurs des universités et les organisations scientifiques.

CONTENTS

ECONOMICS

*Nehad Hafiz Haidar, Al Saady Wesam, Ibrahim Mustafa Ali,
Batueva Irina Alekseevna*

Analysis the Role of Gold in Different Conditions of the Russian
Financial Market.....10

Gasumov Eldar Ramizovich, Gasumov Ramiz Alijavad-oglu

Caspian region may become one of the main gas suppliers to Eu
rope.....16

Smorodina Elena Anatolyevna, Deresheva Violetta Sergeevna

Formation and execution of local budget expenditures: analysis,
problems, prospects.....24

Muratova Marina Nikolaevna

Selected issues of using a resource-based approach to managing an
industrial enterprise development project.....34

TECHNICAL SCIENCES

Burlov Vyacheslav Georgievich, Polyukhovich Maxim Alekseevich

Integration of a geographic information system and an electric power
networks safety system as the basis for sustainable electric power
supply.....44

Starishko Ivan Nikolaevich

The state of the existing calculation methods and the factors affecting
the strength of bent reinforced concrete elements along inclined se
ctions.....54

Salkutsan Vladimir Ivanovich, Novikova Alexandra Vasilienva

Research and analysis of hygienic regulation on occupational noise.....67

Aleksey Y. Mironov, Anna Y. Mironova, Vyacheslav G. Burlov

Preventive Management of Administrative Production when Resources
Scarcity in the Parties Conflict.....75

PHYSICS AND MATHEMATICS

Inna Yu. Apalikova, Boris A. Markov, Yury I. Sukharev

Characteristics of Quantum Macrosystem as Principal Specific Feature of Colloid Gel Oxyhydrates.....88

MEDICAL SCIENCES

Muhitdinova Hura Nuritdinovna

Correlation relations of mean arterial pressure with hematopoietic parameters during burn toxemia depending on age.....116

*Ponomareva Maria Nikolaevna, Petrov Ivan Mikhailovich,
Kalyuzhnaya Elena Nikolaevna, Kalinina Vera Leonidovna,
Bredneva Anna Igorevna*

Etiopathogenetic therapy of microcirculation disorders in patients with COVID-19 associated pneumonia.....126

*Petrov Ivan Mikhailovich, Ponomareva Maria Nikolaevna,
Gribanova Evgeniya Konstantinovna, Bredneva Anna Igorevna,
Kalinina Vera Leonidovna*

Features of somatic polymorbidity in patients with diabetic angioretinopathy in peripheral diabetic neuropathy.....134

*Vozdvizhenskiy Mikhail Olegovich, Gorbachov Andrey L'vovich,
Trubin Alexey Jur'evich*

Surgical treatment options of advanced kidney cancer.....141

Moskalets Oxana Vladimirovna

Diagnostic value of neopterin as laboratory marker of lung sarcoidosis activity.....149

*Pochinok Elena Nikolaevna, Voronova Maria Romanovna,
Fomina Elena Viktorovna, Bedash Kalinka Ivanova,
Ponomareva Maria Nikolaevna*

Features of the state of muscular balance (phoria) in students of the Tyumen State Medical University. The effect of optical correction.....153

*Yushina Maria Alexandrovna, Markova Anastasia Olegovna,
Fomina Elena Viktorovna, Bedash Kalinka Ivanova,
Ponomareva Maria Nikolaevna*

Analysis of chronic ophthalmological pathology of the children's population of the Tyumen polyclinic.....162

*Terentyeva Natalya Aleksandrovna, Bazdyrev Evgeny Dmitrievich,
Krivoshapova Kristina Evgenievna, Pomeshkina Svetlana Aleksandrovna,
Barbarash Olga Leonidovna*

Impact of the musculoskeletal disorders in patients with coronary artery disease on the outcome of coronary bypass graft surgery.....168

BIOLOGICAL SCIENCES

*Gerasimov Vladimir Nikolaevich, Aslanyan Elena Mkritichevna,
Podgornaya Natalia Nikolaevna, Tyryshkina Anna Igorevna,
Khramov Mikhail Vladimirovich*

New opportunities for studying the ovicidal activity of disinfectants and estimating the viability of helminth eggs.....176

Ali J. Othman, Ludmila G. Eliseeva, Majd Alsaady, Vyacheslav V. Latushkin
Overall assessment of The Innovative Preparation "Glauxin" on the Product Quality and Nutritional Value of Hydroponically Grown Oakleaf Lettuce Plants Upon Foliar Treatment.....185

CHEMICAL SCIENCES

Voronin Aleksandr Vasilievich

Quantitative assessment of the content of some chemical elements in expert studies of various objects.....197

GEOLOGICAL AND MINERALOGICAL SCIENCES

Abilkhassimov Khairly

Sedimentation stages of the formation of the Caspian sedimentary basin in the Late Paleozoic.....206

ANALYSIS THE ROLE OF GOLD IN DIFFERENT CONDITIONS OF THE RUSSIAN FINANCIAL MARKET

Nehad Hafiz Haidar

Assistant Professor
University of Kalamoon
Deratia, Syria

Al Saady Wesam

Lecturer
Plekhanov Russian University of Economics
Moscow, Russia

Ibrahim Mustafa Ali

Lecturer
University of Technology
Baghdad, Iraq

Batueva Irina Alekseevna

Lecturer
Plekhanov Russian University of Economics
Moscow, Russia

This study presents the results of testing the relationship between the prices of stocks, bonds, and gold to investigate the existence of hedging or safe havens. The empirical analysis examines the price performance of Russian stocks and bonds and their relationship with gold price performance during a stable economic period and during the coronavirus pandemic.

Keywords: safe haven asset, hedge asset, diversifier asset, weak-form efficiency, financial crisis, economic recession after coronavirus.

Introduction

In the pre-crisis period, it is important to create a portfolio in which, individual assets during the crisis would become hedging assets, having a negative correlation with stocks or bonds in their composition.

It is important to carry out this in the pre-crisis period when this asset is not overvalued since the hedged asset is negative correlated with the

other portfolio assets, then when the crisis began the increase in demand quickly leads to rising its value. Thus, buying the hedged asset during the financial crisis is less useful or not useful at all (Al Saady,2021).

Traditionally, such an asset is considered to be gold, which is often associated with the existence of a safe haven. Published studies do not discuss all the investment characteristics of a safe haven asset; this study attempts to approach this issue in a broader framework. The theoretical reasoning is as follows. If there is an asset that reduces losses during market stress or financial crisis through hedging and portfolio diversification, then it is advisable to include it in the portfolio in the pre-crisis period, when its revaluation does not yet exist. Such an asset can be called a haven asset, since being not overvalued at the first stage, it also performs the function of portfolio diversification during the crisis.

Literature Review

The current approach to portfolio management in a crisis is considered in the context of including in the portfolio those financial assets that, having a negative correlation with stocks or bonds during the crisis. The study of Semenikova E. (2021) mentioned that such instruments in the Russian stock market are gold, shares of IT companies that provide technology for remote work, and shares of alcohol companies. The current study presents the results of testing the correlations between stocks, bonds, and gold to examine the effectiveness and time horizon of hedging.

Kahneman D. and Tversky A. (1979) proposed the prospect theory to create a useful theoretical framework for analyzing the safe haven assets. Later Tversky A. and Kahneman D. (1992) mentioned that people value speculation by thinking about profits and losses, not about the final level of wealth.

Studies of Tully E. and Lucy V. (2007), Semenikova E. and Mazaev. N. (2014), Capie F. et al. (2005). examined the nature and influence of the gold market.

While other studies examined gold as a "safe haven" Upper S. (2000) Kaul A. and Sapp S. (2007).

The current study does not mention a single article that analyzes the role of gold as a safe haven for both bonds and stocks in the Russian financial market.

Research Goals

- Analyzing the role of gold as a safe haven asset, as a hedge asset, or as a diversifier of the Russian security market, which are not weak efficient market, as the current study did not find any study that tests the role of gold in the market that is not efficient from the weak form;

- Analyzing the relationship between stock, bond, and gold markets in Russia during a stable economic period and during the coronavirus pandemic, then provide recommendations to the long-term investors in the Russian security market.

Data and Methodology

The current study covers two periods from 1st October 2017 to 20th February 2019 as a financial stability period, and from 20th February to 31st March 2021 as a financial crisis period. Includes 1046 daily observations. The data of MOEX the general index of the Russian stock market, and the data of the general Russian bond market index collected from the official website of the Moscow Exchange (2021a, 2021b). The data of gold price per gram was collected from the website of the Central Bank of the Russian Federation (2021).

The Russian Ruble was chosen as the currency for the analysis. As the current study aimed to determine the investment role of gold for the Russian investor.

The current study shows that an investors utility increases if they buy an asset that reduces losses outside of hedging or diversifying assets, that does not lose its value during extreme market conditions (for example: during the coronavirus pandemic). Thus, exhibits zero or negative correlation with the benchmark portfolio at such time. Such an asset will be designated as a safe haven asset. To distinguish a safe haven asset from a hedge and diversifier assets, the current study will explicitly explain those three types before proceeding.

Hedging asset: is an asset that is not correlated or negatively correlated with another asset or portfolio on average.

Diversifier asset: is an asset that is positive but not fully correlated with another asset or portfolio on average.

Safe haven asset: is an asset that is negatively correlated or not correlated with another asset or portfolio during the financial shocks or crises on average.

Depending on the above, the current study suggests the following hypotheses:

- Gold is a hedge for the Russian stocks. The price of gold and the price of stocks negatively correlate, or do not correlate on average.

$$R_1 \leq 0 \tag{1}$$

- Gold is a hedge for the Russian bonds. The price of gold and the price of bonds negatively correlate, or do not correlate on average.

$$Y_1 \leq 0 \tag{2}$$

- Gold is a safe haven for the Russian stocks. Gold and stock prices negatively correlate, or do not correlate during the coronavirus pandemic.

$$R_1 + R_2 \leq 0 \quad (3)$$

- Gold is a safe haven for the Russian bonds. Gold price and bond price negatively correlate or do not correlate during the coronavirus pandemic.

$$Y_1 + Y_2 \leq 0 \quad (4)$$

Where:

R_1 - the correlation between gold price and stock price during a period of economic stability.

R_2 - the correlation between gold price and stock price during the coronavirus pandemic.

Y_1 - the correlation between gold price and bond price during the economic stability period.

Y_2 - the correlation between gold price and bond price during the coronavirus pandemic.

Empirical results and discussion

The unconditional correlation matrix for stock, bond, and gold in both a stable economic period and the coronavirus pandemic period is shown in table 1.

Table 1 illustrates the relationship between stock, bond, and gold returns on average. Thus, the findings do not provide enough information to understand whether gold is hedging asset, or diversification asset, or safe haven asset for the Russian stocks and bonds.

The results show a negative correlation in stable economic times between stock and bond returns with gold price implying that gold is a hedge for stock and bond markets during stable economic times.

During the coronavirus pandemic, there is a positive correlation between stock and bond returns with gold price, Thus, gold is diversifier for stocks and bonds during the coronavirus pandemic.

After applying the formula $R_1 + R_2 \leq 0$ to check if gold is a safe haven for stocks. Results show that $R_1 + R_2 = 0.528$ is more than zero, which means that gold is not a safe haven for stocks in the Russian market.

In the same way, after calculated $Y_1 + Y_2 = 0.12$ is more than zero, which means that gold is not a safe haven for bonds in the Russian market.

The results provide convincing evidence for reject the weak form efficiency of the Russian security market, and on the presence of a large number of irrational investors in the market, since stocks and bonds prices did not fall during the coronavirus pandemic, but rose in the same direction as the gold price, as a result of speculation activity.

Table 1. The correlation returns matrix of stocks, bonds and gold

Correlation	Stock	Bond	Gold
Stable economy period			
Stock	1	0.205	(0.032)
Bond		1	(0.023)
Gold			1
Coronavirus pandemic period			
Stock	1	0.232	0.56
Bond		1	0.143
Gold			1

All values are significant at 0.05.

Values in brackets () are negative values.

Source: Prepared by authors.

Conclusion

The current study analyzes the role of gold as a safe haven asset in the Russian financial market and provides evidence that investors in the market did not use gold as a safe haven asset during the coronavirus pandemic. Moreover, gold is a diversifying asset for an investor in Russian security market during the coronavirus pandemic.

While in a period of economic stability, investors in the Russian security market could use gold for hedging in their portfolios.

Fluctuations in stock, bond, and gold prices increase during the coronavirus pandemic, indicating a higher opportunity for the rational investor to achieve abnormal returns during the crisis.

Given this result, it can be assumed that speculators often exacerbate anomalies in the Russian security market. Thus, arbitrage operations will never bring security prices to their fair values. So, the Russian security market looks promising for the long-term investors who have the solvency to seize arbitrage opportunities, and take risks during crisis periods such as the coronavirus pandemic.

References

1. Al Saady W. (2021). Actual approach to portfolio management in a crisis [Aktual'nyy podkhod k upravleniyu portfelem tsennykh bumag v usloviyakh krizisa]. *Financial markets and banks*, 1(1), 37-41. <https://cyberleninka.ru/article/n/aktualnyy-podhod-k-upravleniyu-portfelem-tsennykh-bumag-v-usloviyah-krizisa/viewer>
2. Capie F., Mills T. C. (2005). Wood G. Gold as a Hedge against the Dollar, *Journal of International Financial Markets, Institutions and Money*. 15(4), 343-352.
3. Central Bank of the Russian Federation. (2021). Precious metals courses— Gold price data. Retrieved from Central Bank of the Russian Federation website: <https://mfd.ru/centrobank/preciousmetals/?left=0&right=-1&from=17.03.2005&til=04.04.2021>
4. Kahneman D., Tversky A. (1979). Prospect Theory: An Analysis of Decision under Risk, *Econometrica*, 47(2), 263-292. <https://doi.org/10.2307/1914185>
5. Kaul A., Sapp S. (2007). Y2K fears and safe haven trading of the U.S. dollar, *Journal of International Money and Finance*, 25(5), 760-779. <https://doi.org/10.1016/j.jimonfin.2006.04.003>
6. Semenкова E.V., Investment Instruments of Industry Development in the Stock Market Under Pandemic Conditions// Modern financial markets in a new economy: collection of articles. international scientific and practical conference, (January 28, 2021) -M: Russian Economic university (Plekhanov), – 2021. - PP. 292-298. https://elibrary.ru/download/elibrary_44776175_80448129.pdf
7. Semenкова E.V., Mazaev N.Yu. (2014). Investment analysis: anomalies of the modern stock market [Investitsionnyy analiz: anomalii sovremennogo fondovogo rynka], *finance and credit*, 43(619), 2-9.
8. Moscow Exchange. (2021a). Moscow Exchange— MOEX Stock index data. Retrieved from Moscow Exchange website: <https://www.moex.com/en/index/RTSI/archive/#/from=2017-01-01&til=2021-04-03&sort=TRADEDATE&order=asc>.
9. Moscow Exchange. (2021b). Moscow Exchange— Bond index data. Retrieved from Moscow Exchange website: <https://www.moex.com/en/index/RUCBITR/archive/#/from=2005-03-17&til=2021-04-03&sort=TRADEDATE&order=desc>.
10. Tully E., Lucey B. M. (2007). A power GARCH examination of the gold market, *Research in International Business and Finance*, 21(2), 316-325.
11. Tversky A., Kahneman D. (1992). Advances in prospect theory: cumulative representation of uncertainty, *Journal of Risk and Uncertainty*, 5, 297-323.
12. Upper C. (2000). How Safe was the 'safe Haven'? : Financial Market Liquidity During the 1998 Turbulences (SSRN Scholarly Paper No. ID 1/100). Retrieved from <https://ssrn.com/abstract=219132>. <http://dx.doi.org/10.2139/ssrn.219132>

THE CASPIAN REGION MAY BECOME ONE OF THE MAIN GAS SUPPLIERS TO EUROPE

Gasumov Eldar Ramizovich

Candidate of Economic Sciences, Associate Professor
Azerbaijan State University of Oil and Industry, Baku

Gasumov Ramiz Alijavad-oglu

Doctor of Technical Sciences, Full Professor
North Caucasus Federal University, Stavropol, Russia

The article discusses the prospects of the Caspian region becoming one of the main suppliers of natural gas to Europe. The priority goals of the world states in the Caspian region in the development of hydrocarbon deposits are given. An important geo-economic factor is the fact that the Caspian region can become one of the main reliable suppliers of natural gas to the European region. The Caspian region is becoming one of the suppliers of natural gas to Europe, due to many factors: a favorable geographic transit position; wealth of HC resources; geopolitical significance; energy potential, acquires the status of a stable "economic ring" in the center of Eurasia, where huge investments will be concentrated in the next decade. It is stated that natural gas from the Caspian region is a new source of supply of natural gas to the European market, and the implementation of new gas pipelines, such as the Southern Gas Corridor (SGC), is anew the energy map of the continent. The commercial supply of Azerbaijani gas through the Trans Adriatic Pipeline (TAP), the latest component of the SGC project, creates powerful infrastructures for the supply of natural gas from the Caspian region to Europe via Turkey. The existing international gas pipelines for the transportation of Caspian gas to Europe, the geography of its supply and possible options for the development of new export supplies are analyzed. Possible options for using "SGC" for gas transit from Asian countries were considered.

Keywords: Caspian region, natural gas, European market, hydrocarbon, pipeline.

The Caspian region, due to many factors, such as an extremely favorable geographic transit position connecting through it the West with the

East, as well as the North and South, as well as the richness of hydrocarbon (HC), water and other resources, has historically been one of the most important regions of the world, to which the attention of various countries and leading states has been attracted since ancient times. The geopolitical significance of the Caspian Sea, in turn, is formed under the influence of its natural resources and energy potential, which are of increased interest for non-regional states and neighboring macro-regions. The Caspian region is currently acquiring the status of a stable "economic ring" in the center of Eurasia, where investments, interests and initiatives of regional and global centers of power will be concentrated in the next decade [2, 15].

An important geo-economic factor is the fact that the Caspian region can become one of the main reliable suppliers of natural gas to the European region. According to British Petroleum experts, Turkmenistan, Kazakhstan and Azerbaijan account for a total of 5.85 trillion cubic meters of natural gas. The potential of the states of the Caspian region is confirmed by the volume of their natural gas reserves - 35-40 trillion cubic meters, or 26% of world reserves. With the acquisition of sovereignty by the coastal states of the Caspian region, the structure of international relations has changed. This especially affected the Caspian Sea. According to preliminary estimates, the explored reserves of hydrocarbons on the shelf of the Caspian Sea amount to 12-14 million tons of fuel equivalent (tfe). If the seabed is divided into national sectors, then Kazakhstan will receive 4.5 billion tfe, Azerbaijan - 4 billion tfe, Russia - 2 billion tfe, Turkmenistan - 1.5 billion tfe, Iran - 0.9 billion tfe. Additional research can add another 3.5 and 3 billion tfe to the Kazakh and Azerbaijani shares, respectively [17].

The presence of large reserves of oil and gas is the most important geo-economic factor affecting the alignment of geopolitical forces in the Caspian region. According to a number of Russian experts, with world oil reserves of 150 billion tons, this region accounts for up to 25 billion tons, that is, no more than 10% of world oil reserves. According to the OPEC countries, the reserves of the Caspian basin do not exceed 23 billion tons [16].

According to Western experts, raw materials from the Caspian Sea may be of great importance for Europe as an alternative to Arab oil, while production from the North Sea declines. According to some reports, only Kazakhstan, Azerbaijan and Turkmenistan own more than 100 billion barrels of oil, which makes the Caspian region the third largest oil reservoir in the world after the Persian Gulf and Siberia [13].

The energy sector of the region is formed at the expense of the Cas-

pian basin, as well as the adjacent oil and gas territories of five countries - Azerbaijan, Iran, Kazakhstan, Russia, Turkmenistan. At the same time, Western authors, in addition to these states, additionally include one more Central Asian republic of Uzbekistan in the countries of the Caspian region.

At present, the geographical role of the Caspian Sea in connection with the expected large oil and gas resources is clearly acquiring a geopolitical coloration. Oil and gas reserves of the Caspian basin, routes of their transportation to world markets, participation in the development of subsoil are the subject of special attention, hidden and sometimes open struggle between individual states for access and control over resources.

Different states fighting for influence in the Caspian region often pursue completely different goals, mainly boiling down to solving purely economic problems (tab. 1).

Table 1- Priority goals of world states in the Caspian region

№	Geopolitical role	Group of states	Priority goals
1	Coastal countries of the Caspian basin	Azerbaijan, Iran, Kazakhstan, Russia, Turkmenistan	Use the export of energy resources to the world market to support the state economy and solve internal problems
2	Ensuring the transit of Caspian energy resources	Azerbaijan, Bulgaria, Georgia, Iran, China, Turkey, Turkmenistan, Ukraine, Russia	To consolidate the role of a permanent transit country for Caspian energy resources and ensure a constant income from their transportation
3	Historical regional actors (leading states)	Iran, China, Russia, Turkey	Maximize geopolitical influence in the Caspian region
4	Global actors (leading states)	Russia, Turkey, EU countries, USA, China	Use positions of influence in the Caspian region to fight for dominance over global logistics routes, as well as to diversify mechanisms to ensure their own energy security and influence opposing actors

The countries of the European Union in the Caspian region have predominantly economic interests. The main goal of European policy here is to ensure its own energy security in the XXI century. New suppliers of oil and gas, represented by Azerbaijan, Kazakhstan and Turkmenistan, could significantly reduce Europe's dependence on traditional suppliers. The second main goal of the leading EU countries in this region is to preserve and develop their own oil and gas industry through the work of their large companies in richer fields outside their countries.

To ensure the full use of the potential of the Caspian region and create all the necessary infrastructure for the production and transportation of gas to world markets, large investments are required. All these factors make the Caspian region one of the main centers of the planet's geo-economic influence. In general, American experts do not exclude that over time, the oil-producing Caspian states (Azerbaijan, Kazakhstan and Turkmenistan taken together) may become a serious competitor to countries supplying gas to Europe [15].

The European Union regards the Caspian region not only as a strategically important source of energy resources, but also as a kind of springboard providing direct access to the resources of Central Asia and Iran.

The projects of the transport corridor Europe-Caucasus-Asia (TRACE-CA) and interstate transportation of oil and gas to Europe (INOGATE) are most consistent with the European vision of the development of this region. In addition, the pipeline system can be used here as an important component of the "European enlargement" strategy. The EU proposes to consider the feasibility of the transport route Europe-Turkey-Georgia-Azerbaijan-Caspian Sea-Turkmenistan-Central Asia, which in many respects repeats the ancient Great Silk Road. In turn, the North-South international transport corridor is intended to connect the North of Russia and Europe through the Caspian basin with the countries of the Persian Gulf, India and Pakistan [1, 9].

These transport routes coincide with existing and prospective pipelines for the export of natural gas from the Caspian and Central Asian regions to Europe. Of all the routes under consideration, the most important link (transport) bridge is Azerbaijan. Azerbaijan has already "opened a window to Europe" not only for its gas, but - so far theoretically - for other countries of the Caspian region as well. Azerbaijan has a great prospect to become one of the centers providing the European market with natural gas, this is based on the following factors [2, 12]:

- advantageous geopolitical and geographical location and common borders of the states of the Caspian region, which have huge reserves of HC;

- the presence of powerful international operating gas transmission systems connecting the Caspian region with Turkey and Europe, a significant transit potential allowing it to become an energy bridge;
- the presence of identified and developed large-scale own, the possibility of increasing exports through the development of new HC fields with predicted reserves of up to 7.0 trillion cubic meters (mainly in the western part of the country, on the Caspian shelf and diversified export infrastructure for the transportation of natural gas);
- experience in the development of offshore oil and gas fields, taking into account the concluded international contracts with large consortia, reliable partnerships between suppliers and consumers, involvement of large-scale foreign investments in the gas industry;
- the existence of a historical relationship between world states, the concentration of transit resources in the hands of the state, which allows providing long-term guarantees of stability and a competitive level of tariffs for gas transportation.

To transport Caspian gas, the main South Caucasian gas pipeline (SCT, SCPx) was built in 2006 and began transporting gas from the Azerbaijani Shah Deniz gas condensate field (stage I) to Georgia, and since 2007 to Turkey. Currently, SCPx's capacities are used to supply Azerbaijani natural gas to Europe within the framework of SGC. The Southern Gas Corridor project (SGC is an abbreviated version of the "Nabucco" project) through which gas from the Caspian shelf is transported to Europe, to Italy, with the prospect of the possibility of involving new resources, incl. from the deposits of the countries of the Caspian region and the Middle East, consists of three parts: "SCPx" - going through the territory of Azerbaijan and Georgia to the border with Turkey; Trans-Anatolian Pipeline (TANAP) - running through Turkey; Trans-Adriatic (TAP) - passing through the territory of Greece, Albania and Italy. An additional gas resource for the SGC gas pipeline (and the future of a full-fledged "Nabucco") can be gas from the countries of the Caspian region. According to some sources, the initial throughput of the Nabucco gas pipeline is estimated at 31 billion cubic meters and can be adjusted, and the capacity of TANAP will allow it to supply 10 billion cubic meters of Azerbaijani gas per year to European markets and another 6 billion cubic meters for internal needs of Turkey. There are plans to increase the capacity of TANAP to 24 billion cubic meters by 2023 and to 31 billion cubic meters by 2026. 9 European companies will buy SGC gas: Anglo-Dutch Shell, Bulgarian Bulgargas, Greek DEPA, German Uniper, French Engie, Italian Herf Trading, Edison, Enel and the Swiss "AXPO" [2, 6, 8, 9,11].

According to EU rules, one supplier does not have the right to occupy more than half of its market, but this rule does not apply to Turkey, and it has really become what it has been striving for for so long - a full-fledged energy hub. The Caspian region, represented by Azerbaijan, has entered a new European market, which will give it concrete financial profit and political dividends. Azerbaijan's largest gas project to launch gas supplies from the Caspian Sea to Europe has been officially completed. TAP - the last element of the SGC connecting the Caspian Sea with Southern and Western Europe - has started commercial deliveries [1-5, 7-9].

Natural gas from the Caspian region is a new source of natural gas supply to Europe, and the implementation of "SGC" is reshaping the energy map of the continent. Commercial supplies of Azerbaijani gas began through TAP at the end of 2020, which is the latest component of the SGC project, which provides for the creation of infrastructure for the supply of natural gas from the Caspian region to Europe via Turkey. Azerbaijan will supply more than 16 billion cubic meters of gas to Turkey and Europe annually for 25 years. In the future, Azerbaijan and Turkey are considering the possibility of using "SGC" for the transit of gas from Iraq and Israel. Turkey expressed their intention, the possibility to build in the future a gas pipeline that will connect the Israeli gas fields "Leviathan" and "TANAP" [1-5, 7, 9].

The EU states that the commissioning of the "SGC" gas pipeline from Azerbaijan will improve the situation with gas diversification not only for South-Eastern Europe, but also for the European Union as a whole. With the start of commercial gas supplies to Europe via the "TAP" gas pipeline, the strategic goal of "SGC" has been achieved, gas supplies to the European market open a new page in the development of the Caspian region and are the logical result of exemplary cooperation between partner countries, companies and international financial institutions. The possibility of doubling the export of Azerbaijani gas to the countries of Southern and Southeastern Europe is already being studied, while the studies carried out indicate that the demand for natural gas from the Caspian region also exceeds the agreed volumes.

Conclusions.

The Caspian region is becoming one of the suppliers of natural gas to Europe, due to many factors: a favorable geographic transit position; wealth of HC resources; geopolitical significance; energy potential, acquires the status of a stable "economic ring" in the center of Eurasia, where huge investments will be concentrated in the next decade.

The presence of powerful international operating gas transmission

systems connecting the Caspian region with Turkey and Europe, a significant transit potential allows Azerbaijan to become an energy bridge for the transportation of natural gas to meet the needs of consumers.

The presence of a historical relationship between the world states and the gas producing countries of the Caspian region, the concentration of transit resources in the hands of the state, allows Azerbaijan to provide long-term guarantees of stability and a competitive level of tariffs for gas transportation to the European market.

References

1. Gasumov E.R. Combustible gas in the history of Azerbaijan's development. // Eurasian Union of Scientists. M.: 2020. № 10(79). V. 8. P.7-11.
2. Gasumov E.R. Prospects for cooperation of the Caspian countries in the development of oil and gas fields. // Eurasian Union of Scientists. M.: 2021. № 2(83). V. 5. P.12-19.
3. Gasumov E.R. Formation of a strategy of innovative development of the gas industry of Azerbaijan based on analysis of influencing factors. // Sciences of Europe. European Science. Prague. 2020. № 60. V.4. P.18-24.
4. Gasumov E.R. Improving the efficiency of gas condensate Feld development through the use of innovations. //Wschodnioeuropejskie Czasopismo Naukowe. Warsaw. 2019. №9 (49). P.31-40.
5. Gasumov E.R. Production of natural gas in the economy of Azerbaijan. //European Journal of Economics and Management Sciences. Vienna. 2020. №4. P.56-61.
6. Gasumov E.R. Research on the relationship between investment and innovation as factors of economic growth and development of the gas industry in Azerbaijan. //Colloquium-journal. Warszawa. 2021. №3 (90). Part 4. -P.65-69.
7. Gasumov E.R. Technical and economic aspects of the development of the gas industry in Azerbaijan. //Wschodnioeuropejskie Naukowe. Warsaw. 2020. №10 (62). Part. 4. P.25-28.
8. Gasumov E.R. The role and place of the gas sector in the fuel and energy complex of Azerbaijan. //Colloquium-journal. Warszawa. 2020. №30 (82). Part 3. P.38-41.

9. Gasumov E.R. Use and production of natural gas in Azerbaijan. // American Scientific Journal. 2020. № 42. V. 2. P.24-28.
10. Maksimenko V. Central Asia and the Caucasus: the foundation of geopolitical unity. // Central Asia and the Caucasus. M.: 2000. № 3 (9). P.70-71.
11. Gasumov E.R., Valiev V.M., Gasumov R.A. Features of the development of the gas sector in Azerbaijan. //American Scientific Journal. № 43. Issue 2. P.25-31.
12. Darabadi P. Caspian region in the international geopolitical system of the early XXI century. // Caucasus and Globalization. M.: 2010. V. 4. Issue 1-2. P.7-21.
13. Kyshkumbaev C. Impact of energy resources on some aspects of domestic and foreign policy of Kazakhstan. // Central Asia and the Caucasus. M.: 1998. № 1. P. 41.
14. Litera B. Oil and gas of the Caspian Sea: state and prospects. // Caucasus & Globalization. M.: 2007. V. 1 (2). P.50-54.
15. On the long-term USA strategy in the Caspian region and practical steps for its implementation (Analytical report). // Journal of Theory and Practice of Eurasianism. M.: 2003. № 22. -P.34-36.
16. Cmapchenkov G. Caspian oil in the regional economy and world politics // Central Asia and the Caucasus. M.: 2006. № 1 (43). P.8-14.
17. Preiger D., Omelchenko V. Blue fuel of the countries of the Caspian region: problems of supply to the European market. // Central Asia and the Caucasus. M.: 2005. № 3(39). P.143-144.

FORMATION AND EXECUTION OF LOCAL BUDGET EXPENDITURES: ANALYSIS, PROBLEMS, PROSPECTS

Smorodina Elena Anatolyevna

Candidate of Economic Sciences, Associate Professor
Ural State University of Economics, Yekaterinburg, Russia

Deresheva Violetta Sergeevna

Student
Ural State University of Economics, Yekaterinburg, Russia

The budget expenditure management system allows the state to achieve an effective budgetary policy as a whole. In the context of limited own receipts of financial resources to the local budget, it is quite difficult to ensure the effectiveness of the fulfillment of expenditure obligations. In this regard, local self-government bodies need to ensure the fulfillment of the tasks of redistributing available financial resources in order to ensure their obligations. This article discloses the concept of "budget expenditures", analyzes the execution of the expenditure side of the budget of the urban district of Nizhnyaya Salda for the period 2017 - 2019, and on the basis of this analysis identifies the problems of the execution of the local budget in terms of expenditures and proposes measures aimed at solving them.

Keywords: budget, budget expenditures, local budget, local government bodies, budget system.

In the existing realities of public administration of budgetary funds, local budgets are allocated only a small part of all revenues that are collected on the territory of the country. This moment, cuts the economy and financial capabilities of municipalities, which in turn affects their direct dependence on regional and state budget funds. As a consequence, local governments need to look for options and opportunities to increase profitability from previously income-generating activities.

Unfortunately, alternative ways to improve the financial condition of the local budget often do not bring significant and tangible results, which in turn returns everything to square one, securing the status of "subsidized" municipalities.

Local self-government bodies have the right and responsibility to independently ensure the balance of budgets and the efficiency of the use of budget funds; carry out the budget process; establish, in accordance with the Tax Code of the Russian Federation, taxes, the income from which is subject to transfer to the local budget; to determine the forms and directions of spending budgetary funds, as well as the authority to form local budget revenues [1, art. 31].

The existence of budget expenditures is primarily associated with public needs and the costs necessary to meet them. Most of these costs are channeled through the budget, and only a small part through decentralized public finance or private funds.

In the specialized literature, there are various author's definitions of the concept of "budget expenditures" (tab. 1).

Table 1 – The authors' approaches to the interpretation of the concept and essence of "budget expenditures" [5, p. 125; 6, p. 33; 10, p. 67; 7, p. 251; 8, p. 195; 9, p. 50]

Author	Definition
Yu.S. Dolganova, N.A. Istomina	Budget expenditures in terms of economic content - monetary relations arising between the state (municipality) with legal entities and individuals, between authorities at various levels in connection with the distribution and use of budget funds.
Yu.S. Dolganova, N.A. Istomina	Budget expenditures for material content are funds allocated for financial support of the tasks and functions of the state and local self-government.
N.Yu. Isakova, Yu.A. Dolgikh, A.G. Lachikhina	Budget expenditures - economic relations arising in connection with the use of funds from the state monetary fund.
N.A. Povetkina	Budget expenditures are monetary funds stipulated in a special regulatory legal act, paid from the budgets of the budgetary system of the Russian Federation in a certain amount and effectively used by authorized bodies for strictly defined purposes, within the framework of financing the tasks and functions of the state.

O.V. Malinovskaya, I.P. Skobelev, A.V. Brovkina	Budget expenditures - funds allocated for financial support of the tasks and functions of the state and local government.
M.B. Karaseva	Budget expenditures are public continuous costs of the state or municipalities in the form of economic relations strictly mediated by the norms of law regarding the distribution and use of centralized money of funds in order to ensure the tasks and functions of the state (the Russian Federation, its constituent entities and municipalities).
N.A. Sattarova	Budget expenditures - relations arising in connection with the distribution and use of the centralized money of funds for sectoral, targeted and territorial purposes.

The information presented in table 3 shows that a number of authors such as: N.Yu. Isakova, Yu.A. Dolgikh, A.G. Lachikhina, Yu.S. Dolganova, N.A. Istomina and N.A. Sattarova define the term "budget expenditures" as economic or monetary relations. But only N.Yu. Isakov and Yu.A. Dolgikh consider in their definition the interacting aspects of these relations: the state (municipalities), legal entities and individuals, as well as authorities at various levels. At the same time, all of the above authors come to a single position that these relations arise in connection with the distribution and use of monetary funds (money), but only N.A. Sattarova points out the directions of the use of funds: by industry, target and territorial purpose.

The second half of the authors, namely: N.A. Povetkina, O.V. Malinovskaya, I.P. Skobeleva and A.V. Brovkina, additionally including N.Yu. Isakova and Yu.A. Dolgikh, considering "budget expenditures" also from the point of view of material content, mark "budget expenditures" as funds allocated to ensure the tasks and functions of government bodies at different levels. Additionally N.A. Povetkina emphasizes that "budget expenditures" are enshrined in a special normative legal act with expenditure obligations, which are directed to strictly defined goals.

Only M.B. Karaseva combined in her concept both directions of thought of the above authors, defining "budget expenditures" as public, continuous expenditures of authorities at different levels, enshrined in normative legal acts of economic relations in order to distribute and use funds for needs and assigned tasks.

Thus, budget expenditures in a broad sense are economic relations, enshrined in a regulatory legal act, arising from the distribution and use of the money of funds to ensure the tasks and functions of the state and

municipalities.

Considering the local budget, it should be said that it is formed from: tax and non-tax revenues, budget allocations (grants, subsidies, subventions), and off-budget revenues (profit from the sale and use of municipal property, voluntary donations, etc.).

The main financial support of the local budget is tax revenues.

The assessment of the financial regulation of local budgets consists of a statistical comparison of the numerical indicators of the estimated period with the indicators of previous periods (tab. 2).

Table 2 - Dynamics of revenues and expenditures of the budget of the urban district of Nizhnyaya Salda for 2017-2019, in thousand rubles. [2; 3; 4]

Indicator/year	2017	2018	2019	Growth (decline) rates, in%	
				2018/2017	2019/2018
Tax revenues	164 624.395	178 468.023	205 696.620	108.4	115.3
Non-tax income	18 294.828	21 721.445	14 525.977	118.7	66.9
Grants	3 525.000	1 606.000	15 087.000	45.6	939.4
Subsidies	179 345.098	211 924.343	319 131.548	118.2	150.6
Subventions	167 543.793	176 309.743	190 732.822	105.2	108.2
Other gratuitous receipts	2 988.600	5 715.500	67 313.200	191.2	1 177.7
Return of the remaining subsidies (in both directions)	- 2 313.896	- 1 359.753	- 5 710.075	58.8	419.9
Total income	534 007.818	594 385.301	806 777.092	111.3	135.7
Total expenses	545 673.133	556 223.905	735 815.822	101.9	132.3
Budget surplus / deficit	-11 665.282	38 161.401	70 961.272	372.1	186.0

After examining the data in the table, one can notice a tendency for an increase in the volume of tax revenues in the context of the periods under consideration, when non-tax revenues have a tendency of sharp instability. The increase in budget profitability is ensured in 2019 in relation to previous periods due to gratuitous receipts for the purpose of co-financing from higher budgets of modernization projects that won the selection. For example, from 2017 to 2020, the following facilities were reconstructed and modernized: Metallurgov Park, the main road on Frunze Street, repair of the road along the alley on the bank of Nizhnesaldinsky Pond, commissioning of the 1st and 2nd stages of gas supply lines.

Since 2018, work has been carried out in relation to the following projects: overhaul of a hydraulic structure on the river Salda, major overhaul of the square. A.K. Bykov, overhaul of the Paris Commune street, and the construction of capital construction facilities continues: a biological wastewater treatment facility, three gasification facilities (gas boiler houses), a ski base. For these purposes, funds have been allocated from higher budgets in the form of: grants, subsidies, subventions and other interbudgetary transfers, due to these actions, there is a trend of budget surplus in the budget of the city district of Nizhnyaya Salda.

The study of budget expenditures of the urban district of Nizhnyaya Salda for the analyzed period in the context of their main directions will reveal the problems of their formation and implementation (tab. 3).

Based on the indicators of the above table, it follows that during the period under review, the value of budget execution in the urban district of Nizhnyaya Salda never reached 100%. This observation indicates incomplete spending of budgetary funds in the following areas: health care, national economy, education and housing and communal services. The most problematic area is the housing and utilities sector, since in the period under review, incomplete execution is observed, bordering in the range from 45-60%.

There are several reasons for the existence of this factor: unreliable suppliers selected by concluding a contract in accordance with 44-FZ, who cannot fulfill the terms of the contract on the spot, as a result of which the contract is terminated and the bidding is held again, which increases the time frame project execution and funds are frozen in the budget of the city district of Nizhnyaya Salda. Sharp budget cuts under the influence of compelling forces and reasons, as well as the influence of other factors that led to the non-fulfillment of the budget in terms of expenditures.

Identifying various reasons for the low rates of filling of local budgets, relative to the overall picture in Russia, it is necessary to refer to research

papers presented by the opinions of authors from other territorial entities.

For example, Tishutina O.I., Doctor of Economics, Associate Professor, Head of the Department of Finance and Credit of the Faculty of Economics of the Khabarovsk State University of Economics and Law, in her scientific work identifies the following reasons for the low income of the local budget: first, the predominance of gratuitous receipts in the revenue side of the local budget indicates that the municipality is financially dependent on the federal and regional authorities, is subsidized.

Second, adjustments and numerous significant changes to the budget during the current fiscal year.

Table 3 - Dynamics of execution of the budget of the urban district of Nizhnyaya Salda by expenditures in 2017-2019, in thousand rubles. [2; 3; 4]

Expenditure section	2017			2018			2019		
	Plan	Fact	% fulfilled	Plan	Fact	% fulfilled	Plan	Fact	% fulfilled
Health care	2 587.901	889.984	34.39	861.803	690.918	80.17	4 511.250	2 313.334	51.28
National issues	46 404.817	44 461.776	95.81	46 741.587	45 386.477	97.1	97 791.562	74 589.756	81.26
National security and law enforcement	6 839.533	6 838.101	99.98	7 482.908	7 451.021	99.57	8 608.499	8 558.842	99.42
National economy	118 862.091	93 198.026	78.41	50 799.419	46 386.706	91.31	192 206.577	107 327.556	55.84
Housing and communal services	80 856.608	49 140.542	60.77	93 081.044	42 800.961	45.98	232 887.491	124 995.421	53.67
Environmental protection	156.000	125.497	80.45	128.372	128.370	100.0	1 066.000	933.580	87.58
Education	280 316.313	278 239.177	99.26	355 815.656	337 400.213	94.82	359 356.590	329 368.817	91.66
Culture, cinematography	31 373.300	31 369.218	99.99	31 901.960	31 895.293	99.98	44 355.093	44 352.532	99.99

SCIENCE. EDUCATION. PRACTICE

Social politics	32 728.452	29 085.744	88.87	33 418.600	30 516.123	91.31	31 937.084	29 782.209	98.16
Physical culture and sport	10 212.331	10 125.068	99.15	11 433.366	11 333.823	99.13	11 397.762	11 393.775	99.96
Mass media	2 200.000	2 200.000	100.0	2 244.000	2 244.000	100.0	2 200.000	2 200.000	100.0
Total expenses:	612 537.346	545 673. 133	89.08	633 908.715	556 233.905	87.75	977 295.408	735 815.822	75.29

This happens as a result of the allocation of interbudgetary transfers for various target programs adopted by the state authorities after the adoption and approval of the municipal budget, as a result of which it is necessary to make serious changes in the budget structure [13, p. 72-73].

There are also other opinions on the existing shortcomings in the local budget management system. For example, Ermakova E.A., Doctor of Economics, Professor of the Department of Finance of the Saratov Socio-Economic Institute, identifies the following problems of the local budget:

1) lack of resources for financial support of expenditure obligations to strengthen the material and technical base of social institutions and carry out repair work in municipal institutions;

2) uneven flow of tax and non-tax revenues, leading to the emergence of cash gaps;

3) an increase in ineffective expenses for the execution of court decisions and tax decisions, taking into account penalties, fines and state duties;

4) the suspension of operations to spend funds on personal accounts due to the failure of the debtor institutions to comply with the requirements of the executive documents [11, p. 158].

In scientific research, there are various approaches aimed at increasing the efficiency of budgetary resources and solving the problems associated with this process. For example, O.I. Tishutina. to increase the revenues of the local budget offers the following activities:

1) more attention should be paid to ways to increase non-tax revenues of the municipal;

2) it is necessary to streamline the organization of administration of these incomes, reorganize the management mechanism and choose uniform methodological approaches to the formation of rental payments;

3) strengthen control over the payment of lease payments and toughen administrative liability for their late payment;

4) make an inventory in order to identify property items that are not used by municipal institutions and municipal unitary enterprises, with their subsequent transfer to the treasury for lease or sale [13, p. 74].

On the contrary, Ermakova E.A. to motivate the development of the revenue base of local budgets when calculating the tax potential indicator to determine the level of estimated budgetary provision, he proposes:

1) apply a restriction at the level of average growth rates for all municipalities for the corresponding tax;

2) in order to increase the stability of the local budget, taking into account the high risks of agricultural production, a reduction coefficient was introduced for the unified agricultural tax.

3) apply the mechanism of replacing subsidies to equalize the budgetary provision of municipal districts and urban districts of the Oblast with additional standards for deductions from personal income tax [12, p. 136].

Based on the analysis of the problems of formation of local budget revenues and fulfillment of expenditure obligations, let us systematize the problems of local budget execution (tab. 4).

Table 4 - Problems of formation and execution of local budgets and ways to solve them

Problems of the formation and execution of the local budget	Proposed problem solving activities
Restriction of freedom of choice by local governments of suppliers of goods, works and services through Federal Law 44-FZ	Revise and modernize this law to the existing realities
The need to return subventions from a higher budget, due to the impossibility of implementing a previously planned event	The possibility of revising and redistributing the allocated funds for other urgent needs of the municipality, within the framework of a related area
Lack of tax incentives for the purchase of goods, works and services for municipalities, the livelihoods of which are financed mainly through grants and subventions, in view of the lack of the possibility of replenishing the budget from their own revenues	Development and approval of regulatory legal acts for the implementation and regulation of this issue

Low awareness of the Government about the state of the budgets of municipalities of the constituent entities of the Russian Federation	Organize work on the study and analysis of the budgets of municipalities with a whole reform to improve the welfare of local budgets
Inconsistency of the scope of powers of local self-government bodies with the material and financial resources at their disposal	1) optimization of budget expenditures 2) taking measures to increase budget revenues (increasing the tax base, increasing investment attractiveness of the municipality, optimization of municipal property management).
Achievement of optimization of the expenditure side of the local budget	1) development, improvement and use of mechanisms for assessing the effectiveness of certain costs 2) concentration of resources on socially significant priorities, avoiding their distribution in insignificant amounts between many problems 3) ensuring the discussion of problems with stakeholders, creating an opportunity for everyone to speak, in order to identify especially acute problems and innovative ideas for ways to solve them.

Summing up the scientific work, one can agree with the fact that in Russia at the present stage the budgetary system is far from ideal. At the moment, there are a sufficient number of problems in the formation and execution of local budgets.

Each author under consideration identifies a whole range of pressing problems that are practiced in municipalities from year to year. While the measures for their solution have to wait a long time, and if this does happen, then it is carried out in an imperfect form, which brings even greater discomfort to the budgets of municipalities.

References

1. Budget Code of the Russian Federation of July 21, 1998 N 145-FZ. URL: http://www.consultant.ru/document/cons_doc_LAW_19702/ (appeal date: 09.03.2021).
2. Decision of the Duma of the urban district of Nizhnyaya Salda dated 05.17.2018 № 30/1 "On approval of the report on the execution of the

budget of the urban district of Nizhnyaya Salda for 2017";

3. Decision of the Duma of the urban district of Nizhnyaya Salda dated 23.05.2018 № 47/1 "On approval of the report on the execution of the budget of the urban district of Nizhnyaya Salda for 2018";

4. Decision of the Duma of the urban district of Nizhnyaya Salda dated 26.10.2020 № 66/3 "On approval of the report on the execution of the budget of the urban district of Nizhnyaya Salda for 2019";

5. The budgetary system of the Russian Federation: textbook / Ed. Yu.S. Dolganova, N.A., Istomina, O.A. Boytush, T. D. Odinkova, A.K. Izmodenov; gen. ed. Yu.S. Dolganova, N.A. Istomina. – M.: Publishing house of the Ural un-ty,

2019. – 356 P. - ISBN: 9785-7996-2699-0.

6. Finances and the financial system of the state: textbook / Ed. N.Yu. Isakova, Yu.A. Dolgikh, A.G. Lachikhin. 2nd ed., Rev. and add. - M.: Publishing house of the Ural un-ty, 2019. – 124 P. – ISBN: 9785-7996-2779-9.

7. State and municipal finance: textbook / Ed. O.V. Malinovskaya, I.P. Skobeleva, A.V. Brovkin. 2nd ed. Add. and rev. M.: Knorus, 2016. – 480 P. - ISBN: 9785-4060-2393-8.

8. Financial law of Russia: textbook / Ed. M.B. Karasev. M.: Publishing house. Yurayt, 2015. – 388 P. - ISBN: 9785-9916-3178-5.

9. Budget law: textbook / Ed. N.A. Sattarov. M.: Business courtyard, 2009. – 296 P. - ISBN: 9785-9155-0074-6.

10. Povetkina N.A. Budget expenditures: concept, signs, features // Actual problems of Russian law. – 2015. – N 8 (57) – P. 5 – 10.

11. Ermakova E.A., Features of the financial security of the powers of local self-government bodies // Bulletin of SSEU. – 2019. N 3 (77). – P. URL: <https://cyberleninka.ru/article/n/osobennosti-finansovoy-obespechennosti-polnomochiy-organov-mestnogo-samoupravleniya/viewer> (appeal date 16.03.2021);

12. Ermakova E.A., Approaches to financial incentives for the effectiveness of local self-government activities // Bulletin of SSEU. – 2020. N 3 (82). URL: <https://cyberleninka.ru/article/n/podhody-k-finansovomu-stimulirovaniyu-effektivnosti-deyatelnosti-mestnogo-samoupravleniya/viewer> (appeal date 16.03.2021);

13. Tishutina O.I., Formation of local budgets in modern conditions: analysis, problems, prospects // Bulletin of the Khabarovsk State University of Economics and Law. – 2020. N 3 (104). URL: <https://cyberleninka.ru/article/n/formirovanie-mestnyh-byudzhetrov-v-sovremennyh-usloviyah-analiz-problemy-i-perspektivy/viewer> (appeal date 15.03.2021).

**SELECTED ISSUES OF USING A RESOURCE-BASED APPROACH
TO MANAGING AN INDUSTRIAL ENTERPRISE DEVELOPMENT
PROJECT**

Muratova Marina Nikolaevna

Senior Lecturer
Russian State University of Justice
Moscow, Russia
ORCID: 0000-0003-2533-9521

The approaches to the management of development projects are compared, including the comparison of the resource and market approaches to the management of the development project of an industrial enterprise. It is shown that the resource-based approach is quite costly, both in terms of time and resources. The advantages of the resource approach in assessing development projects, as well as methodological differences in approaches, are described. The features of the approaches are analyzed and conclusions are drawn about the need to combine them to form the most effective management strategy. The process of managing the cost and financing of the project is described. The priority directions of improving the project management of the development of an industrial enterprise on the basis of the integration of the resource approach are identified. A model for assessing the resource efficiency of a project in time is presented.

Keywords: industrial enterprise, development project, resource approach to project management, project cost management.

As noted earlier, a distinctive feature of the use of the resource approach in the implementation of development projects is the analysis of the flow of development resources, as the main object of management. This feature allows us to classify the resource approach to the area of subject management. The essence of the approach lies in the fact that the totality of the resource potential and capabilities of the enterprise, as the basis for the formation of the internal environment of the project, forms activities that are unique in their composition, capable of generating a certain effect.

In other words, each industrial enterprise has a unique resource potential, which can be used as efficiently as possible in its own projects. The advantages and disadvantages of the resource approach to the formation of a project management strategy for the development of an industrial enterprise, as well as its comparison with the market approach, are presented in table 1.

Table 1 – Comparison of resource and market approaches to project management for the development of an industrial enterprise

Approaches to project management for the development of an industrial enterprise	Advantages	Disadvantages
Market approach	is based on a functional concept, which allows you to link the management stages to the stages of the project life cycle or classical management functions; the strategy is based on long-term competition based on quality improvement, cost reduction, product and market differentiation; using the effective Porter model; ensures the interests of external investors by analyzing the risks and factors of influence of the external environment.	the assumption about the perfection of the market for factors of production; erroneous judgments about the homogeneity and high mobility of resources; the focus is on the external competitive environment of the firm; dependence on strong fluctuations in market conditions, crises and volatility of other external factors.
Resource approach	based on a subject concept, which allows you to effectively manage available resources; the strategy is based on long-term competition based on the increment of priority resources; ensures the internal interests of the enterprise in the project for the development of an industrial enterprise; takes into account the uniqueness and variability of development resources, as well as the quality of their management in the process of forming the final result of the project.	the difficulty of implementation arising from the scale of the required analysis, assessments, choice of alternatives, etc.; does not take into account the interests of external investors in terms of the goals of the project, which reduces the interest of investors; the complexity of calculations related to forecasting and controlling the expected resource effect; the management function is reduced to planning and control.

Source: developed by the author.

Analyzing the data in table 1, we can conclude that the existing market approach is universal for organizing project management through simpler mechanisms and techniques. At the same time, it is based on certain assumptions, which are expressed in the stability of the transparency of the general economic situation, as well as the minimum negative impact of the entire set of factors of the internal and external environment.

At the same time, the resource-based approach is quite costly, both in terms of time and resources. But at the same time, it allows not only to take into account possible resulting impacts from the outside, but also to build an effective model of project management in conditions of high risks and uncertainty due to an increased depth of assessment and control. In this case, the main methodological difference between the approaches is the subject of management: in the market - cash flow; in the resource - the flow of development resources.

The difference in the subject of management allows us to draw a conclusion about the possible effective application of one or another approach in the implementation of a development project. Thus, it is advisable to apply the market one in the process of using the mechanisms of project financing and attracting funds from investors and creditors, since external financing is attracted for the potential cash flow generated by the project. The resource-based approach allows us to evaluate the final result of the project from the point of view of the actual goal of its implementation, where the financial assessment is only a litmus of the final capitalization. Based on the development of strategic resources, this method allows the enterprise to assess the real results of the implementation of the development project to the fullest extent.

Analyzing the features of the approaches, it can be concluded that it is necessary to combine them to form the most effective management strategy. At the same time, the elements and methods of the market approach should provide a functional management concept in conjunction with the analysis of external factors of influence.

At the same time, the resource approach in management is focused on the resources and capabilities of an industrial enterprise, as the main subject of management, and also allows us to formulate the features of resource control as the main element of management of an industrial enterprise development project. According to MA Kushner, "the use of a combined approach to project management for the development of an industrial enterprise is primarily due to the imperfection of the existing practice" [3], the main problems of which are:

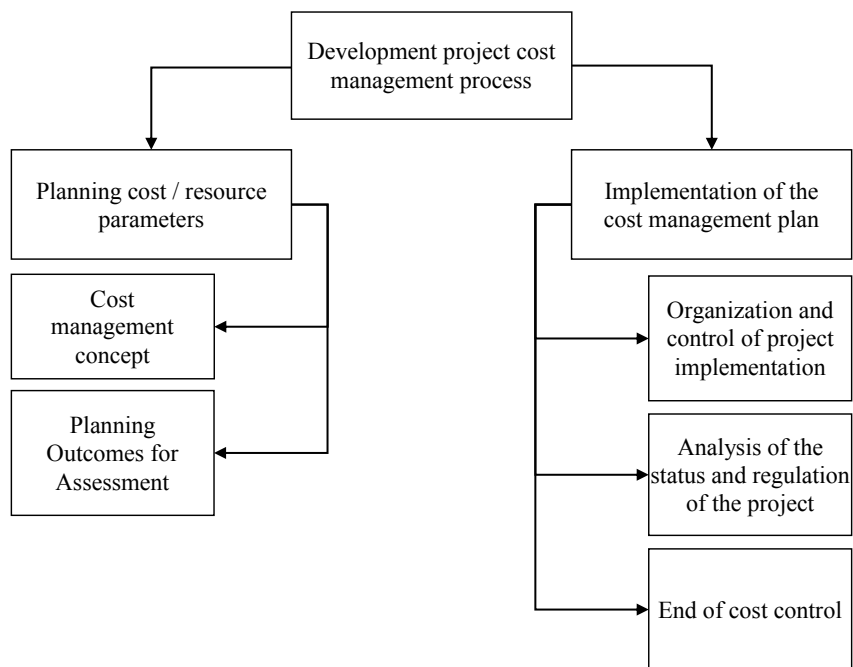
- 1) insufficiently worked out initial assessment of the project;

2) the lack of an effective control system that takes into account the interests of both the owners of the enterprise and external investors and creditors;

3) the allocation of cash flow as an object of management;

4) inaccurate assessment of the effectiveness of the project.

1. Insufficiently developed initial project assessment. This problem is characterized by the absence of a high-quality primary assessment of the project in terms of its main parameters: the amount of resources expended, the timing of implementation, the final result. The project cost management function affects the main aspects of determining the estimate and budget, funding sources, planning the resource flow, forming a single effective control system, etc. The classical cost management process includes five stages, which can be divided into two main stages (figure 1).



Source: Konoreva T.V., Kovalev V.I. Practical aspects of cost management and project financing // Modern problems of science and education.– 2014. – №4.

Figure 1 – Project cost and financing management process

A.S. Medvedev indicates that "at the concept stage, the main stages are the formation of a management strategy and financing a development project" [4]. For each project, its own form of financing is selected, depending on the existing internal capabilities and external capabilities of the enterprise. The choice of the optimal structure of funding sources allows you to level the financial risks arising in the process of project implementation.

Parameter planning involves assessing the total costs of project resources, as well as the time of project activities. Determination of the list and quantity of resources implemented in project activities, as well as the sources of their receipt.

2. Lack of an effective control system that takes into account the interests of both the owners of the enterprise and external investors and creditors. The effectiveness of the control system in the implementation of development projects should be achieved due to the high quality of preliminary control, and not the volume of identified and eliminated actual problems.

3. Allocation of cash flow as an object of management. The limitation of this approach is expressed in the static nature of the control object, since the cash flow is only identified with resources (or equated to the only type of resources, divided by the property criterion), which limits the possibilities of managerial influence. As a result, there is no possibility of high-quality structuring of the control object, that is, dividing it into structural elements that have a resulting impact on the implementation of the project.

4. Inaccurate assessment of the project's effectiveness. Practically applied dynamic and static methods for assessing the effectiveness of a project have a number of disadvantages (table 2).

Table 2 – Comparative analysis of existing approaches to assessing the effectiveness of projects

Advantages	Disadvantages
Dynamic approach (discounting)	
easy to calculate and analyze; takes into account the change in the value of money over time; allows you to calculate the predicted profitability for each investor;	does not take into account the peculiarities and structure of development resources; distorts the final results, appealing only with absolute indicators in monetary interpretation; management is directed only to cash flows; does not evaluate the effectiveness of the project; valuation results are subject to high levels of volatility in an environment of high risks and uncertainty.
Statistical approach (discount rates)	
simplicity of calculations; allows you to assess the liquidity and riskiness of the project; can be used in conditions of high inflation and a shortage of liquid working capital.	does not take into account the value of money over time; does not take into account the peculiarities and structure of development resources; does not give a clear idea of the final results of the project

Source: developed by the author.

The identified problems allow us to say that the priority areas for improving the management of an industrial enterprise development project based on the integration of the resource approach are: a) defining and specifying the object of management and the project management system; b) increasing the level of reliability of the pre-implementation assessment of the project; c) the formation of a qualitative methodology for as-

sessing the effectiveness of the project (table 3).

Table 3 - Directions for improving the management of an industrial enterprise development project based on the integration of the resource approach

Directions for improving the management of an industrial enterprise development project	The use of the resource approach
Definition and concretization of the control object and system	Selection of the flow of development resources as an object of management; Determination of the project management system in terms of the flow of development resources; Implementation of the concept of resource control
Improving the level of confidence in the pre-implementation assessment	Formation of the resource pool of the project / individual project activities based on the principle of sufficiency, not necessity; Formation of alternative options for resource pools of the project; Formation of a resource support system for the project.
Creation of a high-quality methodology for assessing the effectiveness of the project	Determination of the final result as a resource effect; Evaluating the effectiveness of the project in terms of the increment of strategic resources

Source: Developed by the author.

Another possibility of applying this strategy can be a methodology for selecting development projects based on two main aspects: the ability of the enterprise to implement the project, the usefulness of the project for the enterprise. The functional dependence of the choice of the project (or the possibility of its implementation) will be as follows:

$$DP = f(Ab_{com}; U_{com}), \quad (1)$$

where Ab_{com} – generalized ability of an enterprise to implement a development project at the current time;

U_{com} – generalized indicator of the usefulness of the development project for an industrial enterprise.

The ability of an enterprise is a set of internal potentials of an enterprise (production, resource, economic, intellectual, etc.), as well as the ability to use the existing capabilities of the external environment to achieve strategic development goals. Being one of the main pillars of the resource concept, they objectively personify the level of competitiveness of an enterprise. The total assessment of abilities can be characterized by the sum of internal potentials and the capabilities of the external environment:

$$Ab_{com} = \sum(C_{in}; O_{ex}), \quad (2)$$

where C_{in} – internal potential of the enterprise;

O_{ex} – external capabilities of the enterprise;

Ab_{com} – generalized indicator of enterprise ability.

The composition of internal indicators of the potential of an enterprise can be determined in terms of individual activities, as well as a set of strategic resources (table 4).

Table 4 – Composition of internal indicators of enterprise potential

Indicator group name (X_i)	Individual indicators of potential (a_i)
Management model	Organizational structure; Management methods; Management style.
Personnel composition	The number of staff; Structure; Qualification.
Labor productivity	Labor intensity; Number.
Technical equipment	Technical composition; Structure; The quality of technology.
Technological equipment	Technological composition; Structure; The quality of technology.
Financial security	Solvency; Financial stability; Profitability.
Product potential	Nomenclature; Quality.

Scientific and technical component	Number of R&D; Number of innovative projects (introduction of innovations); The volume of innovation in the volume of products.
Production cost potential	The ratio of the cost of production of the enterprise to the cost of competitors' products; The ability to influence the cost.
Pricing reserves	The ratio of the price of the company's products to the price of competitors' products; The ability to influence the price.
Supply potential	Supply costs; Losses due to poor quality supplies.
Sales potential	Sales costs; Losses due to poor quality sales.
Material use potential	Specific weight of material costs; Material utilization rate; Material efficiency.
Information security	Information costs; Losses as a result of poor quality information.
Marketing potential	Marketing costs; Losses as a result of poor quality marketing.

Source: developed by the author using Edziew A.E. Assessment of the economic potential of the enterprise. // Infrastructure sectors of the economy: problems and development prospects.– 2014. – №5. – P. 106-111.

Assessment of resource efficiency in time allows you to identify the real result of the implementation of the project for the development of an industrial enterprise in monetary terms. As an actual management tool, the author proposes to use a financial operator - a resource capitalization mechanism, which determines the dependence of the current cost of resources (Cost - C) on the time moment of assessing their capitalization (Time - t):

$$C = f(t) \cdot . \tag{3}$$

A financial operator can be either a simple interpretation of the re-

source effect through its financial assessment, or any capitalization mechanism based on discounting. The final assessment of the financial efficiency of the project is determined by the difference between the actual and planned financial value of the incremental strategic resources and the newly formed resource rent.

References

1. Edziev A.E. Assessment of the economic potential of the enterprise. // Infrastructure sectors of the economy: problems and development prospects. – 2014. – №5. – P. 106-111.
2. Konoreva T.V., Kovalev V.I. Practical aspects of cost management and project financing // Modern problems of science and education. – 2014. – №4.
3. Kushner M.A. Conceptual model of interaction of elements of management of projects for the development of industrial enterprises. // Relevant problems of economics and law.– 2013. – №3. – P. 124-130.
4. Medvedev A.S. Methodology for assessing and monitoring the state of the economic potential of industrial enterprises. // Sustainable development of mountainous areas. – 2013. – V.5. – №1. – P. 114-121.

INTEGRATION OF A GEOGRAPHIC INFORMATION SYSTEM AND AN ELECTRIC POWER NETWORKS SAFETY SYSTEM AS THE BASIS FOR SUSTAINABLE ELECTRIC POWER SUPPLY¹

Burlov Vyacheslav Georgievich

Doctor of Technical Sciences, Full Professor
Peter the Great St. Petersburg Polytechnic University

Polyukhovich Maxim Alekseevich

postgraduate student
Peter the Great St. Petersburg Polytechnic University

Managing the process of electric power supply to consumers in the interests of sustainable development of society requires the formation of processes with predetermined properties. The implementation of this approach is provided by a management concept based on the integration of a geographic information system and an electric power networks safety system. Applying this concept, it is possible to guarantee the high-quality functioning of the facility (electric power networks) under the influence of meteorological factors.

Keywords: electric power network, safety management system, geographic information system, human decision model, sustainable development

1. Introduction

The electric power industry is one of the key sectors of the economy of each country and consists of a set of processes for the production, transmission and consumption of electricity, as well as the operational management of these processes. These processes form a combination of economic relations that are part of the state's sustainable development program [1]. The operation of electric power facilities is determined, first of all, by the need for electric energy of the complex of socio-economic and industrial facilities [2], and then by the current hydrometeorological conditions [3].

¹The reported study was funded by RFBR, project number 20-38-90225.

To increase the level of technical and economic reliability of the electric power system, it is necessary to apply an integrated approach to the safety management of its elements [4-5]. This is especially true for electric power networks (EPN). At present, in order to improve the level of quality of functioning, all kinds of software and computing systems are used, which make it possible to predict the state of an object in advance under the influence of various meteorological factors [6-9]. But there is a general drawback of these complexes, which complicates their application in EPN, expressed in the uncertainty of the initial information about the state of the environment [10-13].

In the general case, the following types of meteorological factors can be distinguished that affect the transmission of electricity: strong wind, glaze-ice and rime deposition, thunderstorms, temperature effects, frost) [14-15].

The electric power industry is an extremely sensitive type of economic activity to the effects of climatic factors. The dependence of this industry on the hydrometeorological conditions of the area is determined by a significant number of geographically distributed infrastructure facilities, the performance of which is influenced by the indicators of weather and climatic conditions [16-17], which is expressed in the termination of power supply to consumers, an increase in electricity losses, as well as in the application of significant material and economic damage to the infrastructure facilities themselves. In addition, the accompanying losses for energy organizations are additional punitive sanctions damages from consumers caused by short-term or long-term outages and non-compliance of the supplied electricity with the declared and required indicators.

The types of losses in EPN under the influence of meteorological factors are considered and then two generalized types are distinguished [18-19]:

- damage to infrastructure facilities (power lines and power transmission line towers);
- electric power failure.

It is obvious that the influence of climatic factors on electric power losses is significant. This fact leads to the emergence of the problem of ensuring the required quality of power supply to consumers (the object of the electric power complex fulfills its purpose).

When managing electric power supply, the following principles should be followed:

- reliability of electric power supply [19];
- safety of operating personnel during work [20];

– economical operation [21-22].

One of the ways to solve the problem is the use of geographic information systems (GIS) for monitoring the state of the environment. A distinctive feature of GIS is the presence of a connection between various points in space with the provision of typical information from external sources [6].

2. Methods

The main functions of the electric power system are to ensure the reliability of power supply, the quality of electricity supplied to the consumer, and the safety of servicing electric installations. This requires the implementation of certain activities. The basis of the activity is the decision of the decision-maker (DM) [23]. Thus, to create a rationally organized system, it is necessary to have a mathematical model for the DM.

In connection with the instability of environmental conditions, it is also necessary to develop a model for the formation of information on the indicators of meteorological factors.

Thus, the task of integrating two processes arises:

- obtaining information about the environment;
- making of management decision.

In order to achieve the goal of the study, it is proposed to use GIS as a source of data on the state of the environment, which is explained by its functionality for predicting wind load indicators, the intensity of thunderstorm characteristics, precipitation, temperature, and solar radiation. These indicators are the main characteristics of the environmental conditions necessary for the formation of information support for the electric power supply management system. With such data, the DM is able to make an informed management decision to obtain a guaranteed result - the supply of electricity to consumers.

To make a decision corresponding to the current state of the environment, it is required to form processes with predetermined properties [24]. This study presents a synthesis-based control concept that meets these requirements. For the synthesis, it is necessary to apply natural-scientific approach, based on the object integrity maintenance law (OIML) [23].

The main problem arising during the integration of the power supply system and GIS is to establish a connection between geo-data, EPN parameters and the personnel of the operating organization. Management decision-making should be based on a specific methodological basis in the form of a condition for the existence of an integrated process [23]. Only the condition for the existence of the management process solves the problem of establishing a single integral connection between the components of the GIS with the elements of the mathematical model of

the operation of the EPN, which allows transforming resources (information, activities, qualifications, environmental conditions) in the interests of achieving the goal of the activity. Thus, it is possible to form an adequate mathematical model of a person's decision, without which it is rather difficult to guarantee the achievement of the set goals.

Sustainable electric power supply to facilities can only be ensured with constant monitoring of potential hazards [25] and timely response to threats arising in the environment, which are manifested through:

- structural components of the facility itself (in this case, EPN);
- action model;
- resources in the system.

To create safety conditions, restrictions should be imposed on information resources (aimed at recognizing threats), on activity resources (aimed at eliminating / preventing threats) and on environmental resources.

Human activity is based on time intervals, the duration of which can be varied depending on the required indicators. We accept that a threat to the process of activity arises with some frequency – Δt_{PM} . In this case, a person fixes a change in the environment over a certain period of time – Δt_{PI} (identification of threat). Then the DM makes a decision and carries out a certain set of actions to neutralize the threat, which also takes a certain amount of time – Δt_{PN} . At the same time, the control object (EPN) operates in parallel during the average time of the target task (T). The ratio of time intervals is shown in figure 1.

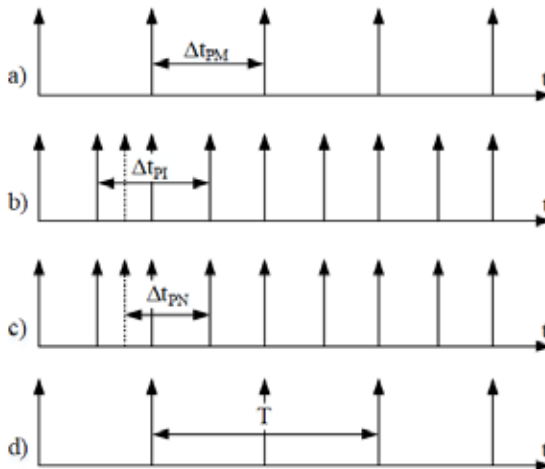


Figure 1. Diagram of the ratio of time intervals

Figure 2 shows a graph of states of an integrated system (combining the safety system of EPN and a GIS). The frequency of transition of the system from state 1 to state 4 (z^+) is equal to the value inverse to the average time for completing the target task (power supply of objects), which characterizes the degree of preparedness for solving target management problems. Frequency z^- characterizes the average rate of failure (electric power outages). The frequency of transition of the system from state 1 to state 2 (λ) is equal to the reciprocal Δt_{PM} . The frequency of transition from state 2 to state 3 (ν_1) is equal to the reciprocal Δt_{PI} . The frequency of transition from state 3 to state 4 (ν_2) is equal to the reciprocal Δt_{PN} .

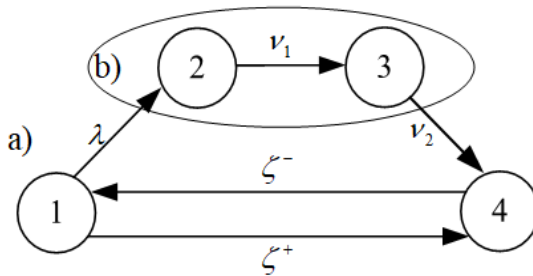


Figure 2. Graph of states of an integrated system

Figure 2 shows two circuits. The first circuit (a) is a consumer electric power supply control system, consisting of sequential control elements. For the stable functioning of the facility of the electric power complex, constant and timely control over meteorological factors is required. For this, GIS (b) is integrated into the power supply management system. This integration provides DM with information about the state of the environment at the moment and in the near future.

Two modes of operation of EPN are considered (figure 2):

- 1) the absence of a destructive impact of the meteorological factor on the control object (1→4);
- 2) the occurrence of the probability of a destructive impact of the meteorological factor on the control object (1→2→3→4).

3. Results

Temporary assumptions make it possible to use the Kolmogorov-Chapman system of differential equations [24].

The solution of this linear algebraic system of equations is the following relations:

$$P_1 = (\zeta^- \cdot v_1 \cdot v_2) / (\lambda \cdot \zeta^- \cdot v_1 + \lambda \cdot \zeta^- \cdot v_2 + \zeta^+ \cdot v_1 \cdot v_2 + \lambda \cdot v_1 \cdot v_2 + \zeta^- \cdot v_1 \cdot v_2) \quad (1)$$

$$P_2 = (\lambda \cdot \zeta^- \cdot v_2) / (\lambda \cdot \zeta^- \cdot v_1 + \lambda \cdot \zeta^- \cdot v_2 + \zeta^+ \cdot v_1 \cdot v_2 + \lambda \cdot v_1 \cdot v_2 + \zeta^- \cdot v_1 \cdot v_2) \quad (2)$$

$$P_3 = (\lambda \cdot \zeta^- \cdot v_1) / (\lambda \cdot \zeta^- \cdot v_1 + \lambda \cdot \zeta^- \cdot v_2 + \zeta^+ \cdot v_1 \cdot v_2 + \lambda \cdot v_1 \cdot v_2 + \zeta^- \cdot v_1 \cdot v_2) \quad (3)$$

$$P_4 = (\zeta^+ \cdot v_1 \cdot v_2 + \lambda \cdot v_1 \cdot v_2) / (\lambda \cdot \zeta^- \cdot v_1 + \lambda \cdot \zeta^- \cdot v_2 + \zeta^+ \cdot v_1 \cdot v_2 + \lambda \cdot v_1 \cdot v_2 + \zeta^- \cdot v_1 \cdot v_2) \quad (4)$$

These ratios determine the probability of finding the obtained integrated control system in the corresponding states.

An indicator of the efficiency of the functioning of the system is the probability that each problem (task) that arises in front of the system will be identified and neutralized. This indicator is determined by the ratio:

$$P_4 = (\zeta^+ \cdot v_1 \cdot v_2 + \lambda \cdot v_1 \cdot v_2) / (\lambda \cdot \zeta^- \cdot v_1 + \lambda \cdot \zeta^- \cdot v_2 + \zeta^+ \cdot v_1 \cdot v_2 + \lambda \cdot v_1 \cdot v_2 + \zeta^- \cdot v_1 \cdot v_2) \quad (5)$$

The impact of wind load on the control object (EPN) is considered.

A meteorological threat to the electric power supply process in the form of a strong wind is especially relevant in the following cases: in case of violation of the maximum allowable wire sag, with an increased maximum allowable distance between power transmission line towers, in the presence of vegetation under the wires. In these cases, a short circuit, breaks or burnout of power lines may occur.

Let's compose an algorithm of actions according to figure 2.

1-2. When analyzing the GIS data, it was recorded that in two days the wind speed is expected to increase above the permissible (48 hours).

2-3. The DM predicts a wire break in the N region (1 hour).

3-4. The monitoring of the state of structures to protect the wires of overhead lines from wind influences (vibration dampers) and their replacement in case of non-compliance with the requirements (8 hours) is carried out.

1-2-3-4. The object fulfilled its purpose (supplying consumers with electricity) (48 hours).

Thus, we get the following values: $I = 0,021$, $n_1 = 1$, $n_2 = 0,125$, $z^+ = 0,021$.

Let us substitute the predicted values into expression (5) and determine the indicator of the functioning efficiency of the integrated control system at various values of the frequency of the target process disruption (from disruption every hour to disruption once a day) (figure 3).

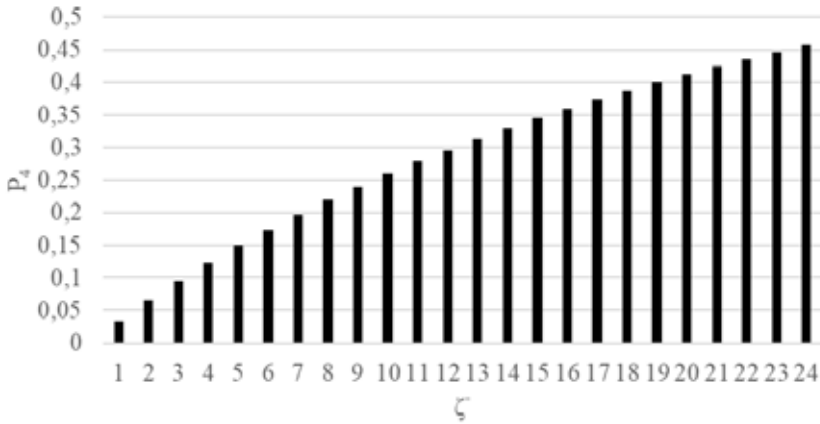


Figure 3. The dependence of the probability P_4 on the frequency z

4. Discussion

This study is devoted to an approach to integrating a GIS and a safety system for EPN for the sustainable operation of the object.

Achieving the goal of the activity (sustainable electric power supply to consumers) is possible only with an adequate management decision based on a mathematical model of the following type:

$$P = f(\lambda, v_1, v_2, \zeta^+, \zeta^-) \tag{6}$$

where P is an indicator of the effectiveness of the implementation of management decisions.

When the control object fulfills its purpose (supplying consumers with electricity), the following ratio must be met:

$$\frac{(\Delta t_{PI} + \Delta t_{PN})}{\Delta t_{PM}} < 1 \tag{7}$$

This study proposes an approach to managing a sustainable electric power supply in conditions of the destructive impact of meteorological factors.

5. Conclusion

The presented simulation of object safety management processes allows to guarantee reliable and safe electric power supply to consumers. Thus, one of the fundamental aspects of sustainable development has been realized.

6. Acknowledgments

The reported study was funded by RFBR, project number 20-38-90225.

References

1. Dertinger, A., & Hirth, L. (2020). Reforming the electric power industry in developing economies evidence on efficiency and electricity access outcomes. *Energy Policy*, 139 doi:10.1016/j.enpol.2020.111348.
2. Wang, M. -, Tsai, C. -, & Lin, W. -. (2021). Towards missing electric power data imputation for energy management systems. *Expert Systems with Applications*, 174 doi:10.1016/j.eswa.2021.114743.
3. Chapagain, K., Sato, T., & Kittipiyakul, S. (2017). Performance analysis of short-term electricity demand with meteorological parameters. Paper presented at the ECTI-CON 2017 - 2017 14th International Conference on Electrical Engineering/Electronics, Computer, Telecommunications and Information Technology, 330-333. doi:10.1109/ECTICon.2017.8096240.
4. Ferreira, T. S. D., Trindade, F. C. L., Pinto, Y. G., & Freitas, W. (2020). New analytical method for analysing the effectiveness of infrastructure reinforcement in electric power distribution systems. *Electric Power Systems Research*, 182 doi:10.1016/j.epsr.2020.106250.
5. Kong, X., Liu, C., Shen, Y., Hu, W., & Ma, T. (2020). Power supply reliability evaluation based on big data analysis for distribution networks considering uncertain factors. *Sustainable Cities and Society*, 63 doi:10.1016/j.scs.2020.102483.
6. Frantasov, D., & Kudryashova, Y. (2021). Information and measurement system for electric power losses accounting in railway transport. Paper presented at the *Transportation Research Procedia*, , 54 552-558. doi:10.1016/j.trpro.2021.02.107.
7. Ferreira, E. F., & Barros, J. D. (2018). Faults monitoring system in the electric power grid of medium voltage. Paper presented at the *Procedia Computer Science*, , 130 696-703. doi:10.1016/j.procs.2018.04.123.
8. Raspopov, D., & Belousov, P. (2020). Development of methods and algorithms for identification of a type of electric energy consumers using artificial intelligence and machine learning models for smart grid systems. Paper presented at the *Procedia Computer Science*, , 169 597-605. doi:10.1016/j.procs.2020.02.204.
9. Arcia-Garibaldi, G., Cruz-Romero, P., & Gómez-Expósito, A. (2018). Future power transmission: Visions, technologies and challenges. *Renewable and Sustainable Energy Reviews*, 94, 285-301. doi:10.1016/j.rser.2018.06.004.

10. Duisebekova, K. S., Kozhamzharova, D. K., Rakhmetulayeva, S. B., Umarov, F. A., & Aitimov, M. Z. (2020). Development of an information-analytical system for the analysis and monitoring of climatic and ecological changes in the environment. Paper presented at the Procedia Computer Science, , 170 578-583. doi:10.1016/j.procs.2020.03.128 .

11. García, C. (2019). From ecological indicators to ecological functioning: Integrative approaches to seize on ecological, climatic and socio-economic databases. *Ecological Indicators*, 107 doi:10.1016/j.ecolind.2019.105612.

12. Molina-Navarro, E., Segurado, P., Branco, P., Almeida, C., & Andersen, H. E. (2020). Predicting the ecological status of rivers and streams under different climatic and socioeconomic scenarios using bayesian belief networks. *Limnologica*, 80 doi:10.1016/j.limno.2019.125742.

13. Wu, X., & Hu, F. (2020). Analysis of ecological carrying capacity using a fuzzy comprehensive evaluation method. *Ecological Indicators*, 113 doi:10.1016/j.ecolind.2020.106243.

14. Sun, L., Su, Z., Tian, M., Xing, D., & Pan, C. (2020). Power flow calculation method of traction network considering geographical and climatic conditions. *Energy Reports*, 6, 228-235. doi:10.1016/j.egyr.2020.11.256.

15. Fikke, S., Nygaard, B. E., & Hawes, H. (2013). Potential effects from global climate change on overhead electric power transmission networks. Paper presented at the 2013 CIGRE Auckland Symposium, 2013-September.

16. Fant, C., Boehlert, B., Strzepek, K., Larsen, P., White, A., Gulati, S., . . . Martinich, J. (2020). Climate change impacts and costs to U.S. electricity transmission and distribution infrastructure. *Energy*, 195 doi:10.1016/j.energy.2020.116899.

17. Zeynalian, M., & Khorasgani, M. Z. (2018). Structural performance of concrete poles used in electric power distribution network. *Archives of Civil and Mechanical Engineering*, 18(3), 863-876. doi:10.1016/j.acme.2018.01.005.

18. Farshchian, G., Darestani, S. A., & Hamidi, N. (2020). Developing a decision-making dashboard for power losses attributes of iran's electricity distribution network. *Energy*, doi:10.1016/j.energy.2020.119248.

19. Ismail, A. G., El-Dabah, M. A., & Nassar, I. A. (2020). Enhancement of electrical distribution networks performance using the load management methodology. *Energy Reports*, 6, 2066-2074. doi:10.1016/j.egyr.2020.07.018

20. Usypko, A., & Uljanov, A. (2020). Improvement of the methodology for calculating damage from possible radiation accidents applicable in energy engineering. Paper presented at the E3S Web of Conferences, , 221 doi:10.1051/e3sconf/202022103003.

21. Zhang, J., Huang, G., Liu, L., Zhai, M., Xie, Y., Xin, X., & Meng, H. (2021). Economic sensitivity analysis of dual perspectives induced by energy scarcity for energy-dependent region. *Science of the Total Environment*, 768 doi:10.1016/j.scitotenv.2020.144876.

22. Kulikov, A., Ivanova, I., Russkova, I., & Veber, J. (2019). The criteria for evaluation of efficiency of heat technical installations considering general energy costs with the aim of increasing their environmental friendliness and reducing negative effect on the environment. Paper presented at the E3S Web of Conferences, , 140 doi:10.1051/e3sconf/201914008010.

23. Burlov, V. (2020). Mathematical model of human decision: A methodological basis for the functioning of the artificial intelligence system. Paper presented at the Proceedings of the European Conference on the Impact of Artificial Intelligence and Robotics, ECIAIR 2020, 38-48. doi:10.34190/EAIR.20.050.

24. Burlov, V., & Grachev, M. (2020). Mathematical model of management decision making that takes into account the technical and human factors. Paper presented at the CEUR Workshop Proceedings, , 2711 597-606.

25. Burlov, V., Uzun, O., Grachev, M., Faustov, S., & Sipovich, D. (2021). Web-based power management and use model doi:10.1007/978-3-030-57450-5_54.

THE STATE OF THE EXISTING CALCULATION METHODS AND THE FACTORS AFFECTING THE STRENGTH OF BENT REINFORCED CONCRETE ELEMENTS ALONG INCLINED SECTIONS

Starishko Ivan Nikolaevich

Candidate of Technical Sciences, Associate Professor
Vologda State University
Vologda, Russia

Almost every theory for calculating the strength of bent reinforced concrete elements along inclined sections, which was developed and laid down in the regulatory documents of many countries, does not in all cases give results that closely match with the experimental results. One of the reasons for this may be the narrow focus of many experimental researches, the results of which are taken for guidance in the development of the theory of calculation. Sometimes the proposed calculation theory is not at all substantiated by experimental research.

The experimental research methodology will give a positive effect for the development of a reliable theory for calculating bent reinforced concrete elements along inclined sections only when it includes the whole complex of a variety of influence of the main factors on the operation of the investigated elements, including the type of loads applied during the test (evenly distributed or focused) with deep analysis of the results obtained.

Keywords: bent elements, load bearing capacity, experimental research, inclined sections, stress-strain state, calculation method.

Introduction

In bent prestressed reinforced concrete elements, as well as in elements without prestressing, due to an insufficient number of experimental researches, the stress-strain state of concrete in a tensioned and compressed section zone, transverse and longitudinal steel reinforcement in the stages of inclined cracks formation, their development and destruction has been little researched, therefore, the existing calculation methods, as a rule, are not sufficiently substantiated. For example, in Russia, on the basis of tests of bent reinforced concrete T-profile beams, in

which the influence of the overhangs of compressed flanges on the bearing capacity along inclined sections was not significant, or is completely absent, in the regulatory documents from the calculations the specified effect of overhangs was removed, which in the previous regulatory documents SNiP 2.03.01-84 in beams with transverse reinforcement was taken into account. The reason for this turned out to be the narrow focus of experimental researches, which were carried out in recent years at small sizes of the shear span $C=(1.5\div 2) h_0$ and large sizes of the rib thickness of T-profile beams with thin and wide overhangs of compressed flanges. In such experimental researches, the effect of overhangs of compressed flanges on the bearing capacity along inclined sections is really not significant, which can be neglected.

However, on the basis of numerous experimental researches of the author of the article on the effect of overhangs of compressed shelves on the bearing capacity of bent reinforced concrete elements along inclined sections, it was found that with an increase in the length of the shear span, the influence of overhangs of compressed shelves on the bearing capacity along inclined sections increases, despite the fact that in general, with an increase in the length of the shear span, the bearing capacity of the bent elements decreases. And when, with an increase in the length of the shear span, the beam becomes equally strong in normal and inclined sections, the effect of overhangs of compressed flanges, when calculating the bearing capacity of a beam along inclined sections, should coincide with the effect of overhangs when calculating its bearing capacity along normal sections.

In the method for calculating a bent reinforced concrete beam along normal sections, laid down in [1], the effect of overhangs of compressed shelves on their bearing capacity is taken into account, but in the method for calculating the same beam along inclined sections, the influence of overhangs is not taken into account at all, for some unknown reason (beam is of equal strength along normal and inclined sections, and the compressed zone of concrete collapses simultaneously over normal and inclined cracks). In the above regulatory documents [1], the effect of prestressing of longitudinal steel reinforcement on the strength along inclined sections of bent reinforced concrete elements and other factors, as a result of which, in some cases, there are large discrepancies between the calculated and experimental data, is not sufficiently substantiated by experimental researches.

The influence of the forces of engagement of the rough surface of the banks in a critical inclined crack, as a rule, with a curved bulge towards

the upper edge of the beam, as well as the influence of the nagel effect in the longitudinal steel reinforcement crossed by an inclined crack, is not taken into account at all, while the significant influence of these factors has been experimentally established.

In addition, in the experimental researches of a number of authors, experimental beams were made using ineffective prestressing steel reinforcement made of steel of grade A-III, which often, even with an insignificant prestressing value, led to the destruction of beams along normal sections.

Main part

From 1973 to the present, first at NIIZhB (Moscow), then working at the Vologda State Technical University, the author of the article conducted extensive experimental research, in which more than 500 bent and eccentrically compressed reinforced concrete elements were tested. 24 experimental prestressed reinforced concrete beams, including six beams without prestressing longitudinal reinforcement were tested at NIIZhB. The tension of the lower and upper longitudinal steel reinforcement was carried out on a stand consisting of three lines (Fig. 1). The strain gauges glued to the longitudinal steel reinforcement from two diametrically opposite sides before its tension, as well as to the transverse steel reinforcement, were carefully protected from their damage during concrete placement, and the wires from the strain gauges were released outside the beams (see Fig. 1). Researching the operation of longitudinal steel reinforcement in the section between the support and the line of action of the load using strain gauges glued on two diametrically opposite sides of this steel reinforcement makes it possible to obtain deformation diagrams of the upper and lower fibers of the bar. In this case, it will be possible to establish the presence of a nagel effect in the steel reinforcement at the intersection of its incline crack. The manufacture of beams with longitudinal prestressing steel reinforcement having different fixing at the ends - with and without anchors - makes it possible to reveal the effect of anchoring of longitudinal steel reinforcement on their bearing capacity along inclined sections. Each series of test samples, consisting of 6 beams, was manufactured on a separate line of the stand, which made it possible for all samples of the series to have the same prestressing value of the steel reinforcement. At the same time, given the same concrete strength in all beams included in the series, it is possible to more accurately identify the influence of the main factors on the strength of inclined sections. The reinforcement was tensioned by a hydraulic jack using a pumping station (Fig. 2). The connection of individual rods of longitudinal steel rein-

forcement along the length of the stand was carried out using couplings and pressed heads at the ends of the longitudinal steel reinforcement (threaded connection), since welding of steel of grades AT- V and AT- VI according to technical conditions is not recommended. On each half of the beams, the step of the transverse steel reinforcement was taken to be different. This transverse reinforcement was adopted in order to obtain as much experimental data as possible with the successive destruction of each half-span. At the same time, after the destruction of the half-span with a smaller amount of transverse steel reinforcement, a bandage was installed on it and another half-span with a large amount of transverse steel reinforcement was brought to destruction.



Fig. 1. General view of prestressed reinforced concrete beams located on the stand and beams without prestressing located outside the stand (see on the right of the stand)



Fig. 2. Tensioning device for longitudinal steel reinforcement located on the stand in the manufacture of prestressed reinforced concrete beams

To research the processes of development and redistribution of deformations in concrete and steel reinforcement when testing only the above 24 beams, about 3 thousand strain gauges and a large number of electronic measuring and mechanical parting were used (Fig. 3). The beams were tested on a jack installation by two forces symmetrically located relative to the middle of the span (see Fig. 3). Dial indicators were installed along the ends of the beams to assess the possible slippage of the longitudinal steel reinforcement under the action of a load, after the formation of inclined cracks near the support.

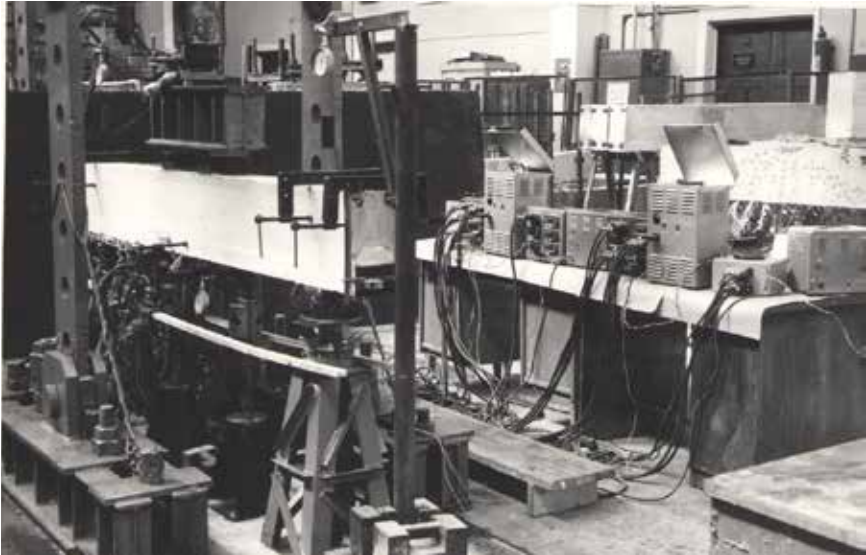
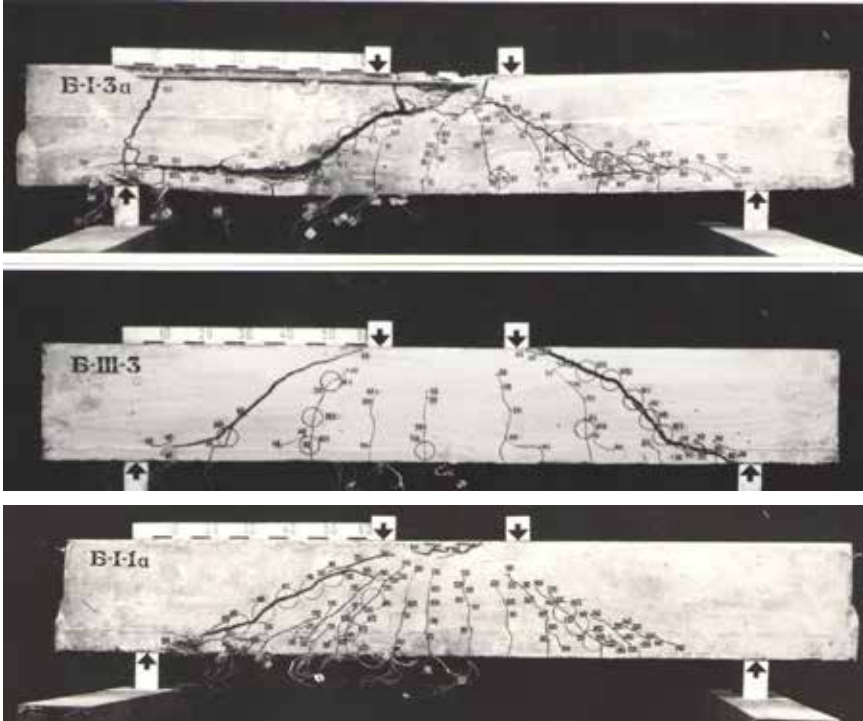


Fig. 3. Instruments and equipment used in the process of testing beams

The experiments of the author of the article, conducted at NIIZhB (1973-1976) showed that in rectangular beams with a relative rib thickness in the cross section $b/h = 15/30=0.5$ with an increase in the prestressing of the longitudinal steel reinforcement, the trajectory of the main compressive stresses in the bearing areas changes. Accordingly, the height of the compressed concrete zone above an inclined crack in prestressed beams, in their limiting state, turns out to be greater in comparison with similar beams without prestressing (Fig. 4). This factor is especially evident in bent prestressed reinforced concrete elements without transverse steel reinforcement ($\mu_{sw}=0$), where, due to the effect of prestressing of longitudinal steel reinforcement, the bearing capacity of prestressed beams exceeds the bearing capacity of similar beams without prestressing up to 2.7 times (see Fig. 4 - prestressed beam Б-I-3a, in comparison with a similar beam without prestressing Б-III-3). With an increase in the amount of transverse steel reinforcement to $\mu_{sw}=0.36\%$ the effect of prestressing of longitudinal steel reinforcement (concrete compression forces N_c) on the bearing capacity of beams along inclined sections, in comparison with similar beams without prestressing, increases slightly to 1.27 times (see fig. 4 - prestressed beam Б-I-1a in comparison with beam Б-III-1). With

a further increase in the amount of transverse steel reinforcement, the indicated difference in the effect of transverse steel reinforcement on the strength of inclined sections of normal and prestressed bent reinforced concrete elements continues to decrease.

In experimental researches of the author of the article, it was also found that in rectangular beams without prestressing longitudinal steel reinforcement with a ratio of cross-sectional dimensions $b/h=0.5$, with a change in the amount of transverse steel reinforcement from $\mu_{sw}=0\%$ to $\mu_{sw}=0.76\%$, the bearing capacity along inclined sections increased quite significantly - 2.8 times (see Fig. 4 - beam Б-III-3 (left half-span) without prestressing and without transverse steel reinforcement in comparison with beam БIII-1 (right half-span) with the amount of transverse steel reinforcement $\mu_{sw}=0.76\%$). At the same time, it was found for the first time that the change in the transverse reinforcement within the same limits, i.e. from 0 to 0.76%, in similar prestressed rectangular beams, the bearing capacity along inclined sections slightly increased - only up to 15% (see fig. 4 - beams Б-I-1a and Б-I-3a).



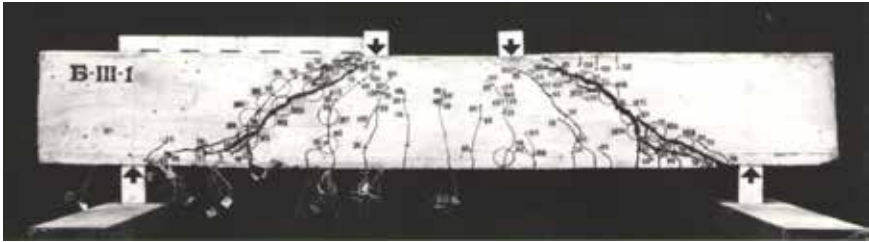


Fig.4 Influence of prestressing and the amount of transverse steel reinforcement on the bearing capacity of bent reinforced concrete beams along inclined sections

It was also found that in prestressed rectangular beams with a ratio of $b/h = 0.5$, the boundary value of the transverse reinforcement should be conventionally considered $\mu_{sw} = 0.3\%$, since with a further increase in the transverse reinforcement, the bearing capacity of the beams along inclined sections practically did not increase. In rectangular beams without prestressing the lower longitudinal steel reinforcement with a ratio of cross-sectional dimensions $b/h = 0.5$ transverse steel reinforcement works most efficiently when it is present within the range of up to 0.4% . With a further increase in the amount of transverse steel reinforcement, the intensity of the increase in the bearing capacity of beams along inclined sections decreases.

Experiments have shown that with an increase in prestressing in the lower longitudinal steel reinforcement of bent reinforced concrete elements, the intensity of stresses in transverse steel reinforcement under the action of a load decreases significantly. The most significant decrease in stresses in transverse steel reinforcement at the time of destruction of bent reinforced concrete elements along inclined sections, due to the effect of prestressing in the lower longitudinal steel reinforcement, occurs with an increase in the width of their cross section.

One of the reasons for this factor is also the following. During the tests conducted by the author of the article, as well as A.S. Zalesov and O.F. Ilyin at the Moscow Experimental Plant of Reinforced Concrete Products (1974) it turned out that in hollow-core bent pre-stressed reinforced concrete slabs used for coatings and ceilings in residential and civil buildings (which have a large width in cross-sections), due to the influence of preliminary stresses of the lower longitudinal steel reinforcement, transverse steel reinforcement increased their bearing capacity along inclined sections insignificantly. At the same time, it even turned out that some

previously manufactured hollow-core standard slabs without prestressing the lower longitudinal steel reinforcement, with the presence of design transverse steel reinforcement located in the longitudinal ribs, had approximately the same bearing capacity along inclined sections as similar prestressed slabs without transverse steel reinforcement. Therefore, by the decision of the USSR State Construction Committee, the above-mentioned typical hollow-core reinforced concrete floor slabs (especially with a length of 6 m and more) began to be made only prestressed, where transverse steel reinforcement, as a rule, is installed only on the supporting sections according to design requirements.

The influence of the sizes of the overhangs of compressed flanges on the bearing capacity of bent reinforced concrete beams along inclined sections [2 and 3], researched at the Vologda Technical University, is expressed through the ratio of the bearing capacity of T-profile beams to the bearing capacity of similar rectangular beams. Experimental researches have shown that in bent reinforced concrete T-profile beams without prestressing longitudinal steel reinforcement, as well as in prestressed beams, the effect of the sizes of the overhangs of compressed flanges on their bearing capacity along inclined sections depends on many factors, including: on the amount of transverse steel reinforcement and the length of the shear span (Table 1), on the thickness of the rib in the cross section of the beams and other factors.

Table 1.
Influence of overhangs of compressed flanges on the bearing capacity of bent reinforced concrete beams along inclined sections (vertically), depending on the size of the cut span and the percentage of transverse reinforcement (horizontally)

Number of cross-sectional diagrams of beams	Cross-section diagrams of beams	The ratio of the bearing capacity of T-profile beams according to schemes 2,3,4 ($Q_{\text{c.crem},n}^{\text{on}}$) to the bearing capacity of rectangular profile beams according to scheme 1 ($Q_{\text{c.crem},1}^{\text{on}}$)													
		Distance from the support to the line of action of the load (shear span)					Number of transverse steel reinforcement μ_{sw} (%)								
		$C = 1,5h_0$					$C = 3h_0$								
					$C = 4h_0$										
0	0,167	0,25	0,5	0	0,167	0,25	0,5	0	0,167	0,25	0,5	0	0,167	0,25	0,5
1	167,5	182,5	207,5	50	70	97,5*	125	45	70	75*	102,5*		70	75*	102,5*
2	$\frac{180}{167,5} = 1,07$	$\frac{212}{207,5} = 1,02$			$\frac{110}{70} = 1,57$		$\frac{147,5}{125} = 1,18$			$\frac{90}{70} = 1,29$	$\frac{102}{75*} = 1,36$			$\frac{150}{102,5*} = 1,47$	
3	$\frac{140}{167,5} = 0,84$	$\frac{182,5}{182,5} = 1,0$	$\frac{227}{207,5} = 1,09$		$\frac{97,5}{70} = 1,39$	$\frac{127,5}{97,5*} = 1,31$	$\frac{163}{125} = 1,30$			$\frac{80}{70} = 1,14$	$\frac{112,5}{75*} = 1,5$			$\frac{150}{102,5*} = 1,47$	
4	$\frac{187,5}{167,5} = 1,12$	$\frac{205}{182,5} = 1,12$	$\frac{220}{207,5} = 1,06$		$\frac{120}{70} = 1,71$		$\frac{180}{125} = 1,44$			$\frac{108,5}{70} = 1,55$	$\frac{127,5}{75*} = 1,7$			$\frac{155*}{102,5*} = 1,51$	

Notes: 1) the numbers marked with (*) indicate that the beam collapsed along normal sections; 2) values of shear forces are given in kN

According to Table 1, it can be seen that the smallest influence of the overhangs of compressed flanges on the bearing capacity along inclined sections occurs in T-profile beams with small shear spans ($c=1,5h_0$).

At the same time, in some T-profile beams with wide overhangs of compressed shelves ($bcb/h'f=20\text{cm}/5\text{cm}=4$) with small shear spans ($c=1,5h_0$ and $c=2h_0$ – which is absent in this article due to a reduction in the volume of the table .2), as well as with a small amount of transverse steel reinforcement ($\mu_{sw}=0,167\%$) the bearing capacity along inclined sections turned out to be less than the bearing capacity of similar rectangular beams (see Table 1 - cross-sectional diagram 3).

In T-profile beams, with an increase in the shear span c , their total bearing capacity decreased along inclined sections, however, the effect of the overhangs of compressed flanges on the bearing capacity of these beams significantly increases (see Table 1, cross-sectional diagrams 2, 3 and 4).

It has also been experimentally established that in T-profile beams, under the action of a load, the effect of the shear span on the bearing capacity along inclined sections is significantly less compared to similar rectangular beams. This is the most important factor when choosing the structures of span structures of bridges and other structures subjected to constant effects of moving loads with different values of the shear span.

With an increase in the thickness of the overhangs of compressed flanges with their constant width, the bearing capacity of the beams along inclined sections increases.

The use of transverse steel reinforcement in rectangular and T-profile beams is one of the main characteristics that affect the strength of bent reinforced concrete elements along inclined sections. On the basis of experimental researches, it was found that in rectangular beams with a small rib thickness in the cross section ($b=0,19h$), in the absence of prestressing in longitudinal steel reinforcement, transverse steel reinforcement with a large amount of it ($\mu_{sw}=1,3\%$ и $\mu_{sw}=1,9\%$) increased the bearing capacity along inclined sections by 1.47 and 1.52 times, respectively. This is less than in rectangular beams with a large rib width in the cross section $b=0,5h$, where a smaller amount of transverse steel reinforcement ($\mu_{sw}=0,76\%$) increased the bearing capacity of the beams along inclined sections much more - 2.8 times. In T-profile beams with the width of the overhangs of compressed flanges ($\mu_{sw}=1,3\%$ и $\mu_{sw}=1,9\%$) $bcb=2,58h'f$ and $bcb=5,52h'f$ as well as a small rib thickness in the cross section ($b=0,19h$), with in the absence of prestressing in longitudinal steel reinforcement, transverse steel reinforcement, at ($\mu_{sw}=1,3\%$ и

$\mu_{sw} = 1,9 \%$), increased the bearing capacity along inclined sections by 2 - 2.58 times, which is significantly greater than the effect of transverse steel reinforcement in similar rectangular beams profile with the same small rib thickness (see above).

In similar bent reinforced concrete T-profile beams with thin ribs in the cross section ($b = 0,19h$), in the presence of prestressing in the longitudinal steel reinforcement, the transverse steel reinforcement also significantly increases their bearing capacity along inclined sections - by 1.68 - 2.49 times. So, with an increase in the rib thickness in the cross section of prestressed reinforced concrete T-profile beams, the effect of transverse steel reinforcement on the bearing capacity along inclined sections decreases. In turn, in beams without prestressing the longitudinal steel reinforcement, the opposite effect occurs, where with an increase in the rib thickness in the cross section, the effect of transverse steel reinforcement on the bearing capacity along inclined sections increases.

Conclusion

1. On the basis of experimental researches, it has been established that the greatest effect of the shear span length (that is, the bending moment), which reduces the bearing capacity of bent reinforced concrete elements along inclined sections, occurs in rectangular beams without transverse steel reinforcement or with a small amount of it ($\mu_{sw} = 0,167\%$).

2. An increase in the amount of transverse steel reinforcement more intensively reduces the effect of the shear span on the bearing capacity of bent reinforced concrete elements along inclined sections in rectangular beams in comparison with similar T-beams.

3. Since in bent reinforced concrete T-profile beams, due to the work of the overhangs of compressed flanges, the influence of the shear span (i.e. bending moments) on the bearing capacity along inclined sections is much less compared to rectangular beams, the effectiveness of the use of T-profile beams turns out to be higher in comparison with rectangular beams. This is especially true of bridge beams, crane beams of industrial buildings and other structures that receive loads with constantly changing values of the shear span.

4. As the results of experiments have shown, in bent reinforced concrete T-profile beams with transverse steel reinforcement at shear spans with $c = 3h$ overhangs of compressed flanges with a small rib width ($b=0,19h$) are more intensively involved in the work on the perception of the action of transverse forces compared to beams with a large rib width ($b=0,3 h$). So, the overhangs of compressed flanges with a small rib width in the cross section and large shear spans increase the bearing capacity

of T-profile beams along inclined sections by 2.02 times, which is much higher compared to T-profile beams with a large rib width, where the overhangs of compressed flanges increase their bearing capacity along inclined sections is 1.5 times (sometimes up to 1.7 times).

References

1. SP 63.13330.2012. Concrete and reinforced concrete structures. General provisions SNIP 52-01-2003.
2. Starishko I.N. Results of experimental studies of the influence of the main factors on the bearing capacity across a sloping section in bending concrete beams of rectangular and t-section. Vestnik MGSU. 2016. p.8-18.
3. Starishko Ivan Nikolaevich. Influence of the main factors on the bearing capacity of bent reinforced concrete elements in inclined sections obtained on the basis of experimental studies. Process management and scientific developments. Birmingham, United Kingdom. January 13, 2021. p.140-150.

DOI 10.34660/INF.2021.24.13.007

RESEARCH AND ANALYSIS OF HYGIENIC REGULATION ON OCCUPATIONAL NOISE

Salkutsan Vladimir Ivanovich

Candidate of Technical Sciences, Associate Professor
Graduate School of Technosphere Safety
Peter the Great St. Petersburg Polytechnic University
St. Petersburg, Russia

Novikova Alexandra Vasilienna

Peter the Great St. Petersburg Polytechnic University
St. Petersburg, Russia

This paper sets out the definition of hygienic regulation of industrial noise in Russia and some countries of the world. Based on the analysis of regulatory legal acts, recommendations on hygienic regulation and other literary sources, a comparison of hygienic standards for industrial noise in Russia and in a number of countries of the world was carried out. The calculation of the recommended number of years of the maximum allowable work experience was made in accordance with the current hygienic standards of Russia for industrial noise. Conclusions are made about a significant difference between the current hygienic standards in Russia and some other countries of the world, affecting the duration of safe work experience in hazardous working conditions. Some reasons for the discrepancy in the values of hygienic standards are indicated, and a number of areas of work to improve working conditions with the presence of an increased level of industrial noise are announced.

Keywords: Hygienic rationing, comparative analysis, hygienic standards, industrial noise, maximum allowable work experience in conditions of exceeding hygienic standards.

Introduction

The presence of abnormal exposure to factors of the working environment in the workplace is one of the many aspects of everyday life that negatively affect human health. Some environmental features at this stage of our planet's existence are already difficult to control, but the negative

impact of factors of the working environment at workplaces (WP) can be neutralized. Millions of people around the world are exposed to potentially hazardous noise levels. In addition, the peculiarities of working conditions in WP often make a significant contribution to the overall noise level, which affects a person. In view of this, there is a global urgent need for legislation to provide adequate protection for workers' health.

Legislation on the regulation of factors of the working environment and the protection of workers from their negative impact has been adopted in many countries with varying degrees of completeness and varying degrees of complexity.

It is noteworthy that according to the National Occupational Research Agenda of July 2019, in the long term, the costs of society for the treatment of occupational diseases and benefits for disability in connection, for example, with hearing loss due to occupational noise, will many times exceed the amount of funds required to spend on the stage of enforcement of the relevant legislation. [1]

Thus, we can say that the chosen topic is relevant for study.

The purpose of the work is to carry out a comparative analysis of the hygienic standards of industrial noise in Russia and a number of other countries.

The object of the research is the peculiarities of national hygienic regulation in the countries of the European Union, the USA, Russia, China and India. The subject of the research is the hygienic regulation of industrial noise.

Methods

The problem of the negative impact of noise on human health is not new. Over the past few decades, a large number of studies have been published on occupational hearing loss [2], on the effect of noise at work on the human cardiovascular system [3], on increasing the risk of accidents at work [4].

Hearing loss caused by exposure to noise is influenced by many factors, such as:

- sound pressure level;
- spectral characteristics;
- duration of exposure;
- the nature of the temporary impact (constant, intermittent or impulse noise).

The main parameters used in normalizing industrial noise are the frequency spectrum, sound pressure level, and time characteristics.

An analysis of the legislative and regulatory acts (RA) of some coun-

tries has led to the conclusion that the degree of development of industrial noise regulation varies significantly from country to country. Often laws and standards are contained in a single document covering all occupational health and safety to varying degrees.

In 1979, the International Labor Organization's Convention No. 148 "On the Protection of Workers from Occupational Risk Caused by Air Pollution, Noise and Vibration in the Workplace" was adopted.[5]

24 articles of the document established the fundamentals of legislation, including the established limit values of the impact of production factors and measures for the implementation of protection against their negative impact. The ratification of this convention has led to the emergence of similar RAs in many countries, with or without amendments.

The maximum permissible level (MPL) of industrial noise in the countries of the European Union is indicated in the Directive 2003/10/EC of 06.02.2003 and complies with the ISO 1999: 2013 standard "Acoustics - Assessment of hearing loss due to exposure to noise".

According to the European directive, three normative noise levels are determined, in particular:

- The maximum permissible level is 87 dBA.
- The upper threshold level is 85 dBA.
- The lower threshold level is 80 dBA. [6]

In Russia, noise rationing from March 1, 2021 is carried out in accordance with SanPiN 1.2.3685-21 "Hygienic standards and requirements for ensuring the safety and (or) harmlessness of environmental factors for humans." The document contains the normative noise values, without taking into account the category of severity and intensity of work. For example, for employees in the field of administrative and management activities, the maximum permissible equivalent sound level is 80 dBA, and for lecturers and teachers, the penetrating noise should not exceed 40 dBA. [7]

Results

Based on the analysis of foreign RA, in which the maximum permissible values of the noise level and some features of its regulation are indicated, a summary table 1 was compiled, which compares the hygienic standards for industrial noise by their maximum values.

Table1.
Comparison of hygienic standards for industrial noise

Country Parameter	Russia	EU	USA	China	India
<i>Maximum sound pressure level</i>	135 dBA (in any octave band)	140 dB-peak	115 dB (A) 140 dB-peak	115 dB (A) 135 dBA	115 dB (A) 140 dB-peak
<i>Equivalent sound level, MPL</i>	80 dBA	Germany - 75dBA Netherlands - 80 dBA France - 85 dBA, Directive 2003/10/EC - 87 dBA Spain - 85 dBA (correction - 3 dBA),	90 dBA (correction 5dBA)	90 dBA	90 dBA

Currently, for the hygienic assessment of noise, in accordance with SanPiN 1.2.3685-21, we use an equivalent (in energy) sound level - however, the existing methods of measuring it are either not accurate enough or laborious.

Individual dosimetry is a promising correct method for measuring noise. However, it, in turn, does not take into account the temporal characteristics of non-constant (especially impulse) noise, which can determine the characteristics of an adverse action.

From a physical point of view, the equivalent level and dose are analogs, and their mutual recalculation is possible, however, in physiological and hygienic terms, these two parameters differ fundamentally: the equivalent level is determined on a logarithmic scale in decibels from the threshold of perception, and the dose - in fractions of the permissible dose, which is the threshold of harmful effects, and is estimated in linear values. The equivalent level reflects the average noise value per shift, and the dose characterizes the total noise energy per shift. The dose makes it possible to more adequately assess the actual noise load on workers in order to predict the degree of adverse effects of noise and assess the effectiveness of preventive measures to limit it.

There is a methodology [8] that allows you to calculate the values of

the maximum permissible length of service when a person is exposed to industrial noise. The proposed calculation method is based on the principle of dose assessment of noise.[9]

According to the methodology, the number of years that a person employed in working conditions in which industrial noise is observed was estimated, taking into account the use of personal protective equipment (PPE) during work.

The industrial noise MPLs selected for the assessment comply with the hygienic standards in Russia, the EU, the USA, the PRC and India. The calculation results are presented in table 2.

Table 2.
Calculation of the recommended length of service depending on the value of MPL noise by country

Country	MPL value	Calculated experience	
		without PPE	with PPE
<i>Russia</i>	80 dBA	25 years	25 years
<i>EU</i>	87 dBA	19.3 years	25 years
<i>USA</i>	85 dBA	20 years	25 years
	90 dBA	8 years	25 years
	95 dBA	2 years	24.7 years
<i>China</i>	85 dBA	20 years	25 years
	90 dBA	8 years	25 years
<i>India</i>	90 dBA	8 years	25 years

The values of the calculated recommended experience when working in conditions where the noise level of 80 dB is exceeded - even by 5 dB as part of the correction (USA, China), and without the use of PPE - significantly reduces the number of years that a person working in such conditions can work out. At the same time, in the study of the etiology of occupational hearing loss, the fixed work experience is taken equal to from 10 to 14 years.

So, in order to increase the estimated length of service in such conditions, it is necessary to increase the number and duration of regulated breaks, to carry out annual free medical examinations, to ensure the availability of hearing protection, and also to evaluate the effectiveness of the current safety regulations at enterprises.

Virtually all international regulations regarding noise levels in the work-

place set an upper limit for the equivalent noise level in the range of 85-90 dBA for an eight-hour work shift. This boundary is established based on the recommendations of the ISO 1999: 2013 standard. Developing countries have traditionally copied laws and regulations from developed countries without significant adaptation to local conditions.

This is especially evident in India. Industrialization in India is primarily focused on manufacturing, while health and safety is a very low priority. With the exception of a few large public and private industries, most other industrialists are quite indifferent to providing acceptable working conditions and lag far behind in ensuring worker safety. [10]

At the same time, in India, as well as in China, there is still a problem with the work schedule and shifts of industrial workers. In these countries, it is normal for workers to work extra overtime of 12-24 hours a week, and the working day lasts 10-12 hours six times a week. [11]

In India, the Factories Act of 1948 sets the MPL of industrial noise at 90 dBA, but the same law also sets a limit of 46 working hours per week, which is 6 hours more than the 40 hours per week limit in Russia, the United States and European countries. (at the same time, according to surveys among workers, the overwhelming majority work 2-4 hours a day [12], that is, 12-24 hours a week, and the working week in this case is 60-72 hours). As a result, the total impact of occupational noise on workers in India is many times greater than the permissible in developed countries.

In the United States, OSHA 1910.95 sets the MPL for noise exposure to WP based on worker weighted averages over an eight hour shift. OSHA 1910.95 has a noise limit of 90 dBA for each person working eight hours a day. This level is set taking into account the correction value of 5 dBA. However, the National Institute for Occupational Safety and Health (NIOSH) reports that significant hearing loss is possible under OSHA's MPL of 1910.95. NIOSH recommends limiting the equivalent noise level for a worker on an eight-hour shift to 85 dBA, corrected by 3dBA, with each 3 dBA exceeding the level, the duration of exposure should be halved. [12]

Work in industrial enterprises plays a colossal role in people's lives, since most workers in the Republic of Moldova spend at least eight hours a day at WP. Therefore, working conditions should be as safe as possible for health.

It is worth noting that according to Trading Economics [13], as of December 2020, the unemployment rate in the US is 6.3%, in China 5.2%, in the EU countries 8.3%, in Russia 5.8%, in India 6. five%. In all countries considered in the work, the unemployment rate is now on a downward

trend, but the current levels are still much higher than those before the sharp deterioration of the sanitary and epidemiological situation in the world in early 2020.

Under the current scenario of unemployment, the majority of the employed population has a fear of losing their jobs, including those who are employed in noisy industries. Therefore, they are ready to work even in harmful working conditions.

It should also be understood that in real conditions in a rare production, an employee will be exposed to only one harmful production factor. Therefore, to ensure proper working conditions, one should always take into account the existence of a combined multifactorial effect of harmful factors of the working environment in the WP.

Conclusion

Depending on many factors, the RAs of some countries take into account all the necessary aspects of industrial noise regulation, while others offer only minimal protection against the negative impact of this industrial factor. The presence of current hygienic standards in the country, as well as the development and continuous improvement of sanitary and hygienic, preventive measures aimed at eliminating or suppressing the negative impact of industrial noise, directly affects the health of that part of society that is employed in noisy industries.

It should be noted that, unfortunately, there are no criteria for reaching a consensus on the issue of general unification of hygiene standards in the field of exposure of workers to industrial noise. The main reason for this is the difference between countries in the degree of their economic development. And while for many countries the most important task is to increase production capacities, employees of enterprises continue to lose their health.

References

1. Murphy W.J. National occupational research agenda for hearing loss prevention. / Murphy W.J., Metetic R.J., Masterson E.A. // National occupational research agenda (NORA) – 2019. // [Electronic resource]. – Access. – URL: https://www.cdc.gov/nora/councils/hlp/pdfs/National_Occupational_Research_Agenda_for_HLP_July_2019-508.pdf (Appeal date: 27.12.2020).
2. Al-Arja O.A. Assessment of occupational noise exposure in coffee grinding shops / Al-Arja O.A., Awadallah T.S. // Applied Acoustics. – 2020. Vol. 158. [Electronic resource]. – Access. – URL: <https://www.sciencedirect.com/science/article/pii/S0003682X19304001> (Appeal date: 27.12.2020).

3. Choochouy N. Hearing Loss in Agricultural Workers Exposed to Pesticides and Noise. / Choochouy N., Kongtip P., Chantanakul S., Nankongnab N., Sujirarat D., Woskie S.R. // *Annals of work exposures and health*. – 2019. Vol. 63, P. 707-718.

4. Toppila E. Evaluation of the increased accident risk from workplace noise. / Toppila E, Pyykkö I, Pääkkönen R. // *Int. J. Occupat. Saf. Ergonom.* – 2009. Vol. 15, P. 155-162.

5. Convention of the International Labor Organization No. 148 on the protection of workers from occupational hazards caused by air pollution, noise and vibration in the workplace. Geneva, 11 July 1979

6. Directive 2003/10/EC of the European Parliament and of the Council of 06 February 2003 on the minimum health and safety requirements regarding the exposure of workers to the risks arising from physical agents (noise) (Seventeenth individual Directive within the meaning of Article 16(1) of Directive 89/391/EEC).

7. Hygienic standards and requirements for ensuring the safety and (or) harmlessness to humans of environmental factors [Electronic resource]: SanPiN 1.2.3685-21; approved Resolution of the Chief State Sanitary Doctor of the Russian Federation dated January 28, 2021, № 2 // Reference and legal system "Garant".

8. Salkutsan, V. Methods for assessing safe seniority in high noise conditions. / V. Salkutsan, I. Russkova, S Faustov. // *Conference Series: Materials Science and Engineering*. – 2019. Vol. 666.

9. Guidelines for the dose assessment of industrial noise [Electronic resource]: Developed by the Order of the Red Banner of Labor Research Institute of Occupational Hygiene and Occupational Diseases of the USSR Academy of Medical Sciences. Approved. Deputy Chief State Sanitary Doctor of the USSR from 29.07.1982, № 2908-82 // Professional reference system "Techexpert".

10. Ramachandran. Occupational Health and Safety in India: The Need for Reform. / Ramachandran, Gurumurthy, and Panneer Sigamani // *Economic and Political Weekly*. - 2014. Vol. 49, P. 26–28. [Electronic resource]. – Access: www.jstor.org/stable/24481023. (Appeal date: 28.02.2021).

11. Singh L. Occupational Health and Safety in Work Study and Ergonomics // Cambridge: Cambridge University Press. – 2015. P. 332-353.

12. Centers for Disease Control and Prevention (CDC). [Electronic resource]. – Access: <https://blogs.cdc.gov/niosh-science-blog/category/hearing-loss/>. (Appeal date: 22.03.2021)

13. Trading Economics: [Electronic resource]. – Access: <https://tradingeconomics.com/> (Appeal date: 28.02.2021)

DOI 10.34660/INF.2021.25.96.008

**PREVENTIVE MANAGEMENT OF ADMINISTRATIVE PRODUCTION
WHEN RESOURCES SCARCITY IN THE PARTIES CONFLICT****Aleksey Y. Mironov**

postgraduate student

Russian State Hydrometeorological University

Anna Y. Mironova

student

ITMO University

Vyacheslav G. Burlov

Doctor of Technical Sciences, Full Professor

Peter the Great St. Petersburg Polytechnic University

In conditions of the narrow departmental management and resource deficiency, the administrative practice integrity is being destroyed by a lack of completeness and authenticity of production on the affairs about administrative offenses complicated by the conflict between the subject of administrative jurisdiction and opposing participants. Timely protection by geoinformatics for reliable detection and proper proof of offenses and rapid provision by geolocation for prompt participants' involvement in the administrative process preventatively guarantee the efficiency and information security of the administrative production. As an adequate mechanism for linking administrative practice and innovation technologies proposed a synthesis of the administrative production management model within a reasonable time, based on the natural-scientific approach to the adoption of managerial decisions. The condition for the existence of preventive management, which relates the characteristics of processes and performance indicators, is concretized by the Kolmogorov-Chapman equations system. In accordance with the structural and functional technology, network models of the target process, the violations occurrence, their identification and neutralization through the managerial impact on the limited resources of the administrative practice by geoinformation and geolocation subsystems are built.

Keywords: preventive management, administrative production, resource deficiency, conflict of parties, geoinformation and geolocation subsystems

1. Introduction

Without innovative technologies, the inefficiency of administrative practice is characterized by failure to detect up to 3/4 of administratively punishable acts, failure to comply with up to 1/4 of rulings on affairs about administrative offenses, failure to pay up to 1/3 of administrative fines. Tragic consequences from fires, illegals construction, and deforestation, from improper use of natural resources and subsoil, from environmental and man-made catastrophes are generated by the random nature of the reasons used to initiate affairs about administrative offenses. The sporadic and post-factum response of law enforcement officials to the flow of administrative offenses retains a vicious punitive-fiscal sense even in risk-oriented production. The administrative law enforcement agencies are focused on collecting fines for committed acts and are indifferent to the damage caused. Overcoming the incompleteness and unreliability of administrative practice is especially relevant in relation to administrative offenses, the traces of which are hidden behind the features of the terrain, or covered by offenders. Administrative prevention, revealing and proving within a reasonable time regularly requires the geographical coordinates with the signs of preparation or commission of offenses to administrative law enforcement agencies in the territory under their jurisdiction, for carryout targeted inspections immediately and for prevent or suppress of harmful consequences. The adequate intensity of the administrative process in the prompt violators' location determination in order to obligation or coerce them to comply with administrative legislation within a reasonable time is ensured by determining the geographic coordinates of unscrupulous production participants [1].

To geocoordinate support of preventive and operational-search activities, it is necessary to systematically analyze cartographic information on tracking changes in the position, shape, and structure of anthropogenic or natural objects with an eye to the ascertainment of administrative offense event and elements [2]. Addresses for targeted inspections can be obtained using the geoinformation system during the monitoring of territories under the jurisdiction of the administrative law enforcement agency. To establish the geographic whereabouts of the participants in the administrative process should be used the geolocation based on ground geodesy of their personal mobiles, their Internet gadgets, anti-theft, and emergency alarms on their vehicles. In addition to GLONASS / GPS positioning of the mobile device of the desired subscriber and triangulation of its connections with GSM or LTE base stations and Wi Fi or WiMAX points, relative geolocation of its computer or other equipment connected to the Internet

can be performed. Dozens of geoportal solutions at the federal, regional, and local levels operate in government or municipal departments, commercial structures of Russia. But due to the failure to timely prevent and suppress of administrative offenses, the catastrophic consequences of destructions, fires, floods, pollutions, misuses of land and forests annually arise. A paradoxical crisis of administrative practice has ripened: when its information security is upset, technological capabilities and production management tools are sprayed into ineffective notification of the dynamics of subordinate problems using geoinformation maps. Therefore, at the junction of administrative practice and geoinformatics or geolocation, an adequate model for preventive managing administrative production using a geoinformation and geolocation subsystems is gaining scientific and practical interest when the resources scarcity and the parties conflict.

According to the theory of functional systems, a decision-maker implements the management process based on the model, which is manifested in the chain of basic elements of its formation: “excitement” - “recognition” - “reaction to the situation” [3]. The relevance of this paper is determined by the lack of an adequate mathematical model necessary to guarantee the preventive management of administrative production and built on ensuring a balanced unity of the functioning rules of law enforcement, geoinformation and geolocation subsystems, of basic world laws within framework of a unified approach to the universal formalized criterion.

In contrast to analysis, synthesis forms processes with predetermined properties. The synthesis of production management when parties conflict will make it possible to preventively guarantee the detection and proof of administrative offenses, the investigation, and consideration of affairs about them, the execution of administrative penalties.

Thus, in this paper, the following tasks are solved:

- synthesis of the appearance of preventive management in case of a conflict between the parties to administrative production;
- synthesis of a mathematical model for managerial decision-making when resource deficiency;
- substantiation of the criterion for preventive management of administrative production within a reasonable time;
- construction of structural-functional technology for automated management of administrative practice using a geoinformation or geolocation subsystem.

2. Materials and Methods

In order to exclude arbitrariness in reasoning and conflicting conclusions, the axiomatic-deductive method is used. To ensure the adequacy

of models for the appearance of preventive management of administrative production and for managerial decision-making, their synthesis is based on the law of object integrity conservation, as a stable repetitive relationship between the properties of the object and the properties of its actions for a fixed mission [4].

2.1. Synthesis of a management appearance in conflict between production parties

Production on affairs about administrative offenses function and are managed in the current situation and the relationship of the circle of subjects of the administrative-jurisdictional process. When modeling the management of administrative practice, it should be borne in mind that at least two parties to administrative procedural legal relationships are involved in administrative production: subject of administrative jurisdiction (body for the execution of administrative legislation or official authorized by it, judge, prosecutor) and opposing participants in the process (offender, representative, defender, witness, expert, specialist), united intentionally or through negligence by a common desire to achieve the goal of the offense. In general, their interaction is considered in the form of a conflict of parties with contradicting interests.

Formalization of the law of object integrity conservation by accumulating the potential effectiveness of the management system for the required space-time states in the area where its main efforts are concentrated has formed a tool for resolving the conflict. The goal arising from interests is achieved through the development, deployment and application of each party to the conflict of its own management system.

In accordance with Figure 1, the conflicting management system counteracts as much as possible by performing three basic functions: target, protective, and providing. Attempts to supplement them give rise to functions similar in content and purpose, which should be taken into account in the basic ones. To implement the main functions, each party to the conflict creates, within the framework of its management system, the corresponding subsystems: target, protective, providing.

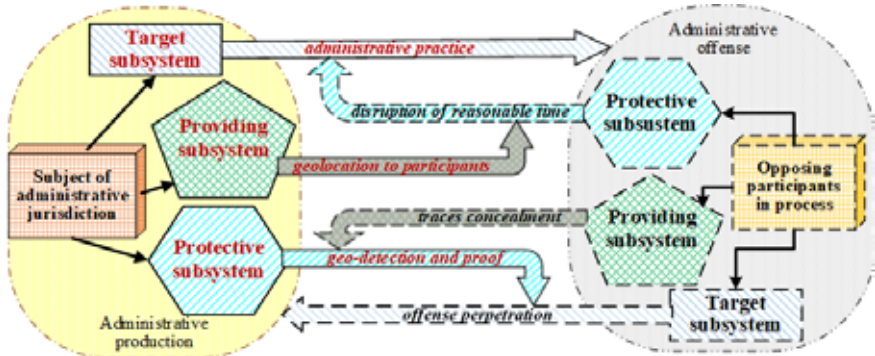


Fig. 1. Interaction of conflict parties due to basic management subsystems

The target subsystem is designed to solve target tasks on a variety of spatio-temporal states: for a subject of administrative jurisdiction – stages of administrative practice, for opposing participants in the administrative process – steps of committing an administrative offense. On the side of the body for the execution of administrative legislation, it forms the standard core of administrative production and is managed within a reasonable time by complementing the protective and providing subsystems.

In parallel with its own target process, the protective subsystem of a party seeks to impede the target's activities of the adversary: the subject of administrative jurisdiction proactively identifies and proves the signs of the event and composition of latent offenses, the opposing participants disrupt a reasonable time of procedural procedures of the target type in administrative production. It is obvious that the protective function prevails in the activity of the conflict party at the stages of initiation and investigation of affairs about administrative offenses. When considering affairs and executing penalties, the protective effect is gradually suppressed by the enemy.

The different directionality of the target and protective functions of each adversary indicates the dialectical contradiction of the realizing subsystems. For their harmonious coexistence and suppression of the counteraction effect, it is natural to assume that the party has a providing subsystem that removes the contradiction: for the subject of administrative jurisdiction – by the geolocation of the participants in the proceedings, which guarantees their presence in the administrative process, for the opposing participants in the proceedings – by actively hiding and destroying the traces of an administrative offense and its consequences. Oppressing

the defensive activity of the enemy in relation to its own target process, the providing function of conflict party is enhanced from the investigation of affairs about administrative offenses to the stages of their consideration and execution of penalties.

2.2. Synthesis of a model for managerial decision-making when resource scarcity

In accordance with the natural-scientific approach, integrating the properties of the world around us, consciousness and cognition, the process of managerial decision-making in Figure 2 is considered in the light of its three properties at each of the three levels of world cognition [5]:

- at the methodological level, based on the law of integrity preservation, the life of administrative production is abstractly presented by the Object in the form of a flow of affairs about administrative offenses and by its Action in the form of administrative practice of the decision-maker to advance affairs hampered by violations of reasonable time, at the expense of resources through the target states of production stages to the Mission of administrative legislation execution within a reasonable time;

- at the methodological level, significant conditions are identified for the current provision of administrative production within a reasonable time, which interact in making a managerial decision through the expenditure of resources, simulating the appearance of the Problem (Offence), its Identification and Neutralization;

- at the technological level, the implementation of the management decision-making process is modeled, which connects the Situation characterizing the current state of administrative production, the Information-Analytical Work within geoinformation or geolocation subsystem on the identification of violations of reasonable time and the Management Decision itself, embodying the Mission of the administrative process to eliminate problems of a reasonable time.

As shown in Figure 3, the formation of an adequate model for managerial decision-making is to establish formal analytical relations between the three technological components that are characterized by temporary resources, irreversible for the decision-maker:

1. Situation (Object) is a set of current state characteristics of the administrative production, factors, and conditions of decision-maker activity, which is identified with the periodicity of offense occurrence (average time to emergence problem) Δt and with the period of the target process ΔT when resources scarcity;

2. Procedural Decision (Mission) is the provision by the decision-maker

of the condition for administrative production implementation within a reasonable time in the current Situation to achieve the management goal, which is identified with an adequate periodicity of response to offenses (average time to neutralize problem) ΔN ;

3. Information-Analytical Work (Action) is the continuous extraction, accumulation, generalization, analysis of geodata about the current Situation, which is generalized into periodicity of offenses detection (average time to identify the problem) ΔI .

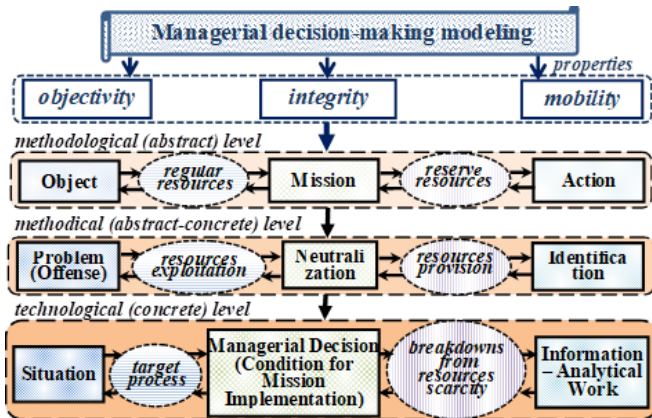


Fig. 2. Awareness by a natural-scientific approach

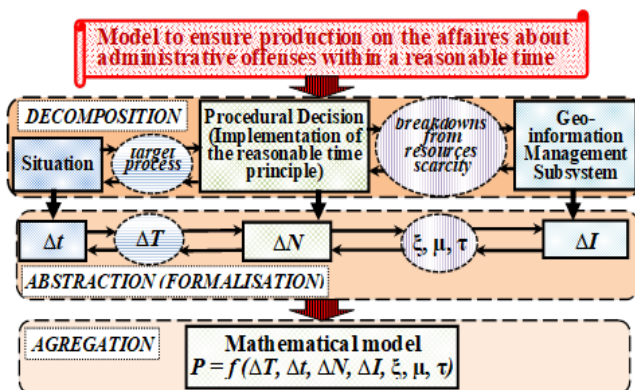


Fig. 3. Cognition of a model synthesis

Using the methods of decomposition, abstraction, and aggregation, the process of managerial decision-making is formalized into the mathematical aggregate of the model:

$$P = f(\Delta T, \Delta t, \Delta N, \Delta I, \xi, \mu, \tau), \quad (1)$$

where P is the probability of finding administrative proceedings during the management in each of its basic states: Initial, Target, Identification or Neutralization;

- ΔT is the generalized characteristic (average period) of the regular implementation of the target process, functionally consolidating acts (works) on the transition through its states to achieve the target task;

- Δt is the generalized characteristic (average time) of problem occurrence, functionally uniting the works for moving through its states to problem maturation;

- ΔI is the average time of problem identification, functionally linking information-analytical works on the passage of process states to identify the problem;

- ΔN is the average time of problem neutralization, functionally linking the acts of decision-makers on advance through process states to eliminate the problem;

- ξ is the average frequency of target process failure within a reasonable time;

- μ is the average frequency of identification breakdown within a reasonable time;

- τ is the average frequency of neutralization breakdown within a reasonable time.

2.3. Criterion for management of administrative production when resource scarcity

In a real environment of administrative production, the decision-maker is focused on the implementation of targeted activities for the prevention, detection, and proof of offenses, for the investigation and consideration of affairs about offenses, for the execution of administrative penalties within a reasonable time due to the procedural methods defined by law and departmental methods. The implementation of proven administrative practice schemes based on normative time and other resources provided is complicated by a stream of objective and subjective circumstances that make it difficult to quickly establish the geographical coordinates of the administrative offense place or production participants indicating signs of the event and corpus delicti. Stochastically emerging problems can and should be proactively identified using a geoinformation or geoloca-

tion subsystem and guaranteed to be eliminated with the involvement of additional resources in the conditions of restrictions on their availability. If the goals of reliable fixing and proving the administrative offense are not achieved within a reasonable time, the decision-maker is forced to delay, procedurally extend or terminate the affair investigation, which is tantamount to the target failure and to the breakdown of production management. On the way to the administrative production goal, the processes of identification in the geoinformation or geolocation subsystem and the neutralization of the problems that have arisen may not give the expected result within a reasonable time and break down to a forced repetition due to a lack of specific resources.

Considering the three-component nature of the basic model of managerial decision-making to protect from the interference of problems (offenses) in the target activity, a continuous Markov chain of administrative production management includes four interacting processes, which is shown in Figure 4. The target process during the execution of administrative practice in the normal mode is objectively accompanied by a Poisson stream of problems leading to failures of a reasonable time. When a reasonable period of implementation is delayed, the target process breaks back to the initial state by the extension or termination of administrative proceedings. In order to prevent the non-fulfillment of the target task and the failure of management, the identification and neutralization processes due to the works of the decision-maker in the automated management subsystem based on geoinformation or geolocation to diagnose the problems occurrence and to take the remedial measures for elimination them with the comparable time and the resources deficiency. In cases of insoluble problems, part of the identification and neutralization processes can also be disrupted to the initial state [6].

The administrative production management model in the form of a continuous Markov chain of Figure 5 is characterized by the probabilities of being in one of four basic states associated with the intensities of target process $\zeta=1/\Delta T$, of problem occurrence $\lambda=1/\Delta t$, of its identification $\nu=1/\Delta I$ and neutralization $\omega=1/\Delta N$, as well as the failure rates of target process $\xi=f(\Delta T)$, of problem occurrence $\lambda=1/\Delta t$, of its identification $\nu=1/\Delta I$ and neutralization $\omega=1/\Delta N$, as well as the failure rates of target process $\xi=f(\Delta T)$, of identification $\mu=f(\Delta I)$ and neutralization $\tau=f(\Delta N)$:

- Θ is the probability of initial state when the administrative practice of the decision-maker is in the initial state of administrative proceedings, which does not require the identification or neutralization of problems;
- Ψ is the probability of target completing when the decision-maker

fulfilled the target task of administrative proceedings with the guarantee of neutralizing the associated problems (offenses) within a reasonable time;

- Λ is the probability of identification when the decision-maker identifies problems leading to a breakdown of a reasonable time for their subsequent neutralization;
- Ω is the probability of neutralization when the decision-maker, based on the results of identification, neutralizes problems that cause disruptions in ensuring a reasonable time.

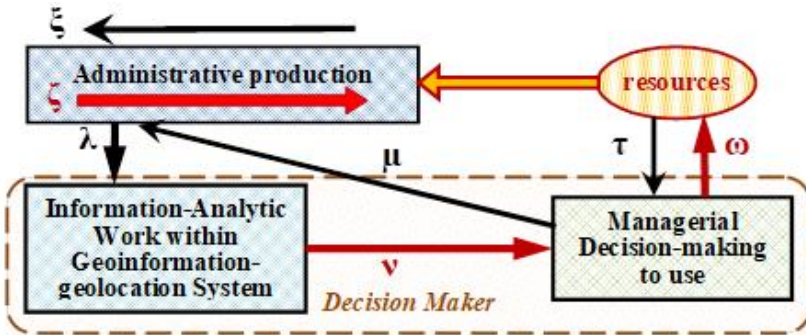


Fig. 4. Scheme for management of administrative production

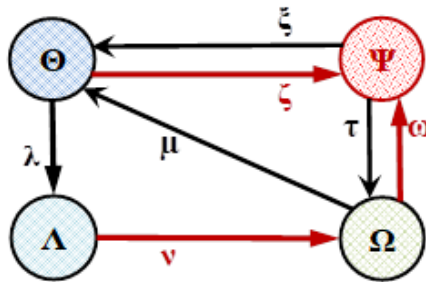


Fig. 5. States graph for management

The relationship (1) of the probability $P = (\Theta, \Psi, \Lambda, \Omega)$ of finding administrative proceedings in each of its basic states, respectively, with the intensities $\zeta, \xi, \lambda, \nu, \mu, \omega, \tau$ of continuous Markov transitions between states of the graph is specified Kolmogorov-Chapman differential equations system:

$$d\Theta(t)/dt = - [\zeta + \lambda] \Theta(t) + \xi \Psi(t) + \mu \Omega(t)$$

$$\begin{aligned}
 d\Psi(t)/dt &= \zeta \Theta(t) - [\xi + \tau] \Psi(t) + \omega \Omega(t) \\
 d\Lambda(t)/dt &= \lambda \Theta(t) - \nu \Lambda(t) \\
 d\Omega(t)/dt &= \tau \Theta(t) + \nu \Lambda(t) - [\mu + \omega] \Omega(t) \\
 \Theta(t) + \Psi(t) + \Lambda(t) + \Omega(t) &= 1
 \end{aligned} \tag{2}$$

When, over time, the Poisson streams of interacting processes tend to the limiting stationary mode, the Kolmogorov-Chapman differential equations (2) are transformed into a system of linear homogeneous algebraic equations, the solution of which using the Cramer method is system-forming factors of management:

$$\begin{aligned}
 \Theta &= \frac{\xi\nu\omega + \nu\mu(\xi + \tau)}{\xi\omega(\lambda + \nu) + \mu(\lambda + \nu)(\xi + \tau) + \nu(\zeta + \lambda)(\omega + \tau) + \nu(\zeta\mu + \xi\lambda)} \\
 \Psi &= \frac{\nu\omega(\zeta + \lambda) + \zeta\nu\mu}{\xi\omega(\lambda + \nu) + \mu(\lambda + \nu)(\xi + \tau) + \nu(\zeta + \lambda)(\omega + \tau) + \nu(\zeta\mu + \xi\lambda)} \\
 \Lambda &= \frac{\xi\lambda\omega + \lambda\mu(\xi + \tau)}{\xi\omega(\lambda + \nu) + \mu(\lambda + \nu)(\xi + \tau) + \nu(\zeta + \lambda)(\omega + \tau) + \nu(\zeta\mu + \xi\lambda)} \\
 \Omega &= \frac{\nu\tau(\zeta + \lambda) + \xi\lambda\nu}{\xi\omega(\lambda + \nu) + \mu(\lambda + \nu)(\xi + \tau) + \nu(\zeta + \lambda)(\omega + \tau) + \nu(\zeta\mu + \xi\lambda)}
 \end{aligned} \tag{3}$$

3. Results

When resources scarcity, modeling management in the form of a state graph in Figure 4 and system-forming factors (3) makes it possible to optimize the continuous Markov chain for realistic costs of the target process and for losses from breakdowns in management subsystem. When studying the work of protective or providing subsystem, for a reasonable time of implementation of which limited resources are reserved, the onset of a resource shortage is fraught with processes breakdowns, that establish the quality of administrative production and management. The criterion of management efficiency from relations (3) is the guaranteed share Ψ^* of time (flow of cases in readiness) for the others functions implementation of production on affairs about administrative offenses:

$$\frac{\nu\omega(\zeta + \lambda) + \zeta\nu\mu}{\xi\omega(\lambda + \nu) + \mu(\lambda + \nu)(\xi + \tau) + \nu(\zeta + \lambda)(\omega + \tau) + \nu(\zeta\mu + \xi\lambda)} \geq \Psi^* \tag{4}$$

4. Discussion

The intensity of the stream depends on the structure and duration of transitions by states (events) within the process. Therefore, it is advisable to obtain the intensity of target process $\zeta=1/\Delta T$, the intensity of problem occurrence $\lambda=1/\Delta t$, the intensities of its identification $\nu=1/\Delta l$ and neutralization $\omega=1/\Delta N$ by the structural-functional method [7]. When using it, by clearly linking the works on transitions and the times spent on them in the network model of each process, network analysis makes it possible to evaluate periods ΔT , Δt , Δl , ΔN through the critical path of each process. According to the observations of administrative statistics regarding the timeliness of the issuance and execution of ordinances on the affairs about administrative offenses, $\xi \approx 0,25\zeta$ and $\approx 0,05\omega$. The probability of technical errors in the functioning of the geoinformation or geolocation subsystem does not exceed $\mu \approx 0,10\nu$.

5. Conclusion

Thus, in an atmosphere of conflicting activity of opposing participants in production on affairs about administrative offenses, the target practice within a reasonable time of the subject of administrative jurisdiction is guaranteed to be managed by its accompaniment with a protective subsystem based on geoinformatics and providing subsystem based on geolocation.

In parallel to the regular process of administrative practice, the protective subsystem of the body for the execution of administrative legislation counteracts the target activities of offenders by early detection and reliable proof of the signs of an event and composition of latent offenses through preventive geoinformation. In an effort to neutralize the protective function of opposing participants in administrative production, the providing subsystem of the body for the execution of administrative legislation preserves a reasonable time of the administrative process by forcing to participate in procedural procedures due to the geolocation search for participants.

The three-functional appearance of the preventive management system in the conflict counteraction of the participants in administrative production gives rise to its protective and supporting reaction, each of which is modeled by a continuous Markov chain through the Kolmogorov-Chapman equations (2).

A numerical assessment of system-forming factors (3) on network models of the processes of administrative practice confirmed that, based on the average statistical duration of the process procedures, the pro-

posed management model (4) is capable of monitoring critical changes in the situation according to the conditions of efficiency and security. It also helps to reconfigure the structure and functionality of the identification and proof of administrative offenses, of the investigation, and consideration of affairs about them, of the execution of administrative penalties within a reasonable time under the current situation.

References

1. V. Burlov, A. Mironov, A. Mironova, J. Idrisova, I. Russkova, Offenses prevention at municipal energy facilities under geoinformation system management, *Advances in Intelligent Systems and Computing* 1258 (2021) 649–658. doi:10.1007/978-3-030-57450-5_56.
2. V. P. Savinykh, V. V. Oznamets, N. N. Selmanova, V. Y. Tsvetkov, System-categorical analysis used while monitoring of the land according to the remote sensing data, *Geodesy and Aerophotosurveying* 62 (2018) 106–113 (2018). doi:10.30533/0536-101X-2018-62-1-106-113.
3. K. V. Sudakov, Theory of Functional Systems: A Keystone of Integrative Biology, in: *Cognitive Systems Monographs*, 2015, pp. 153–173. doi:10.1007/978-3-319-19446-2_9.
4. Alexander G. Sokolov, Valery M. Abramov, Eugene P. Istomin et al, Digital transformation of risk management for natural industrial systems while climate change, *IOP Conference Series: Materials Science and Engineering* 940 (2020) 012003. doi:10.1088/1757-899x/940/1/012003.
5. V. G. Burlov, A. Y. Mironov, Y. V. Baranov, Synthesis of model of management of affairs about administrative offenses, *Information-measuring and Management Systems* 3 (2019) 22–34. doi:10.18127/j20700814-201903-03.
6. V. G. Burlov, A. Y. Mironov, A. Y. Mironova, Application of geoinformation system in prevention, identification and evidence about administrative offenses, *Scientific Notes of the Russian State Hydrometeorological University* 57 (2019) 126–146. doi:10.33933/2074-2762-2019-57-126-146.
7. A. Y. Mironov, A. Y. Mironova, V. G. Burlov, Prevention, Detection, and Proof of Offenses in Road and Bridge Construction Under the Management of Geoinformation System, in: A. Sinitsyn (eds) *SES-2020: Innovative Perspectives: Lecture Notes in Civil Engineering*, volume 141, Springer, Cham, 2021, pp. 214–223. doi:10.1007/978-3-030-67654-4_24.

CHARACTERISTICS OF QUANTUM MACROSYSTEM AS PRINCIPAL SPECIFIC FEATURE OF COLLOID GEL OXYHYDRATES

Inna Yu. Apalikova, Boris A. Markov, Yury I. Sukharev

3. Chelyabinsk State University

Chelyabinsk, Russia

2,3 Chelyabinsk Red Banner Military Aviation Institute for Navigators,
a branch of the Russian Air Force Academy named after Professor N. Ye.
Zhukovsky and Yu. A. Gagarin

To characterize the colloidal system, we introduced the so – called Lisegang operator – a periodic dependence that sets the concentration increase if the concentration has not reached some upper critical value- and sets the concentration drop if the upper critical value at a given point has already been reached; the concentration decrease will continue until the point when the lower critical value is reached. After that, the process is repeated.

It turns out that the system behaves "non – classical"-because of fundamentally complex, transcendental chemical reactions, we can not offer an adequate observable classical model and are forced to declare this behavior of the colloid "characteristic" of multiparticle interactions, observed, nevertheless, experimentally. Of course, such chemical reactions involve multiparticle interactions of molecules and even mesomolecules of the colloid. The concept of "entanglement" of states is much more relevant here than anywhere else.

At the same time, the axiomatically introduced concept of the "Lisegang operator", as a "general property of entanglement of gel systems", needs both research and proof.

Keywords: emission-wave duality, Lagrangian maps, Liesegang operator, oxyhydrate gel systems, colloid clusters, spontaneous pulsation flow, diffuse double electrical layer, topological continuum, dissociation-disproportion mechanism, Whitney theory, geometry of caustics.

LEMMA

If colloid chemical experimental data are in accord with the Liese-

gang operator distribution, then the system in question is a macroscopic quantum correlation system that is describable by the Schrödinger-Batanov equation.

To prove the lemma – the hypothesis, let us consider a few one-to-one maps that share a certain specific feature. Let us consider groups of wave numbers formed by nonzero real numbers according to a set binary multiplication operation. Each real number can be viewed as a complex number.

Introduction

Let us turn our minds to properties of elementary particles to derive the correlation function equation. These properties are as follows: the particles in question are quantum particles, and behaviors of these particles are correlated. Consequently, we are to build an equation for correlated functions of these particles, based on the Schrödinger equation $i\hbar \frac{\partial}{\partial t} \Psi = \Delta \Psi + (E - U)\Psi$.

Let us build a correlation for two various functions $\langle \Psi_1 \Psi_2 \rangle$, where the angle brackets denote averaging. To do so, it is convenient to begin by finding the binary function of multiplication $\psi = \Psi_1 \Psi_2$. Let us take the Schrödinger equation for these functions

$$i\hbar \frac{\partial}{\partial t} \Psi_1 = \Delta \Psi_1 + (E - U)\Psi_1$$

$$i\hbar \frac{\partial}{\partial t} \Psi_2 = \Delta \Psi_2 + (E - U)\Psi_2$$

Let us multiply the first equation by the function Ψ_2 , and the second one – by the function Ψ_1 , and then add the first equation to the second one. As a result, we find that $i\hbar \left(\Psi_2 \frac{\partial}{\partial t} \Psi_1 + \Psi_1 \frac{\partial}{\partial t} \Psi_2 \right) = \Psi_1 \Delta \Psi_2 + \Psi_2 \Delta \Psi_1 + (E - U)\Psi_1 \Psi_2$.

Now, let us transform the equation found $\Psi_2 \frac{\partial}{\partial t} \Psi_1 + \Psi_1 \frac{\partial}{\partial t} \Psi_2 = \frac{\partial}{\partial t} \Psi_1 \Psi_2 \equiv \frac{\partial}{\partial t} \psi$, $\Psi_1 \Delta \Psi_2 + \Psi_2 \Delta \Psi_1 = \Delta \Psi_1 \Psi_2 - (\vec{\nabla} \Psi_1; \vec{\nabla} \Psi_2)$. With the transformations taken into account, we find the final relation for the correlation function

$i\hbar \frac{\partial}{\partial t} \psi = \Delta \psi - (\vec{\nabla} \Psi_1; \vec{\nabla} \Psi_2) + (E - U)\psi$. It is worth noting that the equation contains the term $(\vec{\nabla} \Psi_1; \vec{\nabla} \Psi_2)$ that, in turn, contains the functions Ψ_1 and Ψ_2 that cannot be excluded from the relation. Moreover, the

relation in question – the product of the gradients – bears a resemblance to a nonlinear relation that describes shockwaves.

Thus, from the Schrödinger equation, we derive a relation for the correlation function in a form $i\hbar \frac{\partial}{\partial t} \psi = \Delta \psi - (\vec{\nabla} \Psi_1; \vec{\nabla} \Psi_2) + (E - U) \psi$.

Oscillatory phenomena are also common in colloid systems [1,2]. Consequently, it is advisable to use functions similar to those used in the Schrödinger equation, which set a probability of finding a particle at this or that point by equating the particle and the wave. Then questions arise: “What is a wave in a colloid state?” and “At what coordinates does it propagate?” Let us introduce the coordinates, while assuming that individual molecules of this or that substance can be identified to a certain degree within a colloid substance; this assumption is to a large extent conventional, as there are complex interactions, including physical interactions, between substances within a colloid.

Let us create a phase space where we will plot these gel coordinates along the axes. Let us denote the current state of the gel as a point within the space; any changes in the state of the gel that occur over time build a phase curve of the life and evolution of the gel. Let the phase space be simplest, and contain two coordinates only, namely, the concentration of metal atoms in micelles, and amounts of the substance ready to interact with these micellar atoms. One coordinate will suffice to describe the colloid while it is in the state it is; let us denote this coordinate as Φ .

Thus, we are able to identify the colloid state by the colloid phase Φ . Hence, we can describe quantitatively the colloid state, which means that concentrations, nanocurrents, and other values become dependent on the colloid phase, and that is when the colloid is fully determined by the colloid phase Φ , the way a quantum particle is determined by the wave function of the very particle in quantum mechanics.

This is why we see it convenient to write down an analog to the Schrödinger for the colloid phase. We only make a minor modification to the Schrödinger equation by substituting the Planck’s constant \hbar with the inverse diffusivity $\frac{1}{D}$, which we regard as a complex value. As a result, we obtain a relation for the phase

$$\frac{i}{D} \frac{\partial}{\partial t} \Phi = \Delta \Phi + \frac{1}{D} (E - U) \Phi.$$

All of the above suggests that the colloid phase must be determined by the correlation function of entangled states, which is why the Schrödinger equation for

the correlation function $i\hbar \frac{\partial}{\partial t} \psi = \Delta \psi - (\vec{\nabla} \Psi_1; \vec{\nabla} \Psi_2) + \frac{1}{D} (E - U) \psi$, written down instead of the Schrödinger equation, should be an analog to the latter. For this equation, we are to offer a substitution to the colloid phase caused by interactions between three various colloid phases that are present in the colloid simultaneously and are correlated by quantum particles. As a result, we obtain a relation for the phase.

$$i \frac{\partial}{\partial t} \Phi = D \Delta \Phi - D (\vec{\nabla} \Phi_1; \vec{\nabla} \Phi_2) + (E - U) \Phi$$

The above equation provides no answer to the question how to consider the product of the gradients that correspond to various wave processes; the equation contains a relation that we see fair to call a rule for phase grouping of real numbers. To do so, we are to consider the colloid phase stage that we have not reached yet. Assuming that there occurs a shockwave phenomenon [2, 6, 7] when the colloid phases are being put together, we see it convenient to rewrite the relation for the phase interaction as shown below $(\vec{\nabla} \Phi_1; \vec{\nabla} \Phi_2) = (\vec{\nabla} \Phi)^2$. Thus, we obtain a nonlinear relation in a form $i \frac{\partial}{\partial t} \Phi = D \Delta \Phi - D (\vec{\nabla} \Phi)^2 + (E - U) \Phi$, while assuming that the correlation between various phases is an autocorrelation.

It is the logic behind our assumption that the gel is a whole and is a priori correlated. Besides, we do not rule out a possibility that the diffusivity can be considered as a complex number that has both a real and an imaginary part, so as the difference coefficient $(E - U)$.

All we are to do now is to try and select the coefficients by using this or that method.

Thus, we obtain two groups of real numbers described by the equations

$$i\hbar \frac{\partial}{\partial t} \psi = \Delta \psi - (\vec{\nabla} \Psi_1; \vec{\nabla} \Psi_2) + \frac{1}{D} (E - U) \psi,$$

$$i \frac{\partial}{\partial t} \Phi = D \Delta \Phi - D (\vec{\nabla} \Phi_1; \vec{\nabla} \Phi_2) + (E - U) \Phi$$

The real groups of numbers where all group operations work in the same way are called isomorphous groups. As the isomorphism of the groups has been found from the function that maps one group onto the other, it is fair to call the second group an image (in this case, an isomorphous image) of the first group [3], which means that isomorphous groups, when considered as abstract groups, coincide.

Consequently, macroscopic colloid chemical oscillatory phenomena that occur within gel systems are quantum colloid states of a macrosubstance.

As of now, it is common knowledge in modern physics that matter has lost its tangibility. The mass has become a secondary property, the result of interactions between intangible quantum fields. What we consider the mass is a product of quantum fields, not a property that belongs to or necessarily inherent to them.

Despite the fact that the world is full of rigid and heavyweight objects, it is reigned by the energy of quantum fields. The mass becomes merely a physical manifestation of the energy in question, and not vice versa. However shocking it may appear conceptually, it sounds extremely attractive. The energy of quantum fields, and not rigid impenetrable atoms, is the greatest property that binds the Universe together [4]

This is why colloid chemical phenomena should be described in a similar way, that is, by taking into account the fact that particles under consideration are quantum particles, behaviors of these particles being correlated. The similarity principle is the fundamental law of nature.

Consequently, we are to build a description of the said particles, based on the Schrödinger wave equation, or a similar Schrödinger-Batanov equation [5] describing wave or energy characteristics of macroparticles of particles. We identified the nanocurrent ferroelectric properties of oxyhydrate gels [6].

Liesegang operator

To characterize colloid systems, we earlier proposed so-called Liesegang operator, which is a periodic dependence that either sets an increase in concentrations whenever any of concentrations does not reach a critical upper value, or sets a decrease in concentrations whenever the critical upper value has been reached at this point; a concentration will keep decreasing until it reaches the point of the critical lower value; and then, the process recurs.

The system, to all appearances, behaves in a “non-classical” way; due to essentially complex transcendental chemical reactions, we are unable to propose an observable adequate classical model, and are forced to assert that the colloid behavior in question is “inherent” in multi-particle interactions that, however, can be observed through experiment[7]. Definitely, these chemical reactions imply multi-particle interactions between colloid molecules and even mesomolecules. The concept of “entangled state” is appropriate here as nowhere else.

On the other hand, the concept of the “Liesegang operator”, proposed axiomatically as “a general property of entangled state in gel systems”, still remains both unstudied and unproved. We see “current surges” – currents that were discovered in colloid systems through experiment – a convenient way of studying Liesegang-type structures [1,6].

Model of long molecules

Let us assume that a gel structure is only caused by molecular interactions between long polar molecules of a gel, which are structured in a strictly definite way. For the sake of simplicity, let us consider simple one-dimensional models. Physical behaviors of these cluster oxyhydrate particles, in their tight interaction, imply that they are of special quantum nature. The states in question are called entangled states. Being aware of the fact that they make integral part of reality discovered, e.g., in gel oxyhydrate systems, implies that there exists a special type of interconnections between the components of the system. Any object that interacts with its surroundings is in an entangled state with it. It is important that we are talking about any objects, including macroscopic ones. Interacting with their surroundings, they are linked with it by non-local quantum correlations. Thus, a microscopic entangled system that exists on the boundary with a macroscopic oxyhydrate system is a special quantum form of compound correlations between electromagnetic noise entangled states within cluster systems, which we considered earlier [1].

Now, let us consider in detail the Liesegang operator as a singularity of entangled states, which means it was formulated in a non-classical way. Let there be domains where all chains of molecules, which generate a field, are oriented in the same direction, while other long polar molecules become oriented along the field, and the larger the field, the more oriented by the field they are – under its impact.

On the other hand, sizable gel molecules are complex, and, whenever the potential of a chain is strong enough, it either disrupts the molecule, or changes its orientation. We assume that a part of a molecule is repelled by the field, while a charge or a dipole remains, oriented in a direction opposite to that of the previous dipoles of the chain. Polarized molecules become attached again to this charge or dipole – this time, in an opposite direction. This process recurs multiple times, building molecular chains, with molecules contained in its cell being polarized in the same way, while those contained in neighboring ones have dissimilar directions of molecules and polarization vectors.

It is worth noting that this physicochemical model characterizes posi-

tions of larger molecules and their interactions with small-sized molecules rather than very charged particles detectible by recording cells. Thus, it is very likely that, within the framework of this model, small-sized clusters will not interact (a fact of little interest to us, seeing as their interactions may, quite possibly, be non-essential and classical), yet they will necessarily interact with the Liesegang cell, a spatial structural unit of transcendental entangled quantum chemical reactions. These multi-particle structures and comparatively simple interactions between them and small-sized particles are of a greatest interest to us.

Mathematical model

Let n , the concentration of long molecules, be oriented by the field, rather than be positioned chaotically. The polarization vector \vec{P} that sets the electrical field \vec{E} is linked with the concentration $\text{div } \vec{P} = 4\pi\epsilon n$, where ϵ is the dielectric penetrability.

Let us assume that, in our model, these molecules have not appeared out of anywhere, but they are capable of rotating. Consequently, they follow the law of continuity, which means that the continuity equation $\frac{\partial n}{\partial t} + \text{div}(n\vec{v}) = L[n]$, where \vec{v} is the speed of a flow of long molecules, and $L[n]$ is the Liesegang operator that, depending on concentration values, may be $\pm a n$, where a is a positive number, is true for them.

Then, it is convenient to use a notation to find the polarization vector linked with the electrical field: in a domain where the Liesegang operator bears the plus sign, we use a concentration that bears the plus sign, and, wherever the Liesegang operator bears the minus sign – we use that bearing the minus. Physically, using opposite sign concentrations is attributable to the fact that those concentrations are concentrations of gel dipoles, oriented in opposite directions.

Now that we know concentrations of these molecules, we would like to obtain the electrical field generated by them. While assuming that the flow of molecules $n\vec{v} = -D \text{grad } n$, where D is the diffusivity, and $\text{grad } u$ is the gradient, we obtain an ordinary diffusion equation for concentrations of molecules $\frac{\partial n}{\partial t} = D\Delta n + L[n]$.

Now, let us consider the very Liesegang operator more carefully. Let the molecule disruption potential be Φ_0 . Consequently, if the potential and the field are linked together $\vec{E} = -\text{grad } \Phi$, then, in a one-dimensional case, $\Phi = -\int_0^x E dx$. Taking into account the fact that $P = eE$, we find that

$\Phi = -\frac{1}{\varepsilon_0} \int_0^x P dx$. Thus, the signs of the Liesegang operator will shift signs at a space point and at a time moment whenever $\left| \frac{1}{\varepsilon_0} \int_0^x P dx \right|$ reaches the value

Φ_0 . This is why it is convenient to take, a nonstandard condition – reaching a critical density – and another condition – reaching the critical value $\pm\Phi_0$ by the integral $\Phi = \Phi(0) - \frac{1}{\varepsilon_0} \int_0^x ds \int_0^s n(p) dp$, where $\Phi(0)$ is the potential value at the domain boundary, as a condition for the sift of the sign by the Liesegang operator at a space point x_0 . When values x are higher, the sign born by the Liesegang operator will be opposite – until the potential reaches the value Φ_0 , etc.

The solution to the differential equation $\frac{\partial}{\partial t} P = D \frac{\partial^2}{\partial x^2} P \pm \alpha P$ for the domains bearing the “+” and “-” signs is already known. We are interested in even a simpler equation: as we see gel Liesegang cells as fully formed, we can take a stationary equation.

Substituting the formula for polarization $\text{div } \vec{P} = 4\pi\varepsilon n$ into the equation $\frac{\partial n}{\partial t} = D\Delta n + L[n]$, we find that $\frac{\partial}{\partial t} \text{div } \vec{P} = D\Delta \text{div } \vec{P} \pm \alpha \text{div } \vec{P}$. Then, we separate the solution domain into subdomains where the Liesegang operator does not change its signs. Then, discarding the divergence, we obtain the field $\frac{\partial}{\partial t} \vec{P} = D\Delta \vec{P} \pm \alpha \vec{P} + \text{rot } \vec{S}$, where $\text{rot } \vec{S}$ is a vorticity vector that changes orientations of long heavy molecules.

Now, let us express these multi-particle Liesegang concepts through their respective wave characteristics.

Let us express these concepts through respective wave characteristics.

Data of experiments and discussion of characteristics of gel oxyhydrates

Multiple experiments [6] suggest that between conductive electrodes that are introduced into a rare-earth metal colloid oxyhydrate and wired together via a measuring instrument (see Fig. 1 below), a potential difference of approx 0.2 V is generated, and a weak current runs, ranging between nanoamperes and one microampere (see Fig. 2 below), which we described in multiple publications, e.g., [1-3,6]).

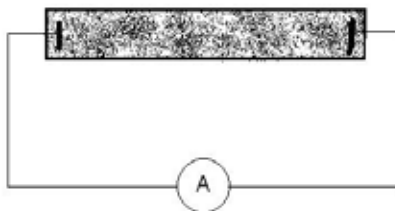


Fig. 1. Layout of electric circuitry to take measurements of current surges

An ammeter is included in the circuit (L-CARD or ZLab-based digital systems), with graphite or platinum electrodes introduced into a rectangular cell designated as a rectangle painted over in gray, the area of the electrodes being approximately one square centimeter.

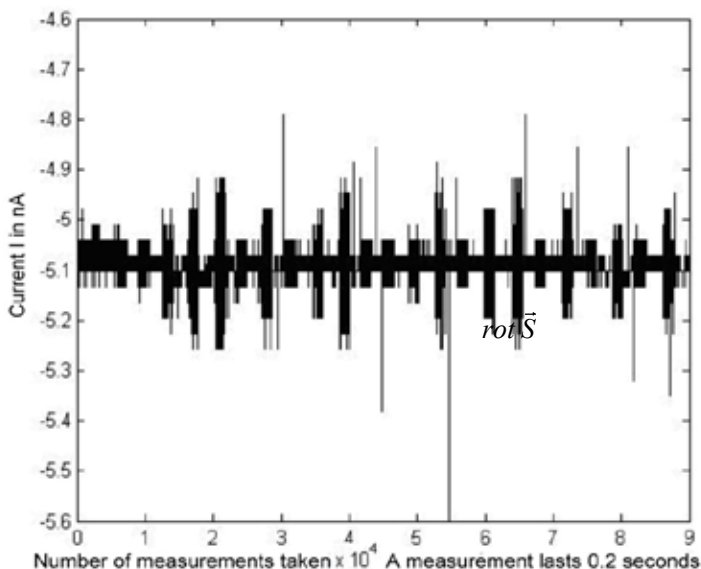


Fig. 2. Current oscillations in time. Results of experiments to measure current surges.

Plotted along the Y axis is measured current in nanoamperes, along the X axis – number of measurements taken in tens of thousands.

10,000 measurements taken correspond to 2,000 seconds, the duration of the experiment being hours.

Periodograms of processes

First and foremost, let us find out if the process is chaotic or it is a total of periodic processes.

Let us resort to the Schuster periodogram method. To use it, let us subtract the mean value of the experimental data obtained, then subject it to the Fourier transformation, and then multiply it by the conjugate value, thus finding the power spectrum, see its respective diagrams on Figs. 3 and 4 below.

According to the periodogram method, a specific value (criterion) of the periodogram for a given amount of experimental data (90,000 measurements taken) corresponds to a specific probability that this value is not a random value.

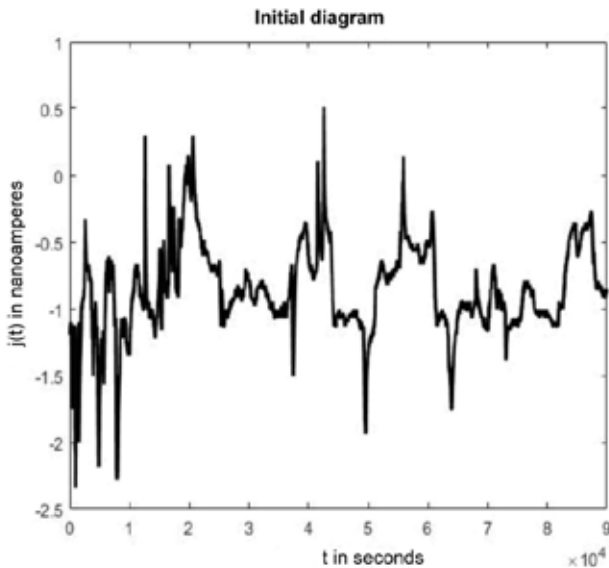


Fig. 3. Initial current diagram (tin, 31st day after colloid was prepared)

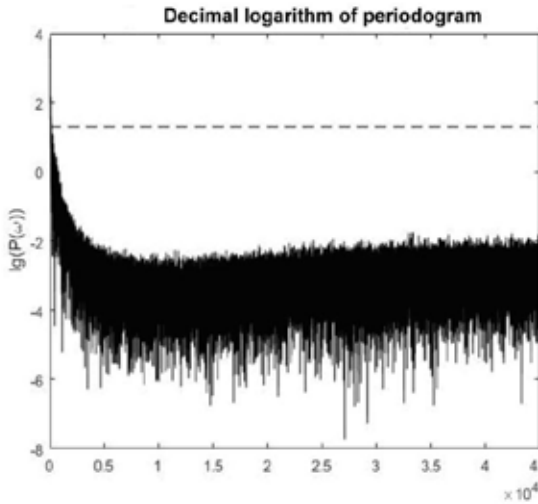


Fig 4. Decimal logarithm of Schuster periodogram. Dashed line denotes criterion value

The criterion value was found from a probability equal to 0.9999, which meant that whenever the periodogram value was below the criterion value, there existed a probability exceeding 0.0001 that the value in question was a result of a random, not an oscillatory process. To present the results in a more convenient way, let us use the periodogram logarithm. Please refer to Figs. 3 and 4 for the results.

It is worth noting that Fig. 4 above suggests that there is only a small range of the periodogram values that exceed the criterion values. Nonetheless, this small range of the periodogram values allows almost a complete reproduction of the initial spectrum.

Discarding the power spectrum values that do not meet the criterion, and restoring the current diagrams, we obtain the result shown on Fig. 5 below.

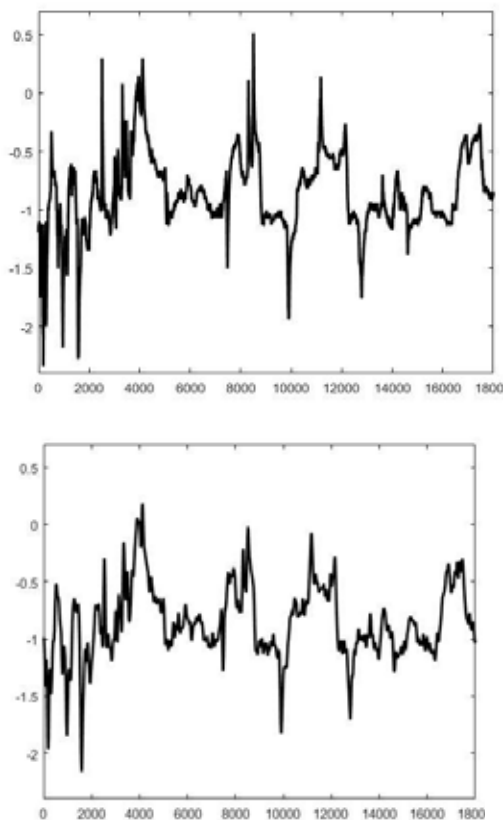


Fig. 5. Left – initial currents diagram; Right – currents diagram restored from small amount of peaks of periodogram

Thus, the “random” part of the periodogram is not influential on the time dependence of the currents, and we see it fair to assume that current oscillations are principally determined by periodic processes.

The physicochemical model of gel colloids

Let there be a chemical reaction occurring at the time moment $t = 0$, leading to a change in the chemical balance. We assume that colloid fragment are not electrically neutral, but they either bear a free electric charge inseparable from its colloid fragment, or they bear an electric momentum

that can be interpreted by ascribing an effective free electric charge to each colloid fragment.

Also, we rely on the assertion that a colloid substance can be represented as an aggregate of both lightweight and significantly heavier fragments. While discarding viscosity, we will only leave colloid elements that are mobile to various degrees. Thus, motions of colloid elements is expressed by the electric hydrodynamics equation.

Let us number the substances by attributing each of them the number j . Thus, the substance concentration numbered j is denoted as c_j , the mass of its individual molecule (or cluster) is denoted as m_j , its effective charge – q_j , and the space travel speed of its molecule – v_j .

We consider motions of colloid particles along the straight line $x \in (-\infty; +\infty)$ within time moments $t \in (0; +\infty)$, where motion begins at the time moment $t = 0$.

The electromagnetic hydrodynamics system of equations can be written down as shown below [7]

$$\left\{ \begin{array}{l} \frac{\partial v_j(x,t)}{\partial t} + v_j(x,t) \frac{\partial v_j(x,t)}{\partial x} = -\frac{q_j}{m_j} E(x,t), \quad x \in (-\infty; +\infty), t \in (0; +\infty), \\ \frac{\partial c_j(x,t)}{\partial t} + \frac{\partial (c_j(x,t)v_j(x,t))}{\partial x} = 0, \quad x \in (-\infty; +\infty), t \in (0; +\infty), \\ \frac{\partial E(x,t)}{\partial x} = 4\pi \sum_{j=1}^N q_j c_j(x,t), \quad x \in (-\infty; +\infty), t \in (0; +\infty), \\ E(x,0) = E_0(x), c_j(x,0) = c_j^{(0)}(x), v_j(x,0) = v_j^{(0)}(x), \quad x \in (-\infty; +\infty). \end{array} \right. \quad (1)$$

The denotations used here are as follows: $E(x, t)$ is the electrical field generated by an aggregate of electrically charged particles, and $j \in \overline{1, N}$, N is the total number of electrically charged particles contained in a specific colloid.

Seeing as a general solution to System (1) is unknown, we will resort to the small parameter method by assuming that there exists a substance that we denote as “1” and that has a considerable higher ratio $\frac{q_1}{m_1}$ than

the rest of the substances $\frac{q_1}{m_1} \gg \frac{q_j}{m_j}, j \in \overline{2, N}$. Let us introduce the

small parameter $\varepsilon_j = \frac{q_j}{m_j} \cdot \frac{m_1}{q_1}$, $j \in \overline{2, N}$, and rewrite the first equation

of System (1) with the small parameter taken into account.

For each number $j \in \overline{1, N}$, we will search for a solution in the form of the serie $c_j(x, t) = \sum_{k=0}^{\infty} \varepsilon_j^k c_{jk}(x, t)$, $v_j(x, t) = \sum_{k=0}^{\infty} \varepsilon_j^k v_{jk}(x, t)$,

$$E = \sum_{k=0}^{\infty} \sum_{l=0}^{\infty} \varepsilon^k \varepsilon^l E_{kl}(x, t).$$

$$\left\{ \begin{array}{l} \frac{\partial v_j(x, t)}{\partial t} + v_j(x, t) \frac{\partial v_j(x, t)}{\partial x} = -\varepsilon_j \frac{q_1}{m_1} E(x, t), \quad x \in (-\infty; +\infty), \quad t \in (0; +\infty), \\ \frac{\partial c_j(x, t)}{\partial t} + \frac{\partial (c_j(x, t) v_j(x, t))}{\partial x} = 0, \quad x \in (-\infty; +\infty), \quad t \in (0; +\infty), \\ \frac{\partial E(x, t)}{\partial x} = 4\pi \sum_{j=1}^N q_j c_j(x, t), \quad x \in (-\infty; +\infty), \quad t \in (0; +\infty), \\ E(x, 0) = E_0(x), \quad c_j(x, 0) = c_j^{(0)}(x), \quad v_j(x, 0) = v_j^{(0)}(x), \quad x \in (-\infty; +\infty). \end{array} \right. \quad (2)$$

Accordingly, System (2) falls into separate equations for the terms of the series.

As any attempt at studying convergence of the formalized series above would be rather cumbersome and is beyond the framework of this Article and the publication, we assume that the initial and the boundary conditions of Problem (2) are such that the series converge as required within the whole range $x \in (-\infty; +\infty)$, $t \in (0; +\infty)$.

To solve (2), we will limit ourselves to two substances to prove that greater amounts of a substance will not destroy the linear sum of oscillations for the minor terms of the series.

Dual-substance model

For the convenience of notation, let us introduce changes to the notation $c_1(x, t) \equiv n(x, t)$, $v_1(x, t) \equiv v(x, t)$, $c_2(x, t) \equiv \rho(x, t)$, $v_2(x, t) \equiv u(x, t)$, $\gamma = \frac{q_1}{m_1}$. As a result, System (2) assumes a form

$$\left\{ \begin{array}{l}
 \frac{\partial v(x,t)}{\partial t} + v(x,t) \frac{\partial v(x,t)}{\partial x} = -\gamma E(x,t), \quad x \in (-\infty; +\infty), \quad t \in (0; +\infty), \\
 \frac{\partial u(x,t)}{\partial t} + u(x,t) \frac{\partial u(x,t)}{\partial x} = \varepsilon \gamma E(x,t), \quad x \in (-\infty; +\infty), \quad t \in (0; +\infty), \\
 \frac{\partial n(x,t)}{\partial t} + \frac{\partial (n(x,t)v(x,t))}{\partial x} = 0, \quad x \in (-\infty; +\infty), \quad t \in (0; +\infty), \\
 \frac{\partial \rho(x,t)}{\partial t} + \frac{\partial (\rho(x,t)u(x,t))}{\partial x} = 0, \quad x \in (-\infty; +\infty), \quad t \in (0; +\infty), \\
 \frac{\partial E(x,t)}{\partial x} = 4\pi (q_1 n(x,t) - q_2 \rho(x,t)), \quad x \in (-\infty; +\infty), \quad t \in (0; +\infty), \\
 E(x,0) = F(x), \quad n(x,0) = n_0(x), \quad v(x,0) = v_0(x), \quad \rho(x,0) = \rho_0(x), \quad u(x,0) = u_0(x).
 \end{array} \right. \quad (3)$$

Let us look for a solution in the shape of the series $n(x,t) = \sum_{k=0}^{\infty} \varepsilon^k n_k(x,t)$,

$$\rho(x,t) = \sum_{k=0}^{\infty} \varepsilon^k \rho_k(x,t), \quad v(x,t) = \sum_{k=0}^{\infty} \varepsilon^k v_k(x,t), \quad u(x,t) = \sum_{k=0}^{\infty} \varepsilon^k u_k(x,t),$$

$$E = \sum_{k=0}^{\infty} \varepsilon^k E_k(x,t).$$

In our considerations, we will not go beyond the zero and the first terms of the said series, while assuming that the rest of the terms are small in comparison to the first two. For the zero terms of the series, from (3), we obtain relations

$$\left\{ \begin{array}{l}
 \frac{\partial v_0(x,t)}{\partial t} + v_0(x,t) \frac{\partial v_0(x,t)}{\partial x} = -\gamma E_0(x,t), \quad x \in (-\infty; +\infty), \quad t \in (0; +\infty), \\
 \frac{\partial u_0(x,t)}{\partial t} + u_0(x,t) \frac{\partial u_0(x,t)}{\partial x} = 0, \quad x \in (-\infty; +\infty), \quad t \in (0; +\infty), \\
 \frac{\partial n_0(x,t)}{\partial t} + \frac{\partial (n_0(x,t)v_0(x,t))}{\partial x} = 0, \quad x \in (-\infty; +\infty), \quad t \in (0; +\infty), \\
 \frac{\partial \rho_0(x,t)}{\partial t} + \frac{\partial (\rho_0(x,t)u_0(x,t))}{\partial x} = 0, \quad x \in (-\infty; +\infty), \quad t \in (0; +\infty), \\
 \frac{\partial E_0(x,t)}{\partial x} = 4\pi (q_1 n_0(x,t) - q_2 \rho_0(x,t)), \quad x \in (-\infty; +\infty), \quad t \in (0; +\infty), \\
 E_0(x,0) = F(x), \quad n_0(x,0) = f(x), \quad v(x,0) = 0, \quad \rho_0(x,0) = q_1 \rho_0 / q_2, \quad u_0(x,0) = 0.
 \end{array} \right. \quad (4)$$

It is obvious that the second equation (4) only has a zero solution, that is, $u_0(x,t) = 0$, and the fourth equation (4) only has a constant solution $\rho_0(x,t) = \text{const}$.

Let an imbalance set in as shown below $n_0(x,t) = -\rho_0 + f_0(x)$, where the function $f_0(x)$ is finite and has a property $\int_{-\infty}^{+\infty} f_0(x) dx$.

This condition corresponds to a local imbalance in the charge, which is caused by force of a chemical reaction, mechanical changes in the clusters, or any other similar phenomena.

Excluding from (4) equations with known solutions, and implementing the reasoning below, we obtain an equation system

$$\left\{ \begin{array}{l} \frac{\partial v_0(x,t)}{\partial t} + v_0(x,t) \frac{\partial v_0(x,t)}{\partial x} = -\gamma E_0(x,t), \quad x \in (-\infty; +\infty), \quad t \in (0; +\infty), \\ \frac{\partial n_0(x,t)}{\partial t} + \frac{\partial(n_0(x,t)v_0(x,t))}{\partial x} = 0, \quad x \in (-\infty; +\infty), \quad t \in (0; +\infty), \\ \frac{\partial E_0(x,t)}{\partial x} = 4\pi(q_1\rho_0 - q_2n_0(x,t)), \quad x \in (-\infty; +\infty), \quad t \in (0; +\infty), \\ E_0(x,0) = F(x), \quad n_0(x,0) = \rho_0 + f_0(x), \quad v_0(x,0) = 0, \quad x \in (-\infty; +\infty). \end{array} \right. \quad (5)$$

From the third equation (5), let us express $n_0(x,t)$: $n_0(x,t) = \frac{q_1}{q_2} \rho_0 - \frac{1}{4\pi q_2} \frac{\partial E_0(x,t)}{\partial x}$, and then substitute it into the second equation (5). Thus, we obtain a relation

$$\frac{\partial}{\partial x} \left(\frac{\partial E_0(x,t)}{\partial t} \right) + \frac{\partial}{\partial x} \left(v_0(x,t) \frac{\partial E_0(x,t)}{\partial x} \right) = 4\pi \frac{q_1}{q_2} \rho_0 \frac{\partial v_0(x,t)}{\partial x}. \quad (6)$$

Removing the coordinate derivative from (6), we get a relation to find $E_0(x,t)$:

$$\frac{\partial E_0(x,t)}{\partial t} + v_0(x,t) \frac{\partial E_0(x,t)}{\partial x} = 4\pi \frac{q_1}{q_2} \rho_0 v_0(x,t). \quad (7)$$

Substituting (5.2) (the second equation of (5)) by the new equation and excluding from consideration $n_0(x,t)$, we find that

$$\begin{cases} \frac{\partial v_0(x,t)}{\partial t} + v_0(x,t) \frac{\partial v_0(x,t)}{\partial x} = -\gamma E_0(x,t), & x \in (-\infty; +\infty), t \in (0; +\infty), \\ \frac{\partial E_0(x,t)}{\partial t} + v_0(x,t) \frac{\partial E_0(x,t)}{\partial x} = 4\pi \frac{q_1}{q_2} \rho_0 v_0(x,t), & x \in (-\infty; +\infty), t \in (0; +\infty). \\ E_0(x,0) = F(x), v_0(x,0) = 0, & x \in (-\infty; +\infty). \end{cases} \quad (8)$$

It is obvious that $F(x) = 4\pi \int_{-\infty}^x f_0(x)dx$ is finite.

Let us look for a solution to (8) in the form $v_0(x,t) = V(x,t) \cos(\omega t) + U(x,t) \sin(\omega t)$, $E_0(x,t) = V(x,t) \sin(\omega t) + U(x,t) \cos(\omega t)$. Then, if $v_0(x,0) = 0$, then, and $U(x,0) = F(x)$, while $\omega^2 = \frac{4\pi q_1^2 \rho_0}{q_2 m_1}$, while. Substituting these expressions into (8), we get an equation

$$\begin{cases} \frac{\partial U(x,t)}{\partial t} + \sin(\omega t) U(x,t) \frac{\partial U(x,t)}{\partial x} = 0, & x \in (-\infty; +\infty), t \in (0; +\infty), \\ U(x,0) = F(x), & x \in (-\infty; +\infty). \end{cases} \quad (9)$$

To solve (9), let us resort to the Florin linearization. Let us look for a solution to the equation for $U_\varepsilon(x,t)$, such that $U(x,t) = \lim_{\varepsilon \rightarrow 0+0} U_\varepsilon(x,t)$.

To obtain a problem for $U_\varepsilon(x,t)$, let us add the term $\varepsilon \frac{\partial^2 U_\varepsilon(x,t)}{\partial x^2}$ to the right-hand part of the first equation (9), and then make the solution $U_\varepsilon(x,t)$ tend to zero at infinity:

$$\begin{cases} \frac{\partial U_\varepsilon(x,t)}{\partial t} + \sin(\omega t) U_\varepsilon(x,t) \frac{\partial U_\varepsilon(x,t)}{\partial x} = \varepsilon \frac{\partial^2 U_\varepsilon(x,t)}{\partial x^2}, & x \in (-\infty; +\infty), t \in (0; +\infty), \\ U_\varepsilon(x,0) = F(x), & x \in (-\infty; +\infty), U(\pm\infty, t) = 0. \end{cases} \quad (10)$$

Let us carry out the linearization in the form $U_\varepsilon(x,t) = -2\varepsilon \frac{\partial}{\partial x} \ln v_\varepsilon(x,t)$. With all the transformations done, we get a problem

$$\begin{cases} \frac{\partial v_\varepsilon(x,t)}{\partial t} = \varepsilon \sin(\omega t) \frac{\partial^2 v_\varepsilon(x,t)}{\partial x^2}, & x \in (-\infty; +\infty), t \in (0; +\infty), \\ v_\varepsilon(x,0) = \exp\left(-\frac{F(x)}{2\varepsilon}\right), & x \in (-\infty; +\infty), v(\pm\infty, t) = 1. \end{cases} \quad (11)$$

The solution to (11) has a form as below

$$v_{\varepsilon}(x, t) = 1 + \int_{-\infty}^{+\infty} \frac{ds}{\sqrt{4\pi \frac{\varepsilon}{\omega} (1 - \cos(\omega t))}} \exp\left(-\frac{(x-s)^2}{\frac{4\pi\varepsilon}{\omega} (1 - \cos(\omega t))}\right) \left(\exp\left(-\frac{F(s)}{2\varepsilon}\right) - 1\right).$$

It is worth noting that the above solution exists always and at any $x \in (-\infty; +\infty)$, $t \in (0; +\infty)$.

The integral cannot be found in a general form, which is why we will provide a few diagrams for the solution to the problem (12)

$$\begin{cases} \frac{\partial U(x, t)}{\partial t} + \sin(\omega t)U(x, t) - \frac{\partial U(x, t)}{\partial x} = 0, & x \in (-\infty; +\infty), t \in (0; +\infty), \\ U(x, 0) = \begin{cases} 0, & x \in (-\infty; -1), \\ \sin(\pi x), & x \in [-1; +1], \\ 0, & x \in (+1; +\infty), \end{cases} \end{cases} \quad (12)$$

at $\varepsilon = 0.2$, see Fig. 6 below.

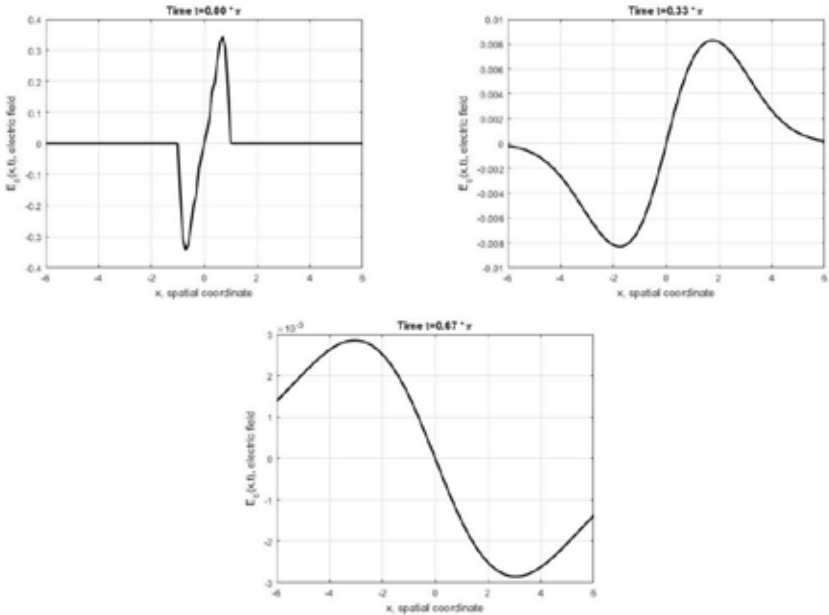


Fig. 6. Solution to (12) for various oscillation phases. Inaccuracy of solution is caused by impossibility of accurate computation of transition to limit

Fig. 6 above suggests that oscillations of the electrical field are reproducible at a period $T = \frac{2\pi}{\omega} = \frac{\pi\sqrt{m_1}}{q_1\sqrt{\pi\rho_0}}$. Consequently, if the assumption that the oscillation found through experiment are of electromechanical nature is true, then each individual oscillations should have a spectrum set by Equation (11).

The spectrum $E_0(x,t)$ may vary greatly, depending on values x (see Fig. 7 below); the spectral lines, however, are rather narrow, so each oscillation can be viewed as an aggregate of individual spectral lines.

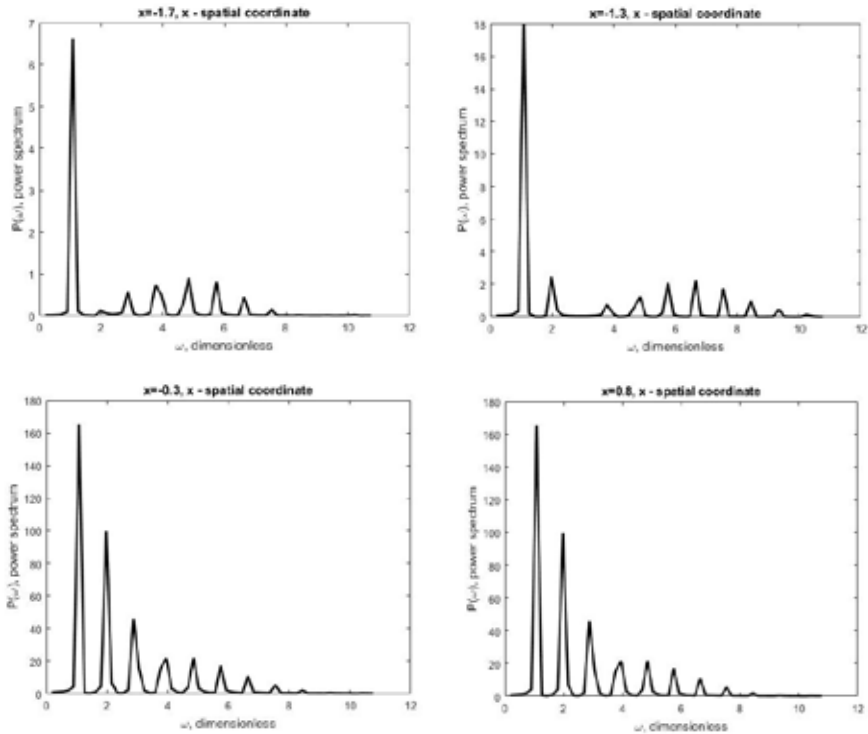


Fig. 7. Power spectrums $E_0(x,t)$ for various values x

Slow motion

Now let us consider the subsequent terms of the series. It is fair to assume that dynamics will also occur among particles having lower charge to mass ratios – due to instability of the electrical charge. Their motions,

within the framework of the electromechanical model, will be determined by the functions $\rho_1(x, t)$ and $u_1(x, t)$.

For the terms $\rho_1(x, t)$ and $u_1(x, t)$ of the series, an equation system can be written down as shown below

$$\left\{ \begin{array}{l} \frac{\partial v_1(x, t)}{\partial t} + v_0(x, t) \frac{\partial v_1(x, t)}{\partial x} + v_1(x, t) \frac{\partial v_0(x, t)}{\partial x} = -\gamma E_1(x, t), \quad x \in (-\infty; +\infty), \quad t \in (0; +\infty), \\ \frac{\partial u_1(x, t)}{\partial t} = \gamma E_0(x, t), \quad x \in (-\infty; +\infty), \quad t \in (0; +\infty), \\ \frac{\partial n_1(x, t)}{\partial t} + \frac{\partial(n_1(x, t)v_0(x, t))}{\partial x} + \frac{\partial(n_0(x, t)v_1(x, t))}{\partial x} = 0, \quad x \in (-\infty; +\infty), \quad t \in (0; +\infty), \\ \frac{\partial \rho_1(x, t)}{\partial t} + \frac{\partial(\rho_0 u_1(x, t))}{\partial x} = 0, \quad x \in (-\infty; +\infty), \quad t \in (0; +\infty), \\ \frac{\partial E_1(x, t)}{\partial x} = 4\pi(q_1 \rho_1(x, t) - q_2 n_1(x, t)), \quad x \in (-\infty; +\infty), \quad t \in (0; +\infty), \\ E_1(x, 0) = 0, \quad n_1(x, 0) = 0, \quad v_1(x, 0) = 0, \quad \rho_1(x, 0) = 0, \quad u_1(x, 0) = 0. \end{array} \right. \quad (13)$$

In System (13), a number of equations can be selected, which can be solved separately.

$$\left\{ \begin{array}{l} \frac{\partial u_1(x, t)}{\partial t} = \gamma E_0(x, t), \quad x \in (-\infty; +\infty), \quad t \in (0; +\infty), \\ \frac{\partial \rho_1(x, t)}{\partial t} + \frac{\partial(\rho_0 u_1(x, t))}{\partial x} = 0, \quad x \in (-\infty; +\infty), \quad t \in (0; +\infty), \\ E_1(x, 0) = 0, \quad \rho_1(x, 0) = 0, \quad u_1(x, 0) = 0. \end{array} \right. \quad (14)$$

The function $E_0(x, t)$ is known; differentiating the first equation (14) by x and substituting the second one into it, we obtain a relation for the concentration

$$\frac{\partial^2 \rho_1(x, t)}{\partial t^2} = -4\pi\gamma(q_1 \rho_0 - q_2 n_0(x, t)) \quad (15)$$

Hence,

$$\rho_1(x, t) = -4\pi\gamma \int_0^t d\tau \int_0^\tau (q_1 \rho_0 - q_2 n_0(x, s)) ds \quad (16)$$

Consequence

Let the expression $4\pi\gamma(q_1 \rho_0 - q_2 n_0(x, t))$ be periodic, with a period T , and, consequently, $\forall t \in (0; T)$ can be expanded into a Fourier series

$$4\pi\gamma(q_1\rho_0 - q_2n_0(x,t)) = \sum_{j=1}^{\infty} \left(a_j \cos\left(\frac{2\pi jt}{T}\right) + b_j \sin\left(\frac{2\pi jt}{T}\right) \right).$$

Then,

$$\rho_1(x,t) = \frac{T^2}{4\pi^2} \sum_{j=1}^{\infty} \left(\frac{a_j}{j^2} \cos\left(\frac{2\pi jt}{T}\right) + \frac{b_j}{j^2} \sin\left(\frac{2\pi jt}{T}\right) \right).$$

Thus, knowing the concentration power spectrum, one can find the density spectrum of heavyweight fragments also, by dividing amplitude squares of each of the frequencies by the fourth powers of the frequencies. We expect that two substances should share one frequency, while more substances will mean more frequencies.

It follows from the considerations of oscillations for the “lightweight fragments- heavyweight fragments” substance pair that other frequencies will only differ by concentrations of fragments and their effective charges.

Indeed, expansion into series is the cause behind the fact that an equation that contains $n_0(x,t)$ and $v_0(x,t)$, which are values related to lightweight fragments, is the only equation to express frequency oscillations for the highest – the zero – term. Subsequent computations identify no changes in the frequencies.

Thus, the frequency diagram, for rather long time spans allows finding the charge vs. the mass of interacting substances.

Another conclusion from the above mathematical considerations is that the currents generated by concentrations of substances will be simply summed up for the first two terms of the series. There will be no non-linear effects of adding the currents for the first two terms of the series.

Building frequency dependence

First and foremost, we should point out that we discovered the current $j(x,t) = n(x,t)v(x,t)$ through experiments, not concentrations of interacting substances. Consequently, before we integrate the concentration over time twice, we are to take into account the travel speeds of lightweight fragments $v(x,t)$

The speed and the electric field are linked by the relation $E_0(x,t)\cos(\omega t) = v(x,t)\sin(\omega t)$. Consequently, multiplying these values by one another will double up the principal frequencies, and changes to minor frequencies will occur. However, the shapes of the electrical field spectrum (see Fig. 7 above) so that the minor frequencies are low, these changes can be discarded, while assuming that the frequencies should be twice as low as those found by measurements.

Thus, the distribution of concentrations by frequencies can be found by using a simple scheme below, namely

➤ Taking measurements of currents at certain time moments $t_i = i \cdot \Delta t$, where Δt is a time span between consecutive measurements, i a number of a measurement taken, and $i \in \overline{1, N}$, N is the amount of measurements.

➤ Carrying out the Fourier transformation against time to get the complex value function $J(\omega) = \sum_{k=0}^{\infty} j(t_k) e^{i\omega t_k}$.

➤ Finding the power spectrum $P(\omega) = J(\omega)J^*(\omega)$ and the normalized Schuster diagram $D(\omega) = NP(\omega) / (Dj)^2$.

➤ Discarding frequencies which have values below the criterion D_{\max} ; the criterion can be found, based on a preferred probability that the frequency is significant.

➤ For the new frequency power $\hat{P}(\omega)$, carrying out division by power four of the frequency to find the function $G(\omega) = \frac{P(\omega)}{\omega^4}$.

➤ In the function found, dividing the frequencies by 2.

➤ To find the percentage of substances that correspond to this or that specific frequency, it is convenient to carry out a transformation by finding

the function $Q(\omega) = \frac{100\% \cdot G(\omega)}{\int_{-\infty}^{+\infty} G(\omega) d\omega}$.

Concentration diagram for tin oxyhydrate

Let us apply the method proposed above to experiments of taking measurements of spontaneous current oscillations in tin oxyhydrate by means of the instrument described earlier in this Article.

Measurements were taken throughout a period of three months; each measurement lasted for six hours. Measurements of spontaneous currents were taken at a rate of five times per second. A total of 46 measurement series were conducted in three months.

Computations were done to a probability exceeding 0.99.

Please refer to Fig. 8 below to see a number of concentration distributions against frequencies. All the forty-six experiment series are provided in Appendix 1.

Fig. 3 provides a general idea of fluctuations in percentages through a 3D diagram.

It is worth mentioning that it is more convenient to consider concentrations, depending on an experiment, by taking the same frequency depending on an experiment number. In other words, if $Q_i(\omega)$ is the power spectrum that corresponds to an experiment number i , then we build a set

$L_{\omega_0}(i) = Q_i(\omega_0)$, $i \in \overline{1, M}$, where M is the total number of experiments, which is 46 in our case. Please refer to Fig. 10 below to see the diagram $L_{\omega_0}(i)$ vs. experiment number at a fixed frequency of $\omega_0 = 10^{-3}$ Hz (the frequency for which computations show the highest concentration practically in all the experiments).

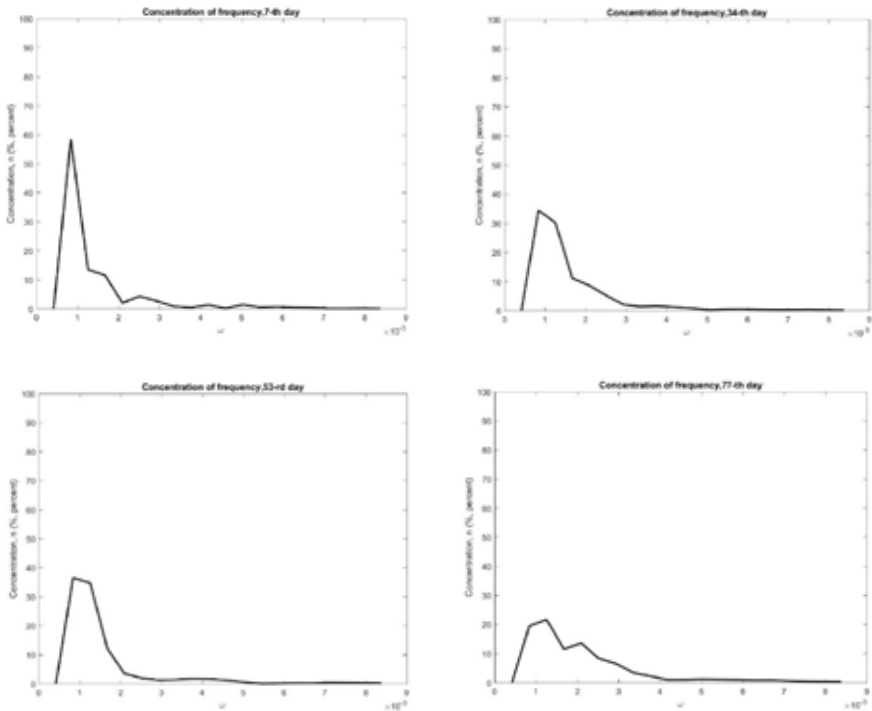


Fig. 8. Concentration diagrams (percentage of general composition), depending on frequencies for various days (7th, 34th, 53rd, and 77th day)

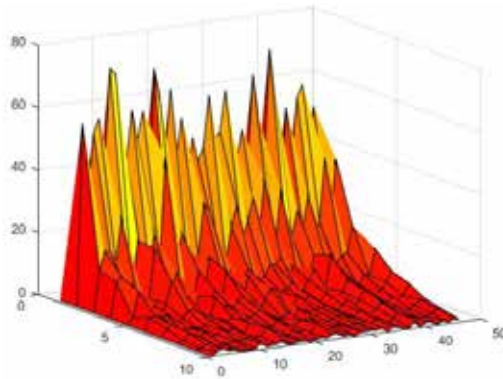


Fig. 9. Composition percentage against frequency and experiment numbers

The above diagram suggests that the process is of oscillatory nature, so it is hard to tell visually if these oscillations are random or not, and to predict if the oscillation amplitude will undergo changes or it will remain unchanged.

To learn more about these patterns, we will resort to the Fourier analysis by using the Schuster diagram again. Thus, the experiments in question comprise three periods (approx 2.4 days, approx 1.3 day, and 1.2 day) that correspond to periodic current oscillations in the group of substances that generate the principal current power.

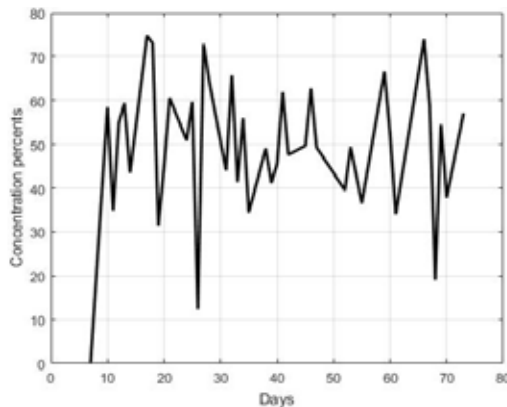


Fig. 10. Concentration oscillations against days

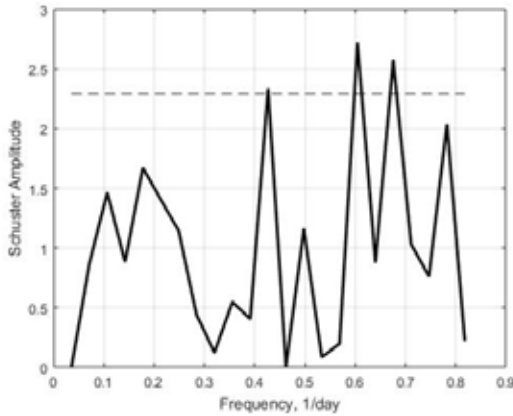


Fig. 11. Schuster diagram for $L_{\omega 0}(\bar{t})$

The dashed line denotes the bottom value of the criterion

Alongside them, there are also oscillations present, which may probably be random.

General equation

Thus, based on the diagrams built, we can conclude that oscillations, firstly, are of electrical nature in any polar oxyhydrate, and, secondly, these oscillations can be observed in practice – in particular, we discovered them in tin oxyhydrate through experiment, which has been considered in detail in this Article. Similar data are also available for iron, yttrium, and other polar oxyhydrates.

Based on the above observations, it is convenient to build a general model of oscillatory motions of particles in polar media.

Let us reiterate the deduction of Formulas (3-9) to get Equations (9) as a result. Let us take the first equation of Model (3), and consider it separately:

$$\frac{\partial v(x,t)}{\partial t} + v(x,t) \frac{\partial v(x,t)}{\partial x} = -\gamma E(x,t), \quad x \in (-\infty; +\infty), \quad t \in (0; +\infty), \quad (17)$$

Let us introduce the function $\Psi(x,t)$, so that $v(x,t) = -2\gamma \frac{1}{\Psi(x,t)} \frac{\partial \Psi(x,t)}{\partial x}$, while taking into account that $E(x,t) = -\frac{\partial \Phi(x,t)}{\partial x}$; as a result, we obtain the equation

$$\frac{\partial \Psi(x,t)}{\partial t} = \gamma \frac{\partial^2 \Psi}{\partial x^2} + (C(t) - \gamma \Phi(x,t)) \Psi(x,t), \quad x \in (-\infty; +\infty), \quad t \in (0; +\infty). \quad (17)$$

According to what was proved earlier, $E(x,t) = \sin(\omega t)V(x,t)$ for a substance pair; and for N substances, it is $E(x,t) = \sum_{j=1}^N \sin(\omega_j t)V_j(x,t)$. Consequently, $\Phi(x,t) = -\sum_{j=1}^N \sin(\omega_j t) \int_0^x V_j(x,t) dx$.

Similarly, $v(x,t) = \sum_{j=1}^N \cos(\omega_j t)V_j(x,t)$. As $v(x,t) = -2\gamma \frac{1}{\Psi(x,t)} \frac{\partial \Psi(x,t)}{\partial x}$, consequently, $\Psi(x,t) = \exp\left(-\frac{1}{2\gamma} \int_0^x v(x,t) dx\right)$. Due to oscillatory nature of the

function, $v(x,t) = \sum_{j=1}^N \cos(\omega_j t)V_j(x,t)$ the function $\Psi(x,t)$ is also of oscillatory nature, and can be expressed through a Fourier series $\Psi(x,t) = \sum_{j=1}^N \cos(\omega_j t)\Psi_j(x,t)$ at the same frequencies.

In this expression, we will, firstly, substitute the sinuses with complex exponents (because earlier we considered a specific initial problem, while initial problems may have various initial conditions), and, secondly, we will assume that the components of the function expansion $\Psi(x,t)$ into Fourier series $\Psi_j(x,t)$ only differ by the coefficients that depend on time: $k_1(t)\Psi_1(x,t) \approx k_2(t)\Psi_2(x,t) \approx \dots \approx k_N(t)\Psi_N(x,t) = \psi(x,t)$. Thirdly, it is worth noting that there exist many substances, so it is fair to substitute the upper limit of the sum with an infinite one, and the integral, whenever necessary, can be substituted with series. Then, the series $\Psi(x,t) = \sum_{j=1}^N \cos(\omega_j t)\Psi_j(x,t)$ can be rewritten as

$$\Psi(x,t) = \psi(x,t) \sum_{j=1}^{\infty} \frac{1}{k_j(t)} e^{i\omega_j t} = \psi(x,t) \int_{-\infty}^{+\infty} e^{i\omega t} K(\omega) d\omega \quad (18)$$

Moreover, due to nonlinear nature of the problem, $\frac{\partial^2 \Psi(x,t)}{\partial x^2} \sim \psi \left(\int_{-\infty}^{+\infty} e^{i\omega t} K(\omega) d\omega \right)^2$ Substituting this expression into (17), we find that

$$\frac{1}{\int_{-\infty}^{+\infty} e^{i\omega t} K(\omega) d\omega} \frac{\partial}{\partial t} \psi(x, t) = \gamma \frac{\partial^2 \psi}{\partial x^2} + (C(t) - \gamma \Phi(x, t) + \zeta(t)) \psi(x, t).$$

$$= \frac{i \int_{-\infty}^{+\infty} \omega e^{i\omega t} K(\omega) d\omega}{\int_{-\infty}^{+\infty} e^{i\omega t} K(\omega) d\omega} \cdot$$

where $\zeta(t) = \frac{i \int_{-\infty}^{+\infty} \omega e^{i\omega t} K(\omega) d\omega}{\int_{-\infty}^{+\infty} e^{i\omega t} K(\omega) d\omega} \cdot$

Substituting the variable, $\tau = \frac{1}{\Omega} \int_{-\infty}^{+\infty} \omega e^{i\omega t} K(\omega) d\omega$, $\Omega = \int_{-\infty}^{+\infty} K(\omega) d\omega$, we obtain an equation similar to the Schrödinger wave equation

$$-i \frac{\Omega}{\gamma} \frac{\partial}{\partial \tau} \psi(x, t) = \frac{\partial^2 \psi}{\partial x^2} + \frac{1}{\gamma} (C(t) - \gamma \Phi(x, t) + \zeta(t)) \psi(x, t).$$

Summary

Thus, the formulated lemma has been proved.

References

1. Yuri I. Sucharev. Electromagnetic Noise Entangled States of Cluster Colloid Systems.2016.Vol.45.№1.C.1-41.R0I:jbc-01/16-45-1-1
2. Yuri Sucharev. Nonlinearity of Colloid Systems: Oxyhydrate Systems. Switzerland, UK,USA: Trans Tech Publications, 2008. P.433.
3. E. Frid. Initial Introduction into Abstract Algebra. Translated from Hungarian.-Moscow.:Mir,1979. 260p.
4. A. I. Akhieker, Yu. P. Stepanovsky. From Light Quanta to Color Quarks. Kiev. Naukova Dumka.1993.; J.-M.Richard. An introduction to the quark model//:1205.4326[heh-ph].
5. Yuri I. Sucharev. The generalized Schrödinger-Batanov equation important fundamental basis for new approaches to the study of physics and chemistry of macrosystems, for example, colloidal-chemical. Butlerov Communications. 2018.Vol.53№2.P.1-27: jbc-01/18-53-2-1

6. Ю.И. Сухарев, И.Ю. Апаликова. НАНОТОКОВЫЕ СЕГНЕТОЭЛЕКТРИКИ ГЕЛЕВЫХ ОКСИГИДРАТОВ. Монография. Серия “Бутлеровское наследие”. Книга1.- Казань: Изд. ООО “Инновационный издательский дом Бутлеровское наследие”.2019.- 440с.

7. I.Yu. Apalikova, B.A. Markov, Yu.I. Sukharev. Characteristics of quantum macrosystem as principal specific feature of colloid gel oxyhydrates. Butlerov Communications A. 2021. Vol.1. No.1. Id.19. DOI: 10.37952/ROI-jbc-A/21-1-1-19

CORRELATION RELATIONS OF MEAN ARTERIAL PRESSURE WITH HEMATOPOIETIC PARAMETERS DURING BURN TOXEMIA DEPENDING ON AGE

Muhitdinova Hura Nuritdinovna

Doctor of Medical Sciences, Full Professor
Center for the Development of Professional Qualifications
of Medical Workers

In the first 10 days of the period of burn toxemia, the tendency towards a decrease in AvBP created a risk of circulatory inefficiency in burned children under the age of 3 years. A gradual decrease in the AvBP mesor within the age norm at the age of 7.1-18 years corresponded in time to a decrease in the systemic inflammatory response of the body to burn stress against the background of effective stress-limiting therapy. Strengthening the inflammatory response of cellular immunity in the form of lymphocytosis created the risk of developing arterial hypertension in group 4. An inverse correlation was found between AvBP and the level of prothrombin index (PI) in persons over 61 years of age.

Keywords: correlation, mean arterial pressure, blood, burn toxemia.

Relevance

Mean arterial pressure (AvBP) is the pressure in the bloodstream during the entire cardiac cycle, regardless of systole and diastole. This indicator reflects the blood supply to vital organs. Higher numbers are an indicator that the heart is working harder than it should. Large AvBP is observed in heart failure, myocardial infarction. Low AvBP can be fatal if left uncorrected. With numbers below 60 mmHg, the organs do not receive the required blood volume, and a state of shock develops. AvBP falls in sepsis, blood loss, stroke, and polytrauma. Sudden pressure drops for people over 60 are more dangerous than consistently high or low readings. They several times increase the load on the heart, accelerating its wear and tear, and provoke a hypertensive crisis, which can cause various complications, including myocardial infarction, can cause cerebrovascular disorders, coronary heart disease, and stroke [1-4]. Insufficient

information on the effect of hemodynamic changes on hematopoiesis in burn toxemia prompted us to study and assess the effect of severe burn toxemia on the relationship between hemodynamic parameters and the function of hematopoietic organs in age groups.

Purpose of the study. Study and assess the correlations between mean arterial pressure and blood parameters during burn toxemia, depending on age

Material and research methods. The studies were carried out in the following age groups: group 1 - 6 months - 3 years, group 2 - 3.1-7 years old, group 3 - 7.1-18 years old, group 4 - 18.1-40 years old, group 5 - 41-60 years old, group 6 - 61-85 years old. The characteristics of the clinical material are presented in tab. 1.

Clinical characteristics of patients, severity of burn injury

Table 1

Groups	Men	Women	Age	Height, cm	Weight, kg	Total burn area, %	area of 3B degree, %	IF, units	days in hospital
1	15	7,0	18.1±7.5 months	77.2 ±5.1	10.7 ±1.4	33.6 ±10.1	9.0 ±6.5	42.1 ±16.6	22.2 ±9.6
2	11	9	4.8±1.0* years	106.2 ±9.3*	21.6 ±10.8	50.8 ±14.9	25.8 ±11.6	88.7 ±36.8	46.3 ±18.4
3	14	4	12.1±3.0* years	147.5 ±14.5*	38.2 ±10.8*	50.7 ±12.7	11.7 ±6.5	76.3 ±19.1	34.3±18.2
4	13	2	27.1±4.8* years	173.5 ±6.3*	70.7 ±7.3*	58.2 ±14.1	20.2 ±12.0	112.3 ±35.6*	48.0 ±19.6
5	5	3	49.4±7.2* years	164.6 ±5.9*	72.0 ±12.8*	53.8 ±15.0	13.3 ±8.1	90.0 ±25.0*	26.5 ±13.4
6	5	3	70.1±6.4* years	169.0 ±10.0*	73.5 ±6.8*	35.7 ±10.6	20.5 ±7.8	77.3 ±30.2	41.6 ±19.3

*-deviation is significant relative to the indicator in group 1

As shown in Table 1, there were 63 male patients, 28 female patients. Age-related, anthropometric differences were significant in the absence of significant differences in the age groups of the total area of the burn, deep damage of grade 3B and the duration of inpatient treatment. A significant predominance of IF in groups 4 and 5 was found, due to the aggravation of the condition by concomitant factors, such as combined trauma, carbon monoxide poisoning, concomitant ischemic heart disease, burns of

the upper respiratory tract.

Modern methods for calculating the average BP:

1. $AvBP = DBP + (SBP - DBP)/3$;
2. $AVBP = 2/3 (DBP) + SBP/3$;
3. $AvBP = [(2 \times DBP) + SBP]/3$;

where AvBP – mean arterial pressure,

DBP – diastolic BP,

SBP – systolic BP. The mean arterial pressure was monitored according to formula 1.

The research data were processed by the method of variation statistics using the Excel program by calculating the arithmetic mean values (M) and the errors of the means (m). To assess the significance of the differences between the two values, the parametric Student's test (t) was used. The interrelation of the dynamics of the studied indicators was determined by the method of paired correlations. In this case, the critical level of significance was taken equal to 0.05. Intensive therapy from the moment of admission was aimed at removing burn shock, adequate anesthesia and intravenous administration of crystalloids, volemic solutions, blood components, parenteral nutrition, metabolic, anti-inflammatory, anticoagulant, according to indications of coronary active, cardiotoxic, antiarrhythmic therapy under volume control.

Results and its discussion

As shown in fig. 1, there were no significant differences by age groups, however, a lower level of AvBP was noticeable in younger groups 1 and 2 of children within 80-85 mm Hg, while in groups 5 and 6 of older patients AvBP was above 90 mmHg. Attention is drawn to the tendency to a gradual decrease in the indicator for 6-10 days in adolescent and adolescent patients (group 3). The latter can be explained by the fact that under conditions when the area and depth of damage to the skin surface did not differ significantly from those in other age groups, the IF was 76.3 ± 19.1 units, a gradual decrease in the AvBP mesor corresponded in time to a decrease in the systemic inflammatory response of the body to burn stress against the background of effective stress-limiting therapy. The most pronounced correlation (fig. 2) of changes in AvBP and the red part of the blood in the first 10 days of toxemia was found in subgroup 1 with a total area of the burn surface of $37.3 \pm 14.7\%$, grade 3B - $3.1 \pm 4.4\%$, IF 42.5 ± 15.7 units, in children (aged 3.1-7 years, who were in intensive care

in the ICU for up to 10 days.

Dynamics of mean arterial pressure depending on age, mmHg

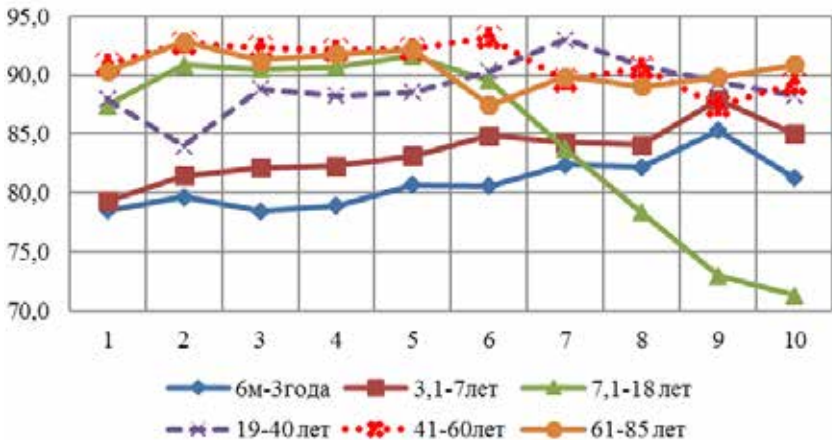


Fig.1

Thus, the inverse correlation of AvBP with the number of erythrocytes, hemoglobin, hematocrit was -0.679 ; -0.705 ; -0.438 , respectively. That is, there was a noticeable likelihood of a side effect of increased blood transfusion in preschool children, when a further increase in erythrocyte, hemoglobin and blood gamatocrit values could lead to a decrease in the average BP, a decrease in the efficiency of blood circulation in severe burn toxemia in children of group 2. The same, but less pronounced trend was observed in subgroup 3 (with a total burn area of $50.8 \pm 14.9\%$, grade 3B - $25.8 \pm 11.6\%$, IF- 88.7 ± 36.8 units, duration of treatment in the ICU for more than 21 days) in toddlers.

Correlation relationships of mean BP with erythrocytes, hemoglobin, platelets and hematocrit during the period of toxemia in children 3.1-7 years old according to the severity of the burn

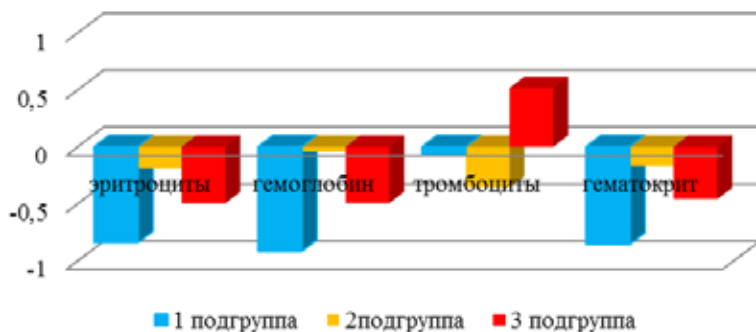


Fig.2

Fig. 3 shows the correlation between AvBP and the parameters of the peripheral blood formula in the first 10 days of treatment. The revealed tendency for a direct relationship between the AvBP level and the ESR indicator indicates a tendency towards a direct influence of the systemic inflammatory response on the AvBP level in all age groups. At the same time, a negative effect of leukocytosis on hemodynamics was revealed in the 1,2,3,4 and 6 age groups. Direct correlation between AvBP and the number of stabs in the peripheral blood was noted in 1,5,6 and negative in 2,3,4 groups. Moderately and weakly positive influence of the acute phase of the inflammatory reaction in the form of growth of segmented nuclei on hemodynamics was found in groups 1,3,5,6, and a statistically significant opposite in group 4. Strong correlations between the number of blood lymphocytes and the level of AvBP in groups 4 and 6 (0.83 and -0.85, respectively) turned out to be oppositely directed. That is, an increase in the inflammatory response in the form of lymphocytosis created a risk of arterial hypertension in group 4, and in group 6, a decrease in the lymphocytic response could provoke an increase in AvBP, which in-

creased the risk of cardiovascular complications in patients over 61 years of age.

Correlation of average BP with indicators of leukocytes, stab, segmented, monocytes, ESR

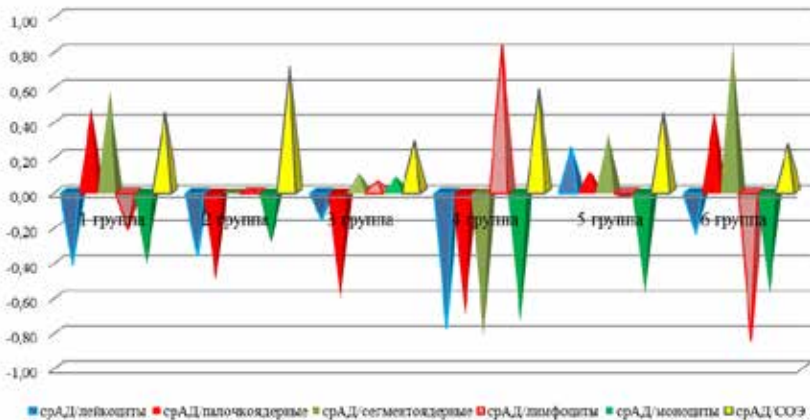


Fig.3

Thus, a rather complex relationship was revealed between the AvBP level and the age-related characteristics of the cellular response of the immune system at different age periods to burn injury. The predominance of the negative effect of an increase in the inflammatory reaction during the period of toxemia of burn disease (an increase in the number of leukocytes, stab, segmented, monocytes) on hemodynamics at the age of 41-60 years, which confirms the opinion about an increased risk of complications of arterial hypotension. An increase in the number of lymphocytes in group 4 and an increase in segmented nuclei in group 6 can serve as a sign of the emergence of a risk of complications of arterial hypertension. A low level of lymphocytes in group 6 is accompanied by an increase in AvBP (-0.85) with a reliable direct dependence of AvBP on segmented (0.78), that is, an acute or exacerbation of the inflammatory reaction in old age is fraught with arterial hypertension, which increases the risk of corresponding complications (heart attack, stroke, etc.).

As shown in fig.4, the direct correlation of changes in AvBP with the level of urea and creatinine in the blood, detected in group 3, and the feedback in infancy (group 1) characterized the oppositely directed effect on hemodynamics of deterioration of renal excretory function in conditions of hypercatabolism, when an increase in intoxication already in the

first 10 days of the toxemia period leads to a decrease in AvBP, inefficiency of blood circulation in burnt children under the age of 3 years. In group 3 (7.1-18 years old), due to the more anatomically and functionally mature characteristics of the cardiovascular system, hemodynamics reacted to the systemic inflammatory response in conditions of hypercatabolism by increasing cardiac output and increasing AvBP.

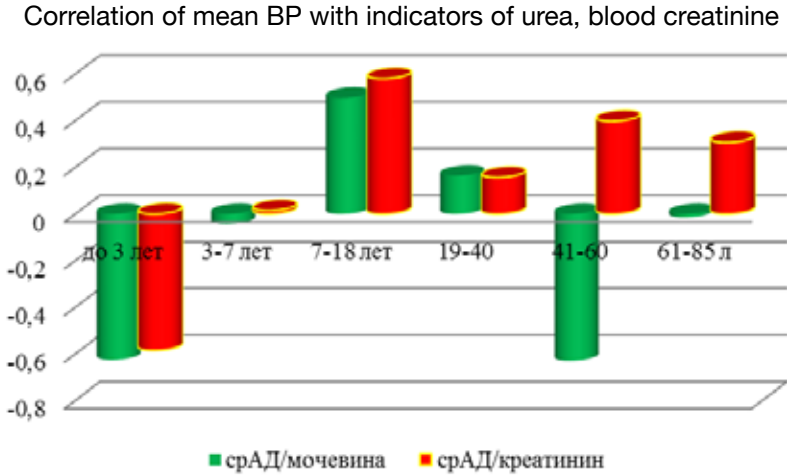


Fig.4

Correlations between mean BP and total protein and albumin values

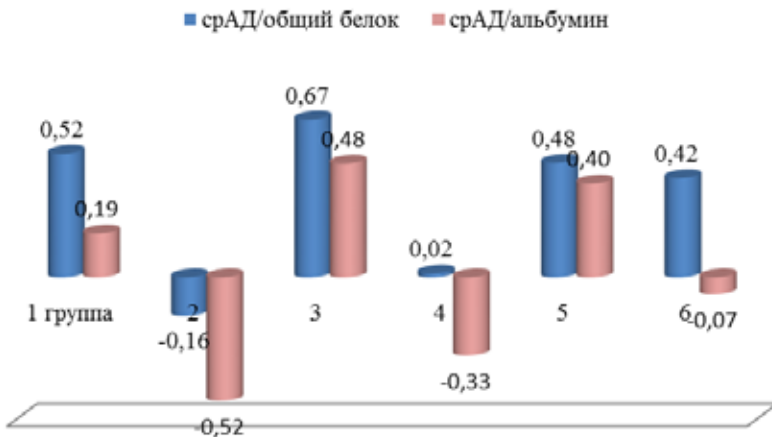


Fig.5

A moderate positive effect of a possible increase in total protein and blood albumin on the AvBP level was found in the 1,3,5,6 age groups, which confirms the timeliness of the corresponding correction (fig.5). The negative effect of an increase in sodium in plasma in groups 4 and 6 on the level of AvBP revealed the appearance of a probability of a decrease in AvBP in conditions of a further increase in hypernatremia (fig.6).

Correlations of mean BP with plasma potassium and sodium levels

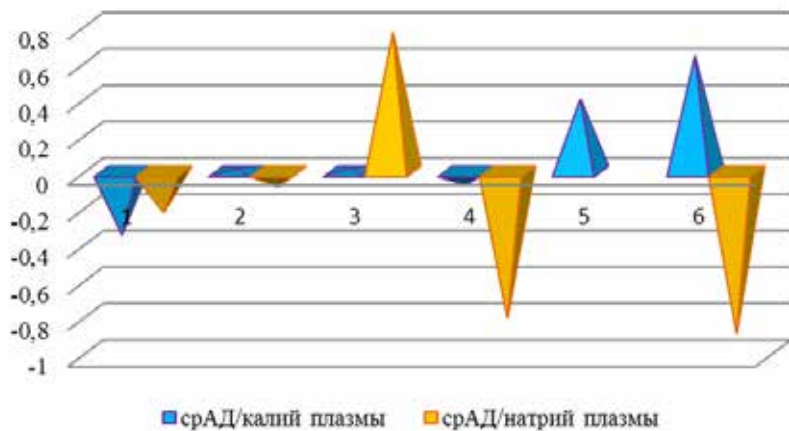


Fig.6

A direct strong relationship between the blood diastase level and AvBP in group 3 (fig. 7) may be a sign of a compensatory hemodynamic response to intoxication caused by pancreatic dysfunction during toxemia in patients aged 7.1-18 years (0.805).

Correlations of mean BP with diastase, AST and ALT values of plasma

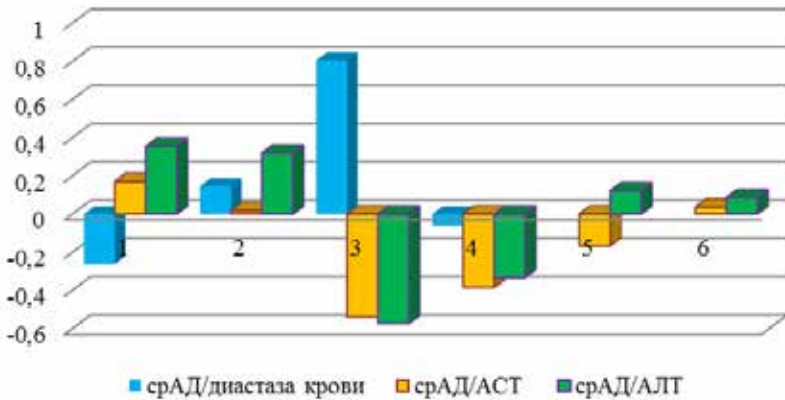


Fig.7

The revealed inverse correlation of AvBP and PI level in group 6 (fig.8) indicated a favorable effect of anticoagulant therapy in persons over 61 years of age (-0.863).

Correlation of mean BP with indicators of fibrinogen, thrombotest, prothrombin index

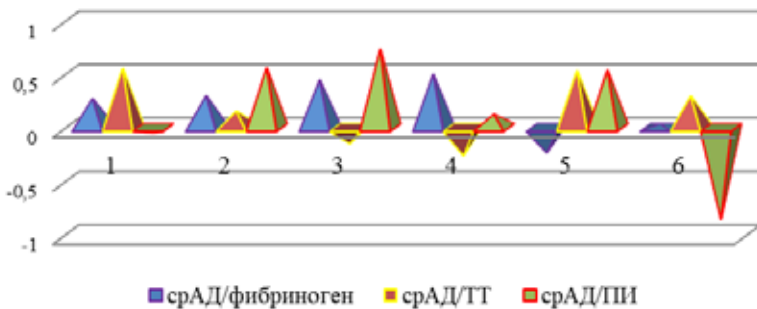


Fig.8

Conclusions

In the first 10 days of the toxemia period, the risk of a decrease in AvBP was revealed in burnt children under the age of 3 years. In group 3 (7.1-18 years old), hemodynamics reacted to the systemic inflammatory

response with a compensatory increase in cardiac output, an increase in AvBP with a tendency to a decrease in AvBP mesor within the age norm for 7-10 days. An increase in the inflammatory response in the form of lymphocytosis created a risk of arterial hypertension in group 4 (41-60 years old). An inverse correlation was found between AvBP and PI levels in group 6 (61-75 years old).

References

1. <http://www.medicus.ru/pediatrics/patient/kriterii-arterialnoj-gipertenzii-u-detej-i-podrostkov-28563.phtml>
2. <https://cardiograf.com/napor/vidy/srednee-arterialnoe-davlenie.html>
3. <https://pansionat-zabota24.ru/polezno-znat/skachet-davlenie-u-pozhilogo-cheloveka-cto-delat/>
4. https://www.bsmu.by/downloads/kafedri/k_poli_ter/stud/15.pdf

**ETIOPATHOGENETIC THERAPY OF MICROCIRCULATION
DISORDERS IN PATIENTS WITH COVID-19 ASSOCIATED
PNEUMONIA**

Ponomareva Maria Nikolaevna

Doctor of Medical Sciences, Full Professor
Institute for Continuing Professional Development
ORCID ID 0000-0001-6522-3342

Petrov Ivan Mikhailovich

Doctor of Medical Sciences, Associate Professor, Head of Department
ORCID ID 0000-0001-7766-1745

Kalyuzhnaya Elena Nikolaevna

Postgraduate

Kalinina Vera Leonidovna

Candidate of Medical Sciences, Associate Professor
Institute for Continuing Professional Development

Bredneva Anna Igorevna

Candidate of Medical Sciences, Associate Professor
Institute for Continuing Professional Development

Tyumen State Medical University
Tyumen, Russia

Purpose: to study the effect of statins, antioxidants and non-steroidal anti-inflammatory drugs on the state of the bulbar conjunctiva.

Material and methods: the study involved 54 patients (108 eyes), 27 people (18 men and 9 women), identical in age with a history of COVID-19-associated pneumonia diagnosis. Group 1 consisted of patients with metabolic syndrome, group 2 did not have metabolic syndrome. Within a month, patients received rosuvastatin, depending on the target indicators, Thioctic acid tablets, topical Emoxipin solution 1% and Broxinac solution.

Results: there was an improvement in conjunctival microcirculation in patients of both groups (54%/50%, respectively) in the form of paravasal changes, (10%/11%, respectively) changes in the shape of blood vessels, (71%/78%, respectively) intravascular changes.

Conclusion: the proposed method of treatment is effective in the presence of changes in the microcirculation of the conjunctiva of the eyeball.

Keywords: bulbar conjunctiva, COVID-19, statins, antioxidants, non-steroidal anti-inflammatory drugs

Relevance

Characteristic of COVID-19 is the presence of a severe acute respiratory syndrome with the development of microangiopathy, hypercoagulable syndrome (thrombosis and thromboembolism) and damage to the organs of the immune system with the interest of the vascular endothelium (development of endotheliosis), which leads to hypercoagulation [1, 2].

Therefore, during the period of convalescence, it is necessary to control the state of organs and systems. Prospective patient follow-up is still scarce and the consequences of this disease should be studied and covered in the modern scientific literature. There are works describing the clinical manifestations of a new coronavirus infection: conjunctivitis, anterior uveitis, retinitis and optic neuritis in the form of single observations. These works describe the clinical manifestations of lesions of the ocular surface with the provision of features of the course of conjunctivitis, treatment of these manifestations, depending on polymorbidity [3,4]. Due to the early detection of cases, timely quality medical care, the number of patients who have had this infection is growing. There is a work devoted to the pathology of the orbit in COVID-19 and the study of the existing eye pathology in patients who could enter a specialized department during the incubation period of the disease (from 7 to 14 days) without clinical manifestations [5].

Our studies of the features of microcirculation of the bulbar conjunctiva from the position of a marker of somatic or ophthalmic pathology showed the presence of microangiopathy and hypercoagulable syndrome with thrombosis of the bulbar conjunctiva as a result of infection in COVID-19 patients with associated pneumonia three months after discharge from the hospital [3,5]. At the same time, patients with cardiovascular diseases are more susceptible to complications against the background of severe endotheliosis, including as a result of atherosclerotic vascular lesions [6,7,8]. Titov V.N., in his studies showed infection (less often genetic factors) can be an etiological factor of atherosclerosis [9,10].

Purpose: study of the effect of statins, antioxidants and non-steroidal anti-inflammatory drugs on the state of the bulbar conjunctiva.

Materials and methods

The study involved 54 patients (108 eyes), 27 people each (18 men and 9 women), identical in age with a history of COVID-19-associated pneumonia diagnosis. Group 1 consisted of patients with metabolic syndrome, group 2 did not have metabolic syndrome.

Patients were examined by a therapist, cardiologist, ophthalmologist, functional diagnostics physician 3 months after discharge from the hospital with informed consent. Median age was 61 years (range 47 to 75 years). An additional criterion for inclusion was dyslipidemia. A history of such diseases as the choroid, optic nerve, retina, and eye trauma before the onset of a new coronavirus infection was an exclusion criterion.

Ophthalmic examination included standard methods (visometry, static and kinetic perimetry, biomicroscopy, direct and reverse ophthalmoscopy, fundus examination using a 78D non-contact aspherical high-diotric lens, Maklakov tonometry). Conjunctival microvessels were examined using a Slim Lamp SL-45 slit lamp using a CMOS video camera (5MP). In the study groups, perivascular changes were determined:

- single pathological foci of microstasis (PFM), widespread edema (WE), single hemorrhages (SH);
- changes in the shape of blood vessels: a decrease in arterio-venous ratio of more than 1/3 (AVR), pathological tortuosity of veins (PTV), aneurysms in venules and capillaries (A), the presence of desolation zones (DZ), the formation of a reticular structure (RS);
- intravascular changes: Sludge phenomenon (Sph).

Biochemical blood test: total cholesterol (TC), high density lipoprotein (HDLP), low density lipoprotein (LDLP), extra low density lipoprotein (EL-DLP), triglycerides (TG). To assess the risk of developing cardiovascular diseases, the atherogenic coefficient (AC) of lipid fractions was calculated using the formula: $AC = (TC - HDLP)/HDLP$.

The therapy consisted in the appointment of rosuvastatin (depending on the target indicators) [6], antioxidants per os - Thioctic acid 600 mg once a day, additionally instilling a non-steroidal anti-inflammatory (NSAI) solution of Broxinac® into both eyes, 1 drop 2 times a day, and antioxidant topically 1% solution of Emoxipin® three times a day) for 1 month [10].

Statistical processing of the results was carried out using the STATISTIC 23.0 software package. The levels of the determined indicators were described on the basis of the median and interquartile range (Me [25%; 75%]). The significance of differences in indicators between groups was assessed by nonparametric methods. Differences were considered statistically significant at $p < 0.05$. Correlation analysis according to Spearman's

method was used to identify links between the studied tests.

Results and Discussion

Analysis of the somatic status of patients revealed a significant ($p < 0.05$) increase in body mass index (BMI) and a tendency to increase in age in group 1 compared with group 2. A large range of lipid spectrum values was revealed in both groups, which is caused by the presence or absence of basic therapy for dyslipidemia. The average values of the lipid spectrum indicators (tab. 1, 2) are within the target levels (according to the European Society of Cardiology (ESC) and European Atherosclerosis Society (EAS) Recommendations for the diagnosis and treatment of dyslipidemia 2019).

Table 1. Levels of the determined indicators of lipid metabolism in patients of group 1 (n=27)

	Min	Max	Average	Mean square deviation
TCH TC	3.18	7.87	5.4889	1.18343
HDLP HDL	0.8	3.1	1.351	0.4976
LDLP LDL	1.46	5.55	3.2867	1.02213
ELDLP PLDL	0.05	4.1	0.8915	0.78143
TG TG	0.1	9.02	1.9604	1.71833
AC AC	2.98	1.54	3.06	-

Table 2. Levels of the determined indicators of lipid metabolism in patients of group 2(n=27)

	Min	Max	Average	Mean square deviation
TCH TC	2.4	9.15	5.3007	1.66169
HDLP HDL	0.89	2.53	1.407	0.41124
LDLP LDL	0.89	6.72	3.2544	1.4091

ELDLP PLDL	0.28	1.46	0.5911	0.27493
TG TG	0.62	3.22	1.3056	0.60301
AC AC	1.70	2.62	2.77	-

The presented results of the study determined that after three months in patients who underwent a new coronavirus infection with lung damage, the most pronounced changes relate to the TCH and LDLP indicators, which are at the upper limit of the target levels. Against the background of changes in the structure of the dyslipidogram (a tendency to an increase in TCH, LDLC) in patients of both groups, hemodynamic disorders of the conjunctiva of the eyeball were revealed. The images of the state of the microcirculatory bed of the conjunctiva of the eyeball in patients with primary treatment (violation of the microvasculature architectonics) are presented: the presence of perivascular changes, the shape of the vessels and intravascular changes (fig. 1).

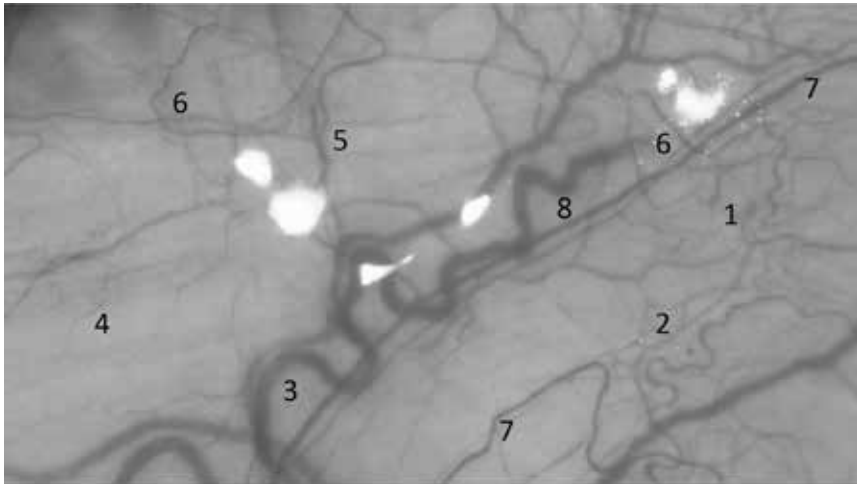


Fig. 1 Biomicroscopy of the conjunctiva of patient D., 62 years old: 1-perivascular edema, 2-single hemorrhage, 3-decrease in the arteriovenous ratio of more than $\frac{1}{4}$, 4 - areas of desolation, 5 - aneurysms in the venules and capillaries, 6-microthrombosis, 7-pathological tortuosity of the veins, uneven caliber, 8-collateral vessels of the conjunctiva

In group 1, there was a tendency towards a decrease in hemorrhagic

manifestations, but an increase in changes in the shape of blood vessels (the presence of aneurysms and RS), which, from our point of view, is associated with the presence of impaired glucose tolerance, more pronounced metabolic changes in the body (fig. 2). Patients of group 2 showed a tendency to an increase in DZ (fig. 2), which may be associated with the frequency of atherosclerotic vascular changes (AB, increased TIMC).

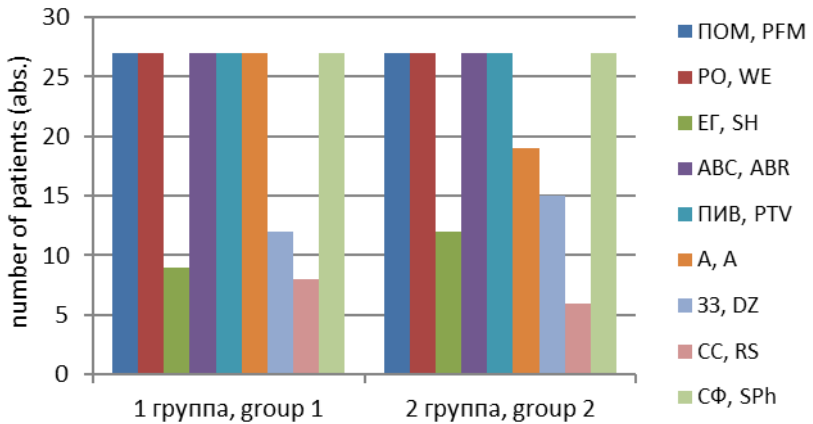


Fig. 2. Conditions of the microcirculatory bed of the bulbar conjunctiva in patients before treatment In English

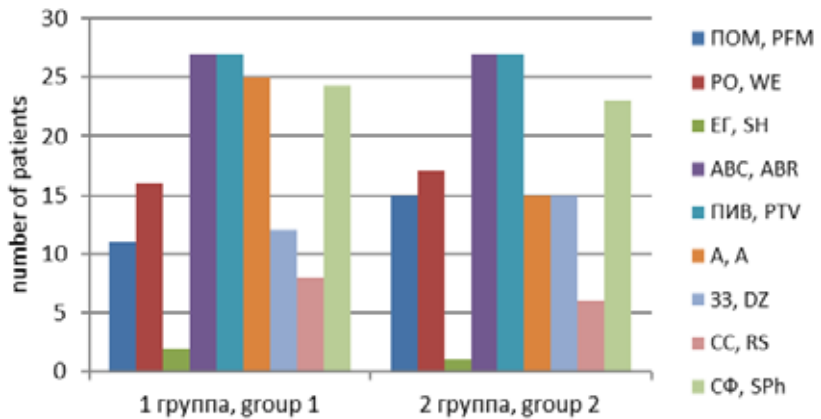


Fig. 3. Conditions of the microcirculatory bed of the bulbar conjunctiva in patients after treatment (In English)

After 1 month, against the background of the therapy, there was a decrease in the severity of hemodynamic disorders of the conjunctiva of the eyeball in both groups (fig. 3): improved intravascular changes (SF) in 71% and 78%, respectively; perivascular changes (PFM, WSE, SH) in 54% and 50%, respectively; changes in the shape of blood vessels (AVR, PTV, A, DZ, RS) in 10% and 11%, respectively. Improvement of the microcirculation of the conjunctiva of the eyeball in the form of perivascular and vascular changes is associated with the administration of antioxidants systemically and locally (Thioctic acid per os and Emoxipin® solution 1%). Bromsinac, with the frequency of instillation of the drug 2 times a day, in this case, performs antiplatelet, anti-inflammatory and decongestant therapy. The absence of significant changes in the shape of blood vessels in this category of patients, both groups 1 and 2, is associated with the presence of chronic endotheliosis due to a combination of dyslipidemia and syntropic chronic diseases.

Conclusion

In patients with dyslipidemia who have undergone COVID-19 associated pneumonia, the use of etiopathogenetic therapy against the background of lipid metabolism correction with rosuvastatin with the prescription of antioxidants systemically and locally, the use of Broxynac locally, is effective in violation of microcirculation in the conjunctiva of the eye.

References

1. The provisional guidelines. Prevention, diagnosis and treatment of new coronavirus infection (COVID-19) Version 7 (03.06.2020). (Electronic resource). (In Russ.)] https://static-0.rosminzdrav.ru/system/attachments/attaches/000/050/584/original/03062020_%D0%9CR_COVID-19_v7.pdf
2. Chan JF, Kok KH, Zhu Z, et al. Genomic characterization of the 2019 novel human-pathogenic coronavirus isolated from a patient with atypical pneumonia after visiting Wuhan [published correction appears in *Emerg Microbes Infect.* 2020 Dec;9(1):540]. *Emerg Microbes Infect.* 2020;9(1):221-236. Published 2020 Jan 28. doi:10.1080/22221751.2020.1719902
3. Kalyuzhnaya E. N., Ponomareva M. N., Petrov I. M., Naimushina A. G., Gapon L. I., Petelina T. I., Yaroslavskaya E. I. Ophthalmological changes in patients with COVID-19 associated pneumonia *Medical science and Education of the Urals.* 2020; Vol. 21;4 (102):117-121 (In Russ.)

4. Grajewski RS, Rokohl AC, Becker M, et al. A missing link between SARS-CoV-2 and the eye?: ACE2 expression on the ocular surface [published online ahead of print, 2020 Jun 4]. *J. Med. Virol.* 2020;10.1002/jmv.26136. doi:10.1002/jmv.26136
5. Polonetsky O. L., L. Z. Polonetsky Endothelial dysfunction and atherosclerosis // *Medical news.* 2012; No. 6. P. 6-11 (In Russ.)
6. Ponomareva M. N., Klyashev S. M., Klyasheva Yu. M., Castro Morales K. A. Diagnosis and treatment of ophthalmopathies in dyslipidemia in the elderly. Tyumen: RIC "Iveks", 2020. 288 p. (In Russ.)
7. Ponomareva M. N., Klyashev S. M., Sakharova S. V., Klyasheva Yu. M., Turlybekova D. A., Novikova N. V., Kalyuzhnaya E. N., Markova A. O., Purtova L. L. Features of ophthalmic diseases in COVID-19 infection *Medical science and education of the Urals.* 2021; Vol. 22, No. 1 (105) pp. 132-136. (In Russ.)
8. Titov V.N. Commonality of atherosclerosis and inflammation: the specificity of atherosclerosis as an inflammatory process. *Russian Journal of Cardiology.* 1999, 5: 3–10. (In Russ.)
9. Titov V.N. Primary and secondary atherosclerosis, atheromatosis and atherothrombosis. M: Triada 2008; 343. (In Russ.)
10. Ponomareva M. N., Petrov I. M., Kalyuzhnaya E. N. Method of complex treatment of bulbar conjunctival hemodynamic disorders in patients with COVID-19 associated pneumonia. Application for invention No. 2021101386 of 23.01.2021. (In Russ.)

FEATURES OF SOMATIC POLYMORBIDITY IN PATIENTS WITH DIABETIC ANGIORETINOPATHY IN PERIPHERAL DIABETIC NEUROPATHY

Petrov Ivan Mikhailovich

Doctor of Medical Sciences, Associate Professor, Head of Department
Tyumen State Medical University
Tyumen, Russia

ORCID ID 0000-0001-7766-1745

Ponomareva Maria Nikolaevna

Doctor of Medical Sciences, Full Professor
Institute for Continuing Professional Development
Tyumen State Medical University
Tyumen, Russia

ORCID ID 0000-0001-6522-3342

Gribanova Evgeniya Konstantinovna

Ophthalmologist G
Multifunctional Clinical and Diagnostic Center,
Tyumen, Russia

Bredneva Anna Igorevna

Candidate of Medical Sciences, Associate Professor
Tyumen State Medical University
Tyumen, Russia

Kalinina Vera Leonidovna

Candidate of Medical Sciences, Associate Professor
Institute for Continuing Professional Development
Tyumen State Medical University
Tyumen, Russia

Purpose - study of somatic status in patients with diabetic retinopathy and peripheral neuropathy. 72 patients with a history of panretinal laser coagulation of the retina were examined. Group 1 (n = 60) included patients with diabetic neuropathy (DNP), group 2 (n = 12) - without it. In group 1, 63.33% of women (38/60) and 36.67% of men (22/60), average age 63.89 + 5.4 years; the duration of the disease is 17.4 + 11.2 years; body mass

index (BMI) 31.98 ± 8.2 . In group 2, patients were represented by 7 women (58.33%), 8 men (41.67%), average age 59.58 ± 8.6 years; the duration of the disease is 11.75 ± 7.7 years; BMI 32.04 ± 7.8 . Obesity affects 71.67% and 83.33% of patients, respectively, arterial hypertension (AH) patients in group 1 have stages 2 and 3, patients in group 2 have stages 1 and 2, chronic heart failure 73.33%/50.0% of patients respectively. In the patients of the study groups, there was a tendency to an increase in the level of low-density lipoproteins. Visual prognosis before and after laser treatment: in group 1, the corrected visual acuity was $0.41 \pm 0.21 / 0.61 \pm 0.59$ before treatment, respectively, after laser treatment $0.69 \pm 2.65 / 0.64 \pm 0.06$ respectively.

Keywords: diabetes mellitus, microvascular changes, comorbidity, diabetic retinopathy.

Introduction

All over the world, there is an increase in the number of patients with diabetes mellitus (DM), called by the experts of the World Health Organization "an epidemic of non-communicable disease" [1, 8.]. Achievements of modern medical science in the treatment of DM are currently bringing to the fore the late complications of the disease as the main medical and social problem, which include, among other things, distal polyneuropathy [4,7]. Diabetic polyneuropathy is a complex of clinical and subclinical syndromes, each of which is characterized by diffuse or focal lesions of peripheral and/or autonomic nerve fibers as a result of diabetes mellitus [2,5]. Diabetic neuropathy is one of the most common complications of diabetes mellitus [7]. It develops in 80% of patients with this disease for more than 10 years [3]. It is known that sensory deficit is the most important risk factor for the development of diabetic foot syndrome, is the cause of disability in DM patients and has a negative effect on the psychosomatic state of patients [3,6]. Currently, the development of the earliest diagnosis and various methods of treatment of diabetic neuropathy is being actively pursued.

Purpose of the study - to study the clinical and statistical features of somatic polymorbidity in patients with diabetic retinopathy and peripheral neuropathy.

Materials and methods

The study was carried out at the SAHCI TO "Multifunctional Clinical and Diagnostic Center" in Tyumen. The object of the study was 72 patients with a history of panretinal laser coagulation of the retina for diabetic retinopathy (DR) using a solid-state laser VISULAS® 532s from ZEISS.

The median age was 65 years, the interquartile range (Q_1 ; Q_3) was 55-71 years old, the share of women was 62.5% (45/72), men 37.5% (27/72). The patients were divided into two groups depending on the presence or absence of such complications as diabetic neuropathy (DNP). Group 1 ($n = 60$) included patients with the presence of DNP, group 2 ($n = 12$) - without it. In group 1, 63.33% of women (38/60) and 36.67% of men (22/60), average age 63.89 ± 5.4 years; the duration of the disease is 17.4 ± 11.2 years; BMI 31.98 ± 8.2 years. In group 2, patients are represented by 7 women (58.33%), 8 men (41.67%), average age 59.58 ± 8.6 ; the duration of the disease is 11.75 ± 7.7 years; BMI 32.04 ± 7.8 . All patients were consulted by a general practitioner, endocrinologist, cardiologist. Among the comorbidities, a study was carried out for the presence of such pathologies as obesity, arterial hypertension (AH), dyslipidemia and chronic heart failure (CHF). As an additional study, we measured weight, height, daily tonometry, venous blood sampling to study the level of total cholesterol, high and low density lipoproteins, as well as electrocardiography and echocardiography. All participants in the study underwent a standard ophthalmological examination: visometry, tonometry (non-contact automatic pneumotonometer from Reichert), perimetry (PNR-2-01), biomicroscopy of the anterior segment of the eye and vitreous (slit lamp "SL-140" from "CarlZeiss Meditec AG"), fundus ophthalmoscopy (using the OcularMaxField 78D non-contact lens). Corrected visual acuity in patients was performed before and after laser photocoagulation of the retina. Statistical analysis was carried out using the statistical packages SPSS for Windows (version 12.0) and STATISTICA (version 7). Continuous variables are presented as $M \pm m$ (mean \pm standard error of the mean) regardless of the criterion used.

Results and Discussions.

The presence of macroangiopathies such as ischemic heart disease (hereinafter IHD), cerebrovascular diseases (hereinafter CVD) is shown in Figure 1. In group 1, IHD was not detected in 27/60 (45%) patients, IHD in various manifestations was detected in 33 / 60 (55%) patients. In group 2, IHD occurred in only 3/12 (25%) patients, while IHD was not present in 9/12 (75%) patients. When examining the presence of CVD, the prevalence of these manifestations was revealed in group 1 - 37/60 (61.6%) patients, in group 2 CVD was revealed in 5/12 (41.6%) patients. From these indicators, it should be concluded that in the presence of diabetic neuropathy, the level of macroangiopathy in its various manifestations also increases.

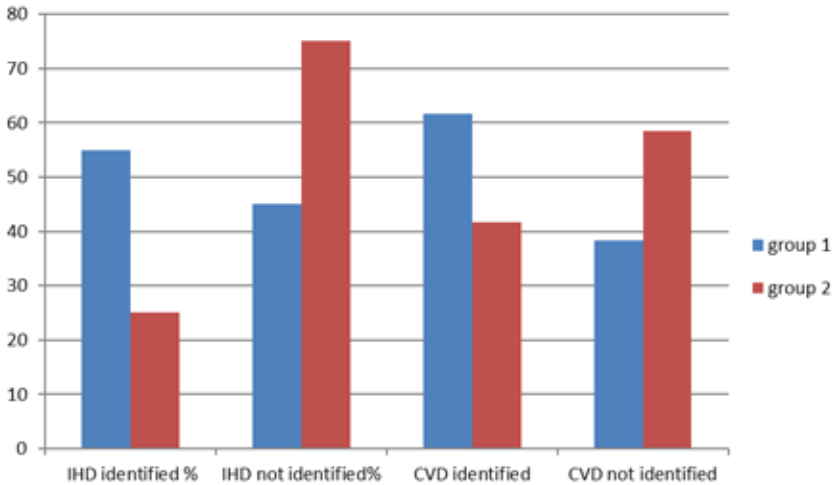


Fig. 1 Distribution of macroangiopathy by groups

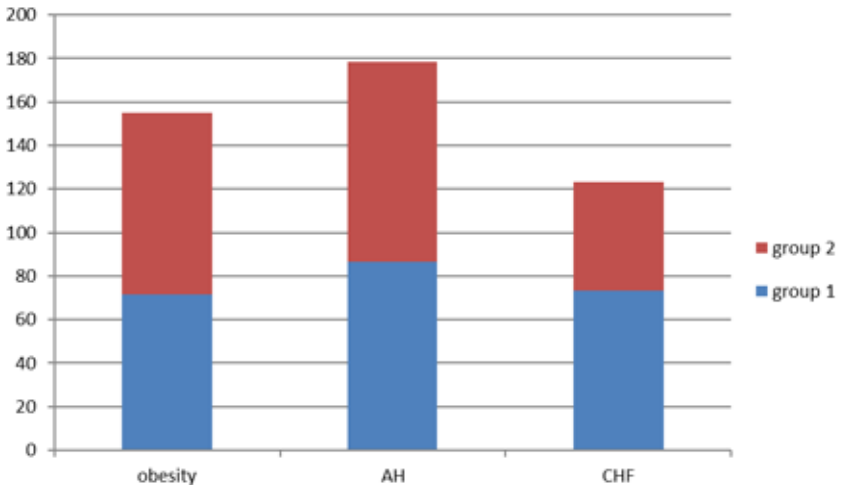


Fig. 2 Distribution of concomitant diseases by groups

Obesity was not detected in only 17/60 patients (28.33%) of the 1st group and in 2/12 patients (16.67%) of the 2nd group. Body mass index (hereinafter BMI) in group 1 was 33.51 ± 6.49 , BMI in group 2 was 32.04 ± 6.92 . From which it can be concluded that 71.67% of patients in group 1 suffer from obesity, 83.33% of patients in group 2 (fig. 2). AH was detect-

ed in 52/60 patients (86.67%) of the 1st group, in 11/12 patients (91.67%) of the 2nd group. The structure of AH in patients of group 1: AH stage 1 - 5/60 (8.3%); 2 stages - 27/60 (45%); 3 stages -20/60 (33.4%). In patients of group 2: AH stage 1 - 4/12 (33.3%); 2 stages - 5/12 (41.6%); 3 stages -2/12 (16.7%). Based on these data, it can be seen that the incidence of AH in both groups is high, however, this disease is more severe in group 1, where stages 2 and 3 AH prevail, while in group 2 patients, stages 1 and 2 are more common (fig. 3).

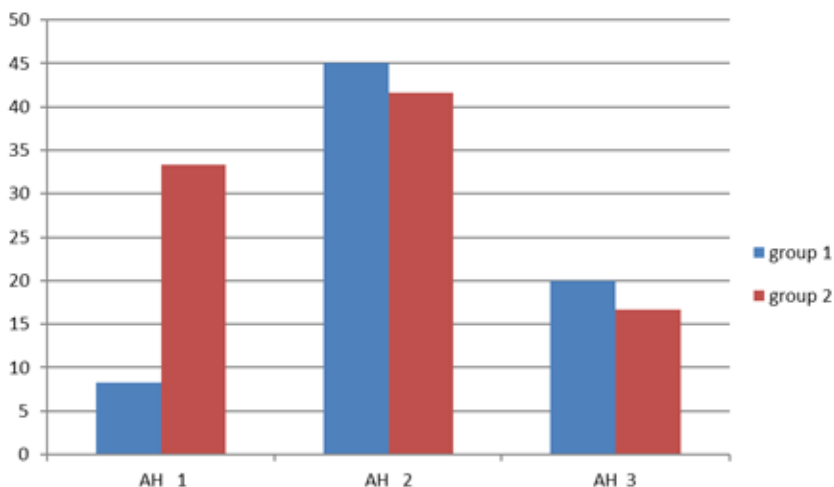


Fig. 3 AH structure by group

Chronic heart failure (hereinafter CHF) was detected in group 1 in 44/60 (73.33%) patients; in group 2 in 6/12 (50.0%) patients.

Dyslipidemia was detected in all patients in both groups, which was accompanied by an increase in low density lipoprotein (hereinafter LDLP) parameters. The average LDLP level in group 1 was 3.85 ± 0.57 mmol/l, (with an optimal / close to normal level of 2.59 - 3.34 mmol/l for patients over 60 years old). In group 2, the average LDLP was 3.36 ± 1.05 mmol/l, which is closer to the upper level of the normal indicator. High density lipoproteins (hereinafter referred to as HDLP) in both groups had approximately the same indicators, for group 1 the HDLP level was 1.45 mmol/l ± 0.38 , for group 2 1.49 mmol/l ± 0.27 , which corresponds to normal values. (0.96-2.36 mmol/l). Based on these data, it should be concluded that patients with DM have a tendency to increase the level of LDLP, regardless of the presence or absence of diabetic neuropathy.

In group 1, visual acuity with correction before laser photocoagulation averaged $0.41 + 0.21$, after coagulation $0.69 + 2.65$. In group 2, visual acuity with correction before photocoagulation $0.61 + 0.91$, after $0.64 + 0.06$. A detailed analysis of the functional outcomes of laser photocoagulation revealed that visual acuity in patients of group 1 in the postoperative period depended on the presence or absence of concomitant micro- and macroangiopathies, such as diabetic nephropathy and diabetic foot syndrome. In 5/60 (8.33%) patients, of which women 1/60 (1.6%), men 4/60 (6.7%), average age $54.8 + 5.4$ years; the duration of the disease is $11.6 + 4.3$ years; BMI $37.61 + 2.9$ with no nephropathy of diabetic genesis, with a history of diabetic foot syndrome and manifestations of neuropathy: among concomitant diseases IHD - 2/5 (40%); AH 1 - 1/5 (20%), AH 2 - 2/5 (40%); AH 3-2/5 (40%) patient; CVD - 1/5 (20%) patient; CHF - 3/5 (60%) patient. In this group, the visual acuity before laser coagulation of the retina was $0.78 + 0.1$, after $0.9 + 0.05$, which corresponds to a sufficiently high visual acuity for patients suffering from diabetic retinopathy in varying degrees of its manifestation.

In 31/60 patients (51.67%), of which 22/60 women (36.67%), 9/60 men (15.0%), average age $58.42 + 7.8$ years; the duration of the disease $17.42 + 4.3$ years; BMI $31.22 + 4.6$ revealed chronic kidney disease in various stages of manifestation (stages 1-2 in 24/31 patients (77.41%), stage 3 A - 7/31 patients (22.58%)), with there were no clinical manifestations of diabetic foot syndrome, but there were manifestations of nephro- and neuropathy of diabetic genesis. In the study, visual acuity before laser coagulation of the retina averaged $0.67 + 0.05$, after the procedure $0.70 + 0.03$. Thus, metabolic disorders associated with CKD, damage to peripheral nerve fibers are combined with damage to the macular region of the organ of vision, which is accompanied by lower indicators of visual acuity both before and after laser coagulation of the retina. In addition, our study showed that the presence or absence of impaired peripheral circulation (diabetic foot syndrome) does not affect the visual prognosis in the post-operative period.

Conclusion

Our study showed an increase in the level of macroangiopathy in its various manifestations in the presence of diabetic neuropathy. Among the comorbidities, an increase in AH of varying severity and CHF was revealed in patients with DNP, in addition, a decrease in the incidence of obesity was noted. In patients with diabetes mellitus, regardless of DNP, there is a tendency to an increase in the level of LDLP. The functional outcomes of laser photocoagulation depend on the presence or absence of

concomitant micro- and macroangiopathies, such as diabetic nephropathy and diabetic foot syndrome.

References

1. Algorithms of specialized medical care for patients with diabetes. // diabetes Mellitus. 2019. Vol. 22. N. 1. P. 1-122. 1.
2. Velichko P. B., Osmanov E. M., Manyakov R. R. Comparative analysis of demographic and medical and social characteristics of people with diabetes mellitus without diabetic retinopathy and with diabetic retinopathy // Bulletin of Russian universities. Math, 2017.22 (4), P. 627-631.
3. Ilyenkov S.S., Inzhutova I.G., Lopatina T.I. Psychological status of patients with diabetic retinopathy // Diabetes mellitus, 2003, № 2. P.26-27
4. Ilyenkov S. S., Inzhutova I. G., Lopatina T. I. Psychological status of patients with diabetic neuropathy // Diabetes mellitus, 2003, no. 2. Pp. 26-27
4. Krasavina M. I., Astakhov S. Yu., Shadrichiev F. E. et al. Ophthalmological markers of diabetic polyneuropathy / / Ophthalmologicheskime Vedomosti, 2016, N. 9 (1), P. 38-46.
5. Meleshkevich T. A., Guryeva I. V., Ametov A. S. Clinical and functional correlations of diabetic foot syndrome and diabetic retinopathy // Mat. 4th all-Russian Congress of Endocrinologists, St. Petersburg, 2001, P. 130.
6. 77. Naidyuk Ya. V. Quality of life and clinical and psychological aspects of therapy of patients with pathology of internal organs on the example of type 2 diabetes mellitus. ... candidate of medical Sciences. - Voronezh, 2007, 25 p.
7. Carrington A.L., Mawdsley S.K., Morley M. et al. Psychological status of diabetic people with or without lower limb disability. // Diabetes research and clinical practice, 1996; 32(1-2):19-25.
8. Chew E.Y., Davis M.D., Danis R.P., Lovato J.F., et al. The effects of medical management on the progression of diabetic retinopathy in persons with type 2 diabetes: the Action to Control Cardiovascular Risk in Diabetes (ACCORD) Eye Study // Ophthalmology 2014. Vol. 121. P.2443-51.

DOI 10.34660/INF.2021.50.43.013

SURGICAL TREATMENT OPTIONS OF ADVANCED KIDNEY CANCER

Vozdvizhenskiy Mikhail Olegovich

Doctor of Medical Sciences, Deputy Chief Physician

Gorbachov Andrey L'vovich

Candidate of Medical Sciences, Head of Department

Trubin Alexey Jur'evich

Oncologist

Samara Oblast Clinical Oncological Dispensary

One of the priority directions in modern oncology is the use of various organ-preserving methods for kidney cancer, which make it possible to avoid a renophobic state while adhering to oncological principles of treatment.

This paper presents a clinical observation demonstrating the potential of the surgical method in mono-mode in the treatment of metastatic kidney cancer.

Patient B., 53 years old, diagnosed with left kidney cancer T2N0M0. Operation - radical left nephrectomy 2005. Progression 2015 metastases in the right kidney, pancreas. Operation - simultaneous extracorporeal resection of the right kidney with autotransplantation. Distal subtotal pancreas resection. Progression 2017 - metastases in the V rib on the left. Operation - removal of the tumor of the chest wall on the left with resection of the V rib. Progression 2018. Metastases to the right parotid salivary gland. Operation - resection of the parotid salivary gland.

In the above observation, due to only the surgical method, it is possible to control the oncological process over a long period of time. Systemic drug therapy was required only with further progression and generalization of the tumor process.

Keywords: renal cell carcinoma, metastatic kidney cancer, nephron-sparing surgeries, extracorporeal kidney resection, targeted therapy for kidney cancer.

Surgical treatment of metastatic kidney cancer in solitary resectable

metastases provides good oncological results [1]. Kidney autotransplantation was first performed and described in 1963 by Hardy JD in the treatment of patients with extensive ureteral involvement [2]. Since that time, this operation has been used in the treatment of various urological diseases [3,4,5]. For tumors of a single kidney, it was first performed by Calne RY, a surgeon at the University of Cambridge (UK) [6], and is currently performed in other clinics [7,8,9]. Later, a group of American authors proposed the term "bench-surgery" - extracorporeal surgery or surgery using a laboratory table. The main surgical moments of the intervention included manipulations on the kidney under conditions of cold ischemia and its transplantation into the contralateral iliac fossa [10].

We present a clinical case of successful surgical treatment of progressive kidney cancer.

Patient B., 53 years old, was admitted to the Oncourology Department of the Samara Oncological Dispensary on July 25, 2015. The patient was observed by an oncologist since 2005, when a radical left nephrectomy was performed for clear cell renal cell carcinoma pT2N0M0G2. Computed tomography (CT) in 2015 diagnosed multifocal cancer of the only right kidney and solitary metastasis to the pancreas. (fig. 1: a, b). This patient had obligate indications for organ-preserving intervention.



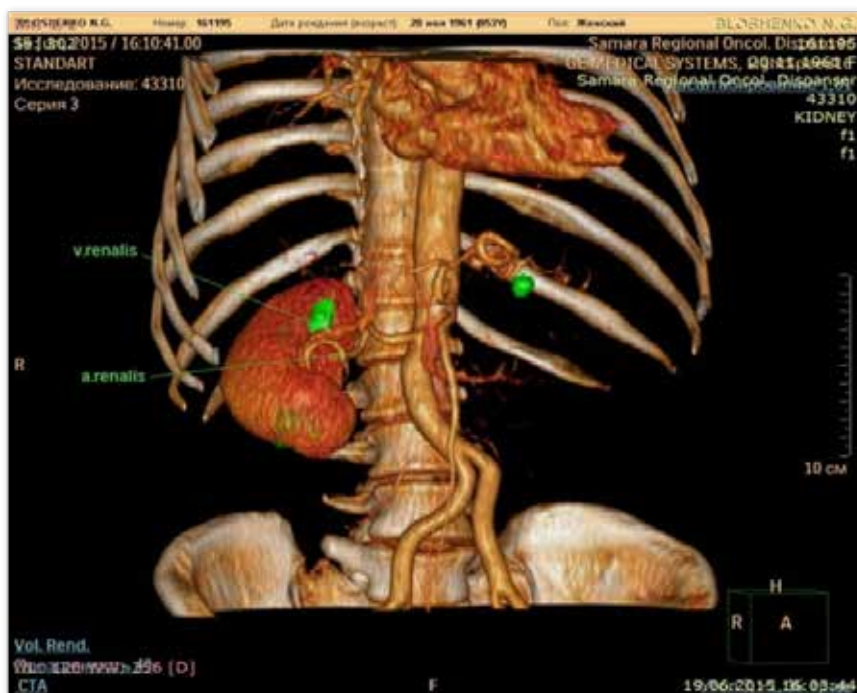


Figure 1. Computed tomography of the abdominal and retroperitoneal organs (contrast enhancement - Yogeksol TR 350-100.0; 3D image reconstruction); a - sagittal projection; b - frontal projection; in the upper and lower segments of the right kidney, there are 4 nodular formations with uneven contours, with signs of intense contrast enhancement, up to 25 mm in size. On the border of the body and tail of the pancreas, a formation up to 10*9mm is determined, which is identical in structure to the formations in the right kidney

On July 28, 2015, a simultaneous extracorporeal resection of the right kidney with autotransplantation into the left iliac region, distal subtotal resection of the pancreas was performed.

The following are the main stages of the operation. Surgical access - midline laparotomy with widening of the incision in the XII intercostal space. For the subsequent reimplantation of the kidney, iliac lymphadenectomy on the left and mobilization of the iliac vessels were performed. With radical nephradrenalectomy on the right, the renal vein was resected with the wall of the inferior vena cava. The removed kidney was placed

under conditions of cold ischemia on a laboratory table (ice crumb coating with saline 0.9% NaCl solution, perfusion with Custodiol solution). 2 tumor foci of the lower pole of the kidney, each about 2 cm in size, were resected. Further - enucleoresection of a 1 cm tumor, localized in the region of the hilum of the kidney, 1 cm in size. To visualize another lesion, an intraoperative ultrasound was required, the results of which diagnosed a tumor in the upper pole of the kidney, located completely intrarenal and resection of the kidney in this area. Hemostasis of parenchymal defects in the area of resection was carried out by the imposition of U-shaped absorbable sutures, as well as additional strengthening with the hemostatic material "Sergisel" (ETHICON, Johnson & Johnson) and the imposition of the Tachocomb plate. The cold ischemia time was 170 minutes. The next step was renal reimplantation in the left iliac region by end-to-end renal artery anastomosis with the proximal end of the internal iliac artery with interrupted sutures and end-to-side anastomosis of the renal vein with the common iliac vein with a continuous vascular suture. The warm ischemia time was 30 minutes. Visually, the viability of the renal parenchyma recovered 5 minutes after the formation of vascular anastomoses, and 15 minutes later, light urine was excreted through the ureter. At the final stage, a ureterocystoneoanastomosis was formed and a distal subtotal resection of the pancreas was performed (figure 2).



Figure 2. General view of the reimplanted right kidney 10 minutes after the imposition of vascular anastomoses (the viability of the renal parenchyma was visually restored)

The postoperative period was uneventful. No hemodialysis was required. The patient was discharged from the hospital in satisfactory condition on the 28th day after the operation (figure 3).

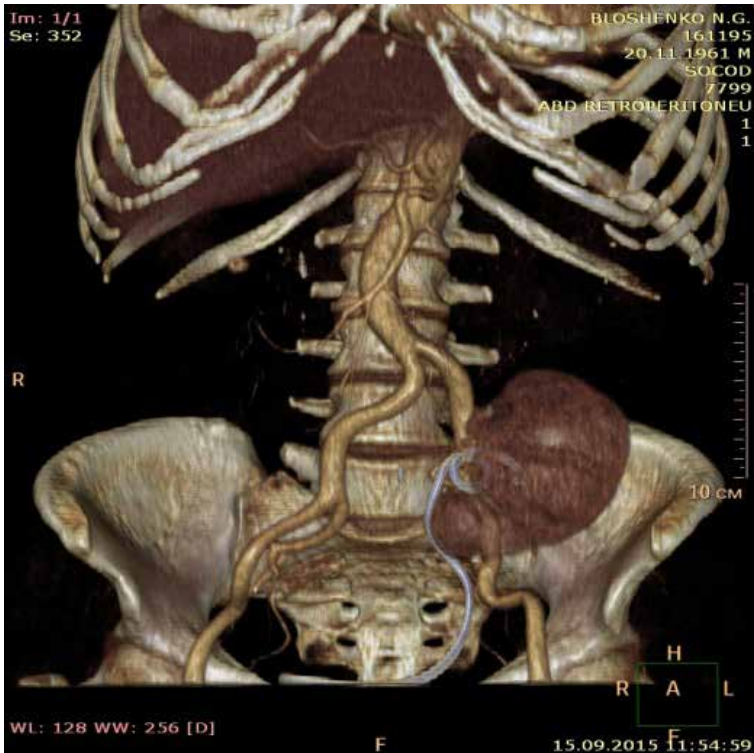


Figure 3. Computed tomography of the abdominal cavity and retroperitoneal space (contrast enhancement - Yogeksol TR 350-100.0); 12 weeks after surgery (3D image reconstruction): The excretory function of the kidney is preserved

According to the results of histological examination, clear cell carcinoma of the kidney G2 was verified in all tumor nodes, as well as metastasis of clear cell carcinoma in the pancreas. No drug treatment (targeted therapy) was prescribed at this stage due to the lack of a morphological substrate.

Further, with dynamic observation 18 months after the operation (January 2017), the progression of the disease in the form of metastasis in the V rib on the left was diagnosed (Figure 4).

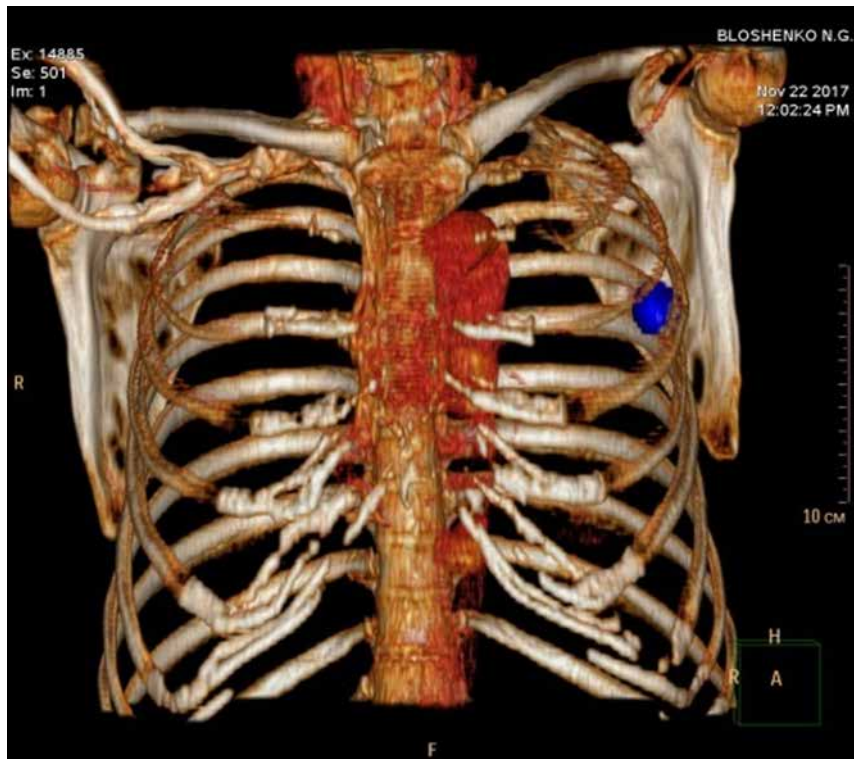


Figure 4. Computed tomography of the chest with contrast enhancement (Omnipak 350 - 50ml); 18 months after surgery (3D image reconstruction): In the lateral segment of the 5th rib on the left, a solid, formation up to 26x21mm in size with the destruction of the rib is determined

On March 17, 2017, the tumor of the left chest wall was removed with resection of the V rib. According to the data of the histological study, metastasis of clear cell carcinoma was verified.

Upon further observation, in December 2018, the progression of kidney cancer was again diagnosed in the form of metastases in the right parotid salivary gland measuring 15 * 11.5 mm and 9 * 8 mm. In this regard, another surgical intervention was performed - resection of the right parotid salivary gland. According to the data of histological examination, renal cell carcinoma metastasis was also verified. No drug treatment was indicated at this stage.

With further observation of the patient, in March 2020, further progression of renal cell carcinoma was diagnosed: metastasis to the only right kidney, liver, left pleura, pancreas. In this connection, the first line of therapy for metastatic kidney cancer was started according to the Interferon-alpha + Bevacizumab scheme. With the next computed tomography in July 2020, negative dynamics of the disease was stated, which manifested itself in an increase in the size of metastatic foci. Further therapy was continued according to the second line scheme, Sunitinib. In March 2021, in connection with a further increase in the size of metastatic foci, therapy for generalized kidney cancer of the 3rd line, Nivolumab, was started.

Dynamic monitoring of the patient continues to this day.

Discussion. Thus, for a long time, for 15 years (since 2005), it was possible to control the development of a malignant process using surgical treatment in a mono-mode, without special drug treatment. Surgical treatment of metastatic kidney cancer, with resectable metastases, provided satisfactory oncological results. In this case, there were obligate indications not only for organ preservation, but also for the use of an extracorporeal technique for intervention on a single kidney. A successfully performed simultaneous operation made it possible to avoid a renoprivative state, thereby increasing not only the expected duration, but also the patient's quality of life. However, such interventions can only be performed in highly specialized centers, where, among other things, there is experience in complex vascular reconstructions. Targeted therapy of kidney cancer in this case was considered as a reserve method in the generalization of a malignant disease, and the preservation of the excretory function of the kidney during surgery provided the conditions for its implementation.

References

1. I. N. Ognerubova, L.L. Gurari, Ya. V. Gridnev. Possibilities of surgical treatment of metastatic renal cell carcinoma (description of a clinical case). "Onokurology" 2011, №4; P.
2. Hardy JD, Eraslan S. Autotransplantation of the kidney for high ureteral injury. J Urol. 1963, Nov; 90:563-74.
3. Stewart BH, Hewitt CB, Banowsky LH. Management of extensively destroyed ureter. Special reference to renal autotransplantation. J Urol 1976; 115: 257-261.

4. Galeev R.Kh., Galeev Sh.R. Kidney transplant for ureteral injuries. "Urology" 2005, №2; P. 28-31.
5. Early progression of hypernephroma after extracorporeal kidney resection [Text] / S.V. Shkodkin, Yu.B. Idashkin, A.S. Pairchuk [et al.] // Experimental and Clinical Urology. – 2017. - №3. – P. 32-37
6. Calne RY. Tumour in a single kidney: nephrectomy, excision, and autotransplantation. Lancet. 1971 Oct 2; 2(7727):761-2.
7. Komyakov B.K., Zamyatnin S.A., Novikov A.I., Kurkov A.S., Popov S.V., Tovstukha D.V., Tsygankov A.V. Extracorporeal kidney resection for tumor. "Urology" 2013, №4; P.
8. V.B. Matveev, D.V. Perlin, A.D. Panahov, A.V. Klimov. Resection of a single left kidney performed 5 years after extracorporeal resection: a clinical case. "Oncourology" 2011, №1; P.
9. Early functional results of surgical treatment of tumors of a single kidney [Text] / L.N. Suslov, O. G. Sukonko, O. V. Krasko [et al.] // Oncourology. – 2017. - V.13, №1. – P. 45-52
10. Gittes RF, McCullough DL. Bench surgery for tumor in a solitary kidney. J Urol. 1975 Jan;113(1):12-5.

DOI 10.34660/INF.2021.83.40.014

DIAGNOSTIC VALUE OF NEOPTERIN AS LABORATORY MARKER OF LUNG SARCOIDOSIS ACTIVITY

Moskalets Oxana Vladimirovna

Candidate of Medical Sciences, Senior Research Officer
Moscow Regional Research Clinical Institute named after M.F.Vladimirskij

Sarcoidosis is an inflammatory granulomatous disease of unknown etiology. To assess the course of the inflammatory process, it is necessary to determine the criteria for the activity of the disease. In clinical practice, for this purpose, the determination of the content of neopterin in the serum of peripheral blood is often used. This article presents data concerning the assessment of the reliability of the determination of serum neopterin as a laboratory marker of the activity of the inflammatory process in pulmonary sarcoidosis. In 111 patients with pulmonary sarcoidosis with different radiological stages of the disease, the number of lymphocytes in the bronchial lavage and the content of neopterin in the serum of peripheral blood were determined. When analyzing the results, a positive correlation was noted between the level of serum neopterin and the number of lymphocytes in bronchial lavage, as well as the level of neopterin and the radiological stage of the disease. At the same time, in 40% of patients with disease progression, the serum neopterin level was within the normal range. Based on the data obtained, it was concluded that monitoring the level of neopterin in the serum of peripheral blood is not a reliable tool for assessing the activity of inflammation in sarcoidosis of the respiratory system.

Keywords: sarcoidosis, neopterin, activity of inflammation

Introduction

Sarcoidosis is a multisystem disease of unknown etiology, the morphological substrate of which is noncaseating epithelial cell granuloma [1]. In 80-90% of cases, the lungs and intrathoracic lymph nodes are affected, and generalization of the process is often found [4, 12]. The nature of the course and features of the clinical manifestations of sarcoidosis are determined by its localization and the inflammatory activity of the process. The

literature data concerning the immunological mechanisms of sarcoidosis are rather contradictory, with the main attention being paid to the T-cell link [1, 3, 6, 7]. Despite the development of radiation diagnostic methods, the search for reliable laboratory criteria that allow assessing the activity of the disease and predicting its course is still relevant. The most informative is the study of bronchial lavage, but technically it is not always feasible. One of the most well-known serum markers is angiotensin-converting enzyme, however, this test has low sensitivity, and at present it is not recommended for routine clinical practice. Quite a lot of works are devoted to gamma-interferon, soluble interleukin-2 receptor, neopterin, as well as various subpopulations of lymphocytes[2,5,6, 8].

The aim:to assess the reliability of the determination of neopterin in the serum of peripheral blood as a laboratory marker of the activity of the inflammatory process in pulmonary sarcoidosis.

Materials and methods

The study included 111 nonsmoking patients with pulmonary sarcoidosis (98 women and 13 men aged 30 to 68 years, mean age 47.6 years). In 12 (10.8%) patients, further examination revealed Löfgren's syndrome. All patients underwent computed tomography of the lungs and organs of the mediastinum, as well as cytological examination of bronchial lavage (BL) with counting lymphocytes. Determination of the level of neopterin in the serum of peripheral blood was carried out by the method of enzyme-linked immunosorbent assay on a test system from IBL (Austria).

Results

Analysis of the results obtained revealed the presence of a direct correlation between the number of lymphocytes in the BL and the level of serum neopterin ($r = 0.26$, $p = 0.027$). At the same time, there was no significant change in the number of lymphocytes in the BL with an increase in X-ray changes.

When comparing the level of serum neopterin with the X-ray picture, the following data were obtained. The first X-ray stage of the disease was in 39 patients, the content of neopterin in this group was 9.0 nmol / L (7.0-4.4). The second stage - in 57 patients, the third - in 15 patients. The content of neopterin in these groups, respectively, was 16.0 (11.5-22.3) and 10.2 (4.7-21.0) ($p = 0.01$ in comparison with the first stage).

Discussion

Neopterin (2-amino-4-hydroxy-6- (D-erythro-1', 2', 3'-trihydroxypropyl) belongs to the compounds of the pteridine class. Despite numerous studies, its biological role has not yet been fully elucidated. Physiological the concentrations of neopterin and its derivatives are low, in the blood

serum they do not exceed 10 nM / L. Small fluctuations may occur depending on age, race, smoking, physiological state.

The main interest in neopterin is associated with the fact that it is a marker of cellular immunity activation. In pathological conditions associated with the activation of the immune system, the concentration of serum neopterin can reach 100-250 nM / L [8].

It has now been established that the main source of neopterin in the human body is monocytes / macrophages. They begin to actively produce neopterin under the influence of γ -interferon (γ -IFN), which is produced by activated T-lymphocytes (mainly, this is a subpopulation of type I T-helpers). Under the influence of γ -IFN, the GTP CH-I enzyme is activated in macrophages and lymphocytes. Some other cells of the immune system are also capable of producing γ -IFN, but their role in the induction of neopterin synthesis has not yet been fully elucidated. In particular, there is evidence that dendritic cells under the influence of γ -IFN are able to produce neopterin, but, unlike macrophages, they are more sensitive to the action of other types of interferons (α -IFN and β -IFN). In addition, γ -IFN can induce the production of neopterin and other cells: endothelial, renal epithelium, fibroblasts. However, it should be noted that the level of production is significantly lower than in macrophages.

Neopterin, produced by alveolar macrophages, is involved in the pathogenesis of sarcoidosis and other interstitial lung diseases. It enhances the processes of transcription of various pro-inflammatory cytokines in cells participating in the inflammatory process. An increase in the level of neopterin was found not only in the peripheral blood serum, but also in the BALF. The amount of synthesized neopterin also correlates with other indicators of the activity of the inflammatory process: reactive oxygen species produced by alveolar macrophages, proinflammatory cytokines, etc. [5, 8].

In this study, it was possible to confirm the relationship between serum neopterin level and the radiographic stage of sarcoidosis. At the 1st stage, when the lesion of the pulmonary parenchyma is minimal, this indicator remained within the normal range. The increase in the concentration of neopterin at the 2nd stage can be explained by an increase in the number of epithelioid cell granulomas in the lung tissue. The disappearance of hilar lymphadenopathy with persisting changes in the pulmonary pattern, which is characteristic of the 3rd stage, was accompanied by a tendency towards a decrease in the level of neopterin. At the same time, in 6 out of 15 (40%) patients with nonspecific symptoms of inflammation (subfebrile fever, arthralgia, weight loss), increased acute phase proteins (CRP,

fibrinogen), radiological signs of disease progression, the content of neopterin did not exceed normal values.

Conclusion

The content of neopterin in the serum of peripheral blood mainly coincides with the X-ray stage of sarcoidosis of the respiratory system, but does not always coincide with the degree of inflammatory activity. Therefore, laboratory monitoring of this marker cannot be a reliable criterion for assessing the dynamics of the inflammatory process in sarcoidosis.

References

1. Dmitrieva L.I., Stepanyan I.E. Sarkoidoz organov dyhaniya: voprosy etiologii, patogeneza, klassifikaciya, rentgenodiagnostika // Voprosy rentgenol. radiol. - 1998. - №4. - S.33-39.
2. Ses' T.P. – Osobennosti vospalitel'nogo processa pri sarkoidoze legkih//Citokiny i vospalenie – 2002. - №3.-S.3-6.
3. Stepanyan I.E., Ozerova L.V. – Sarkoidoz organov dyhaniya //Russkij medicinskij zhurnal – 1998. – t.6. - №4. – S.221-227.
4. Cuchalin A.G,red. - Sarkoidoz. Uchebno-metodicheskoe posobie dlya slushatelej poslevuzovskogo i dopolnitel'nogo professional'nogo obrazovaniya // Kazan':KGMU. – 2010. – 58 s.
5. Bargagli E., Mazzi A., Rottoli P. Markers of inflammation in sarcoidosis: blood, urine, BAL, sputum and exhaled gas. Clin.Chest Med. – 2008. – v.29(3). – P.445-458.
6. Gerke A.K., Hunninghake G. – The immunology of sarcoidosis // Clin. Chest Med. – 2008. – v.29(3). – P.379-390.
7. Semenzato G., Maschio N., Agostini C. – Immune mechanisms in interstitial lung disease //Allergy – 2000. – v.55(2). – P.1103-1120.
8. Wachter H., Fuchs D., Hausen A., Reibnegger G., Werner E.R. Neopterin as marker for activation of cellular immunity: immunologic, basis and clinical application //Adv. Clin. Chem. – 1998. – v.27. – P.81-141.
9. Zhou Y.,Laver E.E., Li H., Baughman R.P. Clinical management of pulmonary sarcoidosis//Expert Rev. Respir. Med. - 2016. - v/10(5).- P.577-591.

DOI 10.34660/INF.2021.73.83.015

FEATURES OF THE STATE OF MUSCULAR BALANCE (PHORIA) IN STUDENTS OF THE TYUMEN STATE MEDICAL UNIVERSITY. THE EFFECT OF OPTICAL CORRECTION

Pochinok Elena Nikolaevna

Candidate of Medical Sciences, Associate Professor
Institute for Continuing Professional Development
Tyumen State Medical University
Tyumen, Russia

Voronova Maria Romanovna

Nurse
Limited Liability Company City Center for Vision Correction
Tyumen, Russia

Fomina Elena Viktorovna

Candidate of Medical Sciences, Associate Professor
Institute for Continuing Professional Development

Bedash Kalinka Ivanova

Candidate of Medical Sciences, Associate Professor
Institute for Continuing Professional Development

Ponomareva Maria Nikolaevna

Doctor of Medical Sciences, Full Professor
Institute for Continuing Professional Development
Tyumen State Medical University
Tyumen, Russia
ORCID ID 0000-0001-6522-3342

Purpose of work. To analyze the state of muscular balance of the visual system in students with different types of clinical refraction. To assess the features of the manifestation of phoria in certain types of refraction, as well as the influence of the complete usual optical correction of myopia on the value of phoria.

Materials and methods. The study was conducted among fourth-year students of the Tyumen State Medical University. 149 people were randomly selected (110 women and 39 men).

Research results. According to the results of the study of distance phoria using the Cover test, deviation of the visual axis to the nose (esophoria) was observed in 8% (12/149), deviation of the visual axis to the temple (exophoria) - in 43% (64/149), in the vast majority - 49% (73/149) had orthophoria. When analyzing distance phoria using a Meddow prism, exophoria also prevailed - 41.6% (49/149), esophoria was often detected - 32.9% (49/149), orthophoria was noted less often - 25.5% (38/149). At the same time, a significant ($p \leq 0.05$) increase in exophoria was observed in the third group, while in the first and second groups, different types of phoria were distributed more evenly. The study of muscle balance near the Howell test in all groups without correction in total revealed the following state of phoria: orthophoria - 30% (44/149), exophoria - 58% (87/149), esophoria - 12% (16/149), which shows a significant predominance of the deviation of the visual axis of the eye outward. Thus, the state of muscle balance in patients of the second and third groups in the optical correction is normalized and becomes comparable to the first group.

Conclusion. Among medical students, emmetropic refraction occurs in only 33% of cases. Myopic refraction was noted much more often - 67%. At the same time, myopia is mild - 40.5%, the percentage of myopia of moderate and high degree is very high - 26.5% of cases (every fourth). Optical correction of myopia leads to a significant decrease in exophoria near and in some patients turns into orthophoria. Thus, the optical correction of myopia not only improves visual acuity, but also leads to a decrease in the imbalance of the oculomotor muscles (phoria), eliminates asthenopic complaints and visual discomfort when working at close range, prevents the development of divergent strabismus, thereby improving the quality of life.

Keywords: myopic refraction, orthophoria, exophoria, esophoria, strabismus.

Relevance

Phoria is an imbalance in the action of the oculomotor muscles while maintaining binocular vision. Weak or excessive convergence can affect not only visual ability, but also a person's personality traits. The state of phoria affects the direct perception of small objects and is the reason for the selective performance of various visual tasks related to learning or hobbies. In contrast to distance phoria, near phoria is prone to significant individual variability [3]. The tendency of the eyes to diverge at a close distance is so constant that it does not allow us to consider the orthophoria

at this distance as the ideal position of the eyeballs. Exophoria from 3 to 6 prism diopters (Δ) at a distance of 40 cm is considered physiological. The concept of "physiological exophoria" to some extent depends on the state of equilibrium of muscle balance for a distance. Sergievsky L.I. [7] understood physiological exophoria as the difference between the equilibrium state of muscular balance at distance and the state of equilibrium at near. At the same time, even weak degrees of exophoria for nearness with orthophoria for distance can be the cause of asthenopia. Grosvenor T. [11] indicates that normally the expected phoria for near is from 3 to 5 Δ exophoria, but often there are patients with exophoria near 10 to 12 Δ , or esophoria 4-5 Δ . The tendency towards asymptomatic exophoria near leads to the introduction of the concept of physiological exophoria. In heterophoria, visual work, especially at close range, requires more than usual neuromuscular tension in order to overcome the tendency to deviate one of the eyes [6]. Strong deviations lead to decompensated heterophoria, this condition is accompanied by increased fatigue, headaches and, as mentioned above, asthenopic complaints and diplopia. Much more often phorias manifest themselves clinically in the form of asthenopic complaints with near vision [8]. When the eyes are disconnected, a relative weakness of any muscle is noted, and the visual axis of one of them deviates inward (esophoria), outward (exophoria) upward (hyperphoria) or downward (hypophoria), less often incyclophoria or excyclophoria is observed. The causes of heterophoria are congenital or acquired anomalies in the structure of the orbits and eyeballs, anomalies of attachment or location of the eye muscles, uncorrected ametropia, and disturbances in the relationship between accommodation and convergence [3]. Most people have some degree of heterophoria. According to a number of authors, the frequency of heterophoria is 62.8%. Optical correction has a positive effect on the muscular balance of the eyes: the frequency of exophoria and its degree are reduced [9, 12]. Under normal conditions, due to the fusional ability of the visual analyzer, muscle balance disturbance is not observed [5]. In practice, phoria should only be corrected if the patient experiences symptoms such as asthenopia, double vision or blurred vision, fogging, or has signs of functional impairments such as abnormally short or long reading distance, while decompensation of phoria leads to overt squint and requires special treatment [1]. At present, myopia is on the rise all over the world. According to statistics in the world for 2000, myopia was observed in 23% of the world's population, and in 2050 this figure is expected to be about 50%, of which 20% of people will have high myopia [14]. In our region, analysis of eye diseases in young men of military age category B

for 2016-2017 revealed a stable increase in myopia from 11.6% to 23.0% and a decrease in hyperopia from 1.7% to 0.5% [2]. And myopia of medium and high degree often leads to the formation of degenerative changes in the peripheral parts of the retina over the years, which aggravates not only the state of the organ of vision, but also affects other functions of the body. Peripheral vitreochorioretinal dystrophy accompanying myopia in women of childbearing age with the threat of retinal detachment is an indication to exclude the laboring period during labor, which is most often an indication for a cesarean section [10]. In modern literature, it is noted that among students of higher educational institutions the incidence of myopia is significantly higher than in the population, especially in medical universities, which is undoubtedly associated with intense visual stress [4], leading not only to accommodative disorders, but also to muscle imbalance of the visual system. In the literature available to us, we did not find works devoted to the study of the frequency and types of muscle balance disorders among organized groups of students, including medical universities, which was the motivation for this study.

Purpose of the study

To analyze the state of muscular balance of the visual system in students with different types of clinical refraction. To assess the features of the manifestation of phoria in certain types of refraction, as well as the influence of the complete usual optical correction of myopia on the value of phoria.

Research materials and methods

The study was conducted among fourth-year students of the Tyumen State Medical University. 149 people were selected by random sampling (110 women and 39 men). The inclusion criterion was the presence of emmetropic or myopic refraction. The exclusion criteria were hyperopia, astigmatism over 1 diopter, anisometropia over 2.0 diopters, overt strabismus, retinal and optic nerve diseases. Ophthalmological examination included standard techniques: visometry with and without correction was performed using a trial set of lenses, a Rota apparatus with a Golovin-Sivtsev table, and an autorefractometer. Binocular vision was tested using a four-point test. Additionally, techniques were used to identify muscle balance. The direction of the latent deviation of the eyes and the magnitude of the phoria when looking into the distance were determined in two ways: using the Cover test, and also using the Maddox cylinder, a trial set of prisms, and a point light source. Near phoria was determined using the Howell test and a 10 prdptr prism pointing downwards.

Distance visual acuity with correction ranged from 0.8 to 1.5 (average

visual acuity = 1.1 ± 0.4). All patients (100%) had binocular distance vision. None of the examined patients actively presented complaints characteristic of decompensated heterophoria (asthenopia, loss of a line during reading, forced position of the head during reading, diplopia).

According to the state of clinical refraction, the patients were divided into 3 groups: the first group - emmetropia, $n = 49$ people (33%), the second group - mild myopia, $n = 60$ people (40.5%), the third group - moderate and high myopia, degree $n = 40$ people (26.5%). To calculate the statistical data, the Excel program (version 10: 0) was used. That is, the overwhelming majority of the surveyed had myopic refraction. All patients showed binocular vision according to the four-point distance test.

Research results

Analysis of heterophoria by gender showed its higher frequency in men (74.8%) than in women (66.4%).

Table 1
The relationship of heterophoria with gender

Sex	Heterophoria
Men	Orthophoria 10 (25.2%) Exophoria 25 (63%) Esophoria 5 (11.8%)
Women	Orthophoria 37 (33.6%) Exophoria 63 (57.3%) Esophoria 10 (9.1%)

According to the results of the study of distance phoria using the Cover test, deviation of the visual axis to the nose (esophoria) was observed in 8% (12/149), deviation of the visual axis to the temple (exophoria) - in 43% (64/149), in the vast majority - 49% (73/149) had orthophoria.

When analyzing distance phoria using a Meddox prism (Fig. 1), exophoria also prevailed - 41.6% (49/149), esophoria was often detected - 32.9% (49/149), orthophoria was noted less often - 25.5% (38/149). At the same time, a significant ($p \leq 0.05$) increase in exophoria was observed in the third group, while in the first and second groups, different types of phoria were distributed more evenly.

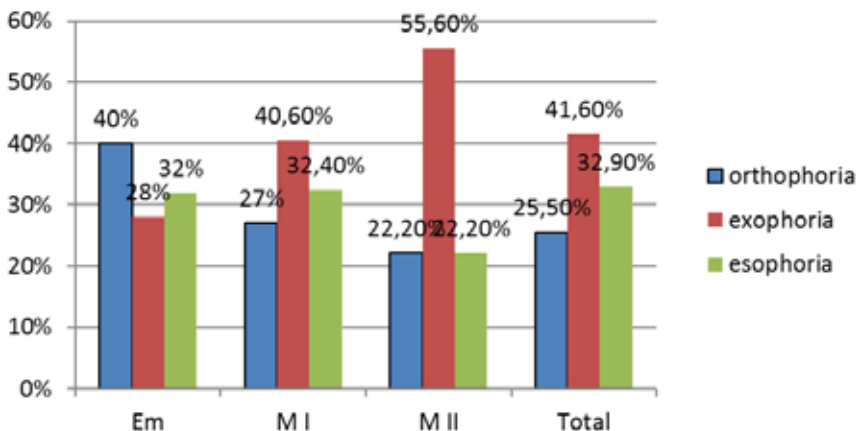


Fig 1. Foria distribution depending on refraction (Meddox distance test)

At the same time, the quantitative characterization of muscle balance disturbance according to the Meddox test into the distance showed that in 91% of cases the value of phoria did not exceed 3Δ , and only in 4.5% it was significant (more than 6Δ).

The study of muscle balance near the Howell test in all groups without correction in total revealed the following state of phoria: orthophoria - 30% (44/149), exophoria - 58% (87/149), esophoria - 12% (16/149), which shows a significant predominance of the deviation of the visual axis of the eye outward.

Next, the analysis of the state of muscular balance in the vicinity of the groups was carried out.

**Table 2
Muscle balance in emmetropia (first group)**

Phoria near Δ ptr	Orthophoria	Exophoria >5	Exophoria <5	Esophoria <5	Total
Emmetropia	20 (40.8%)	9 (18.4%)	14 (28.6%)	6 (12.2%)	49 (100%)

Orthophoria prevailed in the first group (40.8%). Quite often, exophoria less than 5Δ - 28.6% is noted, which is regarded as a variant of the norm. Significant deviations from the norm (exophoria $> 5\Delta$ and esophoria) were less common.

Table 3
Muscle balance in mild myopia
(second group)

Phoria near Δ ptr	Orthophoria	Exophoria >5	Exophoria <5	Esophoria <5	Total
Without optical correction	14 (23.4%)	25 (41.6%)	15 (25%)	6 (10%)	60 (100%)
With full optical correction	31 (51.7%)	15 (25%)	10 (16.7%)	4 (6.6%)	60 (100%)

The analysis of phoria in the second group without optical correction showed a very high percentage of exophoria (2/3 of all subjects), while in 41.6% (25/60) there was a deviation of more than 5Δ (this degree of exophoria can lead to decompensation and the development of a clear divergent squint). Examination in full optical correction showed the normalization of muscle balance, which was expressed in a decrease in exophoria to 41.7%, and especially in its decompensating values (more than 5Δ), an increase in the percentage of orthophoria.

Table 4
The state of muscular balance in moderate and high myopia
(third group)

Phoria near Δ ptr	Orthophoria	Exophoria >5	Exophoria <5	Esophoria <5	Total
Without optical correction	10 (25%)	10 (25%)	14 (35%)	6 (15%)	40 (100%)
With full optical correction	25 (62.5%)	3 (7.5%)	10 (25%)	2 (5%)	40 (100%)

In the third group of patients in the study without optical correction, exophoria also prevailed - 60% (24/40), although its decompensating degree was noted less often than in the second group (25%). We explain the relative decrease in the amount of exophoria exceeding 5Δ by the greater adherence to optical correction in this group (patients with moderate myopia due to low uncorrected visual acuity constantly use glasses, and many - contact lenses). Research in optical correction also demonstrates a decrease in the number and magnitude of phoria, a transition to orthophoria. That is, the optical correction of myopia reliably ($p \leq 0.05$)

contributes to the compensation of phoria.

Thus, the state of muscle balance in patients of the second and third groups in the optical correction is normalized and becomes comparable to the first group.

Conclusion

Among medical students, emmetropic refraction occurs in only 33% of cases. Myopic refraction was noted much more often - 67%. At the same time, myopia is mild - 40.5%, the percentage of myopia of moderate and high degree is very high - 26.5% of cases (every fourth). The frequency of heterophoria is high and averages 53.2%, but the results of the study largely depend on the method used. Thus, when assessing distance phoria using the Meddow prism, heterophoria was detected much more often than according to the Cover test, which is associated with a more severe separation of the binocular visual system by the first method. When working at a close distance, heterophoria is detected more often than at a distance (70%). Exophoria is especially often observed near, and its frequency and degree increases in proportion to the degree of myopia in the absence of optical correction. So with uncorrected myopia of a weak degree, exophoria was noted in 2/3 of patients, and clinically significant exophoria was more than 5Δ in 41.6%. Optical correction of myopia leads to a significant decrease in exophoria near and in some patients translates it into orthophoria. Near esophoria occurs in patients with myopia much less frequently than exophoria, and does not reach pronounced degrees. Thus, the optical correction of myopia not only increases visual acuity, but also leads to a decrease in the imbalance of the oculomotor muscles (phoria), eliminates asthenopic complaints and visual discomfort when working at close range, prevents the development of divergent strabismus, thereby improving the quality of life, which is especially important for medical students. Intense visual loads and high mental activity affect the quality of vision, therefore, it is very important for us to investigate this particular social category in order to find the cause of visual impairment in time, since students of medical universities, like no one else, need the correction to fulfill the set of tasks before them.

References

1. Myagkov A.V., Parfenova N.P., Demina E.I. Guide to medical optics. Part 1. Basics of optometry. 2016 Moscow: April. 205 P.

2. Ponomareva M.N. Modern trends in the dynamics of the state of ophthalmological health of persons of military age / M.N. Ponomareva, A. Yu. Kuzmina, D.A. Karpova // Point of view. East-West. – 2019. - №3.- P. 86-89.
3. Pospelov V.I. Etiology, pathogenesis and principles of pathogenetic therapy for the progression of myopia in children / V.I. Pospelov – M., – 1986. – 180 P.
4. Pochinok E.M., Khaziakhmetova E.R. Analysis of the effectiveness of hardware (functional) treatment of patients with refractive anomalies in the conditions of the university multidisciplinary clinic of the Tyumen State Medical University // University Medicine of the Urals. 2017. - №1. – P.71-72.
5. Rinskaya NV, Optometrist's Handbook. Refraction selection algorithm. 2019 Moscow: FARB-IT.560 P.
6. Rosenblum Yu.Z. Optometry. Selection of vision correction means. Second edition / Yu.Z. Rosenblum.- SPb.: Peter, 1996.- 249 P.
7. Sergievsky LI Conjugate strabismus and heterophoria / LI Sergievsky. Sergievsky. - M., - Medgiz, 1951.- 244 P.
8. Handbook of ophthalmology / [E.S. Avetisov, L.A. Katsnelson, Yu.F. Maychuk and others]; Ed. E.S. Avetisova. - Moscow: Medicine, 1978. - 382 P.
9. Fomina E.V. The value of the study of accommodation and binocular balance for the risk of myopia progression / E.V. Fomina, E.M. Pochinok // Point of view. East-West. – 2020. - №2.- P. 53-55.
10. Fomina I.V. Caesarean section in women with pathology of the organ of vision / I.V. Fomina, M.N. Ponomareva, Alyeva A.A. // Eurasian Scientific Association. – 2017. V.1.- №3(25). - P. 85-86.
11. Grosvenor T. Primary Care Optometry. 5-th ed. Butterworth-Heinemann; 2007.
12. Fomina E.V. Disorders of binocular balance and accommodation as myopia progression criteria / Fomina E.V., Pochinok E.M., Bedash K.I., Ponomareva M. N. // Proceedings of the International Conference “Scientific research of the SCO countries: synergy and integration”. Part 1. - Reports in English (December 8, 2020. Beijing, PRC). - P. 61-65.
13. Holden B.A., Fricke T.R., Wilson D.A., et. al. Global prevalence of myopia and high myopia and temporal trends from 2000 through 2050

ANALYSIS OF CHRONIC OPHTHALMOLOGICAL PATHOLOGY OF THE CHILDREN'S POPULATION OF THE TYUMEN POLYCLINIC

Yushina Maria Alexandrovna

Ophthalmologist
City polyclinic № 1, Tyumen, Russia

Markova Anastasia Olegovna

Clinical Resident
Institute for Continuing Professional Development

Fomina Elena Viktorovna

Candidate of Medical Sciences, Associate Professor
Institute for Continuing Professional Development

Bedash Kalinka Ivanova

Candidate of Medical Sciences, Associate Professor
Institute for Continuing Professional Development

Ponomareva Maria Nikolaevna

Doctor of Medical Sciences, Full Professor
Institute for Continuing Professional Development

Tyumen State Medical University
Tyumen, Russia
ORCID ID 0000-0001-6522-3342

Relevance. The implementation of the national project "Health", the effectiveness of social programs of the government of the Russian Federation (improvement of housing conditions for young families, purchase of a mortgage loan/loan on preferential terms, etc.) leads to stimulation of the appearance of large families. In addition, migration of the population from the Northern districts of the Tyumen Oblast, both pensioners and young families, was noted, in connection with which, the emergence of new buildings is observed. According to the Office of the Federal State Statistics Service for the Tyumen Oblast, the Khanty-Mansiysk Autonomous Okrug - Yugra and the Yamalo-Nenets Autonomous Okrug, in 2016 there was a mechanical increase in women of childbearing age (20-29 years) in the region of 60.12% [3]. Over the past 5 years, in the service

area of the "City Autonomous Healthcare Institution of the Tyumen Oblast" City Polyclinic № 1 "there has been an increase in the child population by 1.6 times. From 10,061 pediatric patients in 2016 to 16529 in 2020. This is primarily due to the increase in the child population leads to an increase in the load on the ophthalmological service in the region, including the outpatient network [1,2,4]. According to the analysis of the available modern scientific literature, the growth of premature babies [2,5], congenital pathology [5], the severity of childhood injuries, neoplasms, refractive errors [1,2,6] is noted. In this situation, it seems relevant to us to study the structure of chronic eye pathology, the causes of disability in order to provide affordable specialized qualified assistance (staffing, purchase of modern diagnostic and therapeutic equipment).

Purpose of the study. To analyze the indicators of chronic eye pathology of the child population in the Tyumen city polyclinic for 2020.

Material and methods.

The study was carried out in the "City Autonomous Healthcare Institution of the Tyumen Oblast" City Polyclinic № 1 "of Tyumen (hereinafter - the Polyclinic) in 2020. The study included 3787 patients from birth to 17 years old, which amounted to 22.9% (16.529) of the total child population polyclinics. During the analyzed period, cases of admission or examination at preventive examinations were taken into account (at the prescribed age: 1 month, 1 year, 3 years, 10 years, 11 years, 15-17 years). The examination included standard ophthalmic research methods (visometry, tonometry, perimetry, skiascopy, biomicroscopy of the anterior segment of the eye and vitreous body, fundus ophthalmoscopy). Statistical processing of the research results was carried out using the STATISTIKA 6 program.

Results and discussion. The structure of ophthalmological pathology, according to the results of referrals and preventive examinations of the organized child population (preschool and school on decreed dates) for the analyzed period, is presented in table 1.

Table 1
The structure of ophthalmic pathology

Pathology	Revealed total N (%)	First time in life	During preventive examinations
Inflammatory diseases of the anterior segment	210(19.59%)	36(13.29%)	-
Diseases of the fibrous membrane	4 (0.38%)	4(1.48%)	-

Diseases of the vascular tract	1(0.09%)	1(0.37%)	-
Diseases of the optic nerve	13(1.21%)	-	-
Diseases of the muscles of the eye	72(6.72%)	5(1.84%)	-
Refractive and accommodation anomalies	756 (70.52%)	213(78.59%)	104(100%)
Injury to the organ of vision	9(0.84%)	9(3.32%)	-
Neoplasms of the organ of vision	1(0.09%)	1(0.37%)	-
Violation of hydrodynamics	2(0.18%)	1(0.37%)	-
Lens pathology	4(0.38%)	1(0.37%)	-
Total	1072(100%)	271(100%)	104(100%)

Inflammatory diseases are mainly characterized by conjunctivitis 78.6% (165/210). Diseases of the fibrous membrane are mainly represented by keratitis 75.0% (3/4). It is noteworthy that with retinal pathology, only background changes (hypertensive angiopathy) were noted, and in 50% of cases they were first detected at the age of 14 years. A relatively high increase in the indicator of pathology of malignant neoplasms is associated with an increase in prematurity of newborns in the service area, and therefore, the disability of this nosology was revealed in 46.2% of cases (only in premature infants 6/13), the rest of the nosology was noted with decompensation of intracranial pressure (complicated and uncomplicated congestive optic discs). Diseases of the muscles of the eye, as a rule, are diagnosed with congenital pathology of the central nervous system 33.3% (24/72) and impaired binocular vision, with abnormalities of refraction and accommodation 66.7% (48/72). Among the anomalies of refraction and accommodation, the largest proportion is myopia, 71.4% (397/556) in adolescents under 14 years of age, with 39.8% (217/556) newly diagnosed. In adolescents 15-17 years old, myopia was detected in 25% (50/200). These indicators correspond to the average statistical indicators for the Russian Federation [6]. Patients with eye trauma went to see an ophthalmologist at the polyclinic after visiting the emergency room for ophthalmological care CAHI TO "OCH № 2" for further follow-up and observation. During the analyzed period, 1 patient applied with a benign

neoplasm of the orbit, no malignant neoplasms were detected. Among the pathology of the lens, 5 patients with a diagnosis of congenital cataract are observed, with a visual acuity higher than 0.5 (requiring dynamic observation) 40% (2/5 of the patient), received surgical treatment without IOL implantation - 40% (2/5) and 10% (1/5) requires surgical treatment. Violation of hydrodynamics is characterized by congenital glaucoma (2 patients), disability was obtained almost after birth, which indicates the severity of the disease, despite the early diagnosis. Patients with refractive errors and ($p < 0.003$) patients with inflammatory diseases of the anterior segment of the eyeball prevail reliably ($p < 0.001$) at outpatient visits.

Thus, the structure of ophthalmic pathology is as follows: the first place is taken by refractive errors, the second place is the inflammatory diseases of the anterior segment, the third place is the diseases of the eye muscles, the fourth place is the diseases of the optic nerve. For effective medical examination and control of myopia, as well as hyperopia, an ultrasound machine is needed, which is not available in the clinic. To control the pathology of binocular vision, Worth's four-point color test (which is available) is required. Additionally, it is necessary to purchase a synoptophore for both diagnosis and possible treatment.

The structure of nosologies in the dispensary group shown in Figure 1 demonstrates the general trend of nosologies that require dynamic observation and treatment of patients in the pediatric population throughout the Russian Federation.

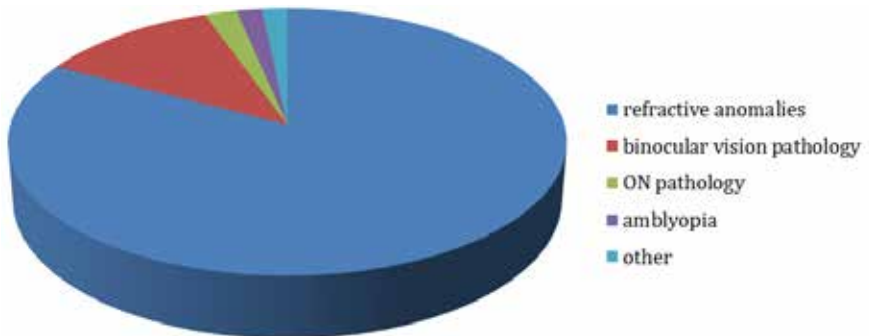


Fig. 1. The structure of nosologies of the dispensary group is presented

Among the group of patients with refractive errors, only patients with 80.54% myopia are observed (352/437). Within the group, the structure

is presented as follows: the first place is taken by patients with a weak degree of myopia 66.76% (235/352), the second place - with an average degree of myopia 26.1% (92/352), the third place - with a high degree of myopia - 7.1% (25/352). The pathology of binocular vision traditionally ranks second, which corresponds to the average statistical indicators for the Russian Federation. Attention is drawn to the fact that in the structure of registered diseases in children, the pathology of ON is 13 cases of the disease, and in the dispensary group there are 9 patients. This can be explained by the fact that patients with an established diagnosis of congestive discs of the ON are observed by a neurologist. The category of other diseases includes: retinal diseases 0.91% (4/437), patients with inflammatory diseases of the cornea and glaucoma 0.45% each (2/437 each), neoplasms 0.22% (1/437). Thus, the structure of nosologies in the dispensary group reflects the general trend of ophthalmic outpatient admission to the child population and is aimed at the treatment and monitoring of chronic diseases. The first two groups (refractive errors and binocular vision pathologies) are those nosologies, the progression of which is associated with poor control of the disease, lack of compliance. Attention is drawn to the growth of pathology of the optic nerve and retina, which has a tendency throughout the Russian Federation, which is associated with an increase in the number of premature babies. From our point of view, this is subject to further study with the aim of the etiology of the origin of these diseases and the development of effective rehabilitation programs.

Conclusion. Despite the increase in the child population in a separate polyclinic in Tyumen, the structure of indicators of chronic ophthalmopathy remains in line with the average statistical indicators for the Russian Federation: in the first place are refractive errors, in second place - diseases of the muscles of the eye, in third place - diseases of the visual nerve. Diseases of the optic nerve occupy one of the leading places only in the last 5 years, which is associated with the effectiveness of medical care and nursing of premature babies. Acute inflammatory diseases traditionally rank second in the overall structure of eye pathology at an outpatient visit. The structure of nosologies of the dispensary group is similar to the structure of the primary outpatient admission and the leading position in it is occupied by an anomaly of refractions. In this regard, it is necessary to provide additional equipment for ophthalmological recep-

tion rooms with ultrasound devices (to control the anterior and posterior size of the eyeball), a synoptophore apparatus (to improve the diagnosis and treatment of binocular vision pathology).

References

1. Drevnitskaya T.S. Analysis of the revealed ophthalmological and somatic pathology of schoolchildren based on the results of preventive examinations / T.S. Drevnitskaya, [et al.] // In the book: Congress "Man and Medicine. URAL - 2019". Collection of materials (abstracts). 2019. P. 28-29.
2. Koptseva T.A. Issues of pathology of refraction from the position of an ophthalmologist at the outpatient reception of the child population / T.A. Koptseva, E.M. Pochinok, E.V. Fomina // In the book: Materials of the Xth Anniversary Therapeutic Forum "Actual issues of diagnosis and treatment of the most common diseases of internal organs". Materials of the X Anniversary Therapeutic Forum. 2018. P. 45.
3. Krasnova L.A. Migration of the population in Tyumen Oblast: causes and impact on the socio-demographic composition of the population. / L.A., Krasnova, A.P. Ked // Internet magazine "Science". – 2017. – V.9. – №4. – P.1-10.<http://naukovedenie.ru/PDF/31EVN417.pdf>. P. 1-10.
4. Makarova D.M. School medicine: conducting preventive examinations by an ophthalmologist and organizing treatment at the territorial level / D.M. Makarova, N.I. Kharitonova, E.V. Fomina, E.M. Pochinok // In the book: Materials of the Xth Anniversary Therapeutic Forum "Actual issues of diagnosis and treatment of the most common diseases of internal organs". Materials of the X Anniversary Therapeutic Forum. 2018. P. 58-59.
5. Ponomareva M.N. On the issue of retinopathy of premature/ M.N. Ponomarev, V.N. Alekina, E.M. Pochinok, D.A. Karpova // In the book: Congress "Man and Medicine. URAL - 2019". Collection of materials (abstracts). 2019. P. 66-67.
6. Fomina E.V. The value of the study of accommodation and binocular balance for the risk of myopia progression / E.V. Fomina, E.M. Pochinok // Point of view. East - West. 2020. № 2. P. 53-55.

IMPACT OF THE MUSCULOSKELETAL DISORDERS IN PATIENTS WITH CORONARY ARTERY DISEASE ON THE OUTCOME OF CORONARY BYPASS GRAFT SURGERY¹

Terentyeva Natalya Aleksandrovna

Postgraduate

Bazdyrev Evgeny Dmitrievich

Doctor of Medical Sciences, Head of the Laboratory

Krivoshapova Kristina Evgenievna

Candidate of Medical Sciences, Researcher

Pomeshkina Svetlana Aleksandrovna

Doctor of Medical Sciences, Head of the Laboratory

Barbarash Olga Leonidovna

Doctor of Medical Sciences, Full Professor,
Corresponding Member of the RAS, director

Research Institute of Complex Problems for Cardiovascular Diseases
Kemerovo, Russia

A single-center, cohort study was conducted among patients with stable coronary artery disease (CAD), admitted for coronary artery bypass grafting (CABG). The aim of the study was to assess the prevalence of musculoskeletal disorders in patients with CAD and to determine their impact on the outcomes of CABG. It was revealed that one-third of patients had prior musculoskeletal disorder (MSD). Sarcopenia and osteopenia increase the risk of early postoperative complications. The study demonstrated that the MSD in combination with prior stroke, myocardial infarction, diabetes mellitus, and age are risk factors for early postoperative complications in CABG patients.

Keywords: coronary artery disease, coronary artery bypass grafting,

¹The study was supported by Federal State Budgetary Institution of Higher Education “Kemerovo State University” (Contract №1327/2020/223, under the Agreement №075-15-2020-766 made as of 14th of December, 2020, entitled “Patient-centered care for patients with coronary artery disease and osteosarcopenia who underwent coronary artery bypass graft surgery”).

prognosis, musculoskeletal disorder, osteopenia, osteoporosis, sarcopenia, osteosarcopenia.

Circulatory system diseases (CSD) are a priority in modern healthcare. Coronary artery disease (CAD) is one of the most significant CSD due to high rates of morbidity, disability and mortality worldwide. Myocardial revascularization has been an established mainstay in the treatment of CAD for almost half a century, improving the prognosis and quality of life of patients [1]. The patients undergoing cardiac surgery are mainly persons over 60 years. The patient's age alone is not a contraindication to cardiac surgery. However, the risk of postoperative complications and fatal outcome in elderly patients is much higher in comparison to younger patients [2]. On the one hand, elderly patients have more than one concomitant pathology. The most common concomitant diseases in this group of patients include arterial hypertension (AH), type 2 diabetes mellitus (DM), chronic obstructive pulmonary disease, peripheral atherosclerosis, cerebrovascular diseases and renal failure [2]. On the other hand, primarily due to age elderly patients have their own features [3].

Aging is associated with many changes in the human body, including the musculoskeletal system. Upon reaching age of sixty, elderly people will experience a gradual decrease in bone mineral density (BMD) (1-1.5% per year), muscle mass (1% per year) and strength (2.5-3% per year), and a simultaneous increase of the risk of developing age-related diseases of the musculoskeletal system, such as osteopenia, sarcopenia and osteosarcopenia [4].

Aim: to assess the prevalence of musculoskeletal disorders in patients with coronary artery disease and to determine their impact on the outcomes of coronary artery bypass grafting surgery.

Materials and methods

A single-center, single-stage cohort study was conducted among 387 patients with stable coronary artery disease, admitted to the "Research Institute of Complex Problems for Cardiovascular Diseases" for coronary artery bypass grafting (CABG). The criteria for inclusion in the study were: signed informed consent, age over 50 years, CAD, scheduled for CABG. The exclusion criteria were: neuromuscular disorders, long-term use of skeletal muscle relaxants, glucocorticosteroids, barbiturates, antidepressants and cytostatics, and refusal to participate in the study.

Sarcopenia was diagnosed according to the European Working Group on Sarcopenia in Older People (EWGSOP, 2019) [5] and osteopenia for postmenopausal women and men over 50 years was diagnosed according to the World Health Organization (WHO, 2008) [6].

All patients underwent typical CABG via median thoracotomy and cardiopulmonary bypass. In order to assess the impact of the prior musculoskeletal disorder (MSD) on the development of early postoperative complications, the development of the composite endpoint (CE) was evaluated. CE was defined as the development/absence of any complication (cardiovascular, surgical, pulmonary) in patients treated with CABG.

Statistical analysis was performed using the Statistica software (v. 6.1.).

Results and discussion

Out of 387 all the patients included in the study, 27.1% of patients with CAD demonstrated signs of sarcopenia and osteopenia/osteoporosis. In order to assess the clinical status, a comparative analysis of patients with CAD was performed depending on the MSD (Table 1).

Table 1. Comparative characteristics of patients with CAD depending on the musculoskeletal disorder

Clinical and anamnestic factor	Group I (with musculoskeletal disorders), n=105 (27,1 %)	Group II (without musculoskeletal disorders), n=282 (72,9 %)	p
Men, n (%)	81 (77,1)	202 (71,6)	0,2
Age, years, Me (Lq; Uq)	66 (61;70)	65 (59;69)	0,4
BMI, kg/m ² Me (Lq; Uq)	28,1 (25,2;30,8)	30 (27;32,6)	0,006
Arterial hypertension, n (%)	93 (88,6)	230 (81,6)	0,09
CCS FC of angina, Me (Lq; Uq)	2 (2;2)	2 (2;2)	0,48
Duration of CAD, years, Me (Lq; Uq)	2 (1;5)	2 (1;5)	0,5
Prior MI, n (%)	65 (55,3)	156 (61,9)	0,2
Cardiac arrhythmias, n (%)	14 (20,9)	24 (14,6)	0,2
Prior type 2 DM in medical history, n (%)	26 (24,8)	72 (25,5)	0,8
Prior stroke in medical history, n (%)	8 (7,6)	28 (9,9)	0,4
SARC-F score, Me (Lq; Uq)	5 (1;6)	2 (0;1)	0,003
T-score at femoral neck, Me (Lq; Uq)	-1 (-1,5;-0,3)	-0,2 (-0,7;0,6)	0,001

Muscle area, cm ² , Me (Lq; Uq)	138,6 (112;155,2)	161,5 (122;174,3)	0,04
Dynamometry			
Men, kg, Me (Lq; Uq)	26 (25;26)	30 (28;34)	0,001
Women, kg, Me (Lq; Uq)	14,5 (13;15)	20 (18;30)	0,017
Skeletal muscle index			
Men, cm ² /m ² , Me (Lq; Uq)	48,76 (43,7; 51,6)	56,8 (54; 60,6)	0,03
Women, cm ² /m ² , Me (Lq; Uq)	34,06 (33,04; 37,06)	42,3 (40,3;43,6)	0,045

Note: AH – arterial hypertension, CAD – coronary artery disease, MI - myocardial infarction, BMI - body mass index, DM - diabetes mellitus, CCS FC - The Canadian Cardiovascular Society functional classification of angina, SARC-F - Strength, Assistance for walking, Rise from a chair, Climb stairs, and Falls score.

Two groups were comparable with respect to baseline characteristics, however standard deviation was present. The patients with MSD had lower values of body mass index (BMI) (28.1 kg/m² vs. 30 kg/m² p=0.006), lower mean SARC-F score (5 vs. 2 score, p=0.003), lower bone density (-1(-1.5;-0.3) vs. -0.2(-0.7;0.6), p=0.001), lower values of muscle area (138.6 cm² vs. 161.5 cm², p=0.04), etc. It was similar with respect to the muscular strength and muscle mass estimated by dynamometry and skeletal muscle index in both women and men.

The current study analyzed the incidence of CE. In the group of patients with prior MSD, CE was registered in 80 (76.2%) patients. In the group of patients without MSD, CE was 1.17 times less prevalent - 183 (64.99%), p = 0.034. Calculating the odds ratio (OR) and 95 % confidence interval (CI), the presence of prior MSD was associated with an increase in the risk of CE after revascularization by 1.7 times (OR =1.73 with 95% CI:1.03-2.89, p = 0.035), compared to patients without MSD.

Classification tree analysis was performed in order to assess the significance of impact of risk factors such as age, concomitant pathology (Arterial hypertension (AH), prior myocardial infarction (MI), cardiac arrhythmia, type 2 diabetes mellitus, prior stroke) and the presence/absence of MSD on the probability of developing CE. The discriminant one-dimensional branching technique was used for categorical and ordinal predictors. The significance of risk factors based on the results of the classification tree analysis was assessed on a 100-point scale, and the significance of the predictor that had the maximum impact on the object was taken as 100 conventional units (c.u.). The results of the analysis demonstrated that the greater influence on the development of CE was exerted by concomitant pathology (prior stroke - 100 c.u., prior MI - 97 c.u., DM - 51 c.u.) and MSD

- 27 c.u., while age had lower influence of 19 c.u.

Thus, this study demonstrated that one-third of patients with CAD had MSD. It should be noted that in the inter-group analysis of clinical and anamnestic features of two groups did not show statistically significant differences, with the exception of naturally worse outcomes due to MSD. Prior MSD was a statistically significant predictor of CE after CABG (76.2% vs. 64.99%, $p=0.034$). During the assessment of the rank significance of the influence of the risk factors, it was revealed that age had a lesser influence than a number of concomitant diseases and MSD.

The process of aging is primarily associated with the development of comorbid conditions and age-related changes in organs and systems that can independently predict morbidity and mortality [4]. Undoubtedly, age plays an important role in the degeneration of the cardiovascular system (CVS), leading to an increased risk of developing CSD in elderly patients. CABG has been established as the most effective treatment for these patients. The surgical risk prediction that includes the age-related features of an elderly patient has become a point of interest for many researchers. A number of authors have demonstrated that sarcopenia and osteopenia are a common pathology in the elderly patients, associated with the risk of developing cardiovascular diseases and unfavorable outcomes after cardiac surgery [7-14] (which is consistent with the data obtained in this study). In the study done by Sumin A.N. et. al, the signs of low muscle mass were detected in 58.44% out of 77 CABG patients with CAD aged 51-59 years. The researchers demonstrated that in patients with initially low muscle mass the incidence of serious postoperative complications (CE) was significantly more prevalent than in patients with higher values of muscle mass (19.05% vs. 3.53%, $p=0.003$) [7]. Hawkins RB et. al revealed that in patients admitted for aortic valve replacement sarcopenia was diagnosed in 33.3% of cases according to the "psoas muscle index" (i.e. by using the skeletal muscle index). Moreover, patients with prior MSD (sarcopenia) had a higher annual mortality compared to patients without MSD (31.9% vs. 16.9%, $p=0.03$). The authors concluded that the skeletal muscle index can be considered as an independent predictor of fatal outcome in early (OR 0.84; $p=0.02$) and late (OR 0.92, $p=0.04$) postoperative periods [8]. Similar results were obtained in a study conducted by Okamura H. et al. - sarcopenia was an independent predictor of lower survival rate among patients undergoing cardiac surgery (valve replacement) (OR 2.22; 95% CI 1.26-3.92, $p=0.006$) [9].

The medical literature analysis pointed out the absence of studies devoted to the impact of osteopenia/osteoporosis on the prognosis of cardi-

ac surgery. However, there are many studies devoted to the prevalence of this pathology, as well as the adverse effect on the course of cardiovascular diseases [10-14]. Thus, the meta-analysis (25 studies, 10,300 patients) conducted by Ye C. et al. revealed that the adjusted incidence of atherosclerosis was significantly higher in patients with low BMD compared to normal BMD (OR 2.96), and in individuals with diagnosed osteoporosis compared to the group without osteoporosis (OR 2.45) [10].

A meta-analysis of 11 studies conducted by Veronese N. et al. demonstrated that subjects with low BMD have an increased risk of developing cardiovascular diseases during follow-up period (OR 1.33). It was noted that a decrease in BMD by one 1SD corresponded to an increase in the risk of developing cardiovascular pathology and cardiovascular diseases by 44% and 28%, respectively [11]. The population-based cohort study in Asia included an analysis of 38,912 respondents, the aim of the study was to assess the risk of developing CAD in patients with osteoporosis. The researchers concluded that the overall incidence of CAD was 23.5 (per 1,000 person-years) in the cohort of patients with osteoporosis and 16.7 in the comparison group, with an average follow-up period of 6.54 years and 6.63 years, respectively. The risk of developing CAD during follow-up was 1.30 (95% CI 1.23–1.38) [12]. Researches Rui Xu et. al demonstrated a parallel between the severity of osteopenia and the degeneration of coronary arteries (OR 2.73; CI 95% 1.06 to 6.13) [13]. Moreover, in a large meta-analysis comprising 110,788 patients, it was shown that low BMD and fractures are associated with a higher incidence of CAD, cerebrovascular diseases, and death due to cardiovascular diseases [14].

Thus, the prior MSD is a risk factor for an adverse prognosis in patients with CSD and a potential complication of cardiac surgery.

Conclusion

Musculoskeletal disorders were detected in one-third of CABG patients with CAD. Sarcopenia and osteopenia increase the risk of early postoperative complications. The study results demonstrated that the prior musculoskeletal disorder with prior stroke, MI, DM, and age are factors of adverse prognosis.

References

1. Prevention of respiratory complications in subjects with coronary artery disease when performing planned coronary artery bypass grafting / E. D. Bazdyrev, S. V. Ivanov, V. Yu. Pavlova, O. L. Barbarash // *Complex Issues of Cardiovascular Diseases*. – 2016. – Vol. 5, № 1. – P. 37-50. doi:10.17802/2306-1278-2016-1-37-50.
2. Dodson, J. A. Changing nature of cardiac interventions in older adults / J. A. Dodson, M. S. Maurer // *Aging Health*. – 2011. – Vol. 7, № 2. – P. 283-295. doi: 10.2217/ahe.11.12.
3. Fatima, M. Therapeutic approaches to osteosarcopenia: insights for the clinician / M. Fatima, S. L. Brennan-Olsen, G. Duque // *Ther. Adv. Musculoskelet. Dis*. – 2019. – Vol.11. – 1759720X19867009. doi: 10.1177/1759720X19867009.
4. Kirk, B. Osteosarcopenia: epidemiology, diagnosis, and treatment – facts and numbers / B. Kirk, J. Zanker, G. Duque // *J. Cachexia Sarcopenia Muscle*. – 2020. – Vol. 11, № 3. – P. 609–618. doi: 10.1002/jcsm.12567.
5. Sarcopenia: revised European consensus on definition and diagnosis / A. J. Cruz-Jentoft, G. Bahat, J. Bauer et al. // *Age Ageing*. – 2019. – Vol. 48, № 1. – P. 16–31. doi: 10.1093/ageing/afy169.
6. Russian federal clinical guidelines on the diagnostics, treatment, and prevention of osteoporosis / G. A. Mel'nichenko, Zh. E. Belaya, L. Ya. Rozhinskaya et al. // *Problems of Endocrinology*. – 2017. –Vol. 63, № 6. – P. 392-426. doi: 10.14341/probl2017636392-426.
7. Sumin, A. N. Assessment of skeletal muscle in patients with stable coronary artery disease: clinical significance and associations / A. N. Sumin, P. A. Oleinik, A. V. Bezdenezhnykh // *Cardiovascular Therapy and Prevention*. – 2020. – Vol. 9, № 1. – P. 895. doi:10.15829/1728-8800-2019-895.
8. Psoas muscle size predicts risk-adjusted outcomes after surgical aortic valve replacement / R. B. Hawkins, J. H. Mehaffey, E. J. Charles et al. // *Ann. Thorac. Surg*. – 2018. – Vol. 106, № 1. – P. 39-45. doi:10.1016/j.athoracsur.2018.02.010.
9. The impact of preoperative sarcopenia, defined based on psoas muscle area, on long-term outcomes of heart valve surgery / H. Okamura, N. Kimura, K. Tanno et al. // *J. Thorac. Cardiovasc. Surg*. – 2019. – Vol. 157, № 3. – P. 1071-1079. doi: 10.1016/j.jtcvs.2018.06.098.
10. Decreased bone mineral density is an independent predictor for the development of atherosclerosis: a systematic review and meta-analysis / C. Ye, M. Xu, S. Wang et al. // *PLoS One*. – 2016. – Vol. 11. – e0154740. doi: 10.1371/journal.pone.0154740.

11. Relationship between low bone mineral density and fractures with incident cardiovascular disease: a systematic review and meta-analysis / N. Veronese, B. Stubbs, G. Crepaldi et al. // *J. Bone Miner Res.* – 2017. – Vol. 32. – P. 1126-1135. doi: 10.1002/jbmr.3089.
12. Osteoporosis is associated with high risk for coronary heart disease: a population-based cohort study / S. J. Chen, C. S. Lin, C. L. Lin, C. H. Kao // *Medicine (Baltimore)*. – 2015. – Vol. 94, № 27. – e1146. doi: 10.1097/MD.0000000000001146
13. Association of severity of coronary lesions with bone mineral density in postmenopausal women / R. Xu, X. C. Cheng, Y. Zhang et al. // *Arq. Bras. Cardiol.* – 2018. – Vol. 110, № 3. – P. 211–216. doi: 10.5935/abc.20180035.
14. Relationship between low bone mineral density and fractures with incident cardiovascular disease: a systematic review and meta-analysis / N. Veronese, B. Stubbs, G. Crepaldi et al. // *J. Bone Miner. Res.* – 2017. – Vol. 32, № 5. – P. 1126–1135. doi: 10.1002/jbmr.3089.

**NEW OPPORTUNITIES FOR STUDYING THE OVICIDAL ACTIVITY OF
DISINFECTANTS AND ESTIMATING THE VIABILITY OF HELMINTH
EGGS**

Gerasimov Vladimir Nikolaevich

Doctor of Biological Sciences, Head Research Officer, Head of Division

Aslanyan Elena Mkritichevna

Lead Engineer

Podgornaya Natalia Nikolaevna

Engineer

Tyryshkina Anna Igorevna

Research laboratory assistant

Khramov Mikhail Vladimirovich

Candidate of Medical Sciences, Deputy Director

State Research Center for Applied Microbiology and Biotechnology

The work is devoted to the creation of a methodological base for the experimental selection of effective antiparasitic agents for environmental protection from contamination with invasive material.

An improved method for determining the ovicidal efficacy of chemical compounds using a multifunctional microcamera is presented. A comparative characteristic of the traditional and improved methods for determining the ovicidal efficacy of disinfectants is given. It is shown that the use of a multifunctional microchamber for setting up experiments to study the effect of disinfectants on helminth eggs makes it possible to significantly simplify the process of washing eggs from a disinfectant, to abandon the use of a neutralizer, to reduce the time for setting up an experiment, to simplify the process of determining the viability of eggs by staining and cultivation methods, to reduce the loss of eggs at the stage washing them from disinfectant.

Keywords: infestation, disinfectants, disinfestation, helminth eggs, methods for determining ovicidal efficacy, multifunctional microchamber, egg viability

The search for new highly effective antiparasitic agents is an important direction in the field of environmental protection from contamination with invasive material [1-6]. The criterion for the experimental selection of effective disinfection agents, in particular, is the degree of ovicidal action of disinfectants and other chemical compounds on helminth eggs. The methodological basis for work in this area of research has long been developed [7-9]. However, conventional methods for testing the ovicidal effect of disinfectants and other chemical compounds involve laborious or technically difficult steps to complete. So, for example, when setting up an experiment in Petri dishes or weighing bottles, the treated eggs must be washed with water from the disinfectant at least 5 times by hand, or at least 2 times using a centrifuge [8, 9]. These operations take a lot of time, require certain skills and are associated with partial loss of eggs. The use of neutralizers to suspend the action of disinfectants further complicates the process.

Such an important stage in setting up experiments for testing ovicidal action, as assessing the viability of helminth eggs after exposure to disinfectants, also contains a number of difficulties. To determine the viability of immature helminth eggs, the method of their cultivation under optimal conditions is most often used. Usually, cultivation is carried out in the same containers in which the tests were carried out (Petri dishes, weighing bottles, watch glasses). After washing the eggs from the disinfectant, a thin layer of water or some solution suitable for cultivation is poured into these containers and placed in optimal conditions (24-30°C) for 2-4 weeks until the larva forms. During this period, at the specified temperature, the water evaporates quickly and you have to add it several times. Some authors even write about the need for periodic replacement of solutions in order to prevent the development of microorganisms [7, 10]. Adding water to all containers with eggs (and there are quite a few of them) and, moreover, replacing solutions for cultivation complicate the course of the experiment. It should also be noted that traditional cultivation containers take up a lot of space and their placement in a thermostat creates a certain difficulty when several experiments are performed. Determination of the viability of helminth eggs by the staining method includes such operations as processing with a dye, removing the dye and, if necessary, washing off the dye. These operations are also time consuming and lead to the loss of eggs.

In order to optimally solve the above problems, we have developed a multifunctional microcamera [11] and proposed a method for its application to determine ovicidal activity.

The purpose of the research. Improvement of the method for determining the ovicidal efficacy of chemical compounds using a multifunctional microcamera. Comparison of traditional and advanced methods.

Materials and methods. To improve the method for determining the ovicidal activity of disinfectants, it is proposed to use a multifunctional microchamber, which is a translucent cell in the form of an inverted truncated cone. The diameter of the larger (upper) base of the cone is 8 mm, the smaller (lower) one is 5 mm, the height of the cone is 6 mm. A trapping membrane (track membrane), which is a thin polymer film with a pore diameter of 2 to 5 microns, is tightly attached to the lower base.

Our proposed improved method for determining the ovicidal efficiency of chemical compounds using a multifunctional microcamera is as follows. First, helminth eggs are treated with a disinfectant in the traditional suspension method. For this purpose, 20 μl of egg suspension is poured into Eppendorf tubes with a volume of 1500 μl , and 1000 μl of disinfectant at the tested concentrations is added. The same amount of distilled water is added to the control variants. All subsequent operations are performed using a micro-camera. At the end of the exposure, to stop the action of the disinfectant, it is removed by passing the treated suspension of eggs through a microchamber installed in a Petri dish on a lining of coarse calico folded in 8-16 layers. To accelerate the passage of the liquid through the microchamber, it is tightly pressed against the tissue with tweezers. After that, the microchamber with the treated eggs is transferred to a clean lining of coarse calico and water is passed through it three times, 1000 μl each, thus removing the remainder of the disinfectant. Further, to determine the viability of eggs, microchambers are installed in 4-well culture plates with a lid. If the viability is determined by the cultivation method, then 500 μl of distilled water is added to each microchamber with eggs installed in the well of the plate, after which the plates are placed in a desiccator in a thermostat to maintain optimal cultivation conditions. Ongoing observation of the development of eggs in microchambers is carried out under a microscope at a magnification of 100x directly in the plates. To account for the number of live and dead eggs at the end of cultivation, the microchambers are removed from the wells of the plate, excess liquid is removed, placed on a glass slide and examined at the same magnification. For better viewing, 1-2 drops of distilled water are added to the micro-camera, if necessary. If the viability is determined by the staining method, then 500 μl of dye is added to each microchamber with eggs installed in the well of the plate, which at the end of staining can be easily removed by filtering on a calico lining. If necessary, dyed eggs in

microchambers are washed with water also on a calico lining. The colored eggs are examined in microchambers under a microscope at a magnification of 100x.

Comparison of the traditional and improved methods was carried out on the material obtained during the study of the ovicidal effect of disinfectants on *Ascaris suum* eggs. For setting up the experiments, we used non-invasive roundworm eggs isolated from the middle section of the uterus of an adult female. The experiments were performed in duplicate. At the initial stage, the treatment of eggs with a disinfectant was carried out in the same way - by the suspension method. At the stage of freeing the eggs from the action of the disinfectant, 2 methods were used: an improved one, using a multifunctional microchamber (described above) and a traditional one, using a centrifuge. When setting up experiments by the traditional method, the disinfectant was removed from the tubes to a volume of 50 μ l, 1300 μ l of distilled water was added and centrifuged for 5 minutes at 800 rpm. Then the supernatant was taken to a level of 50 μ l, water was added in the above volume and centrifuged again. The centrifugation operation was repeated three times. Comparison of the methods was carried out according to two parameters: the duration of the process of freeing the eggs from the action of disinfectants, and the number of eggs remaining after this manipulation for the subsequent determination of their viability. The viability of the treated eggs, freed from the action of the disinfectant by two different methods, was determined in one way - by cultivation under optimal conditions using a multifunctional microchamber. Comparison of methods at this stage of research is not carried out in this work.

The material for comparing the two methods was obtained as a result of studies by different operators of the ovicidal action of the disinfectants "Enke mod", "Pharmades" and "Povidone Iodine". In the course of the work, the time required to free the eggs from the action of disinfectants was recorded using two methods. Before setting up for cultivation, the number of eggs remaining after the previous operation performed by two methods was counted. Eggs were counted in microchambers under a microscope at 100x magnification.

Results and discussion.

The stage of freeing eggs from the action of disinfectants for the convenience of recording the time of its execution and comparison of methods was conditionally divided into separate operations and actions.

In the experiments performed by the traditional method, the following operations were distinguished at this stage: centrifugation (three times),

preparation for it (three times), preparation of eggs for cultivation. The operation of preparation for centrifugation included such actions as removing the preparation from the tubes (before 1 centrifugation) or the supernatant (before 2 and 3 centrifugations), adding water for washing the eggs, mixing the contents of the tubes. The centrifugation operation began with the installation of tubes in the centrifuge, included the centrifugation time (from start-up to complete stop of the centrifuge), and ended with the removal of the tubes from the centrifuge for subsequent manipulations. Preparation of eggs for cultivation consisted of transferring, after centrifugation 3, the egg suspension into the microchamber, removing the liquid, installing the microchamber in the well of the plate and adding the culture liquid. Thus, the stage of freeing eggs from the effects of a disinfectant, performed by the traditional method using a centrifuge, consisted of 7 basic operations, each of which, in turn, was split into several simpler actions (21 actions in total). Each operation was performed at once for all variants of the experiment, recording the time of its performance. The total duration of the stage of freeing eggs from the action of disinfectants for all variants of the experiment was obtained by adding up the time for performing individual operations.

The release of eggs from the action of the disinfectant, carried out by a modified method using a microchamber, consisted in transferring the processed egg suspension from the test tube to the microchamber, straining the disinfectant, washing the eggs three times in the microchamber with water, installing the microchamber in the well of the plate, and adding water for cultivation (7 actions in total). For each variant, all actions were performed at once. The total processing time for all variants of the experiment was recorded from the beginning of work with the first variant to the end of work with the last variant. Table 1 shows data on the time required to complete the stage of freeing eggs from the action of disinfectants using two methods.

Table 1– Time to complete the stage of freeing eggs from the action of disinfectants by two methods

Drug name	Operator number	Experiment variants number	Stage execution time for all variants of the experiment (min.)		Average stage execution time for one experiment variant (min.)		Correlation of the operation execution time by two methods "C"/"M"
			"C" *	"M" **	"C"	"M"	
Encke Mod	1	10	95	38	9.5	3.8	2.5
Pharmades	2	8	65	29	8.1	3.6	2.2
Pharmades	1	6	64	21	10.7	3.5	3.0
Povidone Iodine	3	6	51	22	8.5	3.7	2.3
Notes * "C" – traditional method (using a centrifuge) ** "M" – improved method (using a micro camera)							

Summing up the above, we can say that the improved method for determining ovicidal activity is simpler in comparison with the traditional one, and at the stage of freeing eggs from the action of disinfectants, it requires fewer operations (7 instead of 21). In addition, according to Table 1, the processing of one variant of the experiment by the improved method occurs, on average, 2.5 times faster than the traditional one (from 2.2 to 3 times). Analyzing the data on the processing time of one variant of the experiment by different operators, we can say that in the case of using the improved method, it depends less on the operator's speed. Thus, the spread of time when processing one variant of the experiment by different operators by the traditional method is 2.5 minutes (from 8.1 to 10.6 minutes), and by the improved method - 0.3 minutes (from 3.5 to 3.8 minutes).

In addition to simplifying the work and saving time, when using a microcamera in the formulation of experiments to study the ovicidal action of disinfectants, there is also a saving (preservation) of material for testing. Table 2 shows data on the number of eggs remaining for the subsequent determination of viability, after freeing them from the action of drugs by two methods.

Table 2 - The number of *A. suum* eggs remaining after they were freed from the action of disinfectants by two methods

Drug name	Operator number	Estimated number of eggs in the experiment	Experiment variants number	Actual number of eggs in all variants of the experiment		Average number of eggs in one variant of the experiment		Share "C" of "M" %	Excess "M" over "C" %
				"C" *	"M"***	"C"	"M"		
Encke Mod	1	1800	10	1137	1741	114	174	66	34
Pharmades	2	530	8	428	510	54	64	84	16
Pharmades	1	840	6	614	842	102	140	73	27
Povidone Iodine	3	840	6	522	847	87	141	62	38
Notes * "C" – The number of eggs after freeing them from the action of a disinfectant using a centrifuge ***"M" – The number of eggs after freeing them from the action of a disinfectant using a microcamera									

Analysis of the data in the table shows that in the experiments performed by the improved method, the number of eggs is always higher than in the experiments performed by the traditional method. The difference in the number of eggs averages 29% (from 16% to 38%). In other words, at the stage of freeing the eggs from the action of the disinfectant by the traditional method using a centrifuge, more than a quarter of the eggs are lost. In addition, the actual number of eggs is more consistent with the calculated in the experiments carried out by the improved method as compared to the traditional one. The calculated number of eggs was determined by multiplying the density of eggs in the working suspension by the volume of the suspension in each variant and by the number of experimental variants.

Conclusion

The use of a multifunctional micro-camera for setting up experiments to study the effect of disinfectants on helminth eggs makes it possible to significantly simplify the process of washing eggs from the disinfectant, to abandon the use of a neutralizer, to reduce the time for setting up the experiment, to simplify the process of determining the viability of eggs by staining and cultivation methods, to reduce the loss of eggs at the stage of their washing from disinfectant.

References

1. СанПиН 3.2.3215 – 14. Профилактика паразитарных болезней на территории Российской Федерации. [SanPiN 3.2.3215 - 14. Prevention of parasitic diseases in the territory of the Russian Federation [in Russian].
2. МУ 3.2.1022 – 01. Мероприятия по снижению риска заражения населения возбудителями паразитозов. [MU 3.2.1022 - 01. Measures to reduce the risk of infection of the population with parasitic pathogens [in Russian].
3. Постановление Главного государственного врача РФ от 25 декабря 2007 г. № 94 «Об усилении мероприятий по предупреждению паразитарных заболеваний и элиминации малярии в Российской Федерации». [Resolution of the Chief State Doctor of the Russian Federation of December 25, 2007. №94 "On strengthening measures for the prevention of parasitic diseases and elimination of malaria in the Russian Federation" [in Russian].
4. Долбин Д. А., Хайруллин Р. З. Устойчивость яиц гельминтов к неблагоприятным физическим, химическим и биологическим факторам окружающей среды (обзор литературы). // Российский паразитологический журнал. – М., 2017. – Т.39.- Вып.1 . – С. 14-19. [Dolbin D.A., Khairullin R. Z. Resistance of helminth eggs to adverse physical, chemical and biological environmental factors (literature review). // Russian parasitological journal. - M., 2017. - V.39. - Issue 1. – P. 14-19 [in Russian].
5. Черникова, Е.А. Геогельминтозы в Российской Федерации / Е.А. Черникова, Л. Миглиорини, С.К. Литвинов, Н.Н. Дарченкова, К.А. Новожилов // Мед. паразитол. – 2015. – № 2. – С.51-54.[Chernikova E.A., Migliorini L., Litvinov S.K., Darchenkova N.N., Novozhilov K.A. Geohelminthiasis in the Russian Federation. // Med. parasitol. - 2015. - №2. - P.51-54 [in Russian].
6. Новиков Н. Л. Разработка средств и методов обеззараживания животноводческих помещений от возбудителей инвазионных и инфекционных заболеваний.// Автореферат диссертации ... канд. ветеринарных наук. – Москва. – 2004. [Novikov N.L. Development of means and methods for disinfecting livestock buildings from pathogens of invasive and infectious diseases. // Abstract of thesis ... Cand. veterinary sciences. - Moscow. - 2004.[in Russian].

7. Симонов А.П. Методика испытания и отбора овоцидных химических соединений для обеззараживания объектов с твердым покрытием (помещений, пола, клеток и др.). – Бюллетень Всесоюзного ордена Трудового Красного Знамени ин-та гельминтологии им. К.И. Скрябина, 1977, вып.19. – С.51.

8. Романенко, Н.А. Санитарная паразитология / Н.А. Романенко, И.К. Падченко, Н.В. Чебышев. – М.: Медицина, 2000. – С. 182-191. [Romanenko, N.A. Sanitary parasitology / N.A. Romanenko, I.K. Padchenko, N.V. Chebyshev. - M.: Medicine, 2000. - p. 182-191]

9. МУК 4.2.2661-10. Методические указания. Методы санитарно-паразитологических исследований. [MUK 4.2.2661-10. Methodical instructions. Methods of sanitary parasitological research]

10. Krotov A.I. Methods of modeling and experimental therapy of helminthiasis // Biochemistry and physiology of helminths and immunity in helminthiasis: collection of articles; ed. B. A. Shishova. – М.: Science, 1984. – P. 58-63.

11. Patent for invention № 2699664 "Multifunctional microcamera and method for experimental selection of ovocidal chemical compounds for disinfection (disinfestation) of surfaces and objects contaminated with helminth eggs." The date of state registration in the State Register of Inventions of the Russian Federation is 09 September 2019.

DOI 10.34660/INF.2021.11.14.020

**OVERALL ASSESSMENT OF THE INNOVATIVE PREPARATION
"GLAUXIN" ON THE PRODUCT QUALITY AND NUTRITIONAL VALUE
OF HYDROPONICALLY GROWN OAKLEAF LETTUCE PLANTS UPON
FOLIAR TREATMENT**

Ali J. Othman

Plekhanov Russian University of Economics, Moscow, Russia

Ludmila G. Eliseeva

Plekhanov Russian University of Economics, Moscow, Russia

Majd Alsaady

Damascus University, Damascus, Syria

Vyacheslav V. Latushkin

Institute for Development Strategies, Moscow, Russia

*"Glaxin" is a phytomineral preparation based on glauconite mineral with the addition of bacteria autolysates of the and other components gives a positive effect when growing lettuce in a phytotron on a mineral wool substrate. This article demonstrates the effect of the "Glaxin" on the growth and development of oakleaf lettuce (*lactuca sativa* var. *Dubachek MC*). The yield of the treated samples increased by 20.7%, the content of chlorophyll "a" and chlorophyll "b" in the leaves increased. The overall quality of products improved, in particular, there has been an increase in the accumulation of the content B vitamins in the shoots. However, the content of residual amounts of nitrates recorded only a slight change. According to the results of biotesting, the phytomineral "Glaxin" does not deactivate the test cultures of *Daphnia magna* and *Paramecium caudatum*, which suggests a high level of food safety and quality.*

Keywords: Glaxin, phytotron, lettuce, vitamins B content, biotesting, product quality, chlorophyll content, ascorbic acid.

Introduction

Currently, plenty of biological preparations are used in agriculture plants as growth stimulants or plant growth promoters. The term glauconite has been employed in two senses. It is most commonly used as a morphological term for sand-sized greenish grains found in sedimentary

rocks, but also as a name for a specific mineral species, a hydrated iron-rich micaceous clay mineral [1, 2].

Glaucanite is a dioctahedral micaceous phyllosilicate mineral with variable chemical composition and a high content of interlayer potassium (up to 8–9%) [1]. It is widely distributed in ancient coastal marine sedimentary deposits [4, 5]. Glaucanite contains many trace elements including Cu, Zn, Fe, Mn, B, Se, Co, Mo, Cr, Vd, which serves as necessary micro-nutrients for plant growth. Furthermore, glaucanite rocks improve soil texture, porosity, and permeability because of the uniform and Pelletal texture [6, 7]. The fertilizer potential of glaucanite is indicated in recent studies on olive trees. A recent study demonstrating the application of glaucanitic rocks for raising the level of potassium in agricultural soil. Few studies reported a positive impact of glaucanite and indicated its fertilization potential on the growth of agricultural plants, such as olive trees [8], sunflowers [9], oat [10]. Glaucanitic rock may be used right away after crushing as a soil fertilizer [11].

However, in natural ecosystems, most nutrients such as N, P, and S are less bioavailable and sometimes difficult for the plants to absorb because they are bound in organic molecules. To access these nutrients, plants got adopted for their growth on soil microbes such as bacteria and fungi, which act as metabolic machinery to depolymerize and mineralize organic forms of N, P, and S [12].

Currently in agriculture, a number of biological preparations are used as plant growth promoters (PPP) [13]. Most of these preparations are based on microorganisms' content that is capable in its nature to do one or more of the following functions including inhibition the development of fungi and bacteria, stimulating the growth and development of plants, enhancing nitrogen fixation [13], converting insoluble soil phosphates into soluble forms [15, 16, 17].

Glauxine is a Phyto mineral of a complex composition based on two parts, the first one is biological which is represented by autolytic bacteria while the second one is mineral and characterized by its content of glaucanite mineral.

Bacterial autolysates are enriched with α -alanine, α -glutamic acid, 3-indoleacetic acid, protease and hydrolytic enzymes, folic acid, and other biologically active substances that actively contribute to plant growth in nature and protect them from diseases, while disodium salt of ethylene diamine Tetraacetic acid allows converting salts into chelated easily digestible forms, and the use of glaucanite enriches the composition with mobile forms of trace elements [18, 19].

These preparation “Glauxin” were designed on the basis of one or more culture of microorganisms in order to perform one of the functions: (1) inhibiting the development of phytopathogenic fungi and bacteria; (2) stimulating the growth and development of plants; (3) enhancing nitrogen fixation or converting insoluble soil phosphates into soluble forms [26, 27, 28, 29].

Studies of complex compositions of a wide spectrum of action made it possible to create a highly effective biological product. The innovative phytomineral “Glauxin” is based on mineral glauconite with a content percentage of 11-15%, coniferous extract 8%, chlorophyll-carotene paste 1-2%, solution of macro- and microelements 15-25%; Trilon-B – 0.5-2%. The content of bacterial autolysates in the preparation is of the following ratio of components (% wt.): autolysate of *Pseudomonas Aureofaciens* – 15-25; autolysate of *Bacillus Megaterium* containing poly- β -hydroxybutyric acid – 15-25; autolysate of *Bacillus subtilis* – 15-25; Autolysates of bacteria, components of the biological product are enriched with α -alanine, α -glutamic acid, 3-indoleacetic acid, protease, hydrolytic enzymes, folic acid, and other biologically active substances that promote plant growth and protect them from diseases, the disodium salt of ethylenediaminetetraacetic acid (Tri-sodium diamine Tetraacetic acid) convert salts into easily digestible chelated forms, and the use of glauconite enriches the composition with mobile forms of microelements [30].

The biological plant growth promoter “Glauxin” is registered in the Russian Federation as a mineral fertilizer and is produced by LLC (ГЛАУКОНИТ-НЕБА, St. Petersburg – Russian Federation).

The purpose of this research is to study the effectiveness of foliar treatment of the biological plant growth promoter “Glauxin” on product quality and nutritional content of oakleaf lettuce plants (*Lactuca sativa* var. Dubachek MC) grown in closed climatic chambers (phytotrons).

Materials and methods

The trial of Glauxin preparation on lettuce plants (*Lactuca sativa* var. Dubachek MC) was carried out under hydroponic culture on a substrate based on mineral wool in the conditions of phytotron ISR 0.1 in REU named after G.V. Plekhanov in Summer 2019.

Glauxin (Phytomineral) is a biological product containing glauconite mineral and based on the bacterial autolysates of *Pseudomonas aureofaciens* holding poly- β -hydroxybutyric acid, *Bacillus megaterium* and *Bacillus subtilis* with the following ratio of components in % wt (Autolysates of *Pseudomonas aureofaciens* 15-25; autolysates of *Bacillus megaterium* containing poly- β -hydroxybutyric acid - 15-25; autolysates of *Bacillus*

subtilis 15-25; glauconite mineral - 8-15; coniferous extract -3-8; chlorophyll-carotene paste 1-2; a solution of macro- and microelements 15-25; Trilon-B (EDTA) - 0.5-2; water D.S). The phytotron is a closed climatic chamber with dimensions of 1800 mm high, 1000 mm long, 500 mm width. Plants were placed in in three tiers: shelf sizes 920 mm * 350 mm. Material - smooth PPU sandwich panels 40 mm thick, painted white on both sides. Doors are double-glazed windows, open outwards and covered from inside with aluminium-light reflective material to ensure maximum light to be reflected into plants. The phytotron is equipped with a timer for optimizing the lighting and ventilation. The lighting system consists of (RAYWAY LED, China) with photosynthetic photon flux density (PPFD) of 180 lumen per one rod. three LED rods were installed on the top and two on the sides of each roof. The total lighting spectrum was determined by handed spectrometer (PG 100N UPRtek, Taiwan). The actual overall irradiation intensity (photon flux density) was 176 $\mu\text{mol m}^{-2} \text{s}^{-1}$, of which 105.9 $\mu\text{mol m}^{-2} \text{s}^{-1}$ accounted for in the red spectrum, 34.5 in the blue, and 20 $\mu\text{mol m}^{-2} \text{s}^{-1}$ in the green spectrum. Two fans (Radial fan BDRS 120-60, Turkey) were installed on the opposite sides of the phytotron to ensure the airflow in and out of the phytotron. Fans are 134*173*183, with 2325 rpm.

Lettuce plants were grown hydroponically on substrate medium from mineral wool blocks. A specially designed nutrient solution developed by (Rijk Zwaan, Netherlands) was used. Foliar treatment with Glauxin (phytomineral) preparation took place once by spraying the lettuce leaves on day 14 from development of first true leaves with a concentration of 5 ml.L-1. Product quality was determined by the following methods:

1. Dry matter Determination of dry matter took place by drying lettuce leaves until constant weight was reached according to Russian GOST 28561-90 [20].

2. Determination of nitrates - by the Ionometric method according to Russian GOST 29270-95 [21].

3. Determination of vitamin C by titration with a solution of sodium 2,6-dichlorophenolindophenolate until a light pink color was reached according to Russian GOST 24556-89 [22].

4. Determination of B vitamins by using capillary electrophoresis on the device " Drop 105M " [23].

5. Photosynthetic plant pigments (chlorophyll a, chlorophyll b and carotenoids) Photosynthetic plant pigments were determined spectrophotometrically according to the method and equations used by Lichtenthaler and Wellburn [24].

6. Determination of Heavy Metals Cadmium and Mercury by Inversion Voltammetric Method in accordance with Russian GOST R 51301-99 with slight modifications [25].

7. Biotesting method using test cultures of *Paramecium caudatum* and *Daphnia magna*.

8. Test culture *Daphnia magna*. The bioassay was performed as follows: the leaves were added to shredded lettuce varying degrees and cultured in medium for *Daphnia magna*, which was prepared by mixing Niemi 50% of the original culture medium and 50% tap water is prepared. In containers with 100 ml of medium, 5 pieces of 6-7-day-old individuals were introduced. They were cultivated under standard conditions for 20 days. During the experiment, *Daphnia* were not fed. The activity, the nature of movement, and the number of individuals were recorded. The counting was carried out visually.

9. Test culture of *Paramecium caudatum*. Experimental procedure: chopped lettuce was added in an amount of 0.1% of the cultivation medium into the *Paramecium caudatum* culture with a density of 1.2 cells in 10 μ l of cultivation medium, grown in the presence of lettuce under standard conditions. The number of cells was counted in 10 μ l of the medium. Cell counting was performed in 10 μ L on a glass slide under microscopy with a magnification of x40.

Results and Discussion

The current study demonstrates the effect of the "Glauxin" on the growth and development of oakleaf lettuce by examining the following factors: The growth rate and productivity of plants, The content of photosynthetic pigments, Dry matter content of lettuce leaves, The content of nitrates and toxic elements in lettuce leaves, The content of vitamins C and B in lettuce leaves, and The Biotesting of oakleaf lettuce leaves

1. The growth rate and productivity of plants

The assessment of the overall quality of oakleaf lettuce plants treated with phytomineral "Glauxin" (on a 5-point scale) was carried out according to a set of indicators: appearance, taking into account color, size, shape, leaf development, the presence of small and substandard leaves. As can be seen in (Table.1), when using the phytomineral "Glauxin", a significant improvement in the assessment of the overall quality of plants was observed. The plants were well developed, bright green in color, with large, wide, aligned leaves with high turgor and were rated 5 points.

Table 1. Comparison of productivity and overall quality assessment between foliar treatment with "Glauxin" and control plants

Nº n/n		Control treatment	Glauxin treatment
1	Assessment of the overall quality of plants, point	3,5	5,0
2	Plant height at the time of harvest, cm	23,5	25,0
3	Average weight of the shoots, g	32,2	38,9
4	Productivity, g.m ²	2254,0	2720,7
	% of control	100,0	120,7

Source: prepared by authors

An increase in the growth of lettuce plants was noted. The average plant height in "Glauxin" treated plants reached 25.6 cm comparing to 23.5 cm in the control treatment. The increase in yield when using phyto-mineral "Glauxin" recorded 20.7% compared to the control.

2. The content of photosynthetic pigments

The activity of photosynthetic pigments affects the entire complex of metabolic processes in plants, the rate and direction of biochemical processes in plant tissues and can serve as an indicator of the physiological state of a plant as an object [31].

It is believed that the ability of the plant to react and change the direction of physiological and biochemical reactions upon changing environmental conditions is associated with the change in the pigment complex of leafy plants. In optimal conditions for the plants leaves, the content of chlorophyll "a" should exceed the content of chlorophyll "b" (the ratio "a": "b" is higher than one). Violation of the physiological state of green plants leads to a decrease in this ratio to values less than 1. [32, 33].

According to the data shown in Figure 1, it can be seen that there is a clear increase in the content of chlorophylls "a" and "b" after treatment with the phyto-mineral "Glauxin". The content of total carotenoids and chlorophyll "a" dramatically increased in comparison with the control.

Both in the experimental and control variants the content of chlorophyll "a" exceeded the content of chlorophyll "b", which indicates the normal course of metabolic processes in oaklettuce leaves. The data obtained fully correlate with the results of evaluating lettuce leaves in appearance, one of the main criteria of which was the intensity of the color of lettuce leaves in appearance, the main criterion of which was the intensity of color.

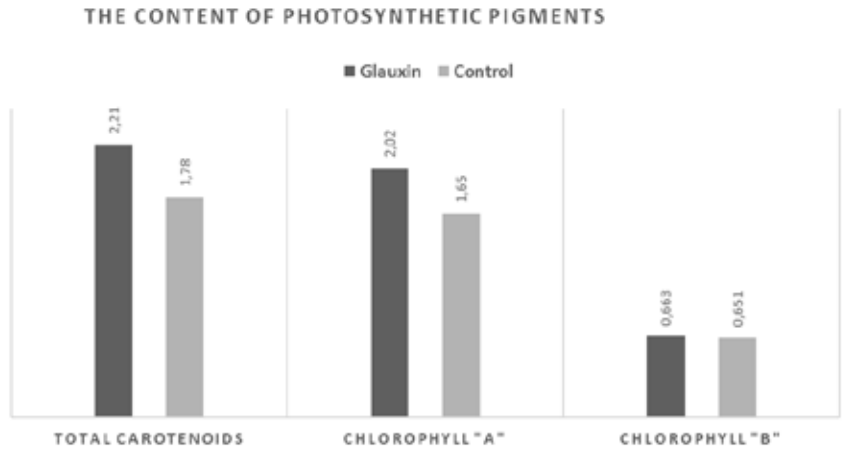


Figure - 1 The content of photosynthetic pigments in lettuce leaves

Source: prepared by authors

The data obtained fully correlate with the results of evaluating lettuce leaves in appearance, one of the main criteria of which was the intensity of the color of lettuce leaves in appearance, the main criterion of which was the intensity of color. Apparently, the treatment with "Glauxin" improves the work of the photosynthetic apparatus and, as a result, increases the productivity of plants. Data on yield (Table 1) support this assumption.

3. The dry matter content of lettuce leaves

The results of determining the content of dry matter in lettuce leaves are shown in the table

Table 2. The content of dry matter in oaklettuce leaves

Option	Control (no processing)	phytomineral "Glauxin"
Dry mass fraction x substances, %	6.9	6.4
Change in relation to control, %	-	-0.5

Source: prepared by authors

The analysis data showed that there is a tendency to a decrease in the accumulation of dry matter after foliar treatment with the preparation "Glauxin".

4. The content of nitrates and toxic elements in lettuce leaves

The results of determining the residual amounts of nitrates and toxic elements are presented in table. 3. For comparison, the maximum permissible concentrations of toxicants in the production of salad crops are given according to Russian sanitary regulations 2.3.2.1078-2001 [34].

Table 3. Content of nitrates and toxic elements in oaklettuce leaves

	Control	phytomineral "Glauxin"	Threshold limit value, mg/kg
Nitrate's residues, mg/kg	178	177	3500 * - 4500 **
Lead (Pb)	0.077	0.027	0.5
Cadimium (Cd)	Not found	Not detected	0.03

* Fresh lettuce, grown in greenhouses grown in greenhouses from April 1 to September 30, from October 1 to March 31

** Fresh lettuce, grown in greenhouses grown in greenhouses, from April 1 to September 30

Source: prepared by authors

The residual content of nitrates in lettuce leaves was low and did not differ from the control treatment. The accumulation of a toxic element (lead) decreased upon foliar treatment with "Glauxin". Residues of Cadmium were not found in both treatments.

5. The content of vitamins C and B in lettuce leaves

Analysis data showed that the accumulation of vitamin C, ascorbic acid, increases with in oakleaf lettuce plants treated with "Glauxin" and recorded (9.6 mg/100 g compared to 8.95 mg/100 g in the control treatment).

Data on the content of B vitamins in lettuce leaves are shown in Fig. 2:

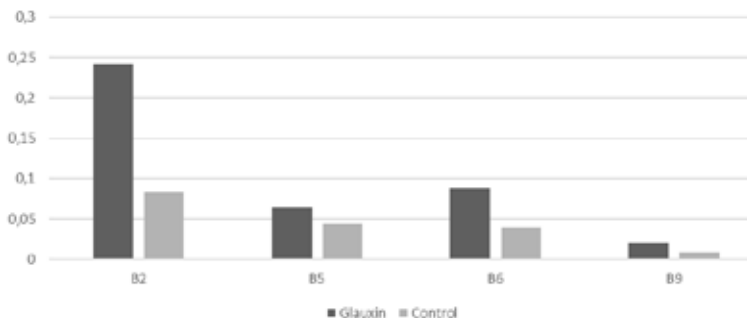


Figure 2. The content of vitamin B2, B5, B6, B9 in oakleaf lettuce under foliar treatment with "Glauxin"

Source: prepared by authors

6. The Biotesting of oaklettuce leaves

Table 3. Intensity of reproduction of daphnia magna in the nutrient medium with the addition of lettuce leaves

Culture	Control	Phytomineral (Glauxin)
Daphnia magna test culture		
Total number of large, medium and small <i>Daphnia magna</i>	10.4 ± 3.5	10.8 ± 2.5
<i>Daphnia magna</i> with eggs in the brood chamber	14.0 ± 2.7	15.7 ± 3.2
Test culture Paramecium caudatum		
Total number of cells in 10 µl	11.7 ± 3.1	11.0 ± 2.4

Source: prepared by authors

According to the results of biotesting (Table 3), the phytomineral preparation "Glauxin" did not deactivate the test cultures of *Daphnia magna* and *Paramecium caudatum* compared to the control, which relatively indicates that the grown products have a sufficient level of food safety and nutritional value of the treated lettuce leaves.

Conclusion

The use of the phytomineral preparation "Glauksin" gives a positive effect upon foliar treatment on oak leaf lettuce leaves grown on mineral wool substrate in the conditions of the phytotron ISR 0.1. We noted a significant improvement in the overall quality of lettuce leaves, plant growth and development, increase in the content of chlorophyll "a", total carotenoids in the leaves, the yield also increased by 20.7%. The content of B2, B5, B6, B9 vitamins also increased in the leaves. The accumulation of the heavy metals Pb and Cd lead in the production recorded a slight decreased. According to the results of biological testing, the phytomineral preparation "Glauxin" does not cause deactivation of test cultures *Daphnia magna* and *Paramecium caudatum*, which indicated the safety and nutritional quality of the lettuce leaves treated with the mentioned preparation.

References

1. Baldermann, A., Grathoff, G. H., & Nickel, C., «Micromilieu-controlled glauconitization in fecal pellets at Oker (Central Germany) » *Clay Minerals*, pp. 513-538, 2012.
2. A Badermann, C., Mavromatis, V., Stickler, C.P., Strauss, H.Bald, «The role of bacterial sulfate reduction during dolomite precipitation: implications from Upper,» *Chem. Geol.*, pp. 1-14, 2015a.
3. Odin, G. S., & Matter, A., «De glauconiarum origine» *Sedimentology*, pp. 611-641, 1981.
4. Meunier, A., & El Albani, A., «The glauconite–Fe-illite–Fe-smectite problem: a critical review» *Terra No-va*, pp. 95-104, 2007.
5. S. G. McRae, «Glauconite» *Earth-Science Reviews*, pp. 397-440, 1972.
6. Shekhar, S., Mishra, D., Agrawal, A., & Sahu, K. K., «Physical and chemical characterization and re-recovery of potash fertilizer from glauconitic clay for agricultural application» *Applied Clay Science*, pp. 50-56, 2017.
7. J. Verma, «Does glauconite be an emerging and potential source of potash fertilizer» *Recent Adv. Petrochem Sci.*, p. 5–8, 2018.
8. Karimi, E., Abdolzadeh, A., Sadeghipour, H.R., Aminei, A., «The potential of glauconitic sandstone as a potassium fertilizer for olive plants» *Arch. Agron. Soil Sci*, p. 983–993, 2012.
9. Torqueti, S.T.S., Boldrin, K.V.F., do Nascimento, A.M.P., Paiva, P.D.O., Furtini Neto, A.E., Luz, I.C.A., «Alternative potassium source for the cultivation of ornamental sunflower | Fonte alternativa de potássio no cultivo do girassol ornamental» *Ciencia e Agrotecnologia*, p. 257–264., 2016.
10. Rudmin, M., Banerjee, S., Mazurov, A., Makarov, B., Martemyanov, D., «Economic potential of glauconitic rocks in Bakchar deposit (S-E Western Siberia) for alternate potash fertilizer» *Applied Clay Science*, p. 225–233, 2017.
11. Castro, L., Tourn, S., «Direct application of phosphate rocks and glauconite as alternative sources of fertilizer in Argentina» *Exploration and Mining Geology*, p. 71–78, 2003.
12. Franzosi, C., Castro, L.N., Celeda, A.M., «Technical evaluation of glauconies as alternative potassium fertilizer from the Salamanca Formation, Patago-nia, Southwest Argentina» *Natural Resources Research*, p. 311–320, 2014.

13. E. Kefeli, "The problem of growth and sustainability regulators, its opportunities and prospects / E.I. Kefeli // Regulators of plant growth and development, "Kiev, Naukova Dumka, p. 325, 1999.

14. Bashan, Y., de-Bashan, L. E., Prabhu, S. R., & Hernandez, J. P., «Advances in plant growth-promoting bacterial inoculant technology: formulations and practical perspectives (1998–2013)» Plant and soil, pp. 1-33, 2014.

15. Ohler, J., Caravaca, F., Carrasco, L., & Roldan, A., «Interactions between a plant growth-promoting rhizobacterium, an AM fungus and a phosphate-solubilising fungus in the rhizosphere of *Lactuca sativa*» Applied Soil Ecology, № 35(3), pp. 480-487, 2007.

16. E. N. Mishustin, "Microorganisms and soil fertility," Publishing house of the Academy of Sciences of the USSR, 1956.

17. N.N. Tereshchenko, Biofertilizers based on microorganisms, 2003, p. 60.

18. R. A. A. S. V. D. Volkov M.Yu., "Biopreparation for increasing the productivity of plants and protecting them from diseases and a method of obtaining." Patent Application for Patent RF 2018113637/10 (021432), 2018.

19. Kohler, J., Caravaca, F., Carrasco, L., & Roldan, A., «Interactions between a plant growth-promoting rhizobacterium, an AM fungus and a phosphate-solubilising fungus in the rhizosphere of *Lactuca sativa*» Applied Soil Ecology, pp. 480-487, 2007.

20. G. 28561-90, "By-products of fruits and vegetables. Methods for determination of dry matter or moisture ", M .: Standartinform, p. 85, 2011.

21. G. 29270-95, "By-products of fruits and vegetables. Methods for the determination of nitrates ". - M .: Standartinform, "p. 11, 2010.

22. G. 24556-89, "By-products of fruits and vegetables. Methods for the determination of vitamin C ". - M .: IPK Publishing house of standards, "p. 10, 2003.

23. N.V. Komarova, Ya. S. Kamentsev., Practical guide to the use of capillary electrophoresis systems "KAPEL", 2006, p. 212.

24. Lapin A.A., Gorbunova E.V., Zelenkov V.N., Gerasimov M.K., «Determination of antioxidant activity of wines by coulometric method» Scientific and methodological guide, Moscow, Russian Academy of natural Sciences RAEN, p. 64, 2009.

25. Kaplin, A. A., Mordvinova, N. M., & Vorob'eva, A. N. (1981). Determination of heavy metals by inversion voltammetric methods. *Gigiena i sanitariia*, (6), 48.

26. Blagoveshchensky, A.V. Biogenic stimulants and harvest / A.V. Annunciation. - M. : Ed. Knowledge, 1962. - p.30.
27. Kefeli, E.I. The problem of growth and sustainability regulators, its opportunities and prospects / E.I. Kefeli // Regulators of plant growth and development. - Kiev, Naukova Dumka, 1999. - p. 325.
28. Mishustin E.N. Microorganisms and soil fertility. Ed. USSR Academy of Sciences, popular science series, 1956. - P.6.
29. Tereshchenko, N.N. Biofertilizers based on microorganisms / N.N. Tereshchenko. - Tomsk: Publishing house of the Tomsk state. University, 2003. -60 p.
30. Volkov M.Yu., Razin A.N., Anikin S.V., Venkov D.A. Application for RF Patent №2018113637 / 10 (021432) Biopreparation for increasing the productivity of plants and protecting them from diseases and a method of obtaining. 04/13/2018.
31. Merzlyak, M.N. The use of reflection spectroscopy in the analysis of pigments of higher plants / M.N. Merzlyak // Plant Physiology. - 2003. - Vol. 50. - S. 785-792.
32. Greenhouse workshop. Plant physiology and biochemistry: digest of the magazine "World of greenhouses" / CJSC "Greenhouse service"; comp. HELL. Tsydendambaev. - M. : World of greenhouses, 2015. —292p.
33. Hit O. Photosynthesis (Physiological aspects) / O. Hit. - M.: Mir, 1972. -315p.
34. SanPiN 2.3.2.1078-2001 Food raw materials and food products. Hygienic requirements for safety and nutritional value of food products. - M. : Federal Center for Sanitary and Epidemiological Surveillance of the Russian Federation, 2002.

DOI 10.34660/INF.2021.52.66.021

QUANTITATIVE ASSESSMENT OF THE CONTENT OF SOME CHEMICAL ELEMENTS IN EXPERT STUDIES OF VARIOUS OBJECTS

Voronin Aleksandr Vasilievich

Doctor of Pharmaceutical Sciences, Head of the Department of Chemistry
Institute of Pharmacy, Samara State Medical University

The aim of the study is to formulate the principles for the quantitative assessment of the content of certain metals and non-metals in expert studies of objects of biological and non-biological origin by methods of X-ray fluorescence and atomic emission spectrometry without the use of standard samples. The objects of research are samples of marijuana seized from illicit trafficking; samples of blue clay from the Undorovskoye deposit, a potential excipient in pharmaceutical technology. Examples of comparative analysis of marijuana and blue clay are considered. In samples similar in structure and chemical composition, the values of analytical signals of chemical elements were compared, and quantitative analysis was also carried out without a calibration step. These techniques make it possible to solve the question of the identity of the elemental composition of the samples. Thus, the problem of quantitative determination of the elements of some metals and non-metals in objects of biological and non-biological origin can be transformed into the problem of assessing the primary analytical signal of the determined elements. Using a formalized mathematical model, for example, the method of fundamental parameters, for the intensity of X-ray fluorescence, it is possible to establish a correspondence with the content of elements in the analyzed object. The described methodological approaches can be applied in forensic chemical, forensic and pharmaceutical analysis.

Keywords: metal compounds, elemental analysis, X-ray fluorescence spectrometry, atomic emission spectrometry, marijuana, blue clay.

Introduction

Atomic spectrometry methods are widely used for routine research in solving problems of forensic chemical, medico-forensic examinations and pharmaceutical analysis [1-3].

Examinations related to the determination of compounds of metals

and some non-metals in objects of biological and non-biological origin, in most cases, involve their quantitative determination. The studied objects have a complex composition, the set of related substances varies greatly in the samples, and the peculiarities of sampling also contribute to the change in the content of the analyzed chemical elements in the object [4].

The possibility of quantitative determination of chemical elements in the objects of study is determined by the availability of available reference standard samples for the calibration procedure and control measurements. However, in the absence of these samples for expert studies, alternative methods of quantitative assessment of the content of chemical elements are required [5].

Purpose of the study – to formulate the principles for the quantitative assessment of the content of some metals and non-metals in expert studies of objects of biological and non-biological origin by methods of X-ray fluorescence and atomic emission spectrometry without the use of standard samples.

Material and methods

Objects of research - samples of marijuana seized from illegal circulation; samples of blue clay from the Undorovskoye deposit as a promising excipient in pharmaceutical technology [6].

X-ray fluorescence spectrometry (RFS) analysis. Equipment: software-analytical complex based on a portable X-ray fluorescent crystal-diffraction scanning spectrometer "Spectroscan MAKS-GV".

Marijuana samples with a moisture content of not more than 15% were ground to a particle size of 0.5 mm. Samples of blue clay were subjected to heat treatment (firing) at a temperature of 800°C to constant weight. It was then crushed on equipment not contaminating the sample to a particle size of 70 µm.

Survey spectra of X-ray fluorescence of the studied samples were recorded in the range of 850.0-13000.0 mÅ.

When determining metals in marijuana samples, the following X-ray fluorescence wavelengths (mÅ) were used: K - 3572.0 (K α -line); Ca - 3360.3 (K α -line); Fe - 1935.0 (K α -line); Sr - 876.7 (K α -line).

Quantitative elemental analysis of blue clay samples was carried out by the standardless method - the method of fundamental parameters [7].

Analysis technique by atomic emission spectrometry (AES). Equipment: spectrographic complex ISP-30 with a modified multichannel spectrum recorder (MIRS). Installation of a light source with a three-lens system. Excitation source - alternating current arc, current strength 7-8 A (generator

DG-2)

A weighed portion of the test object (marijuana sample) was subjected to mineralization by burning at a temperature of 450-500°C and subsequent mixing with spectral coal "extra pure" in a 1:1 ratio.

When determining metals in marijuana samples, the following analytical line wavelengths (nm) were used: Ca - 317.93; Mg - 278.14; Fe - 280.45; Al 396.15; Cu 324.75; Ba - 233.52; 263.48; 277.14; Ti 294.83; V 437.92; Mn 257.61.

Statistical processing of the obtained data was carried out by one-way analysis of variance using the Statistica 6.0 software (Statsoft Inc., USA) [8].

Results and discussion

The intensity of X-ray fluorescence depends not only on the concentration of the element, but also on the chemical composition and surface structure of the sample, which complicates quantitative analysis. There are also no commercial reference materials available for calibration in studies of objects of biological origin.

A methodical approach to assessing the primary analytical signal of elements was used in the study of marijuana samples to establish the unity of the source of origin for the raw materials used (i.e., to determine the identity of the samples).

The elemental composition of marijuana samples was determined in the course of registration of a survey X-ray fluorescence spectrum. Comparison of the samples was carried out for the elements: calcium, potassium, iron and strontium. All elements were measured in five analytical replicates to ensure the possibility of statistical processing.

As an alternative analysis, the above post-mineralized marijuana samples were analyzed by the AES method.

Table 1 – Analytical Signals of Elements in Marijuana Samples by RFS and AES Methods

Test samples	X-ray fluorescence intensity, imp/s				Analytical line intensity, standard units		
	Ca	K	Fe	Sr	Cu	Mn	V
sample №1 Average value, A_i	23473.60	10343.60	8009.80	17076.00	62.00	56.00	37.20
Standard deviation, S_{A_i}	64.49	76.52	19.12	74.18	2.74	4.18	4.38

sample № 2 Average value, A_i	13782.00	8730.60	8453.40	16236.60	55.00	50.40	32.40
Standard deviation, S_{Ai}	91.19	45.29	26.94	117.78	7.07	4.28	3.36
sample № 3 Average value, A_i	17734.80	8072.80	8413.80	15774.40	66.00	54.60	34.00
Standard deviation, S_{Ai}	135.26	47.17	30.82	37.88	7.18	3.13	5.48

It was found that all samples have the same elemental composition: calcium, magnesium, iron, sodium, aluminum, copper, barium, titanium, vanadium, manganese, and also non-metal - silicon. The differences in the lists of the determined elements are associated with the difference in the detection limits of the RFS and AES methods, as well as the loss of metals during the mineralization of the object of study.

The results of measuring the intensity of the $K\alpha$ lines of calcium, potassium, iron, and strontium, as well as the intensities of the analytical lines of copper, manganese, and vanadium are presented in tab. 1.

To check the significance of the difference in the mean values of the analytical signals, one-way analysis of variance was used.

Table 2 – Results of analysis of variance for comparison of the content of elements in marijuana samples (RFS and AES methods)

Element	SS_{total}	MS_{ef}	SS	MS_{error}	F-criterion	p
Ca	237475940.0	118737970.0	123076.0	10256.3	11577.0	< 0.01
K	13651670.8	6825835.4	40525.2	3377.1	2021.2	< 0.01
Fe	602608.5	301304.3	8164.8	680.4	442.8	< 0.01
Sr	4353972.9	2176986.5	83240.4	6936.7	313.8	< 0.01
Cu	310.0	155.0	300.0	25.0	6.2	0.014
Mn	84.9	42.5	182.4	15.2	2.8	0.10
V	59.7	29.9	242.0	20.2	1.5	0.27

The statistical hypothesis about the equality of the contents of elements: calcium, potassium, iron and strontium in samples № 1-3 can be rejected. When using the AES method, all the studied samples of mari-

juana significantly differ in the content of copper and do not differ in the content of manganese and vanadium (tab. 2).

To detail the differences in the content of each element, post hoc comparisons of the means were used using Fisher's least significance test (tab.3).

In the considered case, all three studied samples of marijuana significantly differ in the content of calcium, potassium, iron and strontium. However, the transition to a higher level of statistical significance - 0.01, allows us to make a conclusion about the similarity of samples № 2 and № 3 in terms of iron content.

Table 3 – Results of a posteriori comparison of quantitative assessment of the content of elements in marijuana samples (RFS method)

	Sample №1	Sample №2	Sample №3
Ca			
Sample №1		< 0.01	< 0.01
Sample №2	< 0.01		< 0.01
Sample №3	< 0.01	< 0.01	
K			
Sample №1		< 0.01	< 0.01
Sample №2	< 0.01		< 0.01
Sample №3	< 0.01	< 0.01	
Fe			
Sample №1		< 0.01	< 0.01
Sample №2	< 0.01		0.034
Sample №3	< 0.01	0.034	
Sr			
Sample №1		< 0.01	< 0.01
Sample №2	< 0.01		< 0.01
Sample №3	< 0.01	< 0.01	

When using the AES method, the samples were compared in terms of the content of elements with the most intense analytical lines in the emission spectra - copper, manganese, and vanadium.

Table 4 – Results of a posteriori comparison of the quantitative assessment of the content of elements in marijuana samples (AES method)

	Sample № 1	Sample № 2	Sample № 3
Cu			
Sample №1		0.047	0.23
Sample №2	0.047		0.0046
Sample №3	0.23	0.0046	
Mn			
Sample №1		0.042	0.58
Sample №2	0.042		0.11
Sample №3	0.58	0.11	
V			
Sample №1		0.12	0.28
Sample №2	0.12		0.58
Sample №3	0.28	0.58	

Detailing the differences in the content of elements showed the difference between samples № 1 and № 2, № 2 and № 3 in terms of copper content, as well as samples № 1 and № 2 - in terms of manganese. When passing to the level of statistical significance of 0.01, only samples № 2 and №3 differ in copper content (tab. 4).

The method of reference-free quantitative analysis (method of fundamental parameters) of blue clay was also considered. The calculation of the content of elements in this version is based on the use of theoretical values - the mass absorption coefficients of radiation of the corresponding analytical lines of the sample under study.

Table 5 – Elemental composition of blue clay samples

Samples	Element concentrations,% (wt.)							
	Al	Si	S	K	Ca	Ti	Fe	Sr
Sample №1	1.31 ±0.20	4.52 ±0.27	0.087 ±0.004	0.60 ±0.046	3.70 ±0.24	0.091 ±0.008	0.84 ±0.072	0.013 ±0.001

Samples	Element concentrations, % (wt.)							
	Al	Si	S	K	Ca	Ti	Fe	Sr
Sample №2	1.65 ±0.31	5.55 ±0.57	0.26 ±0.029	0.72 ±0.045	5.15 ±0.58	0.12 ±0.013	1.08 ±0.15	0.013 ±0.001
Sample №3	1.26 ±0.17	4.35 ±0.35	0.84 ±0.023	0.58 ±0.041	3.56 ±0.49	0.088 ±0.005	0.81 ±0.029	0.012 ±0.001
Sample №4	1.71 ±0.24	5.75 ±0.42	0.27 ±0.021	0.75 ±0.10	5.35 ±0.57	0.12 ±0.012	1.12 ±0.14	0.013 ±0.003

Analysis of the X-ray fluorescence spectra of blue clay samples indicated the presence in the following metals - aluminum, potassium, calcium, iron, strontium, and titanium, as well as non-metals - sulfur and silicon.

The results of the quantitative analysis of various samples of blue clay from the Undorovskoye field are presented in tab. 5.

Comparison of the elemental composition of four samples of blue clay with different time and place of sampling in the field shows a significant difference in the content of silicon, sulfur and all metals, except for strontium (tab. 6).

Table 6 –Results of analysis of variance for comparison of the composition of blue clay samples

Element	SS _{total}	MS _{ef}	SS	MS _{error}	F-criterion	p
Al	0.59	0.20	0.88	0.055	3.61	0.037
Si	6.90	2.30	2.77	0.17	13.27	< 0.01
S	1.64	0.55	0.0074	0.00046	1186.15	< 0.01
K	0.054	0.018	0.067	0.0042	4.31	0.021
Ca	12.08	4.03	3.84	0.24	16.77	< 0.01
Ti	0.0095	0.0032	0.0017	0.0001	30.45	< 0.01
Fe	0.32	0.11	0.19	0.012	8.85	< 0.01
Sr	0.00002	0.000008	0.00005	0.000003	2.78	0.075

A detailed comparison of the content of some metals in blue clay samples shows that samples № 1 and № 2, № 1 and № 3, № 2 and № 4 do not differ in the content of aluminum; samples № 1 and № 3 do not differ in calcium content, on the contrary, in strontium content it differs only in samples № 3 and № 4 (tab. 7).

Table 7 – Results of a posteriori comparison of the content of a number of elements in blue clay samples

	Sample №1	Sample №2	Sample №3	Sample №4
Al				
Sample №1		0.083	0.76	0.029
Sample №2	0.083		0.046	0.59
Sample №3	0.76	0.046		0.015
Sample №4	0.029	0.59	0.015	0.029
Ca				
Sample №1		< 0.01	0.87	< 0.01
Sample №2	< 0.01		< 0.01	0.017
Sample №3	0.87	< 0.01		< 0.01
Sample №4	< 0.01	0.017	< 0.01	
Sr				
Sample №1		0.55	0.25	0.13
Sample №2	0.55		0.089	0.33
Sample №3	0.25	0.089		0.012
Sample №4	0.13	0.33	0.012	

Conclusion

Thus, the problem of quantitative determination of the elements of some metals and non-metals in objects of biological and non-biological origin can be transformed into the problem of assessing the primary analytical signal of the determined elements in the object under study. Using a formalized mathematical model, for example, the method of fundamental parameters, for the primary analytical signal - the intensity of X-ray fluorescence in the RFS method, it is possible to establish a correspondence with the content of elements in the analyzed object. When conducting a comparative analysis of samples in order to establish their identity, the establishment of a functional relationship between the value of the analytical signal of the element being determined and its content is no longer appropriate.

Comparative quantitative elemental analysis of objects is possible in the following areas: comparison of analytical signals of chemical elements

in samples similar in composition and structure to prove their identity; performing quantitative determination by a standardless method without a calibration step.

The necessary conditions for the implementation of the above methodological approaches are: standardization of conditions for measuring the analytical signal of an element (analytical equipment, sample preparation, objects of study similar in structure and chemical composition); the need for statistical processing of measurement results using parametric methods.

The described methodological approaches to the study of samples of biological and non-biological origin can be used in forensic chemical, forensic and pharmaceutical analysis.

References

1. Bezpaly, Yu.B. X-ray spectral fluorescence analysis: generalization of the ten-year practical / Yu.B. Bezpaly, E.Kh. Musin, N.A. Romanko // Forensic medicine. – 2016. – № 2. – P. 162-163.
2. Aspects of studying hashish by inductively coupled plasma mass spectrometry / V.Yu. Kuzovlev [et al.] // Advances in chemistry and chemical technology. – 2015. – № 9. – P. 24-25.
3. X-ray fluorescence trace metal analysis of environmental liquid samples after membrane preconcentration / E. Margui [et al.] // Spectroscopy Europe. – 2008. – V. 20, № 1. – P. 11-14.
4. Sidorina, A.V. Optimization of the method for determining the elemental composition of biological objects by the XRF-SI method: abs. diss. ... cand. chem. sci. – Novosibirsk, 2014. – 26 P.
5. Oskolok, K.V. Quantitative X-ray fluorescence analysis of multielement objects of complex shape without using reference samples / K.V. Oskolok, A.V. Garmay, A.V. Monogarova // Bulletin of Moscow University. Series 2. Chemistry. – 2014. – V. 55, № 1. – P. 10-14.
6. Simakina, A.A. Blue clay as a promising excipient in the technology of sorption-active drugs / A.A. Simakina, P.G. Mizina // Bulletin of the Samara Scientific Center of the Russian Academy of Sciences. – 2009. – № 1 (6). – P. 1308-1310.
7. Artamonov, D.O. Application of the method of fundamental parameters in determining the chemical composition of stratal waters on an X-ray fluorescence spectrometer / D.O. Artamonov, P.A. Ivanov, O.V. Orlova // Lithology, petrography, mineralogy, geochemistry. – 2013. – № 1 (13). – P. 79-84.
8. Khalafyan, A.A. Statistical data analysis. Statistica 6.0.: Textbook / A.A. Khalafyan. – Krasnodar: KubSU, 2005. – 192 P.

DOI 10.34660/INF.2021.27.27.022

UDC 553.98.061: 552.54.73. (470.4+574.1)

SEDIMENTATION STAGES OF THE FORMATION OF THE CASPIAN SEDIMENTARY BASIN IN THE LATE PALEOZOIC

Abilkhassimov Khairly

Doctor of Geologo-Mineralogical Sciences,
Academician of the Academy of Mineral Resources
Of the Republic of Kazakhstan, General Director of the
LLP "GEO-Munai XXI"
Almaty, Republic of Kazakhstan

In the sedimentary complex of the Paleozoic of the Caspian Basin, there are several carbonate platforms of different ages, as well as zones with predominantly terrigenous deposits. The complex geological structure of the region is due to the influence of collisional processes that took place in the junction zone of the East European platform and the Ural paleocean.

The review presents the results of paleogeographic reconstructions of the main stages in the development of the Late Paleozoic sedimentary basin, which reflect the features of the formation of sedimentary complexes of the Caspian Basin. The influence of the block structure of the basement on the duration of sedimentation stages and the formation of carbonate platforms has been substantiated. Different depths of the basement, determine the variability of the lithological composition and thickness of the Paleozoic deposits. The typification of sections of carbonate platforms within the side zones of the Caspian Basin was carried out, which made it possible to identify the relationship between the conditions of sedimentation and the block structure of the basement.

In recent decades, the so-called "carbonate platform" model has been used to interpret the Paleozoic stage of carbonate accumulation. It (the model), in contrast to the models of carbonate reefs and atolls, is characterized by successively replaced facies belts: from the shallow waters of the transitional tidal plain, the inner shelf lagoon, the intramarine sand-bank of the margin, through the carbonate slope and reef complexes into a relatively deep-water basin cavity (depression). In international geological practice, such formations are called isolated carbonate seamounts

and the term "carbonate massif" is the closest in meaning in Russian-speaking geology.

It was found that the carbonate massifs are characterized by an increase in the power (thickness) of the sediments, compared with their same-age framing, and the narrow transition zone, where a change in thickness is noted, was called the carbonate scarp (slope). The carbonate massifs themselves are almost entirely composed of different facies of limestones and dolomites, painted mainly in light tones, with interlayers of volcanogenic-terrigenous and terrigenous material. Sediments developed along the framing of carbonate massifs with a condensed (relatively thin) section are represented by dark-colored carbonate-argillaceous and carbonate-terrigenous, and in more remote parts of the basin - by thin-layered argillaceous-shale and terrigenous material.

In such a model, reefs, as organogenic structures of the Paleozoic stage of evolution, are one of the constituent parts of the carbonate platform. The model of the Paleozoic carbonate platform was successfully used to interpret the carbonate strata of East Kazakhstan - Cambrian-Ordovician Small Karatau and North-Western Balkhash and Devonian-Carboniferous Big Karatau.

Votsalevsky E.S., Pilifosov V.M. et al. (2000) believed that the development of these carbonate massifs in the paleogeographic respect was determined by their location in the junction zone of the structures of the southeastern margin of the East European Platform with the Ural paleo-ocean and Paleo-Tethys. At the same time, the formation of the Tengiz-Kashagan carbonate platform was associated with the period of the opening of the Ural paleo-ocean. This resulted in a wider stratigraphic range and more significant thickness of carbonate deposits. In contrast, the origin of the South Emba carbonate platform occurred during the closure of the Ural paleo-ocean and is associated with a relatively short-term process of shallowing of the territory (compression period). The same reasons determined the different degree of preservation and morphological manifestation of the structures under consideration.

The lithological-facies analysis carried out by the author confirms the geodynamic constructions proposed by the above researchers, and proves that the Central Caspian depression throughout the history of its development was the most submerged parts of the sedimentation basin, where the deep-water and most distant from the sources of drift sediment facies were concentrated. In the side zones, carbonate platforms and reef massifs are developed. The active supply of clastic material is provided by powerful paleo-channel systems that form clinofolds facing deep into

the depression. The complex, long and multidirectional process of the formation of the sedimentary complex of the Caspian basin is reflected in the lithological and paleogeographic schemes compiled by the author.

Late Devonian-Early Visean stage. In the Late Devonian - Early Carboniferous, the opening of the Central Caspian rift was accompanied by the formation of a narrow deep strait of the Ural paleocean. A huge amount of terrigenous material, represented by volcanic-sedimentary, siliceous-clayey sediments and basalts, was introduced into the depression by alluvial cones from the Urals through the Central Caspian rift. The accumulation of thick terrigenous strata in the area of the South Emba rift has drawn the southeastern periphery of the Caspian basin into a stable compensated subsidence.

The carbonate stage of sedimentation, which began in the Devonian in most of the framing of the south, southeast and north of the Caspian region, continued without sharp facies changes in the Carboniferous period. This was established from the sections of wells in the Primorskiy uplift zone in the south and on the northern side of the depression. The total thickness of the carbonate strata in the sections of the wells in the Yuzhnaya area is more than 1660 m. It is represented by a stratum of limestones, dolomites, less often marls from the lower Tournaisian stage of the Lower Carboniferous to the eroded surface of the Middle Carboniferous carbonates. In the Astrakhan and Tengiz-Kashagan zones, where gravity flows did not reach, there was a calm tectonic regime, which contributed to the emergence of the Late Frasnian-Early Turnean carbonate platform. The lithological-paleogeographic scheme compiled by the author (fig. 1) shows that in the southern part of the basin - in the Late Devonian time, an extensive carbonate platform was formed, the dimensions of which cover the area, including the Astrakhan and Tengiz-Kashagan zones, on which large reef buildings. In addition, it is possible that the boundaries of carbonate accumulation were wider and covered the Novobogatinskoe and Guryevsko-Kulsarinskoe arched uplifts. Carbonate accumulation processes also occur in the eastern and northern flank zones of the Caspian Basin.

In the structure of the deeply submerged subsalt complex in the northern side zone of the Caspian depression Devonian, Carboniferous and Lower Permian sediments, which are distinguished by the diversity of facies and the originality of their lateral and vertical alternation, take part. The study of the sections and their correlation made it possible to identify various types of sections, which are characterized by a complete and reduced stratigraphic sequence. The Lower Devonian sediments within

the Karpovskoe uplift of the basement were formed in a shallow sea basin during the epoch of the elevated position of the sea level. Within the boundaries of the Border elevated zone and the Chinarevsky ledge, there was land for a long time, since the Lower Devonian deposits are represented here, in fact, by the basement weathering crust about 60 m thick. The seas accumulated clay and carbonate deposits. The latter could be accompanied by reef formation at the border of shallow water and relative deep water with a presumably uncompensated type of sedimentation. According to existing concepts, the Lower Devonian deposits mainly act as a stratum filling the unevenness of the basement relief and developing mainly consedimentary. The sections of the central part of the Karpov uplift were formed in shelf conditions. The Boundary Uplifted Zone is characterized by a shallower-water character of carbonate formations. In the southern part of the ledge (West Kamenskaya area), conditions were also optimal for the formation of shallow carbonate deposits. The optimal conditions for the development of stromatoporous carbonate organogenic structures were the conditions within the Chinarevsky uplift of the basement. The distribution of the thickness of carbonate rocks was influenced by the difference in the depths of the bed of the troughs and the surrounding paleo-uplifts inherited from the basement protrusions. In the uplifted areas, shallow-water carbonates could be deposited, a shelf and its barrier-reef framing could be formed. In the troughs, the sedimentation process was slowed down and mainly deep-water siliceous-carbonate sediments were deposited. Lower Eifelian carbonate deposits in even greater thicknesses can be developed in submerged parts of the paleobasin. Bysk carbonate deposits were formed during the epoch of high sea level and are represented mainly by deep-water deposits. Shallow sediments were formed within the Chinarevsky uplift, the Border elevated zone, the Karpovsky uplift and, possibly, in the form of several areas on the eastern and southern extensions of the latter.

The supposed reef Middle Devonian belts of the northern and southern marginal parts of the Pogodaevo-Ostafyevsky trough are currently submerged in the trough along faults that developed consedimentary.

At the beginning of the Givetian time, the sea level dropped, and sedimentation was actively occurring in the lower parts of the territory, which is associated with the active input of terrigenous material, most likely, by water flows and its distribution in the sedimentary basin. However, the deposits of the complex, due to the Middle Frasnian phase of tectogenesis and the subsequent erosion, were not preserved or were preserved in a reduced volume within the basement protrusions (uplifts). The complex is

also absent on its uplifted part within the Chinarevsky basement ledge. It was exposed along the periphery of the ledge by wells 11 Chinarevskaya, P-25 Tashlinskaya, 101, 106 Dolinnye, etc. At the beginning of the Givetian time, the sea level decreased and sedimentation took place in the lower parts of the territory. The general paleogeographic environment for such sedimentation was favorable; however, to the east (Koshin area), the Vorobyevsky horizon is significantly reduced in thickness and resembles deep-sea deposits in composition and structure.

S.S. Konovalenko (Konovalenko, 1999) associates the presence of coarse sandstones in the sections of a number of wells in the Chinarevsky uplift with the transportation of coarse material along the axial part of the trough, where fluvial sleeve-like deposits are predicted.

The erosion of coarse-grained Riphean sediments, cemented by clay cement, could cause the formation of extensive sandy (sand and gravel) shoals (beaches) or fan lobes along the periphery of the uplift. During periods of carbonate sedimentation in Givetian time (Ardatov layers), organogenic structures were formed in relatively uplifted zones, primarily along the periphery of the Chinarevsky ledge of the basement (Dolinaya area). According to seismic data, many clinoforms are distinguished in the compensation sequence of the Pogoda-Ostafyevsky trough, which indicates a high rate of sedimentation due to the transportation of terrigenous material from west to east along the trough. The Upper Frasnian-Tournaisian carbonate complex is composed of the Frasnian and Famennian stages of the Upper Devonian and the Tournaisian stage of the Lower Carboniferous.

Compared with the previous, Middle Devonian, stage of carbonate accumulation, this stage is characterized by a significant expansion of the area of shallow-water carbonate accumulation, which encompassed not only the uplifted areas, but also the western part of the Rubezhinsko-Perelyubsky trough and a significant part of the territory south of the Karpov ledge. With the formation of this complex, the active manifestation of local tectogenesis is practically completed, and only individual tectonic disturbances are manifested along the roof of the complex. The Lower Viséan terrigenous-carbonate complex is represented by the Bobrikovsky horizon (20-60m), and in the Pogodaevo-Ostafyevsky trough and at its outlet into the Caspian depression, the Kozhinsky overhorizon as part of the Kosva (terrigenous) and Radaevsky (mainly carbonate) horizons, with a maximum thickness of up to 1000m. The lithofacial setting of the Kozhinsky superhorizon, which plays a decisive role in the formation of the Pogodaevo-Ostafyevsky trough, has not been completely studied.

Judging by the seismic data, its strata is divided into several successive filling levels. In the lower one, corresponding to the Kos'va horizon, the gradual character of the deposits is traced towards the trough with clinoform terrigenous strata of filling.

In the Late Devonian - Early Carboniferous (during the accumulation of an analogue of the Zilair Formation), *the eastern margin of the Caspian Basin* developed in a compression mode. This is evidenced by the flysch appearance of the formed terrigenous-clayey deposits. Mountain coastal terrigenous deposits developed here, which filled, in all likelihood, the boundary myogeosynclinal troughs and lowered parts of the platform. This is evidenced by the data of drilling and geophysics of the region of the South Emba uplift, Biikzhal and Isembet. Compression in the late Visean led to uplift and gradual shallowing; therefore, in the Tula-Aleksin time, sandy-silty-clayey sediments in the Zhanazhol zone were probably formed in a shallow environment. A similar pattern was established by us for the southern parts of the South Emba region. Later, the Zhanazhol carbonate platform arose on this uplift. Thus, the shallowing caused by the regional compression processes predetermined the subsequent biogenic carbonate accumulation in the shallow shelf environment of the warm sea.

At the base of the section of the carbonate platform, boreholes have exposed terrigenous-argillite strata, dominated by black mudstones with charred plant detritus. Gray sandstones are medium- and fine-grained, have a graywacke composition. Above, there are two carbonate strata - Late Visean-Kashirian (KT-II) and Late Moscow-Gzhel (KT-I), characterized by thicknesses of 600-750 m and 700-830 m, respectively. They are separated by terrigenous-argillite strata of the Upper Kashir and Podolsk horizons of the Moscow stage of the middle carbon. Its thickness is 400-500 m.

It is important to note that the upper KT-I carbonate unit is distributed in the indicated stratigraphic volume only in the Zhanazhol facies zone. Of the sections of the southern, southeastern, and eastern side zones of the Caspian depression, the most ancient are the deposits of the Frasnian and Famennian stages in the Karaton, Zhanasu, North Minsualmas, Isembet, Kokpekty.

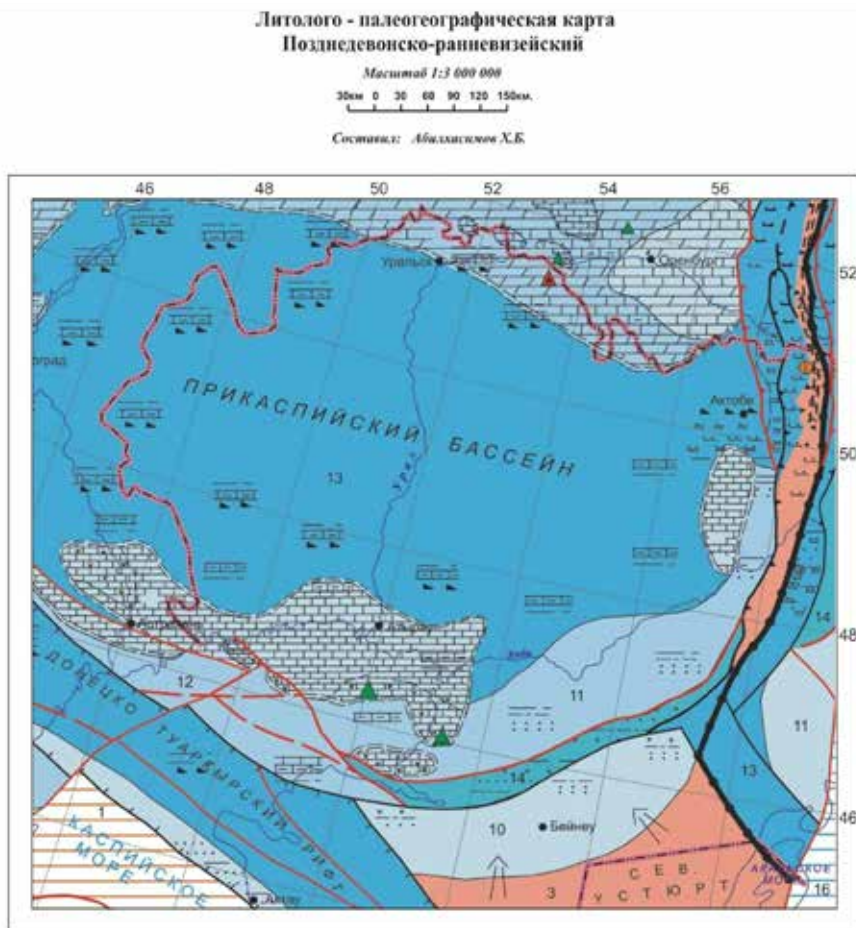


Fig. 1 Lithological-paleogeographic map of the Late Devonian – Early Visean stage. Compiled by Kh.B. Abilkhassimov

The Devonian carbonate deposits uncovered by drilling are part of a single Upper Devonian-Carboniferous carbonate platform shallow-sea stratum.

Within the southeastern flank of the Caspian Basin, the introduction of terrigenous material did not contribute to the formation of carbonate deposits. The extensive areal development of Devonian carbonate deposits in the south of the Caspian Basin is also indicated by the materials of geophysical studies.

Geological and geophysical studies of the southeast and east of the Caspian Basin made it possible to distinguish, in addition to the platform facies proper, the accompanying myogeosynclinal terrigenous and terrigenous-carbonate molassoid and flyschoid rocks. They were opened on the South Emba uplift (Zhanasu - G-10, G-11, Turesay - G-7, Northern Minsualmas - P-1, P-2, P-3) and on the eastern side of the depression (Kokpekty and Isembet areas). The marine genesis of most of the Devonian deposits of this area is beyond doubt (foraminiferal fauna, carbonate content, bedding, etc.), and a number of facies data, including paleontological characteristics, indicate traces of shallow water. The thickness of the characterized strata in the P-1 - North Minsualmas section is 2100 m. The section is represented by mudstones, sandstones, and conglomerates. The Frasnian stage of the Upper Devonian sediments (well G-11 Zhanasu) contains interlayers of marls and limestones. The exposed thickness of the Upper Devonian is 760 m here. The flysch-like sequence of sandstones, siltstones, mudstones of the section of well G-6 is also attributed to the Upper Devonian terrigenous sequence. Isembet with a thickness of 1600 m, as well as the Devonian deposits of the section of the well G-22 Kokpekty. The presence of coarse clastic material, effusive rocks, poorly rounded fragments, and charred detritus indicates the proximity of the source of drift.

Within the southern flank of the Caspian Basin, in the zone of the Tengiz-Primorsky uplifts, the Carboniferous carbonate sections exposed by drilling are part of a single Upper Devonian-Carboniferous carbonate stratum formed in shallow sea water conditions. With slight changes in composition, it can be traced westward to the Astrakhan arch, possibly capturing the southern part of the Novobogatinsky and Guryevsko-Kulsarinsky paleo-basins. Facies conditions were favorable for the formation of reef structures. From the second half of the Middle Visean time, the development zone of the shallow marine platform carbonate strata began to move northward along the eastern flank of the basin due to the development of carbonate shelf facies. And the band of terrigenous sections shifts further to the northwest, bending around the forming underwater accumulative uplifts - areas of shallow water. Carbonate deposits of the Tengiz-Kashagan carbonate platform cover a wide stratigraphic interval - from the beginning of the Late Frasnian (according to seismic data) to the Middle Carboniferous. It includes two structural levels - the Upper Devonian-Lower Turneian and Carboniferous, separated by a short-term stratigraphic hiatus, the time of occurrence of which is defined as the middle of the tour. In the Carboniferous structural level, two complexes are

distinguished - the Tourne-Lower Visean and Oka-Bashkirian, separated by a volcanogenic-sedimentary member of the Tula age, which is a confidently traceable geophysical benchmark between the carbonate massifs.

In the Late Devonian, a raised surface of the uplift was formed, on which shallow-water carbonate sediments of the carbonate platform formed from the middle of the Frasnian of the Late Devonian to the Early Turneian of the Early Carboniferous. At the end of the early tour, a hiatus in sedimentation is recorded. In the late tour, vertical movements began on the Tengiz-Kashagan platform, which led to the formation of uplifted and lowered blocks (structures). The Tengiz block was an uplift. On this uplift and its periphery, as well as on the Karaton and Royal uplifts, the facies of silt hills formed in the late tour and early Visean.

Within the Astrakhan carbonate platform, the most ancient deposits of the Lower Devonian, most likely their basal part, were opened only by the Devonskaya-2 wells in the interval of 7003-6550 m. Quartz sandstones, gravelly sandstones and gravelstones occur at the bottom of the well, which are replaced higher by tephrogenic siltstones and sandy siltstones, which are products of rhyolite tuffaceous material washed out in a shallow water environment. Detrital grains of aleurite and fine-sandy size consist of potassium feldspar (sanidine) and quartz of volcanic origin. From a depth of 6690 m, there is an alternation of feldspar-quartz sandstones, clayey siltstones, silty mudstones with interlayers of vitro-crystalloclastic tuffs of medium-basic composition. At the top of this interval of the section, single interlayers of calcarenites appear, in which the Lower Devonian conodont is found. These deposits are considered as sediments of the slopes of volcanic edifices of the central type and products of their redeposition and mixing with terrigenous clastic material from the underlying older strata in shallow and coastal marine environments. The thickness of the Lower Devonian deposits varies from 150 to 500 m.

In the second half of the Early Devonian and the beginning of the Middle, within the volcanic uplift of the Astrakhan arch, volcanic activity gradually began to fade. As a result, shallow-water sediments were replaced by deeper-water ones, and carbonate caps of bioherms began to form on volcanic edifices. The products of destruction and partial erosion of biogenic structures are calcarenites of turbidite origin, calcilyutites and slime limestones exposed by wells. The bioherms themselves were delineated by us only according to seismic data. Probably, the sedimentation area was distinguished by a rather dissected relief inherited from the volcanic relief of the previous epoch. This is evidenced by traces of slumping of unconsolidated sediments, the presence of interlayers of turbidites. At the

contact of slumped members and undisturbed sediments, the angle of inclination of bedding changes, which suggests that there were significant slopes of the basin bottom.

This explains the proximity of bioherm structures formed in a shallow water setting and depressive carbonate-clayey facies containing remains of relatively deep-water forms of conodonts. The increased carbon content of clay deposits and the depressed composition of the benthic fauna in them are most likely the result of postvolcanic hydrothermal activity.

During perestroika, the greatest uplift and erosion was experienced by the southwestern part of the Astrakhan arch. Perhaps this is due to the processes of pre-rift arcogenesis of the Donbass-Tuarkyr zone in the vicinity of the Karpinsky ridge. A feature of these structures is the alternation of large uplifts with narrower troughs. Orographically, these are mountain ranges separated by intermontane depressions. Depressions are usually separated from ridges by a zone of faults or flexures.

After the attenuation of the volcanic activity of the Early-Middle Devonian, structural restructuring, which led to the uplift and erosion of the southern part of the Astrakhan arch at the end of the Middle Devonian, sedimentation resumed at the beginning of the Frasnian. It is interesting to note that the zone of erosion of the end of the Middle Devonian was also found in the area of relatively deep-sea sedimentation. In all likelihood, this is associated with the processes of extension and subsidence in the rifting zone of the Karpinsky Ridge (Volozh et al., 1999). In the area of shallow-water sedimentation, among the Lower Frasnian deposits with a thickness of 100-300 m, two facies are distinguished: biogenic carbonate structures such as shell banks and shallow-water, predominantly silty-clayey and carbonate-detrital deposits. *The facies of biogenic structures* was penetrated by the wells Devonskaya-1 (interval 6087-6096 m) and Devonskaya-3 (interval 5994-6057 m). In the Devonskaya-1 borehole, it is represented by completely dolomitized biogenic and bioclastic limestones of the shellstone type with a layered arrangement of whole large scattered shells of castle brachiopods and their fragments, as well as single corals. In the ***facies of shallow carbonate-clayey and carbonate-clastic rocks***, two subfacies are distinguished, characterizing, on the one hand, the proximal slopes of shell banks, on the other hand, the distal parts of the slopes and depressions between the banks.

More distal and basin subfacies were discovered in the Pravoberezhnaya-1 wells (interval 6368-6494 m), where white limestones with a small amount of gray clayey and slightly clayey ones are observed. Limestones recrystallized with single grains of pyrite, in separate interlayers their pri-

mary detrital (fine-grained calcarenites) and organogenic-detrital texture are visible. The thickness of the deposits varies from 50 to 500 m.

In the Middle Frasnian, the transgression and differentiated subsidence of the Astrakhan Rise continued, which began in the Early Frasnian, which led to an almost complete leveling of facies settings both within the Astrakhan Rise and adjacent parts of the water area. The accumulation of black bituminous mudstones, clayey siltstones, sludge limestones and calcilyutites (the so-called Domanic facies) of small thickness (condensed sediments) prevails everywhere. More intense subsidence of the southern part of the uplift, adjacent to the Karpinsky Ridge, led to a tilt of the entire geoblock of the Astrakhan arch. As a result, its northern edge experienced an uplift, and the northern slope acquired a steeper slope compared to the southern one. This trend continued in subsequent periods.

As a result, on the site of the Early-Middle Devonian volcanic Astrakhan uplift, an intra-basin carbonate platform of sub-latitudinal strike with steep northern and gentler western and southern slopes arose, which developed in a regressive mode in a subsidence setting up to the end of the Tournaisian time of the Early Carboniferous. As a result, up to 1600 m of carbonate deposits have accumulated in some parts of the platform over the period under consideration.

The complete absence of terrigenous material in the composition of sediments indicates the isolation of the carbonate plateau and its elevated position in the relief of the bottom of the Caspian basin. In the modern structure, its southern slope is partially cut off by a Permian fault. Among the carbonate deposits of the platform, we have identified two facies: carbonate biogenic structures and shallow-water carbonate-detrital deposits. Within the latter, two subfacies are distinguished, which characterize environments with passive and active hydrodynamic modes of accumulation.

The most complete section of ***the facies of carbonate biogenic structures*** was penetrated by the Tabakovskaya-1 well (interval 5050-5580 m). This facies is dominated by lumpy-spherical-clotted algal, sometimes oncoid limestones, dolomitized to varying degrees, containing also the remains of foraminifera, gastropods, ostracods, coniconchia and echinoderms. Algal limestones contain interlayers of clastic, bioclastic and foraminiferal limestones. Biogenic structures have a layered structure and are similar to biostromes in terms of accumulation conditions.

The facies of carbonate-clastic rocks is the most widespread. Subfacies, which formed during the period under consideration in an active hydrodynamic regime, is closely related to the biogenic facies vertically

and laterally, differing from the latter by the predominance of clastic varieties of rocks over biogenic clot-algal ones. This facies is also characterized by diagenetic dolomitization. The most typical section was penetrated in the Pravoberezhnaya-1 well. The subfacies of carbonate-clastic rocks, accumulated in a passive hydrodynamic regime, were more widespread within the carbonate platform, as well as its gentle southern and southwestern slopes.

By the expansion of the platform area into the regressive stage of the cycle under consideration (Famen-Tournai), one can speak of the progressive nature of the slopes development, especially in the north and south. In addition, we can talk about the predominant development of carbonate and carbonate-clayey turbidites of various distalities on the slopes of the platform, since clinoform occurrence conditions characteristic of this type of sediment are clearly visible in the wave field. The turbidite character of sedimentation is also supported by the presence of turbidites and traces of slumping of unconsolidated sediments among the shallower facies of the platform and its upper gentle slope.

At the end of the Tournaisian century, due to the northward movement of the Karabogaz-Karakum and North Caspian microplate systems, the North Ustyurt block approached the edge of the East European platform.

Intense compressional deformations led to the fracture of the platform base of the terrigenous wedge and the formation of condensed folds in the Upper Devonian-Lower Turneian terrigenous complex of the South Emba zone. According to the results of the carried out lithological-facies studies, fanning cones are distinguished. Within the South Emba uplift - Sholkarinsky, Tortaysky, Vostochno-Tabynaisky and Arman-Airshagylsky, and along the eastern side - Ostansuk-Dzhurunsky, Kozdysai-Akzharsky and Vostochno-Zhanazholsky. The composition of clastic material and clay minerals differs significantly in each of the identified fans.

In the eastern side zone (Zhanazhol-Tortkol), the Tournaisian sediments accumulated in the shallow-sea regime, as evidenced by the presence of carbonate cement, limestone interlayers, fauna finds, and the appearance of different-grained sandstones at different levels. In the section of the lower Visean of this zone, several members of mudstones, siltstones and sandstones are distinguished, containing interlayers of coarse-grained sandstones and gravelstones, less often conglomerates, the nature of interlayering is pseudo-horizontal and horizontal, with interlayers of carbonaceous material. Ripple marks can be seen on the bedding planes. These deposits probably accumulated in the underwater part of the river delta. In the southern part of the zone (V. Tortkol 'square), the accumula-

tion of terrigenous rocks gradually moved to the area of the coastal delta. This is evidenced by the appearance in the section of fine-grained sandstones and siltstones with interlayers of gravelstones and traces of marine fauna. From time to time, deltaic sediments were overlapped by coarse detrital sediments of an alluvial plain protruding towards the sea (well P-1 Teresken). In the northeastern part of the Zhanazhol structure, sulfate, sulfate-dolomite, clayey rocks, and dolomites were deposited at that time. This is due to a stagnant hydrogeological regime and an increase in water salinity. A feature of the section of this zone is the presence of 3 terrigenous strata.

The lower terrigenous sequence of the Visean stage (1300 m) corresponds in stratigraphic position and is close in lithological composition to the sections of the Zhanazhol-Tortkol zone. However, it is possible to trace some differences in the sedimentation conditions of the Lower Visean deposits, for example, in the sections of the Laktybai area, graywacke sandstones prevail, composed of fragments of effusive, siliceous, carbonate and clay rocks of poor sorting and weak roundness. The accumulation of these deposits took place on the continental slope in the underwater fans. These sediments lack textures indicative of wave activity. The plastic material was supplied by grain and turbidity flows that appeared from time to time in the submerged part of the river valley located near the shelf edge.

Significant variability of the Lower Visean deposits is noted near the Tortkol area. Gravel-pebble and sandy-argillaceous deposits are traced here, represented by mudstones, silty-sandstones, less often gravelstones and conglomerates. The sections of the upper Visean are distinguished by a more clayey composition and some reduction in silty-sandy interlayers. Sandstone and silty-sandstone beds (15-30 m) are interbedded by mudstones with a platy or layered texture. In the section, several large cyclites are distinguished, at the base of which coarse-detrital deposits lie, which are gradually replaced by finer and finer-grained ones. At the top of cyclites, clays are often overlain by micro-grained limestones and tuff limestones.

Studies of clay minerals of subsalt deposits in the southeast of the Caspian depression, carried out by the author, revealed that, in their distribution, there is a certain dependence on the hydrochemical and hydrodynamic regimes of sedimentation. The mineralogical composition of clay minerals shows that they were formed on land in a hot humid climate in weathering crusts of a linear type with different rock compositions. In the eastern part - according to rocks of basic and ultrabasic composition,

according to the presence of nontronite, palygorskite and clinochrysotile in the clay association (ultrabasic massif of the southern Urals). The presence of a horizon with a high content of palygorskite indicates a close source of drift, since in the parts of the basin more distant from the coast, the finest palygorskite individuals are easily destroyed with a slight increase in the transport paths. In the Arman-Aiyrshagyl zone, the southwestern part of the South-Emba uplift and in the Tengiz-Kashagan zone, clayey associations with a predominance of hydromicas and mixed-layer minerals are characteristic. A specific feature is the presence of corrensite tuffaceous clays in the sections of the Vostochny Arman, Arman, Saztobe and Tengiz areas. The composition of the clastic material is volcanic, andesitic; there are interlayers of lithic - nitroclastic tuffs.

In the southeastern part of the Caspian Basin, a wide manifestation of andesite volcanism in the Predoksk time is associated with the activity of single volcanoes directly in the Arman-Aiyrshagyl zone. Terrigenous material, within the Caspian Basin, was still brought along the already formed fan lobes.

The sections of the South Emba type in the areas of Tortai, Molodezhnaya, Tabynai, Yuzhno-Embinskaya, Yuzhno-Molodezhnaya, Ravninnaya and others are characterized by a montmorillonite-hydromica-mixed-layer association formed in the weathering crusts of volcanic-sedimentary rocks of basic and middle age, possibly of Devonian, which were exposed by drilling in the Zhanasu-Minsualmas mountain-coastal zone, close to the Northern Ustyurt. This fact confirms the proximity of the North Ustyurt microcontinent in the Devonian.

In the area of the Minsualmas-Teresken uplift, composed of Devonian and Tournaisian terrigenous deposits, there is a scaly uplift of the base of the sedimentary cover along a series of the area of the Tohtkol-2 well reaches 10-11 km. The Teresken trough is separated from the bulge by a regional fault (or a system of faults) of possibly ancient origin, but most actively manifested in the Late Permian-Triassic time, since the Permian-Triassic deposits to the southeast of the fault become the dominant complex of the entire pre-Jurassic section.

The Tournaisian-Visean coastal-marine terrigenous strata was penetrated by wells in the Turesai, Northern Minsualmas, Yuzhno-Molodezhnaya, Teresken areas. Its analogs can be traced in a strip through the areas of Tortkol, Tokhutkol, Yu. Tuskum, Vostochny Tobusken, Kuantai, Kozhasai, Zhanazhol, Sinelnikovskaya, etc. to Isembet in Primugodzharye. Coarse-detrital deposits of abrasion terraces, sandy-argillaceous deposits of underwater coastal-marine gently sloping accumulative plains, ele-

ments of graywacke and flyschoid sedimentation take part in the structure of the stratum. The sections that make up the stratum are represented by alternating gray-colored varieties of mudstones, siltstones of coarse and medium-grained sandstones, and high-thickness gravelstones. In the section of well P-1 Teresken, the thickness of the stratum in the volume of the Tournaisian-Visean stages reaches 2506 m. It also reflects elements of flysch sedimentation. A characteristic feature of the strata sections are the presence of large thicknesses, rhythmic structure, fine alternation of rocks, finds of ostracods and brachiopods, the presence of plant coalified organic matter, and angular roundness of clastic material. Up the section, it has a thinner silty-clayey composition, carbonate cement, and thin limestone interlayers, which record the rhythm of sedimentation. Fully in the scope of the Tourne-Upper Visean stages, the coastal-marine terrigenous stratum is represented in the sections of the Teresken, Isembet-Dzhilansaid areas. The rocks are represented by mudstones, siltstones, sandstones, gravelstones and conglomerates.

Coarse-grained sediments occupy a wider area than the paleochannels themselves in the coastal-marine zone as a result of channel migration. Straight channels also experience migration, which we observe in the section of the Tortai area. Areas of distribution of underwater-channel sediments are noted in the areas of Zhanasu, Turesay, Tortay, Ravninaya, where they are composed of alternating gravelstones, less often of conglomerates with siltstones and mudstones. The rhythm of the underwater-channel currents in time is observed. In the sections in the Tortkol, Tokhutkol, Zhanazhol, and Tuskum areas, the terrigenous stratum has an incomplete exposed thickness of 700-800 m. slope of the South Emba uplift. The standards of the section are gray-colored terrigenous rocks (siltstones, sandstones, less often mudstones, gravelstones). The thickness of the Turne-Serpukhovsky terrigenous complex in the P-1 Tortai well reaches 1570 m, and in the SG-2 Biikzhal well it decreases to 870 m.

So, at the end of the early Visean, an important stage in the formation of the Caspian basin proper was completed: the South Emba inversion uplift and the North Ustyurt microcontinent bounded the basin from the southeast. In the second half of Vise, a new stage in the formation of carbonate platforms of the Caspian Basin begins, which significantly differed from the previous stage, both in the essence of carbonate sedimentation processes and in the location of carbonate platforms.

An extensive carbonate shelf, limited by uncompensated troughs, formed in the Famennian-Tournaisian time.

Late Visean-Bashkir stage. In the Late Visean time, in addition to the Astrakhan and Tengiz-Kashagan carbonate platforms in the south, Zhanazhol and Temir in the east, and Karachaganak in the north, a new Late Visean-Bashkir carbonate platform appeared on the most elevated part of the denuded South Emba uplift, moreover, due to the sea transgression expanded significantly towards North Ustyurt, and the platform boundary ran from east to west. Areas of carbonate accumulation, possibly, remained within the Novobogatinsky and Guryevsko-Kulsarinsky arched uplifts (fig. 2). In the Late Tula and Early Aleksinian times, ash-tuff material of andesite composition and graywacke terrigenous clastic were supplied from the southeastern framing of the Paleo-Caspian basin.

In the northern side zone, the Visean-Lower Bashkirian carbonate complex consists of the Tula, Aleksinian, Mikhailovsky and Venevian horizons of the Visean stage, the Serpukhovian stage (Lower Carboniferous) and the Lower Bashkirian substage of the Middle Carboniferous. The main feature of its development, like other carbonate complexes, is the change of shallow-marine carbonate sedimentation of the platform type through the reef, in the area of the platform margin, to the deep-water depression.

The carbonate complex was formed under the conditions of a high sea level position, and corresponds to the high-level group of sequences of the Visean-Bashkir composite sequence. The Visean-Bashkir reef belt is displaced to the south in relation to the Devonian-Tournaisian, and in the eastern part of the region it is controlled by the clinofold of the Kozhin superhorizon.

In the east, in the Zhanazhol-Tortkol zone, the Upper Visean sandstones are mainly of petroclastic-quartz composition and are better sorted. Fine-grained silty sandstones are characterized by layering due to enrichment with coalified plant residues and mica, and clay lumps are also present. It is possible that such sandstones accumulated in the underwater channels and grooves of the delta front, including during the washing and partial destruction of the channel shafts. Above the Lower Carboniferous terrigenous complex lies a carbonate complex (KT-II) up to 1115 m thick, composed of rocks of organogenic origin (algal, brachiopod, crinoid, detrital, foraminiferal, oolitic limestones) with insignificant interlayers of terrigenous rocks and partly dolomites. The stratigraphic range of deposits is the Mikhailovsky, Venevian horizons of the Visean stage of the Lower Carboniferous - the Kashirian horizon of the Moscow stage of the Middle Carboniferous. Sediments were formed during the period of a regressive cycle of carbonate accumulation in warm shallow waters with isolated lagoons, bays, in a semi-isolated sea shallow, as well as in a shallow-wave zone.

In some periods of time, the introduction of terrigenous material was noted. Limestones KT-II are overlain by terrigenous strata (up to 600 m) of the lower half of the Podolsk horizon of the Upper Moscow substage (MKT). The accumulation of predominantly dark-colored clayey, silty rocks with thin horizontal and lenticular bedding, the presence of spicular clayey varieties, limestones testifies to the calm hydrodynamic regime of the bottom waters and the relative deepness of the sediments. The presence of coarse-grained sandstones, gravelstones and conglomerates in the section is associated with the introduction of coarse-grained material from the source of deposition, i.e. land area located in the immediate vicinity.

In the area of the Zhagabulak - V. Tortkol', Tokhutkol' structures, which were probably more elevated areas, shallow-water carbonates were deposited, alternating with interlayers of terrigenous rocks. The thickness of MKT here does not exceed 100-120 m. Further, the section is built on by a carbonate complex (KT - I) of the Upper Moscow Substage - Upper Carboniferous, in a number of wells (on V. Tortkol, Tokhutkol, Ts. Yakut, Nikolaevskaya squares, the southern end of the Alibekmola structure). The upper carbonates are complemented by the Asselian stage of the Lower Permian. Carbonate deposits of the Upper Moscow substage are represented by a wide variety of lithotypes of limestones: organogenic-lumpy-clotted, organogenic-pelitomorphic with depleted organic matter, with an insignificant presence of clayey rocks. They were mainly formed in the conditions of an isolated shelf lagoon, which were replaced with the conditions of the open shelf.

This complex is composed of thin-layered sandy-argillaceous deposits with small limestone interlayers formed in shallow-water shelf conditions. On the structures of V. Tortkol (well G-3), Tokhutkol, V. Zhanazhol, Kindyky, Ts. Yakut, shallow algal limestones of the Asselian stage with a thickness of 500-700 m are widespread.

The intercarbonate terrigenous strata is composed of clays with interlayers of calcareous sandstones, siltstones with intercalations of gravelstones and, more rarely, limestones, with charred plant detritus. The strata is not developed everywhere. Its thickness varies from 53 m to 406 m (Kozhasai II-3, Zhanazhol G-56). The greatest thicknesses are revealed in the sections of the Zhanazhol, Sinelnikovskaya, Zhagabulak, Alibekmola areas. The reduction in the thickness of the deposits, which are noted in the areas of Yu. Mortuk, Kozhasai, Urikhtau, Zhantai, Tokhutkol and is absent in the Kenkiyak area, is explained by interruptions in sedimentation and erosion.

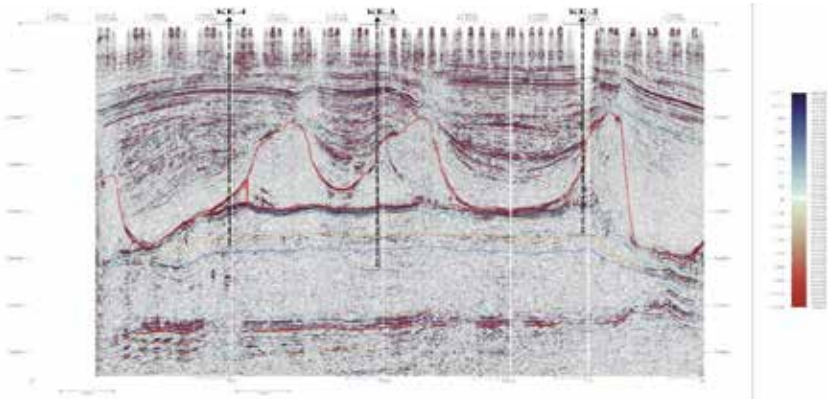


Fig. 2. East Kashagan. Seismic profile through wells VK-4, VK-1 and VK-2

In the south, within the Tengiz-Kashagan carbonate platform, in the late Viséan (Aleksin and Mikhailovskoe time), crinoid and brachiopod-crinoid banks were formed on the surface of silt hills. Silt hills formed paleogeomorphological heights, on which crinoid and brachiopod-crinoid banks, in turn, created a solid substrate for reefs.

The carbonate reservoir, including the western and eastern sections of the Kashagan platform, is a single large uplift, outlined by a closed isohypse of -5000 m along the reflective horizon P2, confined to the top of the Bashkirian deposits of the Middle Carboniferous. Its size along the long northeastern axis is 70 km. In its middle part, the width of the carbonate platform is 8-10 km and expands both in the west and east by almost two times. The marginal parts of the platform are complicated by narrow linear or isometric uplifts with an amplitude of up to 300 m - a rim frame. The most extended Rome is expressed in the extreme northeastern part of the Kashagan structure (fig. 2).

From the end of the late Viséan (Venev time) and in the Serpukhovian, an atoll existed, with reef facies. In the after-reef zone, facies of biostromes, organogenic banks and shoals, and calcareous silts of the lagoon were formed. The period from the early Viséan to the Serpukhovian, from the beginning of the formation of hills, then crinoid banks and reefs, was a stage of compensated subsidence of the Tengiz condensed uplift. At this time, on the border of the early and late Serpukhovian time, as well as Protvinskaya and Zapaltyubinskiy, breaks were established. They contributed to the leaching processes and the formation of secondary voids in the reservoir of the Tengiz field.

ПЕРИОД	ЭПОХА	В Е К	ПОДЪЯРУС	ГОРИЗОНТ	ЛИТОСТРАТИГРАФИЧЕСКАЯ КОЛОНКА	КРАТКАЯ ХАРАКТЕРИСТИКА ФАЦИЙ	ЦИКЛ РИФООБРАЗОВАНИЯ	НЕФТЕГАЗОНОСНОСТЬ	СЕЙСМИЧЕСКИЙ ГОРИЗОНТ	
КАМЕННОУГОЛЬНЫЙ ПЕРМСКИЙ РАНИЯ	РАНИЯ	АРТИНСКИЙ				Карбонатно-алевритово-глинистые осадки относительно неглубокого моря на внутривосставном поднятии			П ₁	
		САКМАРСКИЙ								
		АССЕЛЬСКИЙ								
	РАНИЯ	СРЕДНЯЯ	БАШКИРСКИЙ		pk-kr		Биокластические банки и отмели			П ₂
			ВИЗЕЙСКИЙ							
		vn								
		mh								
		НИЖНИЙ		al		Криноидные и брахиоподово-криноидные банки				
				tl						
		ТУРНЕЙСКИЙ		bb-ks		Иловые холмы				
ksl-gm										
ДЕВОНСКИЙ ПОЗДНЯЯ		ФАМЕНСКИЙ		zv-el		Мелководная карбонатная платформа. Седиментация комковато-стучковых и фораминиферо-водорослевых известняков			Dt	
		ФРАНСКИЙ								lv-sr

Fig. 3 Vertical facies row of the Tengiz-Kashagan carbonate platform (on the example of the Tengiz field)

In the Bashkir Age (from Krasnaya Polyana to the Kama Time inclusive), bioclastic banks, shallows and underwater shafts were formed. At the border of the Serpukhov and Bashkir centuries, a break is recorded - there was a shallowing and cessation of reef formation. In the sediments of the Bashkir age, a small height of cans, erosion and frequent surface breaks are found. This can be explained by the fact that sedimentation

was not compensated by subsidence. The formation of the Tengiz-Kashagan carbonate platform was associated with the period of the opening of the Ural paleocean. This resulted in a wider stratigraphic range and more significant thickness of carbonate deposits. Carbonate deposits of the Tengiz-Kashagan carbonate platform cover a wide stratigraphic interval - from the beginning of the Late Frasnian to the Middle Carboniferous.

The peculiarity of the cycle on the Tengiz uplift is that reef formation here stopped at the end of the Serpukhovian. This could be due to the fact that compensated subsidence, which is so necessary for the existence of reefs, ceased in the Bashkir Age. Fig. 3 shows the vertical facies row of the Tengiz-Kashagan platform.

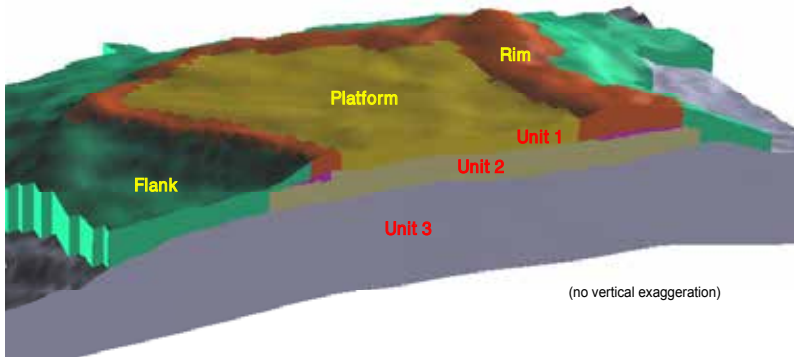


Fig. 4 Tengiz carbonate structure

The Late Visean-Sakmarian coastal-marine shelf carbonate stratum also developed in the zone of the South Emba uplift. The stratum is represented by sections of the wells Sarykum, Urtatau-Sarybulak, Bekbulat, Saztobe Yuzhnoye, Turesai, Tortai (G-23, G-12), Yuzhno-Molodezhnaya and Yuzhno-Embinskaya, drilled on the northwestern slope of the Yuzhno-Emba uplift. Its analogue is found along the eastern flank, where it is dissected into two carbonate strata by terrigenous sediments of the lower Podolsk horizon of the Moscow stage. Carbonate sections of the South Emba uplift differ in stratigraphic completeness, content of terrigenous interlayers, and structural-genetic types of carbonate sediments.

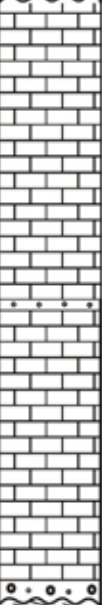
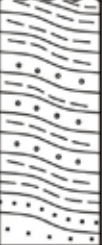
КАМЕНЕУГОЛЬНЫЙ ПЕРИОД ЭПОХА	ВЕК	ЛИТОСТРАТИГРАФИЧЕСКИЙ КОМПЛЕКС	ЛИТОЛОГО-ФАЦИАЛЬНАЯ КОЛОНКА	КРАТКАЯ ХАРАКТЕРИСТИКА ФАЦИЙ	НЕФТЕГАЗОНОСНОСТЬ	СЕЙСМИЧЕСКОСТЬ ГОРНОТЫ
КАМЕНЕУГОЛЬНЫЙ ПЕРИОД ЭПОХА	САКМАРСКИЙ (?)	КАРБОНАТНЫЙ ОБЛОМОЧНЫЙ ДОЛОМИТИЗИРОВАННЫЙ		Во внешней части мелководного шельфа на глубине 50-130 м сформировались банки грейстоунов		П1
	АССЕЛЬСКИЙ					
	СРЕДНЯЯ	МОСКОВСКИЙ	ТЕРРИГЕННО-КАРБОНАТНЫЙ		Внутренняя и средняя части шельфа глубиной 30-70 м. Преимущественно переотложенный органино-обломочный материал. Слагает банки и уплощенные холмы. Терригенные компоненты образовались при размыве преимущественно платформенного чехла Устьуртского микроконтинента	
БАШКИРСКИЙ						
РАНИЯ	СЕРПУХОВСКИЙ	ТЕРРИГЕННО-АРГИЛЛИТОВЫЙ		Подножие предостроводужного, активного, а затем - пассивно-океанического бассейна: иловая седиментация в сочетании с гравитационными потоками, в песчаниках пачки присутствует переотложенный вулканомиктовый материал андезитового состава		П2 ¹
ВИЗЕЙСКИЙ						

Fig. 5 Vertical facies row of the northwestern margin of the South Emba carbonate platform

The accumulation of carbonate sediments took place in a shallow coastal sea basin under conditions favorable for carbonate sedimentation. The thickness of the Carboniferous part of the stratum in the section of the Turesay area is 1043 m. The lower carbonate stratum is composed of limestones of various genetic types, in varying degrees of dolomitized, foliated and massive with different densities, with interlayers of mudstones. The stratigraphic volume of the strata is determined by the Oka, Serpukhov, Bashkir, and Early Moscow ages.

The stratum was formed in a shallow sea basin over a vast area of the entire eastern part in the form of a carbonate platform.

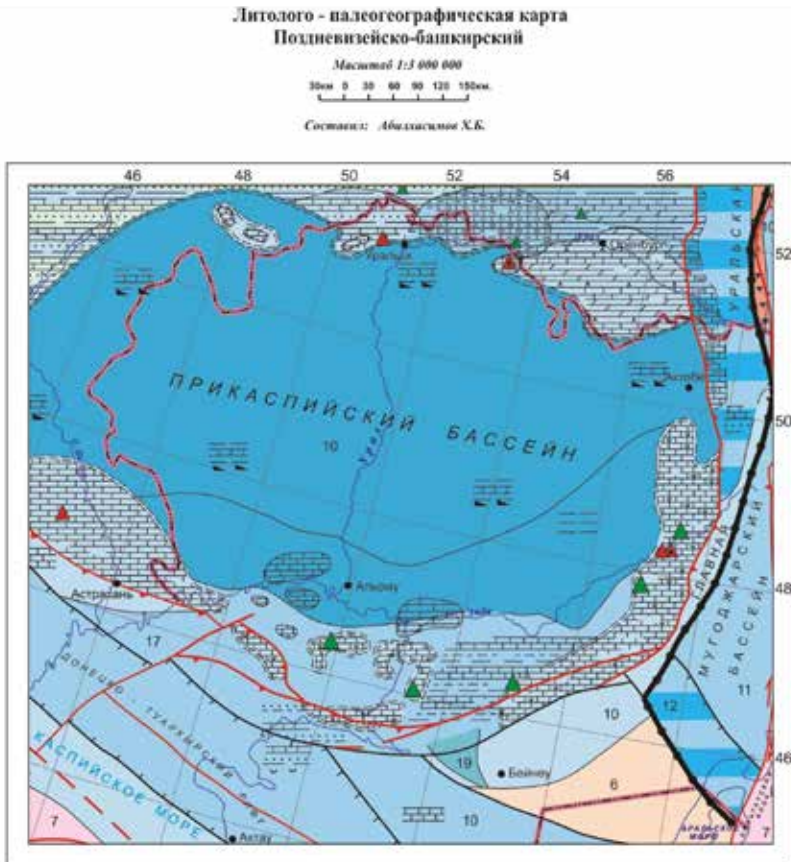


Fig. 6 Lithological-paleogeographic map of the Late Visean-Bashkir stage. Compiled by: Kh.B. Abilkhassimov

The thickness of the lower carbonate stratum (KT-II) decreases from east to west from 650 m to 250–136 m, and towards Biikzhal and Tortay it is replaced by a shelf terrigenous-carbonate stratum.

The vertical facies series of the northwestern margin of the South Emba carbonate platform is shown in fig. 5.

Within the Astrakhan carbonate platform, in the Late Visean-early Bashkirian time, mainly shallow-water carbonate formations accumulated, and in the lower parts of the troughs, clay-carbonate, relatively deep-water sediments. Areas of shallow carbonate sedimentation have decreased. In the early Bashkir, the sedimentation conditions correspond to lagoon environments, in which the products of the destruction of reef structures accumulated. The deposits are represented by biomorphic, biomorphic-detrital, biochemogenic and organogenic-detrital limestones.

In the Late Paleozoic, the Astrakhan dome was in the area of active carbonate accumulation (fig. 6), at times replaced by the introduction of terrigenous material. The most ancient deposits uncovered by drilling are the Lower Carboniferous limestones. On the erosional surface of the Serpukhovian deposits of the Lower Carboniferous, there is a stratum of organogenic limestones of the Bashkirian stage.

Moscow-Late Carboniferous stage. The Moscow basin of sedimentation inherited the character of the sedimentation regime from the Bashkir one. In the Tengiz-Kashagan zone, there was a hiatus in sedimentation during this period. The end of the Bashkirian - early Moscow centuries marked the beginning of the third (Late Bashkirian - Early Gzhelian) stage in the development of carbonate platforms, associated with intense tectonic processes in the south of the depression - in the Karpinsky ridge, where the process of sedimentation of thick terrigenous strata began (fig. 8).

Carbonate platforms remained in shallow-sea conditions for a long time, periodically drained, which contributed to the development of karst processes. The accumulation of the terrigenous complex was accompanied by consedimentation deformations of compression and thrust on the Astrakhan carbonate platform and a chain of other carbonate massifs in the south of the Caspian basin.

Serpukhovsko-Moscow - shelf terrigenous-carbonate strata developed in the zone of junction with the South Emba uplift. The stratum is represented by a section of wells in the Biikzhal, Tortai, Yu.Z. Ulkentobe, Sholkara, Tabynai, Kumshety, Urtatau-Sarybulak, etc.) Serpukhov, Bashkir and Moscow age. The predominance of limestones is noted in the upper parts of the sections of the Serpukhov, Bashkir and Moscow age and

their decrease in the lower. The total thickness of the Serpukhov-Moscow terrigenous-carbonate strata in the Biikzhal area is 174 m.

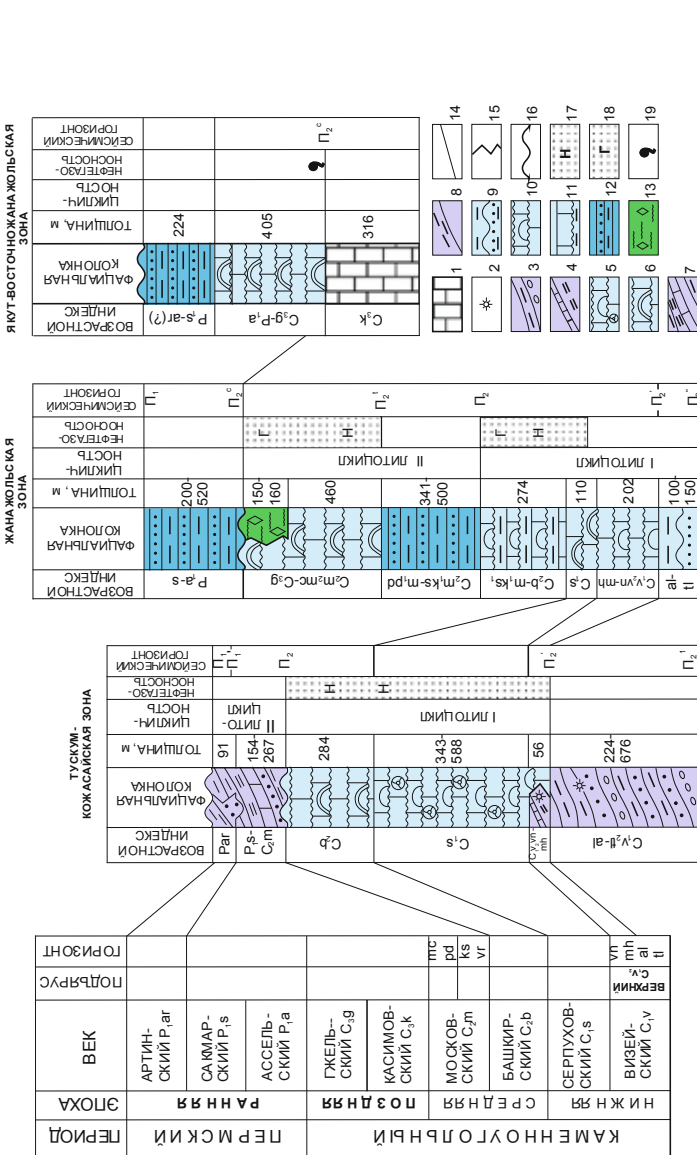


Рис. 7 Фация льные колонки структурно-фациальных зон Жанажольской карбонатной платформы. По материалам С.М. Бланк, О.И. Вадеевой, П.Б. Гибшман, Ю.А. Иванова, Л.Н. Ивановой, И.Н. Иванова.

1 - известняк; 2 - известняк с раковинами; 3 - известняк с раковинами; 4 - известняк с раковинами; 5 - известняк с раковинами; 6 - известняк с раковинами; 7 - известняк с раковинами; 8 - известняк с раковинами; 9 - известняк с раковинами; 10 - известняк с раковинами; 11 - известняк с раковинами; 12 - известняк с раковинами; 13 - известняк с раковинами; 14 - известняк с раковинами; 15 - известняк с раковинами; 16 - известняк с раковинами; 17 - известняк с раковинами; 18 - известняк с раковинами; 19 - известняк с раковинами.

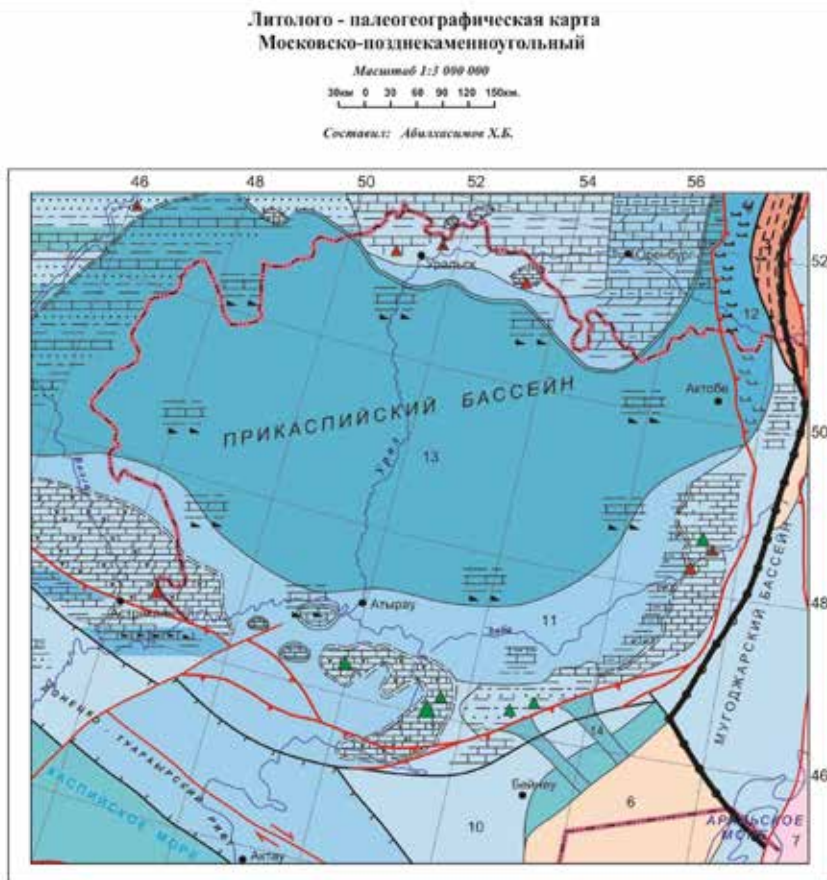


Fig. 8 Lithological-paleogeographic map of the Moscow – Late Carboniferous stage. Compiled by: Kh.B. Abilkhassimov

In terms of its genetic content and completeness, the Biikzhal section can be classified as a reference.

The Upper Visean-Upper Carboniferous platform shallow-marine complex of the terrigenous-carbonate strata is widely developed in the subsalt sediments of the *eastern near-belt zone of the Caspian Basin*: Tokhutkol, Tortkol, Vostochny Tortkol, Kindysai, Vostochny Tobusken, Kuantai, Zhanatan, Akzhar-Tashiy, Kozhasai, Sinelnikovskaya, Zhanazhol, Urikhtau, Alibekmola, Yu. Mortuk, Kenkiyak, etc. It contains two carbon-

ate strata, KT KT-I (-II) and the stratum of terrigenous deposits separating them. The thickness of the entire complex decreases from east to west from 1800-1500 m until it disappears completely. There is a reduction in the thickness, first of the Upper Moscow-Upper Carboniferous carbonates (KT-I), then the intercarbonate terrigenous strata and the Upper Visean-Lower Moscow limestones (KT-II) with the formation of clinoforms due to erosion. The depth of erosion of Carboniferous deposits increases towards the Karaulkeldinsky paleo-uplift. The Late Carboniferous is marked by a sharp drop in sea level, which led to partial erosion of previously accumulated deposits in the area of uplifted areas and carbonate structures: Tengiz-Kashagan and Yuzhno-Embinskaya; reduction of the carbonate shelf zone, the formation of underwater shoals and an increase in the role of terrigenous material.

On the Astrakhan carbonate platform Upper Carboniferous deposits were preserved fragmentarily due to later erosion. Terrigenous-clastic and carbonate-clastic deposits prevail here. The thickness of the deposits is 180 - 250m. They were penetrated in wells 3-Vysokovskaya, Yuzhno-Astrakhanskaya and Tabakovskaya -1. It is overlapped by a clay-carbonate stratum of the Lower Permian, represented by various genetic types of light-colored limestones of various structures. The total thickness of the Sakmar-Artinsky deposits is 225-330 m.

Assel-Sakmara stage. In the pre-Permian time, the South Emba carbonate platform developed, as in the previous stage, with the entire set of formations characteristic of the platform. After a long Late Carboniferous hiatus in sedimentation and denudation of positive forms of paleo-relief to the depth of the Serpukhovian and sometimes Visean stages, a new transgression of the sea took place. The sedimentation conditions in the southeastern Caspian region in the Asselian and Sakmarian centuries were similar and, probably, formed a single cycle (fig. 8). The distribution of lithofacies zones of deposits of the Asselian-Sakmarian age did not undergo significant changes in comparison with the Late Carboniferous time. Carbonate accumulation remained in a narrow strip on the Urtatau-Sarybulak area and extended to the Zhanazhol-Tortkol zone of the eastern side of the Caspian Sea. (fig. 9). The Lower Permian deposits are represented by light bluish-gray limestones, bioherm, combined with bluish-gray, organogenic detrital limestones, with the accompanying fauna of the Asselian stage.

Thickness - 955 m. In the Temir zone, the section of the Assel-Artinskian stage is argillaceous-sandy, argillaceous-siliceous, with single interlayers of limestones, dolomites and thin lenses of coarse rocks; the upper

part of the Artinskian Stage is dominated by mudstones and clays. The Lower Permian shallow-sea sediments belong to the lithological-facies complexes of underwater paleodeltas and meandering branched channels, with near-channel banks, with the introduction of volcanogenic material from the land area.

On the structures of V. Tortkol (well G-3), Tokhutkol, V. Zhanazhol, Kindykty, Ts. Yakut, shallow algal limestones of the Asselian stage with a thickness of 500-700 m are widespread. The Intercarbonate strata has a smaller age volume - only the Podolsk horizon and a smaller thickness (up to 200 m). The main feature of this zone, as the authors believed, is a larger age range and, accordingly, a greater thickness of the upper carbonate strata. They believed that the upper part of KT-I here includes limestones of the Asselian stage of the Lower Permian.

According to N.B. Gibshman (Geology and oil and gas content ..., 1988) in the Vostochny Tortkol G-3 well, the boundary between the Carboniferous and Permian systems is not lithologically pronounced and passes inside the layer of algal limestones at a depth of 1839 m. Thus, judging by this well, between the Carboniferous and Permian deposits is observed the consonant nature of the border (fig. 7).

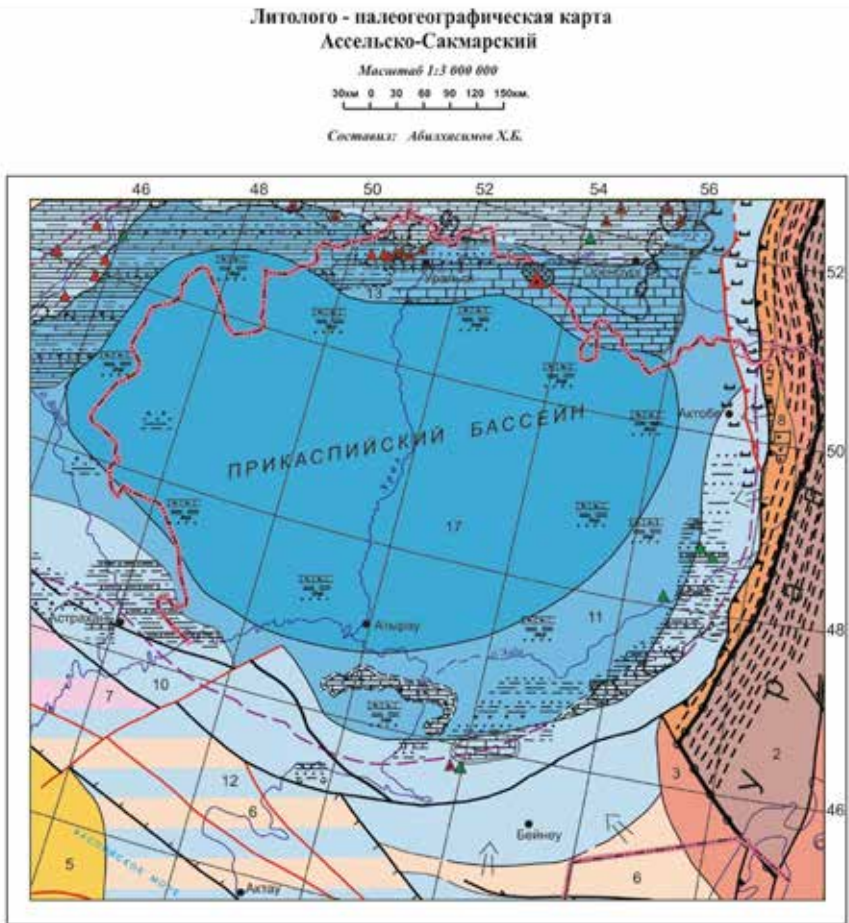


Fig. 9 Lithological-paleogeographic map of the Asselian-Sakmarian stage. Compiled by: Kh.B. Abilkhassimov

Permian deposits begin from the lower subzone of the lower fusulinid zone of the Asselian stage, consisting of bluish-gray tubifite limestones. The middle and upper parts of the Assel section are composed of organogenic detrital limestones alternating with subordinate layers of silty, clayey, and tubiphytic limestones. These parts of the section are characterized by foraminifera of the middle and upper zones of the Assel. The thickness of the carbonate section of the Asselian stage in this well is 339

m. Similar and similar sections were opened in the wells Tokhutkol G-1, G-2, Yakut-1. According to seismic materials, the thickness of the Assel reaches up to 950 m. Unfortunately, the insufficient amount of materials and inconsistency with the seismic data led the authors to several significant inaccuracies. The Assel (later Sakmarian) carbonate deposits cannot be attributed to the KT-I carbonate strata, since the seismic horizon P, which characterizes the surface of the KT-I complex in the Zhanazhol region (where, in fact, the abbreviation KT-I came from), is clearly traced in the considered zone at the usual stratigraphic level - in the thickness of Late Carboniferous limestones. The opinion about the lithological indistinctness of the boundary between the Carboniferous and Permian deposits (well Yakut-1) is not confirmed either. Therefore, the Early Permian carbonate stratum is designated by the KT-O index. The facies boundary between the Upper Carboniferous and the Assel corresponds to a clear change from mudstones to carbonates. In this zone (in two wells: Vostochno-Zhanazholskaya G-1 and Yakut-1), the most complete sections of KT-O were penetrated. The Yakut-1 well was drilled on a carbonate platform near the scarp along the Early Permian complex. In the interval 3455 (bottomhole) - 3104 m, it exposed the carbonate complex KT-II as part of the Bashkirian stage and the Vereisk-Kashirian horizons of the Moscow stage of the Middle Carboniferous. The sedimentary complex is represented by white and gray crystalline limestones. In the interval of 3104-2784 m, the intercarbonate stratum MKT, represented by dark mudstones of the middle of the Moscow stage (Podolsk horizon), was crossed. Carbonate complex KT-I (Late Moscow-Kasimov age) is represented by light limestones with subordinate interlayers of mudstones (2784-2398 m). The Gzhel Stage (Late Carboniferous) is composed of gray mudstones, and the Asselian-Sakmarian deposits form the upper carbonate complex KT-0, which has anomalously high thickness (926 m) for the entire eastern part of the Caspian Basin (depth interval 2071-1145 m).

In the western part of the northern side zone, the Asselian deposits in the volume of all three fusulinid zones overlie the deposits of the Upper Carboniferous or the Moscow Stage of the Middle Carboniferous. On the rest of the northern flank, deposits of the Asselian stage unconformably overlap the deposits of the Middle and Lower Carboniferous. Within the shallow carbonate shelf, the Asselian stage, 50-200 m thick, is composed of carbonate deposits. In the zone of the side scarp, where organogenic structures are widely developed, the Asselian stage is composed of biohermal and layered shallow-water shelf formations containing organogenic structures.

In the Asselian sediments within the Karachaganak reef, there are three biohermal edifices that form hilly peaks within the chest-shaped organogenic edifice with a flat vault and steep wings, formed by the underlying Upper Devonian and Carboniferous deposits.

Sediments of the Sakmarian Stage in the northern side zone are developed everywhere. In the western part of the zone, they are represented only by deposits of the Tastubian horizon, in the eastern part they have a full stratigraphic volume. Within the shallow shelf in the after-reef zone, the Tastubian horizon is composed of micro-fine-grained limestones and dolomites with interlayers of organogenic-detrital and pseudo-oolitic varieties. In the zone of the side scarp, the Sakmara Stage is composed of layered carbonates with bioherm inclusions.

Bioherm deposits are represented by gray and light gray bryozoans and bryozoans-purple, organogenic-detrital, foraminiferal-algal limestones and relict-organogenic dolomites.

On the Karachaganak and South-Emba carbonate platforms, and partly on the Zhanazhol (on the structures of the East Tortkol, and Tokhutkol) and Temir (later cut off by the pre-Kungur erosion), the accumulation of carbonate complexes continued, which deep into the basin were replaced by rhythmic strata of terrigenous deposits, siltstones (sandstones).

Shallow-water sediments are replaced by relatively deep-water ones, developed in the Matken-Ushmola and Tengiz-Kashagan zones, where the Assel sediments overlap with stratigraphic unconformity on the Carboniferous formations of different ages and are represented by volcano-genic-sedimentary formations.

The end of the Sakmarian - the beginning of the Artinskian age corresponds to the regional restructuring of the entire tectonic regime within the territory under consideration. The inversion in the area of maximum thickness of the accumulated Carboniferous and Asselian-Sakmarian sediments led to powerful ascending movements that formed an area with mountainous relief at the site of the South Emba trough.

Artinsky stage. The final Artinsk stage is characterized by mountain building processes in the Urals, i.e. the emergence of a new source of drift of terrigenous material into the Caspian basin. In addition, active denudation of the folds of the Karpinsky Ridge, expressed in relief, continued. The formation of carbonate platforms stops everywhere, with the exception of the central and southern parts of the South Emba uplift and the northern side zone (fig. 10).

In the northern side zone, the Artinskian deposits are developed everywhere in the volume of two substages. Within the shallow-water reef

shelf, the layer deposits with a thickness of 62 to 182 m at the base are composed of pseudo-endotiric pseudo-oolitic, microphytolitic and micro-grained limestones, which are replaced upsection by micro-grained limestones with interlayers of dolomites. The section ends with an anhydrite member 10 to 25 m thick. In the zone of the side scarp, layered and biohermal carbonate deposits are developed. The thickness of the layer deposits in the zone of the side scarp varies from 30 to 338 m (Matloshinsky, 1988; Kabatskaya et al., 1988). The reef deposits of the Kashir-Artinsk carbonate formation have been studied in the northern inner near-edge zone among the depression sediments on the Karachaganak island reef. However, only the upper, lower Permian part of the formation is present within the reef, the lower part of the formation in the volume of the Moscow and Upper Carboniferous deposits falls out of the section and the Asselian deposits unconformably lie on the Serpukhovian formations in the dome and on the lower Bashkirian ones on the wings.

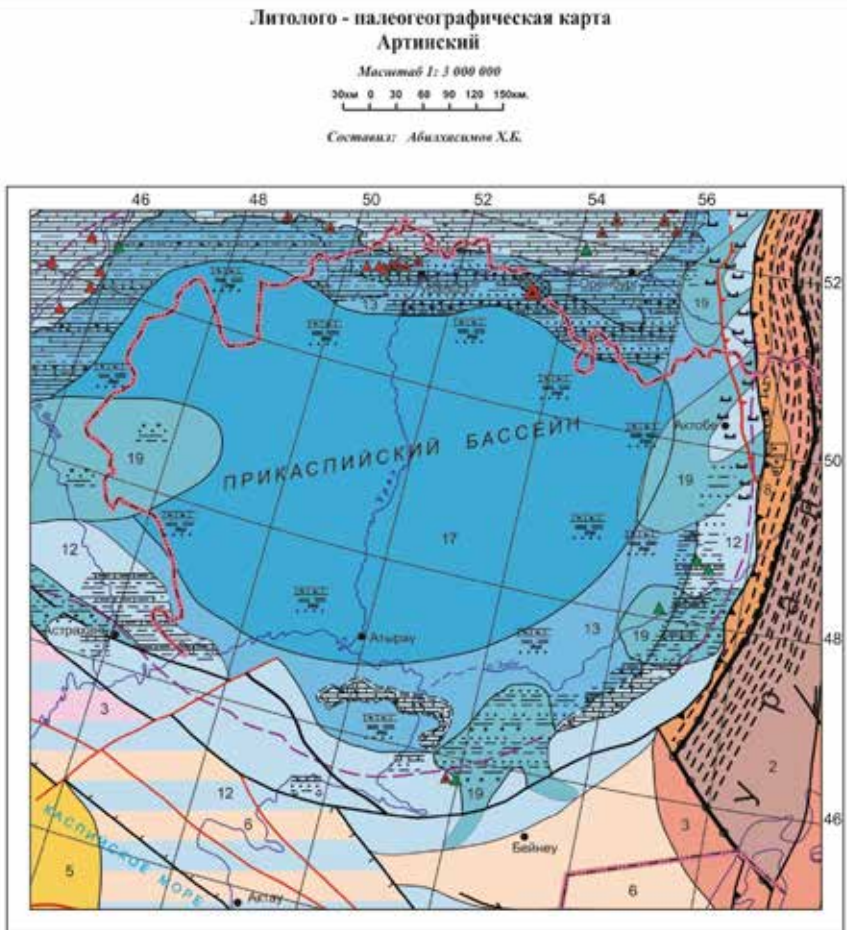


**Fig. 10 Lithological-paleogeographic map of the Artinsk stage.
Compiled by: Kh.B. Abilkhassimov**

The Artinskaya part of the formation of the Karachaganak island reef is represented by a stratum of carbonate rocks with a thickness of more than 200 m. These are formations of bioherm structures, which have somewhat shifted towards the center of the massif. Bioherms are formed by blue-green, siphonic, and crimson algae to a lesser extent tubifites, bryozoans, crinoids, brachiopods, fusulinids, foraminifera, gastropods, trilobites, and solitary corals (Moskvich, 1988).

As follows from the curve of R. Weil, it is in the middle of the Early Permian epoch that there is a sharp decrease in the level of the world ocean. According to A.P. Lisitsin, in this era, most of the shelf, especially its shallow areas, become the scene of numerous subaerial interruptions. At the same time, there is a "discharge" of a significant mass of accumulated sediments to the second global level of sedimentation (continental slope, its foot and abyssal plains); the transfer of sedimentary material from the shelf and its edge is quite probable directly to the foot of the Lower Permian side scarp, and in the case of gentle slopes, to deeper areas.

Here, stable conditions for the accumulation of sediments remain, and as the level falls, they acquire the features of shallow-water sedimentation. This explanation is in good agreement with the structural features of the sections directly adjacent to the steep slopes of the Lower Permian wall (Teplovsko-Tokarevskaya zone, Vostochno-Vetelkinskaya area), and sections of the Artinskian stage of Pavlovskaya, Chinarevskaya, and Rozhkovskaya areas. The set and composition of their constituent rocks are largely determined by the features of sedimentation in the adjacent areas of the side of the depression. So, in the Teplovsko-Tokarevskaya zone, the remains of reef builders - bioherm rocks - are of great importance.

Thus, using the main provisions of the theory of A.P. Lisitsyn on avalanche sedimentation and interruptions in sedimentation, it is possible to approach the interpretation of some paleogeographic settings in the Upper Paleozoic of the northern side zone of the Caspian Basin in a new way.

Sharp drops in sea level in the isolated Caspian basin led to the development of erosional relief in the side parts of the depression and the formation of powerful fan loops in the southeastern part of the basin (Tortaysky, Sholkarinsky, Tabynaisky, Arman-Aiyreshagylsky).

Paleochannels have a flat V-shape with a wide cone, open towards the basin and are filled mainly with medium-coarse-grained sands and gravel in various proportions, with a large amount of large residues of plant detritus. In the cross section away from the thalweg, there is a gradual decrease in the granulometry of sediments. There are inter-channel and dam sediments, which are mainly represented by fine-grained sand. In the inter-channel depressions, a thinner clay material is deposited.

**УСЛОВНЫЕ ОБОЗНАЧЕНИЯ
К ЛИТОЛОГО-ПАЛЕОГЕОГРАФИЧЕСКИМ КАРТАМ**

Палеогеографические обстановки

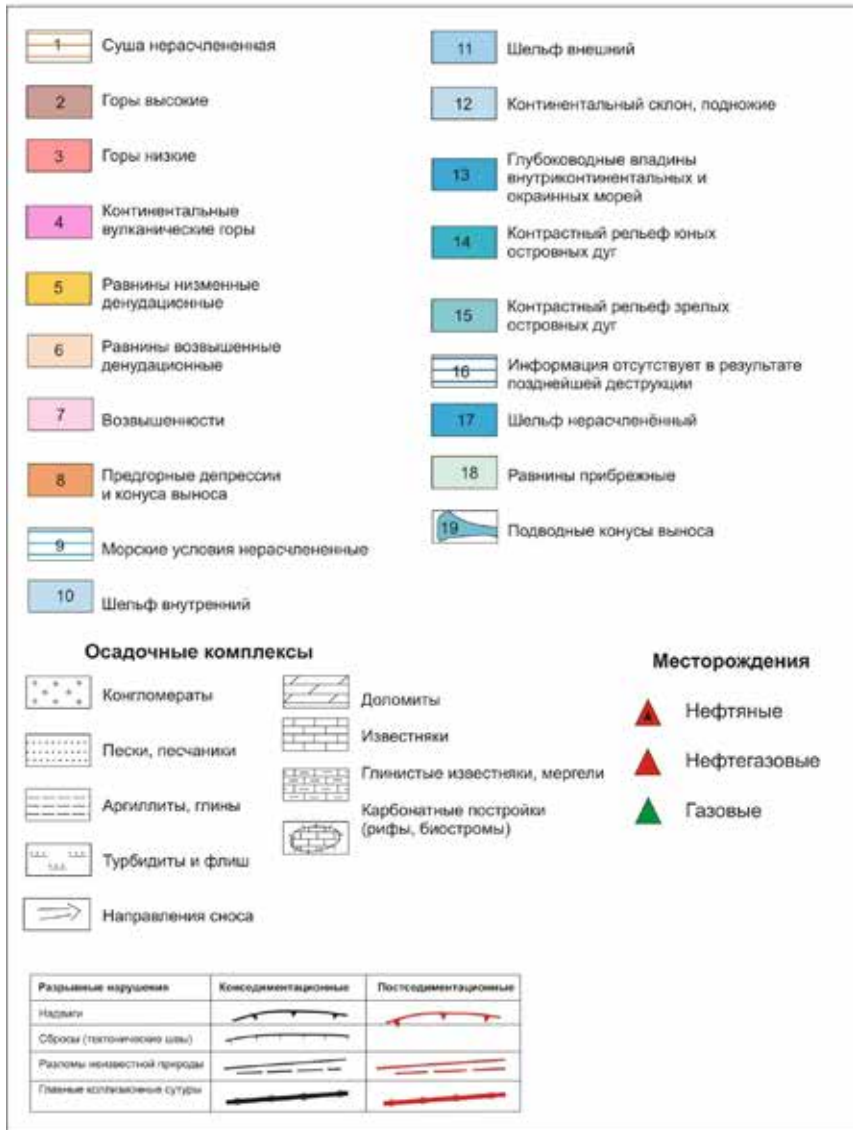


Fig. 11 Symbols for lithological and paleogeographic maps

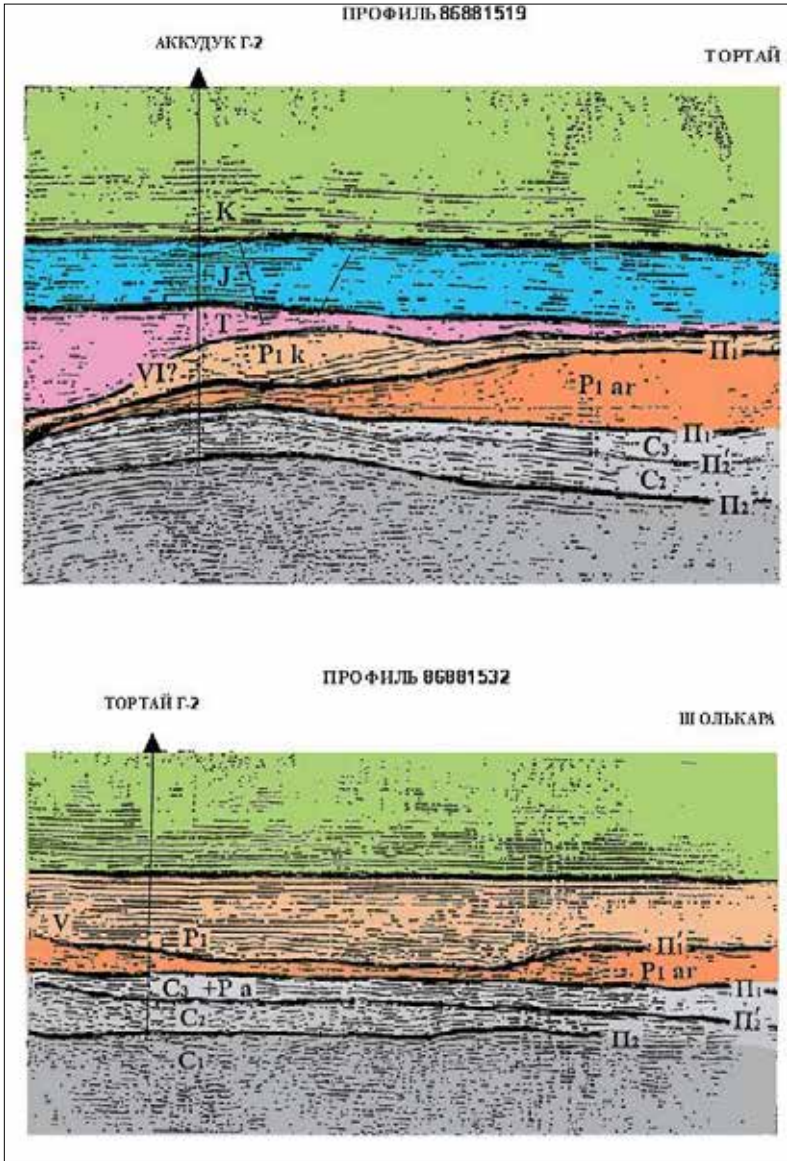


Fig. 12 Seismic sections of the southeastern part of the Pre-Caspian depression, displaying the Tortay (top) and Sholkarinsky fans

Coarse-grained channel sediments occupy a wider area, which is associated with the lateral migration of paleochannels due to their meandering.

Tracing the boundaries of sedimentary seismic complexes and seismic formations, it was possible to establish certain regularities in their distribution in space and to estimate the material composition of individual seismic formations. The main display on time sections is found such elements as shelf side scarps, shelf edges, cross-bedded and sigmoidal formations of lateral build-up and fan cones, erosion and sedimentation scarps within the basin, on the slopes and at its foot.

When drawing up diagrams of the structure of sedimentary complexes, reflecting the paleogeographic situation at the time of their formation, the analysis of time sections was also taken into account, which made it possible to distinguish the characteristic forms of the relief of the basin bottom and geological bodies, to give their more accurate contours and to establish the direction of the main flow of terrigenous material. Among the sedimentation seismic complexes that are confidently distinguished on the time sections is the terrigenous Artinsk seismic complex. The reference reflective horizons, bounding this seismic complex, were referenced by wells.

The Lower Permian Artinskian terrigenous seismic complex overlaps the Carboniferous deposits and is bounded from below by the reflecting horizon P1, and from above by the reflecting horizon P'1 or "b". The internal structure of the seismic complex has a variety of wave characteristics within the study area. The features of the wave field are quite pronounced, characteristic and diagnostic in nature, that is, the seismic complex is easily recognized on time sections and rich information is associated with it about the features of the geological section and its lithological composition (fig. 12). The most pronounced in the wave field is a cross-bedded stratum of lateral build-up, well studied by drilling and seismic exploration in the Tortai, Ravninnaya, Molodezhnaya areas. The thickness of the strata reaches 800–900 m.

As already noted, in the time sections, various kinds of ledges are most clearly visible. The fragments of seismic profiles shown in the figures show how clearly the sedimentation scarps of the Artinskian terrigenous strata appear in the wave field. Here, the edge of the scarp manifests itself in the form of wedging of the P1 horizon under the reflecting horizon V. It should be noted that the main feature of the wave field in the considered zone is a sharp change in wave fields at short distances when the underlying deposits of the Upper and Middle Carboniferous have a polyfacial structure from carbonate in the south to clay-terrigenous in the northwest and are characterized by reflective horizons P2, P'2, occupying a time interval. The convergence of horizons in time sections indicates a decrease in the

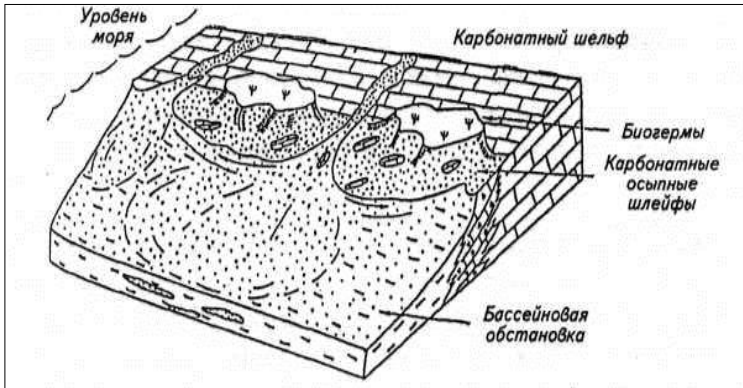
thickness of the Upper-Middle Carboniferous sediments to 100-200 m (within the resolution of seismic exploration in the conditions of a given area), but not about their complete loss from the section, since they are recorded in the sections of wells. The wave field of this complex is characterized by a set of non-parallel, different intensities of differently oriented reflective boundaries of small length, often insignificant in intensity. There is a deterioration in the tracking and expressiveness of these reflections in the area of replacement of lithofacies of Carboniferous deposits.

In the Tengiz-Kashagan zone, in the crestal parts of the Tengiz, Korablevskaya, Tazhigali fields, the thickness of the Artinskian deposits ranges from a few meters to 255 m. The lithological composition is characterized by the predominance of mudstones in the section, the presence of mudstone-like clays, marls and limestones. A characteristic feature is the areal development of tuffacelites and lithiviroclastic tuffs in the lower part of the section. At the base of the stratum, there is a horizon of clayey-carbonate breccia. Tuffaceous rocks are found in the form of separate layers of predominantly light green color. The rocks are dense, robust, with a massive texture, with a conch-like fracture. According to the mineral composition of clay matter, these rocks are divided into two subtypes. The first one is mainly tuffopelites of predominantly hydromica-kaolinite composition with an admixture of mixed-layer formations. The second has a monomineral composition of mixed-layer formations of hydromica - smectite. On the northeastern flank of the Tengiz structure in well 10 under the Kungur salt-bearing strata in the interval 4862-4920, the section is represented by interbedded clay rocks with interlayers of siltstones and marls. Clay rocks are represented mainly by calcareous mudstones, bituminous to varying degrees, silty, thin-horizontally-layered, with a large amount of charred plant detritus, dispersed and fine-aggregate globular pyrite. In some interlayers (4912-4913 m), accumulations of remains of siliceous skeletons of radiolarians, characteristic of the Upper Carboniferous or the Lower Permian (Assel), are noted.

Within the Tengiz-Kashagan zone, the Artinskian deposits are represented by deeper-water formations of the Upper Artinskian substage. The hypsometrically uplifted carbonate massifs in the Asselian and Sakmarian times were subject to periodic erosion of carbonate complexes. For example, foraminifera were found in fragments of slime-detrital limestones, which are common in the upper part of the Lower Carboniferous and in the lower part of the middle. However, the Artinsky clay deposits, 40-100 m thick, were preserved from erosion, which indicates an increase in the level of the Artinsky basin compared to the previous time.

Fig. 13 shows sedimentation models of the southeast of the Caspian Basin during the Paleozoic stage. A feature of the sedimentation environment in the Late Paleozoic basin of the Caspian Sea region is that different geomorphological levels of sedimentation have developed within the same basin. Carbonate platforms compose isolated areas, fixed by positive forms of the relief of the Paleodenum.

MODEL OF CARBONATE-TERRIGENIC SEDIMENTATION (Late Visean-Sakmarian stage)



MODEL OF TERRIGENIC SEDIMENTATION (Artinsky stage)

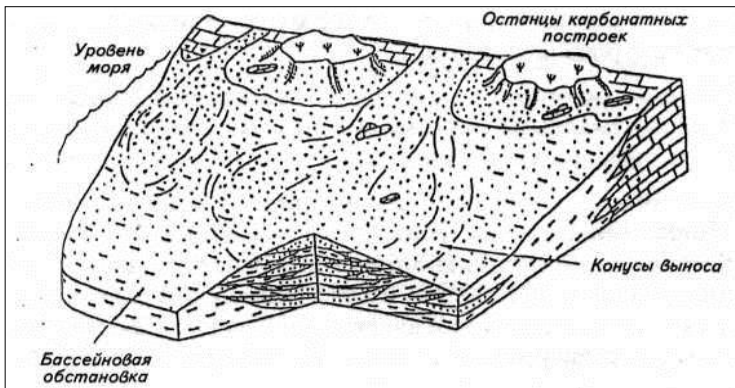


Fig. 13 Sedimentation models of the southeast of the Caspian basin in the Paleozoic stage

A characteristic feature of this stage of sedimentation is the formation of powerful fans, the tongues of which penetrated into the inner part of the basin, forming coarse-detrital interlayers in the sections, as well as inter-cone submarine accumulative swells, predominantly of clay composition with subordinate interlayers of sandstones, less often gravelstones. A special role is played by paleo-channel systems, which were the main arteries in the supply of terrigenous material to the basin. The distal parts of the basin are dominated by terrigenous deposits. The morphological irregularities of the paleogene are recognized by the granulometry of the sediments. In the raised areas - vaults - mainly clay-silty material accumulates.

In the lower parts, in zones with high velocities of bottom currents, due to the washing out of the clay fraction, the coarser material, psammitic, is concentrated.

By the end of the Artinskian time, the Caspian sedimentary basin was bounded from the southwest by the continental Scythian block and the North Ustyurt massif - from the southeast, which is confirmed by integumentary-thrust deformations in the area of the Karpinsky and Donbass-Astrakhan zones. In the isolated Caspian Basin, thick layers of salt accumulated in kungur in a calm tectonic setting.

Conclusions:

- The spatial distribution of carbonate platforms in the Caspian Basin is determined by the different duration of sedimentation stages and the block structure of the basement. In the northern part of the Caspian Basin, carbonate accumulation lasted the longest period, which provided the formation of the powerful Karachaganak platform with a wide stratigraphic range of deposits from the Late Devonian to the Early Permian inclusive. In the eastern and southeastern parts of the Caspian Basin, due to the influence of geodynamic factors of the convergence of the Urals and the North Ustyurt block with the edge of the East European plate, the areas of carbonate accumulation sharply decreased, and a narrow strip of carbonate platforms was formed - Temirskaya, Zhanazholskaya and Yuzhno-Embinskaya. The processes of carbonate accumulation were suppressed by the introduction of a large amount of terrigenous material from the adjacent land. There are no KT-I deposits on the Temir carbonate platform. The South Emba carbonate platform is much younger than the Tengiz-Kashagan one. Carbonate deposits within it occupy a narrower stratigraphic interval, covering the period from the end of the Lower Carboniferous - Early Visean to the Assel-Sakmarian stage of the Lower Permian inclusive.

- The most intense carbonate accumulation took place in the south and southwest of the Caspian region within the Astrakhan and Tengiz-Kashagan platforms; Due to the expansion of the area of carbonate accumulation in the Late Devonian, a single Astrakhan-Zhylyoi platform was formed, which covered the entire modern water area of the North Caspian and adjacent coastal areas.

- The single Astrakhan-Zhylyoi Devonian carbonate platform, within which the Yuzhnoye uplift is located, is delineated by tracing its basement between the regional reflectors P3 and P4. The assumed age of the carbonates enclosed between these horizons is the middle - the Lower Devonian. On this base, there was a growth of reef structures clearly expressed on the seismic profiles - atolls: Koe, Karaton, Pustynnaya, Tazhigali, Kashagan, Aktoty, and other Upper Devonian-Artinskian age.

- Along with the indicated atolls, there are less prominent Upper Devonian-Bashkirian carbonate edifices, such as Ansagan and Amanat, mapped to the east and north of the well-known giant Tengiz field.

- The southeastern remote source of drift, judging by the expansion of the Carboniferous and Permian thicknesses in the southerly direction, supplied at that time a significant amount of predominantly clayey material, leveling the Matken Trough, adjacent to the carbonate platform from the east.

- In the process of the closure of the Kungur basin and the formation of its southern flank, the inclination of the basin bottom towards the north increased, which accordingly led to intraformational disruptions in the terrigenous Lower Permian-Carboniferous sequence and the formation of "rootless" structures Pionerskaya, Kultuk Severny, Yubileinaya, etc. It is natural that such structures were formed only east of the boundary of the carbonate platform and marginal reefs, which at the time of accumulation of the strata that formed the folds were a barrier to the penetration of large masses of terrigenous material into the carbonate platform.

- One of the features of the formation of reef massifs in this region, identified by many researchers, is the arched structure of bioherms, the convex side of which faces the northeast, from where the ocean current took place for a long time.

- The site on which the Yuzhnaya, Ohiskaya reefs are located, for a large period of geological time was at a higher hypsometric level than the surrounding territory. Most of the reefs in this area stopped growing during the Bashkirian Middle Carboniferous, while the South grew up to the Artinskian Stage, the Permian. When the world ocean level dropped, the top of the reef came out to the day surface, which led to the erosion

of its top. Erosion products formed in the Artinskian time on the carbonate platform carbonate-terrigenous breccia, overlapping more submerged reef structures and coming into direct contact with the slopes of the Tengiz reef.

- The Astrakhan carbonate platform is associated with the formation on a volcanic uplift of a limited area carbonate massif up to 500 m high, located along the northeastern edge of the platform.

Conclusion

Summarizing the data on the depositional environments of the Paleozoic, it should be noted that:

1. During the Middle Frasnian-Early Turnean time, within the eastern and southeastern part of the Caspian Sea, there was a sea basin in which carbonate and carbonate-terrigenous deposits were formed. In the southern part of the basin - in the Late Devonian time, an extensive carbonate platform was formed, covering the area including the Astrakhan and Tengiz-Kashagan zones, where, in a calm marine environment, large reef structures were formed over buried volcanic arcs. Sedimentation conditions favorable for the formation of carbonate deposits also existed in the northern flank of the depression, where the Karachaganak carbonate platform is being formed.

2. Transgression in the Late Visean-Bashkirian time led to the expansion of the basin to the south towards the North Ustyurt and the widespread accumulation of carbonates. On the denuded surface of the South Emba uplift, the formation of a carbonate platform was at times suppressed by the introduction of terrigenous material.

3. In the Middle-Late Carboniferous time, the accumulation of carbonates continues in the areas of previously formed carbonate massifs, as well as along the northern side zone, where the Karachaganak carbonate platform is being formed.

4. In the Assel-Sakmara time, carbonate accumulation was preserved in the northern side zone - the Karachaganak platform, as well as in a narrow strip on the Urtatau-Sarybulak area and extended to the Zhanazhol-Tortkol zone of the eastern side of the Caspian Sea.

5. In the Artinskian age, the activation of tectonic movements in the east and southeast led to the formation of underwater fans and to the cessation of carbonate accumulation in the east and southeast. Carbonate accumulation is preserved only within the northern side zone.

References

1. Abilkhassimov Kh.B. Tectono-sedimentation model of the structure and assessment of the oil and gas content of the Paleozoic complex in the southeast of the Caspian syncline M.: OOO Geoinformtsentr 2003. (115 P.) 7.25 print.p.
2. Abilkhassimov Kh.B. Regularities of the spatial distribution of natural reservoirs of the Caspian basin. "Geology of oil and gas" M: LLC "Geoinformcenter" 2007, № 6. P.11-18.
3. Abilkhassimov Kh.B. Geodynamic and sedimentation stages in the evolution of the southeast of the Caspian syncline in the Paleozoic. "Geology, resources, prospects for the development of oil and gas subsoil of the Caspian depression and the Caspian region." International Scientific and Technical Conference: Assessment of the oil and gas potential of the Upper Paleozoic sediments in the southeast of the Caspian syncline. Selected reports/ed. V.P. Gavrilova – M.: MAX Press, 2008. – 388. P.17-27.
4. Astrakhan carbonate massif: Structure and oil and gas content. Edited by Yu.A. Volozh, V.S. Parasyna. M.: Scientific world, 2008. -221 P.
5. Atlas of lithological-paleogeographic, structural, palinspathic and geocological maps of Central Eurasia. Alma-Ata. 2002.
6. Zholtaev G.Zh., Abilkhassimov Kh.B. Sedimentation models and prospects of oil and gas content of Paleozoic deposits of the Caspian syncline and Ustyurt. // Geology of the Caspian and Aral Seas Regions: - Almaty: Kazakhstan Geological Society "KazGEO", 2004. -472. P.296-306.
7. Kuandykov B.M., Matloshinsky N.G., Sentgiorgi K. et al. // Oil and gas content of the Paleozoic shelf margin of the north of the Caspian basin. Almaty, 2011. 280 P.
8. Matloshinsky N.G. Devonian carbonate-terrigenous complex of the northern side part of the Caspian basin // Geology of Kazakhstan.1999. № 1. P. 12-23.
9. Akhmetshina L.Z., Bulekbaev Z.E., Gibshman N.B. Devonian of the eastern side of the Caspian syncline. // Domestic Geology. 1993.№1.
10. Ivanov Yu.A., Blank S.M. Lithological features of carbonate deposits in the eastern part of the Caspian basin in connection with their oil and gas content. // Lithology and minerals, 1986, №3. P.91-102.
11. Ivanova L.N., Yatskevich S.V., Kukhtinova L.V. Isolation of biohermal formations and stratigraphic relationships in subsalt oil and gas complexes of Bashenkol (Zharkamys vault). // Stratigraphy and lithology of subsalt oil and gas complexes of the Caspian basin. Saratov, 1991.P.120-127.

12. Abilkhassimov Kh.B. Geological structure and prospects of oil and gas content of the southern flank of the Cis-Ural trough. "Oil and gas" 2020, №3-4 (117-118) P. 69-84.

13. Abilkhassimov Kh.B. Features of the formation of natural reservoirs of Paleozoic sediments of the Caspian depression and assessment of the prospects for their oil and gas potential. M.: Publishing House of the Academy of Natural Sciences, 2016. (244 P.) 30,5 print.p.

Scientific publication

**International University Science Forum
"Science. Education. Practice"**

Publication scientifique

**Forum Scientifique International des Universités
"Science. Éducation. Pratiquer"**

Toronto, Canada

April 8, 2021

Signed in print 12.04.2021 r. 60x84/16.
Ed. No. 01. Circulation of 500 copies.
Scientific publishing house Infinity, 2021.

